Optimization Under Uncertainty for Management of Renewables in Electricity Markets

Zugno, Marco; Pinson, Pierre; Morales González, Juan Miguel; Madsen, Henrik

Publication date:
2013

Document Version
Publisher's PDF, also known as Version of record

Optimization Under Uncertainty for Management of Renewables in Electricity Markets

Marco Zugno

Kongens Lyngby 2013
PHD-2013-298

Technical University of Denmark
Department of Applied Mathematics and Computer Science
Building 303B, DK-2800 Kongens Lyngby, Denmark
Phone +45 45253031
compute@compute.dtu.dk
www.compute.dtu.dk PHD-2013-298

Summary (English)

This thesis deals with the development and application of models for decision-making under uncertainty to support the participation of renewables in electricity markets.

The output of most renewable sources, e.g., wind, is intermittent and, furthermore, it can only be predicted with a limited accuracy. As a result of their non-dispatchable and stochastic nature, the management of renewables poses new challenges as compared to conventional sources of electricity. Focusing in particular on short-term electricity markets, both the trading activities of market participants (producers, retailers and consumers) and the decision-making processes of system and market operators are challenged.

As far as producers are concerned, participation in electricity markets imposes them to make their trading decisions with a certain advance in time as compared to energy delivery. Since their actual output is uncertain at the time of bidding, the trading problem for a renewable power producer translates into a stochastic optimization problem, whose objective is the maximization of the expected revenues. In this thesis, we consider the trading problem for a wind power producer both in markets with low penetration of renewables, where the producer is a price-taker, and in markets where the producer acts as a price-maker.

Owing to the demand response initiatives to be undertaken in future power systems, the operation of electricity retailers and the behavior of consumers are also going to be influenced by renewable power production. Another focus of this thesis is on time-varying price mechanisms to make the most of end consumers' flexibility. In particular, the problem of managing optimally a virtual power

plant equipped with renewable production facilities and flexible consumers is addressed through control-by-price. In a similar setup, the optimal trading (and pricing) problem for a retailer connected to flexible consumers is considered.

Finally, market and system operators are challenged by the increasing penetration of renewables, which put stress on markets that were designed to accommodate a generation mix largely dominated by conventional sources. Indeed, the traditional market design, based on the sequential clearing of successive market floors and on deterministic rules and criteria, is characterized by higher and higher degrees of suboptimality and lower reliability as the penetration of renewables increases. This work contributes to the state-of-the-art by proposing new mechanisms for day-ahead dispatch and reserve determination in markets with high penetration of renewables, on the basis of stochastic criteria.

Summary (Danish)

Denne afhandling beskæftiger sig med udviklingen og anvendelsen af stokastiske modeller for beslutningsprocesser, som vil understøtte integrationen af vedvarende energi i elmarkeder.

Produktionen fra de fleste vedvarende elkilder, herunder vind, er uregelmæssig og stokastisk, og derudover kan den kun forudsiges med begrænset nøjagtighed. Som følge heraf indebærer driften af vedvarende energikilder helt nye udfordringer i forhold til konventionelle elkilder. Med hensyn til *short-term* elmarkeder er der væsentlige udfordringer både i handlingsaktiviteterne for markedsdeltagere, herunder producenter, detailhandlere og forbrugere, og i beslutningsprocesserne for markeds- og systemsoperatører.

Producenternes deltagelse i elmarkeder kræver, at deres handelsstrategi bestemmes, inden leveringen af energi forefalder. Da den fremtidige produktion fra vedvarende elkilder er usikker, når produktionen bliver udbudt på markedet, er handelsproblemet et stokastisk optimeringsproblem, hvis mål er maksimeringen af indtægterne i gennemsnit. I denne afhandling fokuserer vi på handelsproblemer for vindenergiproducenterne såvel i markeder med lav penetration af vedvarende energi, hvor producenterne er *price-takers*, som i markeder med en høj penetration, hvor de er *price-makers*.

På grund af de initiativer som skal indføre fleksibelt forbrug (*demand response*) i fremtidens elsystemer, vil detailhandlernes drift og forbrugernes vaner være påvirket af vedvarende energiproduktion. Et andet fokusområde i afhandlingen er anvendelsen af dynamiske priser for at udnytte forbrugernes fleksibilitet. Vi studerer især problemet at styre et virtuelt kraftværk optimalt bestående af

vedvarende energiproduktionsfaciliteter og prisfleksible forbrugere. Desuden er vi optaget af et lignende problem, hvor en detailhandler, som forsyner prisfleksible forbrugere, skal optimere sin markedsstrategi.

Endeligt er vi optaget af, hvordan markeds- og systemsoperatører udfordres af den stigende penetration af vedvarende energi, som belaster de nuværende elmarkeder, der oprindeligt var konstrueret til at håndtere en blandet produktion fra konventionelle elkilder. Jo højere en penetration af vedvarende energi, jo mere suboptimal og mindre pålidelig er den traditionelle markedsstruktur, der baserer sig på sekventielle markeds *clearing* procedurer og på deterministiske kriterier. I den forbindelse bidrager denne afhandling til det aktuelle tekniske niveau ved at foreslå nye stokastiske metoder for fastsættelsen af produktionsplan samt reservesstørrelse i markeder med høj penetration af vedvarende energi.

Preface

This thesis was prepared at the department of Applied Mathematics and Computer Science (DTU Compute) at the Technical University of Denmark in partial fulfilment of the requirements for acquiring a Ph.D. degree.

The thesis deals with the development of models of optimization under uncertainty to support the participation of renewables in electricity markets. Various aspects of the topic, addressing the perspective of market participants and operator are considered.

The thesis consists of a summary report and eight papers, documenting the work carried out during the period between January 2010 and March 2013. Four of these papers are either published or in press in international peer-reviewed journals, another paper is currently submitted, and one is a technical report. Finally, the remaining two papers appear in conference proceedings.

Frederiksberg, 31-March-2013

Marco Zugno

Acknowledgements

This thesis concludes a very intense three-year period during which I enjoyed the support of many people. Since it would be really hard to imagine how this thesis would look like without this backing, I feel that I should express my gratitude to some of these people here.

The first acknowledgement goes without doubt to my supervisors, Prof. Pierre Pinson, Assoc. Prof. Juan Miguel Morales and Prof. Henrik Madsen. I have learnt so much from their supervision, and I really appreciated their unceasing support. I am glad to have the chance to collaborate with them again in the future.

I would also like to acknowledge Prof. Antonio J. Conejo, who has been a fantastic host for me at the University of Castilla–La Mancha. My stay in Spain was a very fruitful period, and I owe this to his excellent supervision. I hope I will have the chance to work with him in other occasions.

The Technical University of Denmark should be credited for supporting my Ph.D. financially. Furthermore, I would like to thank all my colleagues at the Department of Applied Mathematics and Computer Science for creating a stimulating research environment. In particular, Pierre-Julien deserves to be explicitly mentioned for sharing innumerable coffee-breaks. Besides, I would like to acknowledge my former long-time officemate, Tryggvi, now at the University of Iceland, for the fruitful collaboration on energy research and the long discussions. For similar reasons I would also like to thank Salvador from DTU Elektro.

I also had the luck of having great friends outside the university, who gave a moral contribution to my research work: my friends and family from Italy and the people I met in Denmark (Riccardo and friends from my Danish classes in particular) and in Spain. I would like to thank them for doing their best to make me feel at home in any of these countries.

My girlfriend Karen deserves very special thanks for sharing both the successful and the stressful times while I was working on this research, and for always being able to cheer me up during the latter ones.

Last, but not least, I would like to thank three special people: my mum, Adelina, my dad, Severino, and my brother, Dario. I could never have done this without their constant support and encouragement.

List of Publications

Papers Included in the Thesis

A Marco Zugno, Pierre Pinson and Henrik Madsen (2013). "Impact of wind power generation on European cross-border power flows," *IEEE Transactions on Power Systems* (in press).

B Pierre Pinson, Tryggvi Jónsson, Marco Zugno, Juan M. Morales and Henrik Madsen (2012). "Statistical analysis of the impact of wind power on market quantities and power flows," invited paper for *IEEE Power and Energy Society General Meeting 2012*, San Diego, CA, USA.

C Marco Zugno, Tryggvi Jónsson and Pierre Pinson (2012). "Trading wind energy on the basis of probabilistic forecasts both of wind generation and of market quantities," *Wind Energy* (in press), DOI: 10.1002/we.1531.

D Marco Zugno, Juan M. Morales, Pierre Pinson and Henrik Madsen (2013). "Pool strategy of a price-maker wind power producer," *IEEE Transactions on Power Systems* (in press), DOI: 10.1109/TPWRS.2013.2252633.

E Marco Zugno, Juan M. Morales, Pierre Pinson and Henrik Madsen (2012). "Modeling demand response in electricity retail markets as a Stackelberg game," in proceedings of *12th IAEE European Energy Conference*, Venice, Italy.

F Marco Zugno, Juan M. Morales, Pierre Pinson and Henrik Madsen (2013). "A bilevel model for electricity retailers' participation in a demand response market environment," *Energy Economics*, 36: 182–197.

G Juan M. Morales, Marco Zugno, Salvador Pineda and Pierre Pinson (2013). "Electricity market clearing with improved scheduling of stochastic production," submitted to *European Journal of Operational Research*.

H Marco Zugno and Antonio J. Conejo (2013). "A robust optimization approach to energy and reserve dispatch in electricity markets," *Technical Report–2013–05*.

Other Publications not Included

The following publications have also been prepared during the course of the Ph.D. study. They are omitted in this thesis either because they are covered by other papers included in the dissertation (conference papers) or because of copyright reasons (book contribution).

I Marco Zugno, Tryggvi Jónsson and Pierre Pinson (2010). "Trading wind energy in a liberalised electricity market: A real world test-case in Western Denmark," poster presentation in *EWEC '10, European Wind Energy Conference*, Warsaw, Poland.

J Marco Zugno, Tryggvi Jónsson and Pierre Pinson (2010). "Decision-making strategies for trading wind power in deregulated energy markets," in proceedings of *IAEE's 33rd International Conference*, Rio de Janeiro, Brazil.

K Tryggvi Jónsson, Marco Zugno and Pierre Pinson (2010). "On the market impact of wind power (forecasts) — An overview of the effects of large-scale integration of wind power on the electricity market," in proceedings of *IAEE's 33rd International Conference*, Rio de Janeiro, Brazil.

L Juan M. Morales, Antonio J. Conejo, Henrik Madsen, Pierre Pinson and Marco Zugno (2013). *"Integrating renewables in electricity markets: Operational problems,"* Springer, International Series in Operations Research and Management, in progress.

Contents

Part I

Summary Report

Chapter 1

Introduction

As far as power systems are concerned, we live in probably the most interesting years since the late nineties, when liberalization took place.

Encouraged by international agreements aiming at reducing CO_2 emissions, and backed by larger and larger shares of the society, renewable energy has experienced an unprecedented growth in industrialized countries during the recent years. This impressive development can partly be explained by the favorable incentives renewables were granted in the early stages of their deployment. Under these schemes, renewable power producers are allowed to contribute to power generation and at the same time sidestep most of the drawbacks and the risks implied by participation in the market.

In parallel to their massive deployment, the per unit cost of renewable energy has constantly decreased, and is approaching grid parity for some technologies like wind and solar. Hence, renewables are able to, and asked to, compete in the marketplace with conventional sources of energy, despite being fundamentally different from these sources. Indeed, renewable sources, with the exception of hydro and biofuels, are *non-dispatchable*, i.e., their output cannot or can only partly be modulated on demand, and their production is *stochastic*, and therefore hard to predict in advance.

As a result of the large-scale deployment and of the peculiar features of renew-

ables described above, there is an increasing need for mathematical tools that can model their impact on, as well as facilitate their optimal participation in, electricity markets.

1.1 Thesis Objective

This thesis aims at developing tools to efficiently manage renewable sources in the framework of liberalized electricity markets. In an economic perspective, efficiency can be interpreted as achieving minimum cost, maximum social welfare or maximum revenue. In mathematical terms, this translates naturally into optimization problems. Furthermore, owing to the uncertain and non-dispatchable nature of renewable sources, their participation in electricity markets can only be modeled and optimized properly by making use of tools accounting for their stochasticity. Hence, the natural choice for tools to attack this type of problems consists in methods of optimization under uncertainty.

As a motivation to this work, we first describe the impact that renewable sources currently have on electricity markets. Owing to their increasing penetration in power systems, and to their peculiar characteristics previously mentioned, renewable sources are expected to have a substantial impact on the market, e.g., on the power flowing on transmission lines and on the market-clearing prices. Papers A and B focus on the development of stochastic models based on nonlinear regression techniques [CD88] to quantitatively describe the underlying relationships between renewable power and market quantities. The focus of these two papers is on modeling rather than optimization, which is the core of this thesis. Hence, their contribution consists in showing how renewables already have a significant impact on electricity markets.

The management of renewables in electricity markets comprises two complementary sides. On the one side are the market participants, mainly producers, retailers and consumers, who either own renewable production capacity or are, more or less directly, influenced by it. On the other side are the market operators and the transmission system operators, which face the challenging problem of operating the market and the transmission grid efficiently and safely as the contribution from renewables increases. Both problems are addressed in this thesis.

The problem of renewable power producers seeking to optimize their revenues in electricity markets is considered first. The uncertain nature of their production, coupled with the advance in time required to participate in electricity markets, result in a problem of optimization under uncertainty. Paper C considers the

case where the producer is a price-taker in the market, which has a certain affinity with the well-known *newsvendor problem* [RS64]. Then, we abandon the price-taker assumption and consider the optimization problem of a renewable power producer having an impact on prices in Paper D. Such problem is modeled as a Mathematical Program with Equilibrium Constraints (MPEC) [GCF+12].

As far as retailers and consumers are concerned, fundamental changes in the way they operate and behave will be brought about in the years to come by demand response initiatives. Being such programmes aimed at increasing the possibility for integrating renewables, the point of view of demand (retailers and consumers) is particularly relevant to this work. In this respect, Papers E and F consider the joint problem of retailers and consumers that interact by means of dynamic prices, broadcast by the former participant, and flexible demand. More specifically, in Paper E, we model the case of a retailer optimally managing a virtual power plant comprising both stochastic generation and flexible consumers exposed to dynamic prices. In Paper F, we consider the hierarchical relationship between flexible consumers and a price-setting retailer, which exchanges power with an infinite market. The models in both papers are based on MPECs.

Market and transmission system operators are also challenged by the development of renewables as they are called to clear and operate markets efficiently, despite the increasing share of non-dispatchable and stochastic power in the system. The "traditional" way of clearing subsequent markets, energy-only or comprising energy and reserve capacity, in a sequential fashion based on deterministic principles is known to be suboptimal when stochastic producers are involved. In Paper G, we consider a clearing procedure for a two-stage (day-ahead and balancing) energy-only market, based on MPECs and on stochastic programming principles [BL11]. Furthermore, in Paper H, we consider the joint optimization of reserve and day-ahead dispatch. Such a problem is approached making use of robust optimization [BBC11], in order to guarantee efficiency in the worst-case realization of the uncertain renewable production.

As a final comment, it should be mentioned that most of the papers included in this dissertation are specifically targeted to wind power, among all renewable sources. There are two reasons for this. The first one is that wind power is by far the most common stochastic, non-dispatchable renewable source in the world nowadays, particularly in Denmark where the share of wind power in the production mix is about 30%. The second reason is that, among these renewables sources, wind was the first one having to participate in markets. However, the results we present could be easily generalized to solar, wave and tidal power, which share many characteristics of wind power, i.e., the stochastic and non-dispatchable nature first, along with intermittency and spatial distribution in the system.

1.2 Thesis Outline

The thesis is structured as follows. Part I is a report introducing and summarizing the papers. Within this part, Chapter 2 comprises a brief introduction to electricity markets, in particular to the Nordic market, Nord Pool, and to how renewables participate in it. Chapter 3 introduces the methodologies employed in the thesis: Mathematical Programs with Equilibrium Constraints (MPECs), stochastic programming and robust optimization. A summary of the main results obtained in the papers is given in Chapter 4. Finally, Chapter 5 concludes Part I.

Part II is a collection of publications including the following papers.

Paper A is a journal article accepted for publication in *IEEE Transactions on Power Systems*. It deals with modeling the impact of wind power production in Germany on European cross-border flows, making use of nonlinear regression coupled with principal component analysis.

Paper B is an invited paper presented at the *IEEE Power and Energy Society General Meeting 2012*, which discusses an analysis similar to the one in Paper A, also including results showing the impact of German wind power production on power flows in Austria, and of the forecast of wind power production on market prices in Western Denmark and in the German EEX market.

Paper C is a journal article published in *Wind Energy* in 2012. This paper deals with the determination of the optimal trading strategy for a price-taker wind power producer, and includes a realistic test-cast simulating the trading activity during a period of 10 months in Eastern Denmark.

Paper D is a journal article accepted for publication in *IEEE Transactions on Power Systems*. This paper deals with the optimal trading strategy for a wind power producer that is a price-maker in the balancing market. It also presents results obtained from a case study based on Nord Pool.

Paper E is a paper presented at the *12th IAEE European Energy Conference* in 2012. The topic of this paper is the optimal management of a virtual power plant comprising wind power production facilities and flexible consumers responsive to dynamic prices.

Paper F is a journal article published in *Energy Economics* in 2013. It presents a hierarchical optimization model for determining the optimal market strategy for a retailer supplying flexible demand, which is responsive to dynamic prices.

Paper G is a journal article submitted to *European Journal of Operational Research*. It presents a novel day-ahead market-clearing model for energy-only markets, accounting for the projected balancing costs of deviations from stochastic producers, and constrained by equilibrium conditions that guarantee cost-recovery for flexible producers.

Paper H is a technical report, which deals with the joint determination of day-ahead energy and reserve dispatch making use of robust optimization.

Chapter 2

Electricity Markets

Electricity is a fundamental resource in modern societies. We make use of it continuously to satisfy our basic household needs. Besides, electrical power is the backbone of our economy, as it is key for the activity in both the manufacturing and the service industry.

Because of the importance of electricity in our society, it is essential that the whole chain of processes from the generation to the delivery of power to the end consumers is managed in a reliable and cost-efficient manner. In a large number of industrialized countries, this is currently performed in the framework of electricity markets.

In this chapter, we review briefly the history of liberalization of the electricity sector and describe the main characteristics of electricity markets in Section 2.1. Then, the structure of the Nordic power exchange, Nord Pool, is sketched in Section 2.2. Section 2.3 discusses the impact of renewables on electricity markets and some of the challenges they pose. Finally, demand response is briefly introduced in Section 2.4.

2.1 Liberalization of the Electricity Sector

Until the last two decades of the 20th century, power systems worldwide were organized in a centralized fashion. State-owned, vertically-integrated utilities were in charge of the whole chain of activity related to electrical power: generation, transmission, distribution and retail. Furthermore, such utilities acted as monopolies in all these fields.

The organization of power systems as state monopolies remained practically unchallenged until the end of the last century. The first steps towards the creation of modern electricity markets were taken by the Chicago Boys in Chile in 1982, during the Pinochet dictatorship, with the separation of generation and distribution activities (unbundling), the introduction of competition between producers, as well as of trading and pricing of electricity according to the production cost (marginal pricing).

As far as Europe is concerned, the first countries to liberalize the electricity sector were the UK, with the creation of an electricity market in England and Wales in 1990, and Norway in 1991. Australia (Victoria and New South Wales market, 1994) and New Zealand (1996) were also among the first movers. The United States followed with the liberalization of markets in California (CalPX), New York (NYISO), Pennsylvania, New Jersey and Maryland (PJM) by the end of the century [Wer06]. Electricity markets worldwide have been implemented in a variety of ways, which would be impossible to review here. However, these implementations share a number of common features.

The first common feature is the separation of generation, transmission, distribution and retail activities. Markets promote competition in generation and retail, while transmission remains a monopoly managed by non-commercial organizations (System Operators, in short SOs).

Trading of electricity is organized in pools or exchanges, where producers and possibly retailers and large consumers submit bids for energy delivery to, or withdrawal from, the grid. Commonly, the preferred marketplace for short-term transactions is a day-ahead market, often referred to as *forward market* in the United States and as *spot market* in Europe. Later adjustments of day-ahead contracts are possible in intra-day markets, and finally in the balancing market, which is also called real-time or regulation market. Contract lengths typically cover one hour or half an hour. Furthermore, most markets provide clearing services for financial contracts (forward, options and derivatives).

In general, liberalization is considered to have improved the efficiency of power systems' management, leading to lower prices for electricity, and to have solved

the overinvestment problem typical of centralized power systems [Wer06]. However, the implementation of electricity markets has not been free of failures, see for example the crisis in California at the beginning of the century [Bor02]. Currently, the traditional market design is challenged by the growth in installed renewable capacity, as we discuss in Section 2.3.

We refer the reader to [Wer06] for a more detailed history and description of electricity markets.

In the next section, we introduce the main features of the Nordic electricity market, Nord Pool. This market is commonly addressed in the research papers included in Part II of this thesis.

2.2 The Nord Pool Market

The Nord Pool market, originally named Statnett Marked AS, was created in Norway in 1991, after the Norwegian parliament imposed the deregulation of the electricity sector. The geographical scope of the market has extended gradually during the years. In 1996, Sweden joined the market to form the first international power exchange worldwide, which was then renamed as Nord Pool ASA. Finland and Denmark joined in 1998 and 2000, respectively. The Baltic countries are currently in the process of being integrated. Estonia and Lithuania have already joined as bidding areas of Nord Pool in 2010 and 2012, respectively, while Latvia is planning to join the marketplace in the near future [Nor13a].

Nord Pool provides clearing services for the short-term electricity markets. Furthermore, it also serves as clearinghouse for financial products (forward, futures, derivatives, etc.). The two types of activities have been separated in 2010, when Nasdaq OMX acquired the financial clearinghouse and consultancy services sections of Nord Pool, now called Nasdaq OMX Commodities Europe, while the short-term electricity market activities are carried out by Nord Pool Spot ASA. The latter company is jointly owned by the Transmission System Operators (TSOs) of the countries participating in the exchange.

Being the focus of this thesis on short-term markets, we describe their functioning in this section, while the financial market is disregarded. First, we present the energy markets, i.e., the the day-ahead, intra-day and balancing markets, according to their sequential order. Then, we deal with capacity markets at the end of the section.

More information on the history of Nord Pool, and on the functioning of the

different markets, can be found in [Nor13b] and [Nor13c].

2.2.1 Day-ahead Market

The day-ahead market in Nord Pool is named Elspot. It is organized as a two-sided auction where producers, retailers and large consumers submit bids for delivery and withdrawal of electricity throughout the following day. Market participants must submit 24 bids in total, i.e., one for each hour of the following day. Each bid is specified as a set of price-quantity pairs, indicating the amount of energy the participant is willing to purchase or sell at a given price.

The deadline for submitting bids is at noon of the day preceding the actual delivery. After this, Nord Pool clears the market by 12:45, publishing the price(s) and communicating the production and consumption schedules to each producer. In order to clear the market, Nord Pool determines aggregate sale and purchase curves by sorting the sale bids according to increasing prices, and the purchase bids in the inverse order. The intersection between the two curves sets the system price. If all transmission constraints are satisfied, this price applies for the whole system: all the sale (purchase) offers whose price is not greater (lower) than this price are accepted, and this determines the day-ahead schedule. The market-clearing procedure is illustrated in Figure 2.1.

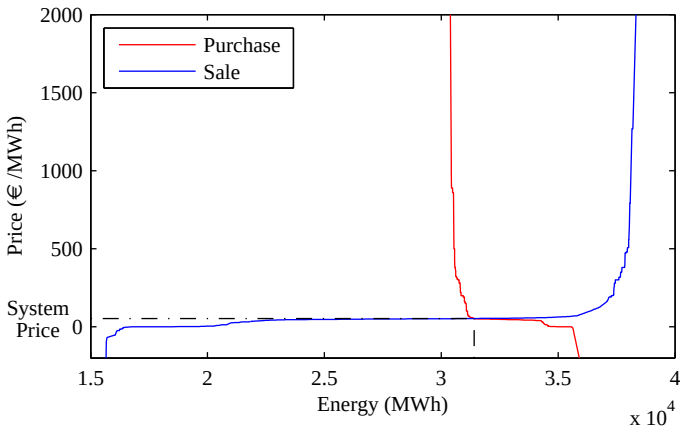

Figure 2.1: Market clearing in Nord Pool based on the purchase and sale curves submitted for the 12th trading period of the 7th September 2011. Data from [Nor13c]

If transmission bottlenecks arise as a result of the production and consumption

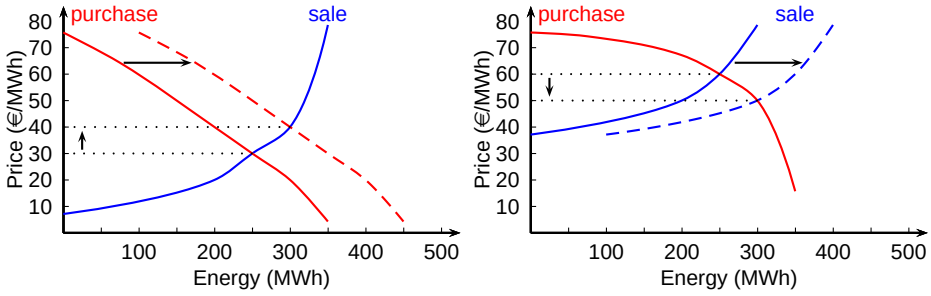

(a) Surplus area (b) Deficit area

Figure 2.2: Market splitting through implicit auctions

plan implied by the application of a unique system price, Nord Pool Spot proceeds with the so-called *market splitting* procedure. In this procedure, different market prices are calculated in market areas linked by congested transmission lines. Area prices are calculated through an *implicit auction*. Aggregate supply and demand curves are determined for each market area where congestion arises. If the area is in surplus of production, the transmission capacity is considered as a price-independent purchase bid, thus shifting the purchase curve to the right. The result is an increase in the area price and, consequently, a larger production and lower consumption. On the other hand, if the area is in deficit of production, the transmission capacity from other Nord Pool areas enters as a price-independent supply bid, thus shifting the sale curve to the right and decreasing the area price. The situation is sketched in Figure 2.2.

The number and geographical extension of the price areas is predefined in Nord Pool. There are five price zones in Norway, four in Sweden, two in Denmark and a single price area for each of the other countries (Finland, Estonia and Lithuania). Basically, the borders between area prices are drawn where the main transmission bottlenecks are located in the power grid. The price zones in Nord Pool are illustrated in Figure 2.3.

The pricing rules in Nord Pool impose that the day-ahead price be equal throughout each individual price zone, despite the fact that internal transmission lines may be congested. Such a pricing system is referred to as *zonal pricing*. In contrast, market prices can be different at each node of the grid when the *nodal pricing* system is employed. In such a system, the price of electricity mirrors the marginal increase in the cost for serving load at any given node of the grid.

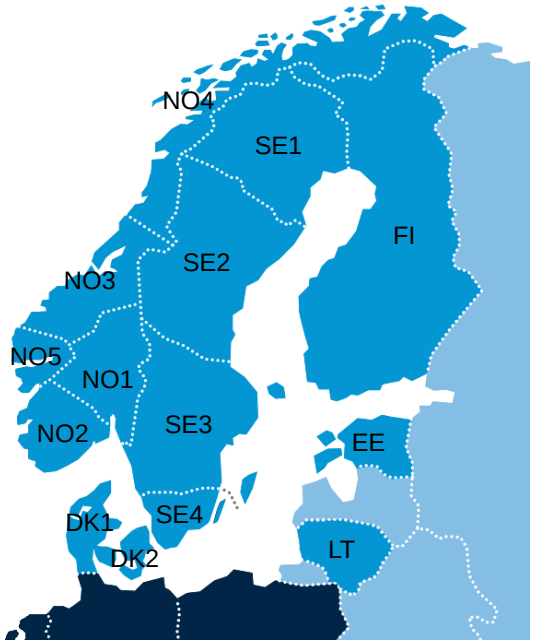

Figure 2.3: Bidding areas in Nord Pool Spot. Figure from [Nor13c]

2.2.2 Intra-day Market

The Elbas market allows intra-day trading in Nord Pool after the clearing of the day-ahead market. Trading in Elbas starts at 14:00 on the day before delivery and is allowed until one hour in advance for any trading period of the day. The organization of the intra-day market in Nord Pool is different from that of an exchange. Indeed in this market, bid and ask offers are matched around the clock on a first-come, first-served basis, rather than being cleared in one shot at the gate closure.

Intra-day markets are indicated by many as a fundamental trading floor to allow the large-scale integration of renewables [Web10]. Nevertheless, Elbas has a very low liquidity, as its trading volume rounds 1% of the total consumption in Scandinavia. This figure is in line with the liquidity of most other European intra-day markets, with the notable exception of the Iberian MIBEL market.

2.2.3 Balancing Market

The balancing market ensures that production equals consumption at any time period in the Nordic region as a whole. This implies that all unwanted deviations from the production and consumption plans resulting from the day-ahead and intra-day markets are offset by the activation of regulating power from other market participants. The balancing market facilitates trading across different price areas of Nord Pool. However, the activation of regulating bids in a certain price area is responsibility of the relevant national Transmission System Operator (TSO), which ensures the stability of the system frequency at 50 Hz within its price area(s).

The distinction between *regulating* and *balancing* power is fundamental. Balance Responsible Parties (BRPs) are allowed to submit bids for regulating power until 45 minutes before delivery. These bids can be for up-regulation (production increase or consumption decrease) or down-regulation (production decrease or consumption increase). On request of the TSO, these bids must be activated within a period of 15 minutes. In Denmark, regulating power is then paid according to the marginal pricing principle, with the price being set as the price offer of the highest (lowest) bid activated for at least 10 consecutive minutes in case of prevailing up- (down-)regulation in the system. Bids that are activated for less than 10 minutes, or that are in the opposite direction to that of the overall system imbalance for the hour, are priced according to the pay-as-bid rule.

Unwanted energy deviations from the aggregated schedules after trading in the day-ahead and intra-day markets constitute balancing power. These imbalances are settled ex post according to the metered production and consumption of the market participant. In the Nordic market, the *one-price* rule applies to deviations in consumption, while the *two-price* rule applies to production imbalances.

In the one-price model, all power imbalances are settled at the balancing market price, i.e., the marginal cost of regulating power for the hour. This implies that an unwanted deviation in the opposite direction as compared to the system imbalance is actually rewarded by a price that is more attractive than the day-ahead price (higher for positive deviation, lower for negative). On the contrary, in the two-price system the balancing market price applies only to deviations in the same direction as the system's. This implies that:

- If the system is in deficit of power (up-regulation), a producer with a negative unwanted deviation (underproduction) must pay the balancing price, which is higher than the day-ahead price, while it receives the day-ahead price for a positive unwanted deviation (overproduction).

- In the case of power surplus (down-regulation), a producer pays the day-ahead price for an unwanted underproduction, while it receives the balancing market price, which is lower than the day-ahead price, for positive unwanted deviations.

The reader is referred to [Ene08] for further information.

2.2.4 Capacity Markets

Day-ahead, intra-day and balancing markets are energy markets, in that the payment to or from the market operator is proportional to the amount of energy actually delivered to or withdrawn from the grid. In addition to energy markets, capacity markets are in place in Nord Pool to guarantee the availability of sufficient regulating power in the market.

The capacity markets are managed by the national TSOs. In Denmark, there exist separate capacity markets for primary, secondary and tertiary (or manual) reserve. The primary reserve market is cleared daily at 15:00 on the day before operation, while the secondary reserve one is cleared on a monthly basis. Instead, the market for tertiary reserve is cleared everyday at 9:30. The acceptance of a reserve bid in the latter market obliges a producer to submit an offer in the regulation market of at least the same size.

Producers participating in capacity markets are paid proportionally to the available capacity (MW). The capacity price is equal to the price of the most expensive bid accepted in the market.

The interested reader is referred to [Ene12] for further details on the functioning of capacity markets in Denmark.

2.2.5 On the Clearing Sequence and Procedures

An important aspect of energy and capacity markets is the relationship between their market-clearing procedures.

In Nord Pool, and in many other electricity markets, the different markets described above are cleared sequentially and in a deterministic fashion. For example, the day-ahead market is cleared on the basis of the bids received from producers and generators, which are known with certainty by the market operator.

On the other hand, there is no regard to the projection of the market-clearing decision on the future cost for the system, e.g., in terms of imbalance. The application of such a straightforward deterministic rule responds to the important criterion of transparency of scheduling and pricing. However, a stochastic criterion such as the minimization of the total expected cost would result in a higher social welfare (in expectation) as soon as renewables penetrate the system, as shown in [PZP10]. The issue is addressed in Paper G in this thesis.

Similarly, the market for manual reserve is cleared before the day-ahead market and according to deterministic criteria (e.g., the $n-1$ criterion). In contrast, the joint optimization of day-ahead dispatch and reserve is advocated in [MCPR09], which shows that significant cost reductions can be achieved by employing a stochastic programming approach. In this dissertation, the topic is addressed in Paper H making use of robust optimization.

2.3 Impact of Renewables on Electricity Markets

In a global perspective, renewable power has been growing at an astonishing pace in the recent years. In particular, wind power has been a booming industry that experienced an almost exponential growth in installed capacity worldwide [Glo12].

Denmark has been at the forefront of the development in wind power. Having enjoyed the first-mover advantage with respect to the deployment of this production technology, this country has one of the highest shares of wind power production worldwide. Figure 2.4 illustrates the evolution in time of the cumulative installed wind power capacity in Denmark, along with the share of wind in the total annual electricity generation, which currently rounds 30%.

As a side effect of accommodating a large share of renewables, Nord Pool has experienced the impact that such sources have on electricity markets. This is particularly true for the Danish price areas DK1 and DK2, where most of the wind power production facilities are installed.

Much of the impact of renewables on electricity markets can be explained by the so-called *merit order* effect. Since their marginal cost is basically zero (or even negative if incentive schemes award price premia to renewables on top of the clearing price), the offer from renewable producers enters the aggregate supply curve from the left-hand side. This implies that renewables are scheduled before conventional power producers.

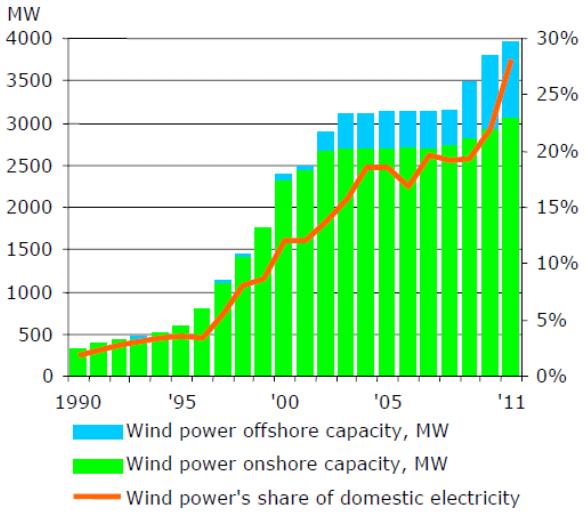

Figure 2.4: Development of installed wind power capacity and wind power penetration in Denmark over the last two decades. Figure from [Ene13b]

The output from renewables directly influences the market price as a result. Since their production is intermittent, the aggregate supply curve for the system is shifted to the left in case of low production from renewables, and to the right in case of high renewable outturn. As illustrated in Figure 2.5, this has an effect on the intersection between the supply and demand curves. In periods with high renewable power production, the amount of scheduled production and consumption increases, and the market price is low. On the contrary, periods with low renewable power production are characterized by higher prices and lower production and consumption schedules.

An implication of the effect of renewable power production on prices is that regions where a high output from renewables is forecast tend to have lower prices than regions with lower renewable production or penetration. In turn, price differentials trigger power flows from low-price areas to high-price ones. Since renewable power production is one of the drivers of the market price, we can expect it to have an effect on regional power flows as well.

Given the stochastic nature of renewable power production, its impact on electricity markets, e.g., on prices and flows, is also stochastic. Furthermore, these effects have a nonlinear nature as well. For example, the relationship between renewable power production and the price is dependent on the shape of the aggregate supply and purchase curves. Similarly, one can expect a nonlinear

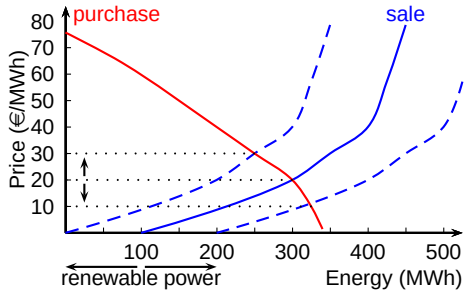

Figure 2.5: The merit order effect and the impact of renewables on the clearing price in an electricity exchange

impact of renewable output on power flows.

In Papers A and B, the impact of renewable power production on electricity markets is studied by making use of nonlinear regression techniques presented in [CD88]. This allows to determine models describing the average behavior of dependent variables (e.g., market prices and power flows) as nonlinear functions of explanatory variables (e.g., wind power penetration).

The relation between forecast wind power penetration, defined as the ratio between the wind power output and load, and the day-ahead price is one of the issues explored in Paper B. Figure 2.6, which is extracted from the paper mentioned above, illustrates this relation in the Western Danish (DK1) price area of Nord Pool. Notably, the day-ahead price is decreasing with wind power penetration, as a consequence of the merit order effect described above. Furthermore, the relation is nonlinear.

Paper A considers the impact of wind power production in Germany on the cross-border power flows among European countries. Figure 2.7 shows the model describing the relationship between forecast wind power penetration in Germany, time of the day and the power flow in the interconnection between Western Denmark (DK1 area) and Norway (NO2 area). As one can see, power flows on average from Norway towards Denmark when low levels of wind power penetration are expected in Germany, while the situation is reversed with high levels of wind power production. Indeed, lower power prices turn Germany and Denmark into net exporters of electricity. On the contrary, the Norwegian generation mix, nearly entirely consisting of hydro units [Nor12], is flexible enough to lower the production, consequently allowing for power import.

The results in Papers A and B confirm that renewables, and in particular wind power, have already become an important player in electricity markets. As such,

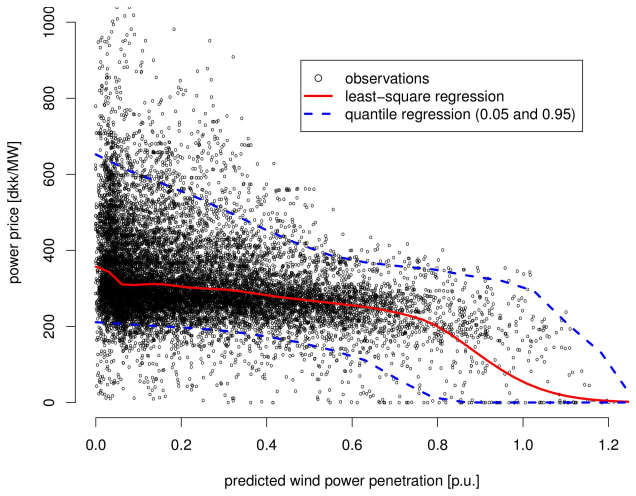

Figure 2.6: Relation between the forecast wind power penetration and day-ahead market price in the Western Danish (DK1) area of Nord Pool. Plot from Paper B

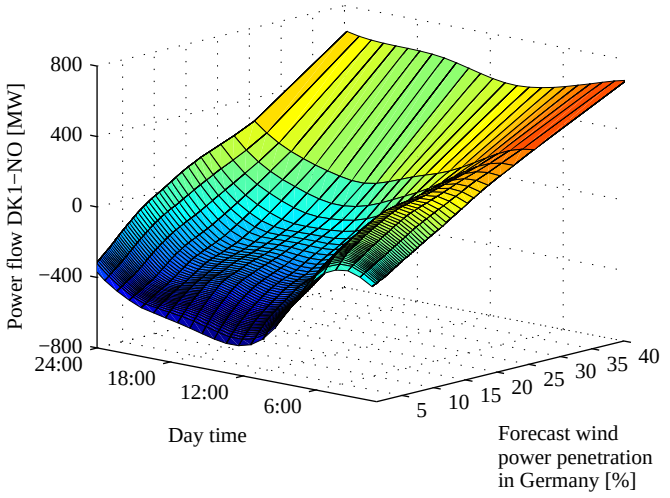

Figure 2.7: Impact of forecast wind power penetration in Germany on power flow between the Danish DK1 area and the Norwegian NO2 area. Plot from Paper A

they are challenging the traditional ways markets are operated.

The uncertain nature of renewable sources, such as wind and solar power, increases the need for backup power to cope with the unpredicted fluctuations of power production. This results in an increasing need for liquidity in markets whose gate closure approaches real-time, as well as for an efficient use of the resources participating in these markets. The balancing market is particularly important to renewable power producers, as it allows them to adjust their contracts so that they match their actual output. Similarly to the case of the day-ahead price, renewable power production impacts the price at the balancing market, too. Increasing the liquidity of intra-day markets [Web10], and improving the functioning of reserve markets [MCPR09] are also paramount to improve the efficiency of electricity markets highly penetrated by renewables. In particular, increasing the efficiency of markets through improved decision making under uncertainty is the topic of Papers G and H.

Another feature of renewables, namely their intermittency, is contributing to reshaping electricity markets. While solar power production peaks at noon, wind power production is generally higher during the night. Increasing renewable power penetration requires a higher degree of flexibility in power systems, as they must be capable of operating safely even when the output from renewables is low. As far as the supply side is concerned, this can be accomplished by installing power plants with large ramping capacity and by deploying storage facilities. Besides, the consumption side offers great potential to increase system flexibility through the development of demand response initiatives.

2.4 The Role of Demand Response

Figure 2.8 illustrates a situation that is becoming more and more common in Western Denmark (DK1 area of Nord Pool): wind power production exceeds total consumption during valley hours. Situations like this normally result in zero or even negative electricity prices. In turn, low prices signal that increasing power supply during these hours has low value for the society, thus discouraging investment in new renewable production capacity.

Demand response has recently emerged as a measure to accommodate increasing penetration of renewables in power systems by making use of the available resources more efficiently. Basically, commercial as well as residential consumers are to be involved in the electricity market and incentivized to adapt to an increasingly intermittent supply.

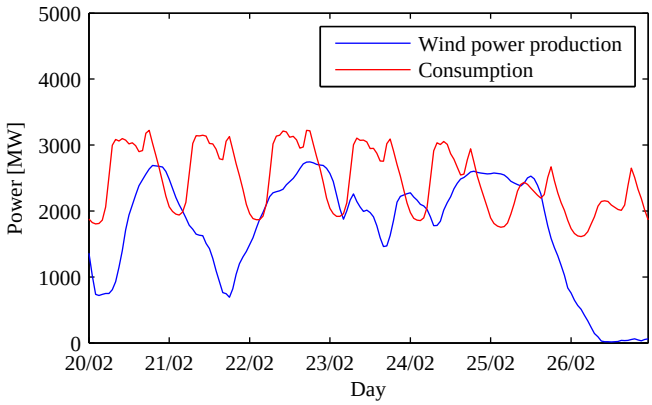

Figure 2.8: Wind power production and consumption in Western Denmark (DK1) during the last week of February 2012. Data from [Ene13a]

Generally demand response initiatives are grouped into either *direct control* or *indirect control*. The former group comprises initiatives aimed at granting TSOs, or other market entities with similar objectives, the right to directly modulate the demand by means of rationing or disconnecting individual consumers, or groups of. Typically consumers involved in these programmes are protected by a contract fixing how often they can be disconnected or rationed.

Indirect control implies the use of economic incentives so that demand adapts to the stochastic and intermittent production. In practice, this would be done by broadcasting time-varying prices to the consumers (time-of-use price or dynamic real-time price). This topic is considered in Papers E and F.

The implementation of demand response requires the installment of infrastructure allowing communication to the consumers (one way or bidirectional), and of consumer appliances able to adapt their consumption to the broadcast signals. This infrastructural upgrade of the grid and of the consumer appliances is often associated with the notion of *smart grid*.

Besides the technical challenges involved with the infrastructural developments just mentioned, demand response poses difficult challenges also in terms of market design. First of all, the introduction of price-incentives will confer dynamic properties to the demand, by increasing its cross-elasticity across different time periods, which needs to be modeled and accounted for by the policy-makers. Furthermore, demand response will require the coordination of a large number of consumers and distributed generators spread around the system, with further complications imposed by the tight capacity constraints that characterize the

power grid at the distribution level. For these and other reasons, demand response is considered one of the most challenging topics of power systems research in the years to come.

We refer the interested reader to [THL10] for a detailed description of the demand response initiatives currently implemented and planned in Europe.

Chapter 3

Optimization Under Uncertainty

Because of the stochastic nature of renewable sources, their efficient management in electricity markets calls for the use of tools for optimization under uncertainty.

In this chapter, we review some elements of optimization theory that support the mathematical developments in the papers included in this dissertation. Section 3.1 summarizes some basic notions of optimization and of linear programming. Mathematical Programs with Equilibrium Constraints (MPECs) are introduced in Section 3.2. Then, we introduce the framework of stochastic programming in Section 3.3. Finally, Section 3.4 deals with robust optimization. Examples focusing on electricity markets are proposed throughout the chapter to illustrate how these optimization tools are employed in the papers in Part II.

3.1 Fundamentals of Optimization

The general mathematical formulation of an optimization problem is the following one:

$$\underset{\mathbf{x}}{\text{Minimize}}\ f(\mathbf{x}) \tag{3.1a}$$

$$\text{s.t. } \mathbf{g}(\mathbf{x}) \leq \mathbf{0}\ , \tag{3.1b}$$

$$\mathbf{h}(\mathbf{x}) = \mathbf{0}\ . \tag{3.1c}$$

Bold fonts indicate vectors, matrices and vector-valued functions. In order to avoid tedious definitions for every optimization model, we will hereinafter assume that all the elements are defined properly, i.e., in this case $f(\cdot) : \mathbb{R}^n \to \mathbb{R}$, $\mathbf{g}(\cdot) : \mathbb{R}^n \to \mathbb{R}^l$, $\mathbf{h}(\cdot) : \mathbb{R}^n \to \mathbb{R}^m$, and $\mathbf{0}$ is a zero-valued vector of the proper size.

The simplest instance of the general optimization problem (3.1) is obtained when the functions $f(\cdot)$, $\mathbf{g}(\cdot)$ and $\mathbf{h}(\cdot)$ are linear. A linear program (LP) can be formulated as follows:

$$\underset{\mathbf{x}}{\text{Min.}}\ \mathbf{c}^T\mathbf{x} \tag{3.2a}$$

$$\text{s.t. } \mathbf{A}_\text{I}\mathbf{x} \leq \mathbf{b}_\text{I}\ , \tag{3.2b}$$

$$\mathbf{A}_\text{E}\mathbf{x} = \mathbf{b}_\text{E}\ , \tag{3.2c}$$

where $\mathbf{A}_\text{I}$, $\mathbf{A}_\text{E}$, $\mathbf{c}$, $\mathbf{b}_\text{I}$ and $\mathbf{b}_\text{E}$ are matrices and vectors of appropriate size.

Linear programs (LPs) model a wide variety of real-world problems. In Example 3.1, we show how a network-constrained market-clearing problem can be modeled as an LP. Notice that very large LPs can be solved using commercially available software.

3.1.1 Duality in Linear Programming

Let us associate the vector $\boldsymbol{\mu} \leq \mathbf{0}$ to the inequalities (3.2b), and the vector $\boldsymbol{\lambda}$, free in sign, to the equalities (3.2c). Both vectors are sized so that one element of the vector corresponds to one constraint. The following problem is the *dual*

version of problem (3.2), which is referred to as *primal*:

$$\underset{\boldsymbol{\mu},\boldsymbol{\lambda}}{\text{Max.}}\ \mathbf{b}_{\mathrm{I}}^T\boldsymbol{\mu} + \mathbf{b}_{\mathrm{E}}^T\boldsymbol{\lambda} \tag{3.3a}$$

$$\text{s.t. } \mathbf{A}_{\mathrm{I}}^T\boldsymbol{\mu} + \mathbf{A}_{\mathrm{E}}^T\boldsymbol{\lambda} = \mathbf{c}\ , \tag{3.3b}$$

$$\boldsymbol{\mu} \leq \mathbf{0}\ . \tag{3.3c}$$

The dual variables $\boldsymbol{\mu}$ and $\boldsymbol{\lambda}$ can be interpreted as marginal costs. Indeed, they represent the per unit change in the optimal value of the objective function (3.2a) if the right-hand side of the associated constraint is increased marginally. Naturally $\boldsymbol{\mu} \leq 0$, since a marginal increase of any element of $\mathbf{b}_{\mathrm{I}}$ would result in a larger feasible space for (3.2).

In a market employing the marginal pricing rule, dual variables are of particular importance as they serve to price the traded commodity.

The following duality results are well known in linear programming. We report them without proof and refer the reader to [LY08] for further detail.

Theorem 3.1 (Weak Duality) *If* $\mathbf{x}$ *is feasible for* (3.2)*, and* $\boldsymbol{\mu}, \boldsymbol{\lambda}$ *are feasible for* (3.3)*, then* $\mathbf{c}^T\mathbf{x} \geq \mathbf{b}_{\mathrm{I}}^T\boldsymbol{\mu} + \mathbf{b}_{\mathrm{E}}^T\boldsymbol{\lambda}$.

Theorem 3.2 (Strong Duality) *If the primal problem has a finite optimal solution* $\mathbf{x}^*$*, so does the dual problem and at optimality it holds that* $\mathbf{c}^T\mathbf{x}^* = \mathbf{b}_{\mathrm{I}}^T\boldsymbol{\mu}^* + \mathbf{b}_{\mathrm{E}}^T\boldsymbol{\lambda}^*$.

Since the dual of the dual problem is again the primal problem, the converse of the previous theorem holds trivially.

3.1.2 Karush-Kuhn-Tucker Conditions

Duality results similar to the ones of linear programming are available for nonlinear convex optimization problems. However, in this dissertation we only deal with Karush-Kuhn-Tucker optimality conditions for convex problems, and refer to [BSS06] for a general introduction to duality theory.

Let us consider the general formulation (3.1), and suppose that $f(\cdot)$, $\mathbf{g}(\cdot)$ are continuously differentiable and convex, and $\mathbf{h}(\cdot)$ is affine.

The Lagrangian function for problem (3.1) is the following:

$$\mathcal{L}(\mathbf{x}, \boldsymbol{\mu}, \boldsymbol{\lambda}) = f(\mathbf{x}) + \boldsymbol{\mu}^T \mathbf{g}(\mathbf{x}) + \boldsymbol{\lambda}^T \mathbf{h}(\mathbf{x}) \ . \tag{3.4}$$

Under the assumptions above, as well as some constraint qualification[1], the following Karush-Kuhn-Tucker (KKT) conditions are necessary and sufficient for optimality for problem (3.1):

$$\nabla_{\mathbf{x}} f(\mathbf{x}) + \boldsymbol{\mu}^T \nabla_{\mathbf{x}} \mathbf{g}(\mathbf{x}) + \boldsymbol{\lambda}^T \nabla_{\mathbf{x}} \mathbf{h}(\mathbf{x}) = 0 \ , \tag{3.5a}$$
$$\mathbf{g}(\mathbf{x}) \leq \mathbf{0} \ , \tag{3.5b}$$
$$\mathbf{h}(\mathbf{x}) = \mathbf{0} \ , \tag{3.5c}$$
$$\boldsymbol{\mu} \geq \mathbf{0} \ , \tag{3.5d}$$
$$\boldsymbol{\mu}^T \mathbf{g}(\mathbf{x}) = \mathbf{0} \ . \tag{3.5e}$$

Equation (3.5a) are stationarity conditions. Constraints (3.5b) and (3.5c) enforce feasibility of the primal problem, while (3.5d) is a feasibility condition of the dual problem. Finally, (3.5e) enforces complementary slackness.

The dual vectors $\boldsymbol{\mu}$ and $\boldsymbol{\lambda}$ retain the interpretation of marginal costs discussed in Section 3.1.1. It should be underlined, however, that the dual variables as defined in (3.5) have opposite sign as compared to the relative definition in the dual of a linear problem (3.3). These definitions are rather typical of the literature on the subject.

In the remainder of this dissertation, we will make use of the $\perp$ operator in the following compact notation for constraints (3.5b), (3.5d) and (3.5e)

$$\mathbf{0} \geq \mathbf{g}(\mathbf{x}) \perp \boldsymbol{\mu} \geq \mathbf{0} \ . \tag{3.6}$$

Example 3.1 (Network-constrained market-clearing problem) *The following LP represents a single-period market-clearing problem in an electricity pool. Its output is the optimal generation dispatch in view of the transmission*

[1] Constraint qualifications are needed for ensuring that KKT conditions are necessary for optimality. This is verified, for example, if $\mathbf{g}(\cdot)$ is affine. Another common constraint qualification requires linear independence of the gradients of active inequality constraints and of equality constraints. We refer the reader to specialized books on optimization, for instance [BSS06]

constraints in the network.

$$\underset{\mathbf{p},\boldsymbol{\delta}}{Min.} \sum_{k} c_k p_k \tag{3.7a}$$

$$s.t. \sum_{k\in\Phi_i^{\mathrm{G}}} p_k - \sum_{j\in\Phi_i^{\mathrm{N}}} B_{ij}(\delta_i - \delta_j) = \sum_{m\in\Phi_i^{\mathrm{L}}} l_m - \sum_{q\in\Phi_i^{\mathrm{W}}} w_q \quad : \lambda_i \ , \quad \forall i \ , \tag{3.7b}$$

$$p_k \le P_k \quad : \mu_k \ , \qquad \forall k \ , \tag{3.7c}$$

$$B_{ij}(\delta_i - \delta_j) \le T_{ij} \quad : \sigma_{ij} \ , \qquad \forall i,j \in \Phi_i^{\mathrm{N}} \ , \tag{3.7d}$$

$$p_k \ge 0 \ , \qquad \forall k \ . \tag{3.7e}$$

In model (3.7)*, we index with* k *the offers for production, with* m *the loads, with* q *the renewable power producers, with* i *and* j *the nodes of the transmission network. Each producer bids a set of pairs* (P_k, c_k)*, where the former element is the size of the production block and the latter one the minimum accepted price for the block. Variables* p_k *represent the decision of the market operator on the energy dispatch for each production block. The parameters* l_m *and* w_q *represent the load and the renewable power production.*

The objective function (3.7a) *represents the production cost for the dispatched quantities. Constraints* (3.7c) *and* (3.7e) *enforce that the dispatch is within the limit specified by the bid and nonnegative, respectively. The situation in absence of transmission constraints is sketched in Figure 3.1. In this case, the minimum-cost dispatch is determined by the intersection between the total net demand and the aggregate supply curve.*

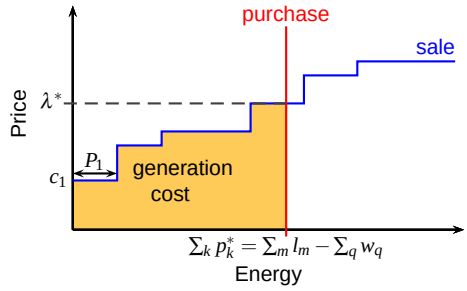

Figure 3.1: Market-clearing in absence of transmission constraints

In order to model the transmission grid, we define the set Φ_i^{G} *of generators located at node* i*. Similarly,* Φ_i^{W} *is the set of renewable power producers at node* i*,* Φ_i^{L} *the set of loads at the same node, while the set* Φ_i^{N} *contains the nodes*

j connected to i by a transmission line. We represent linearly the flow on the interconnection between i and j as the product between the line susceptance B_{ij} and the difference between the voltage angles $\delta_i - \delta_j$ at the ends of the line. Inequality (3.7d) *enforces the transmission limit between nodes i and j, which must be lower than the line capacity, T_{ij}, in absolute value. Finally, equation* (3.7b) *enforces the power balance at each node i, by setting the difference between production and power flowing out of the node equal to the net nodal consumption.*

The dual problem for the network-constrained market-clearing model writes as:

$$\underset{\boldsymbol{\lambda},\boldsymbol{\mu},\boldsymbol{\sigma}}{Max.} \sum_i \left(\sum_{m\in\Phi_i^{\mathrm{L}}} l_m - \sum_{q\in\Phi_i^{\mathrm{W}}} w_q \right) \lambda_i + \sum_k P_k \mu_k + \sum_i \sum_{j\in\Phi_i^{\mathrm{N}}} T_{ij}\sigma_{ij} \tag{3.8a}$$

$$s.t.\ \lambda_{s(k)} + \mu_k \le c_k \quad : p_k\ , \qquad \forall k\ , \tag{3.8b}$$

$$\sum_{j\in\Phi_i^{\mathrm{N}}} B_{ij}(-\lambda_i + \lambda_j + \sigma_{ij} - \sigma_{ji}) = 0 \quad : \delta_i\ , \qquad \forall i\ , \tag{3.8c}$$

$$\mu_k \le 0\ , \forall k\ , \sigma_{ij} \le 0\ , \forall i,j \in \Phi_i^{\mathrm{N}}\ , \tag{3.8d}$$

where $s(k)$ is the index of the node where producer k is located.

The determination of the optimal value of the dual variables $\boldsymbol{\lambda}$ is of particular significance. At optimality, λ_i^* indicates the per unit change in the objective function value of (3.7) *for a demand increase at node i. It should be noticed that this is precisely the definition of marginal price. In a market with nodal pricing, the optimal value of the dual vector $\boldsymbol{\lambda}^*$ provides the price of electricity at each location of the power grid.*

Figure 3.1 illustrates the situation when no congestion occurs in the grid. The marginal price of electricity is equal to the highest-price offer accepted. If demand is increased by a constant, the purchase curve is shifted to the right. This implies an increased cost for the system equal to the size of the shift times the per unit cost of production of the last unit dispatched.

The Lagrangian for the network-constrained market-clearing problem (3.7) *is the following:*

$$\begin{aligned}\mathcal{L} = &\sum_k c_k p_k + \sum_i \lambda_i \left(\sum_{k\in\Phi_i^{\mathrm{G}}} p_k - \sum_{j\in\Phi_i^{\mathrm{N}}} B_{ij}(\delta_i - \delta_j) - \sum_{m\in\Phi_i^{\mathrm{L}}} l_m + \sum_{q\in\Phi_i^{\mathrm{W}}} w_q \right) \\ &+ \sum_k \mu_k (p_k - P_k) + \sum_i \sum_{j\in\Phi_i^{\mathrm{N}}} \sigma_{ij} \left(B_{ij}(\delta_i - \delta_j) - T_{ij} \right) - \sum_k \alpha_k p_k\ .\end{aligned} \tag{3.9}$$

Notice that we assigned the dual variables $\boldsymbol{\alpha} \geq \mathbf{0}$ *to the nonnegativity definition of* $\mathbf{p}$ *in the above derivation of the Lagrangian.*

From (3.9)*, we obtain the following stationarity conditions:*

$$\frac{\partial \mathcal{L}}{\partial p_k} = c_k + \lambda_{s(k)} + \mu_k - \alpha_k = 0 \,, \qquad \forall k \,, \tag{3.10a}$$

$$\frac{\partial \mathcal{L}}{\partial \delta_i} = \sum_{j \in \Phi_i^{\mathrm{N}}} B_{ij}(-\lambda_i + \lambda_j + \sigma_{ij} - \sigma_{ji}) = 0 \,, \qquad \forall i \,. \tag{3.10b}$$

The primal equality constraints

$$\sum_{k \in \Phi_i^{\mathrm{G}}} p_k - \sum_{j \in \Phi_i^{\mathrm{N}}} B_{ij}(\delta_i - \delta_j) = \sum_{m \in \Phi_i^{\mathrm{L}}} l_m - \sum_{q \in \Phi_i^{\mathrm{W}}} w_q \,, \qquad \forall i \,, \tag{3.11}$$

also appear in the set of KKT conditions.

We can write the complementarity conditions in a compact form, including the primal inequality constraints and the nonnegativity definitions of the dual variables, as follows:

$$0 \leq \mu_k \perp p_k - P_k \leq 0 \,, \qquad \forall k \,, \tag{3.12a}$$

$$0 \leq \sigma_{ij} \perp B_{ij}(\delta_i - \delta_j) - T_{ij} \leq 0 \,, \qquad \forall i, j \in \Phi_i^{\mathrm{N}} \,, \tag{3.12b}$$

$$0 \leq \alpha_k \perp -p_k \leq 0 \,, \qquad \forall k \,. \tag{3.12c}$$

Variables $\boldsymbol{\alpha}$ *are in fact slacks. We can get rid of them by recasting conditions* (3.10a) *and* (3.12c) *as follows:*

$$0 \leq p_k \perp c_k + \lambda_{s(k)} + \mu_k \geq 0 \,, \qquad \forall k \,. \tag{3.13}$$

We conclude the example with the following comments.

- *Constraints* (3.11)*, the inequalities on the right-hand side of the* $\perp$ *operator in* (3.12a) *and* (3.12b)*, as well as the ones on the left-hand side of* $\perp$ *in* (3.13) *constitute the definition of the feasible space of the primal problem* (3.7)*.*
- *Equation* (3.10b)*, the inequalities on the left-hand side of* $\perp$ *in* (3.12a) *and* (3.12b)*, as well as the ones on the right-hand side of* $\perp$ *in* (3.13) *correspond to the definition of the feasible space of the dual problem* (3.8)*, after a redefinition of all the dual variables with a change in sign.*

- *The $\perp$ operator implies that either an inequality of the primal (dual) problem holds strictly, i.e., with the equal sign, or the corresponding dual (primal) variable is zero, or both. Such conditions are referred to as complementary slackness.*

3.2 Mathematical Programs with Equilibrium Constraints

A relatively recent area of optimization where KKT conditions are used extensively is the one of Mathematical Programs with Equilibrium Constraints (MPECs). In this section, we consider the use of MPECs to model bilevel programs, i.e., optimization problems constrained by other optimization problems. The reader is referred to [LPR96] and [GCF+12] for an in-depth treatment of the subject.

3.2.1 MPEC Formulation

The general formulation of a bilevel program is the following:

$$\underset{\mathbf{x},\mathbf{y}}{\text{Max.}}\ \theta(\mathbf{x},\mathbf{y}) \tag{3.14a}$$

$$\text{s.t. } \boldsymbol{\phi}(\mathbf{x},\mathbf{y}) \leq \mathbf{0}\ , \tag{3.14b}$$

$$\boldsymbol{\psi}(\mathbf{x},\mathbf{y}) = \mathbf{0}\ , \tag{3.14c}$$

$$\mathbf{y} \in \underset{\mathbf{z}}{\arg\min} \{f(\mathbf{x},\mathbf{z}) \text{ s.t. } \mathbf{g}(\mathbf{x},\mathbf{z}) \leq \mathbf{0}\ , \mathbf{h}(\mathbf{x},\mathbf{z}) = \mathbf{0}\}\ . \tag{3.14d}$$

The fundamental difference with respect to the general optimization problem (3.1) is the enforcement of the optimality conditions (3.14d). This way, we embed a lower-level optimization problem into another, upper-level one. The problems are interdependent, since in general the upper-level objective function (3.14a) and constraints (3.14b) and (3.14c) depend on the lower-level decision variables $\mathbf{y}$. Viceversa, the objective function and the constraints of the lower-level problem (3.14d) depend on the upper-level variable $\mathbf{x}$. It should be remarked that model (3.14) could accommodate several lower-level optimization problems, simply by concatenating multiple optimality conditions of the type of (3.14d).

Under the assumption that KKT conditions are necessary and sufficient for optimality of the lower-level problems, the bilevel program (3.14) can be recast as a single-level optimization problem. This is achieved by replacing the optimality

conditions (3.14d) with the corresponding KKT conditions (3.5). However, the solution of the single-level program is complicated by the fact that KKT conditions are in general nonlinear and non convex, as they involve cross products between variables in (3.5e).

If the feasible space of the lower-level problems is defined by affine equality and inequality constraints, and if the partial derivatives of the objective function with respect to the decision variables are also affine, a linear reformulation of the KKT conditions involving binary variables is available [FM81]. For example, a complementarity condition of the type (3.6) can be recast as follows:

$$g(\mathbf{x}) \leq 0 \,, \tag{3.15a}$$
$$g(\mathbf{x}) \geq -iM_1 \,, \tag{3.15b}$$
$$\mu \geq 0 \,, \tag{3.15c}$$
$$\mu \leq (1-i)M_2 \,, \tag{3.15d}$$
$$i \in \{0,1\} \,. \tag{3.15e}$$

The binary variable i forces at least one between $g(\mathbf{x})$ and μ be equal to 0, as required by (3.5e).

Notice that for the above reformulation to be valid within a bilevel problem of the type (3.14), the constants M_1 and M_2 must be large enough so as not to leave its solution out of the feasible space of (3.15).

If, besides the assumption on the lower-level problems in the paragraph above, $\theta(\cdot)$, $\boldsymbol{\phi}(\cdot)$ and $\boldsymbol{\psi}(\cdot)$ are linear, one can recast the bilevel problem (3.14) as a single-level, Mixed-Integer Linear Program (MILP). Optimization problems of this type can be solved with commercially available software.

Example 3.2 (Offering problem in a market with nodal pricing) *In this example, we consider a simplified case of the trading problem for a renewable power producer in a single market floor, organized as an electricity pool where renewable power enters the supply curve from the left-hand side, by offering production at its zero marginal cost. Without loss of generality, we consider producer 1, located at node $s(1)$. We assume for the sake of simplicity that the maximum renewable power production W_1 is known with certainty at the time of bidding. However, the producer has the possibility of withdrawing production from the market in order to exercise market power.*

Under these assumptions, the optimal offer w_1^* solves the following bilevel problem. It should be noticed that in the formulation below, we employ the definition of the dual variables in (3.8), which requires a change in sign as compared to the standard derivation of the KKT conditions in Example 3.1. The former

formulation is preferred, because nodal prices are equal to the dual variables λ_i. Instead, if the definition of the dual variables as in the KKT formulation were employed instead, prices would be equal to $-\lambda_i$.

$$\underset{\substack{w_1,\mathbf{p},\boldsymbol{\delta},\\ \boldsymbol{\lambda},\boldsymbol{\mu},\boldsymbol{\sigma}}}{Max.} \quad \lambda_{s(1)} w_1 \tag{3.16a}$$

$$s.t. \quad 0 \leq w_1 \leq W_1 \ , \tag{3.16b}$$

$$\sum_{k\in\Phi_i^{\mathrm{G}}} p_k - \sum_{j\in\Phi_i^{\mathrm{N}}} B_{ij}(\delta_i - \delta_j) = \sum_{m\in\Phi_i^{\mathrm{L}}} l_m - \sum_{q\in\Phi_i^{\mathrm{W}}} w_q \ , \quad \forall i \ , \tag{3.16c}$$

$$p_k - P_k \leq 0 \ , \qquad \forall k \ , \tag{3.16d}$$

$$B_{ij}(\delta_i - \delta_j) - T_{ij} \leq 0 \ , \qquad \forall i,j \in \Phi_i^{\mathrm{N}} \ , \tag{3.16e}$$

$$p_k \geq 0 \ , \qquad \forall k \ , \tag{3.16f}$$

$$c_k - \lambda_{s(k)} - \mu_k \geq 0 \ , \qquad \forall k \ , \tag{3.16g}$$

$$\sum_{j\in\Phi_i^{\mathrm{N}}} B_{ij}(-\lambda_i + \lambda_j + \sigma_{ij} - \sigma_{ji}) = 0 \ , \qquad \forall i,j \in \Phi_i^{\mathrm{N}} \ , \tag{3.16h}$$

$$\mu_k \leq 0 \ , \forall k \ , \sigma_{ij} \leq 0 \ , \forall i,j \in \Phi_i^{\mathrm{N}} \ , \tag{3.16i}$$

$$p_k - P_k \geq -z_k^1 M \ , \qquad \forall k \ , \tag{3.16j}$$

$$\mu_k \geq -(1 - z_k^1) M \ , \qquad \forall k \ , \tag{3.16k}$$

$$B_{ij}(\delta_i - \delta_j) - T_{ij} \geq -z_{ij}^2 M \ , \qquad \forall i,j \in \Phi_i^{\mathrm{N}} \ , \tag{3.16l}$$

$$\sigma_{ij} \geq -(1 - z_{ij}^2) M \ , \qquad \forall i,j \in \Phi_i^{\mathrm{N}} \ , \tag{3.16m}$$

$$c_k - \lambda_{s(k)} - \mu_k \leq z_k^3 M \ , \qquad \forall k \ , \tag{3.16n}$$

$$p_k \leq (1 - z_k^3) M \ , \qquad \forall k \ , \tag{3.16o}$$

$$z_k^1, z_k^3 \in \{0,1\} \ , \forall k \ , z_{ij}^2 \in \{0,1\} \ , \forall i,j \in \Phi_i^{\mathrm{N}} \ . \tag{3.16p}$$

The objective function (3.16a) *is the profit of renewable power producer 1, given by the multiplication of the relevant nodal price $\lambda_{s(1)}$ with the offer w_1. Constraint* (3.16b) *ensures that the offer is a feasible production value. Constraints* (3.16c)–(3.16f) *define the feasible space of the primal problem* (3.7)*. Furthermore, the constraints of the dual problem in Example* (3.8) *are included as* (3.16g)–(3.16i)*. Finally, constraints* (3.16j)–(3.16p) *comprise the linearization of the complementarity conditions.*

We remark that the model above is nonlinear, owing to the bilinear product between $\lambda_{s(1)}$ and w_1 in the objective function.

Trading problems formulated as MPECs are often nonlinear as a result of the product between primal and dual variables, where the former are offers, and the latter prices. In the following example, we show how in some cases the problem can be linearized by making use of the strong duality results in Theorem 3.2.

Reformulations of this type are used in Papers D, F and H.

Example 3.3 (Linearization of the objective function via strong duality) *Let us consider the objective functions of the primal and of the dual versions of the market-clearing problem* (3.7) *and* (3.8)*, respectively, presented in Example 3.1. Owing to the strong duality theorem, the two objective function values are equal at optimality, i.e.,*

$$\sum_k c_k p_k = \sum_i \left(\sum_{m \in \Phi_i^{\mathrm{L}}} l_m - \sum_{q \in \Phi_i^{\mathrm{W}}} w_q \right) \lambda_i + \sum_k P_k \mu_k + \sum_i \sum_{j \in \Phi_i^{\mathrm{N}}} T_{ij} \sigma_{ij} \ . \quad (3.17)$$

Solving the previous equation for $\lambda_{s(1)} w_1$ *yields:*

$$\lambda_{s(1)} w_1 = \sum_i \left(\sum_{m \in \Phi_i^{\mathrm{L}}} l_m - \sum_{q \in \Phi_i^{\mathrm{W}} \setminus 1} w_q \right) \lambda_i + \sum_k P_k \mu_k + \sum_i \sum_{j \in \Phi_i^{\mathrm{N}}} T_{ij} \sigma_{ij} - \sum_k c_k p_k \ . \quad (3.18)$$

The expression on the right-hand side of (3.18) *is linear, since* $l_m, \forall m$ *and* $w_q, q \neq 1$ *are constant parameters in the optimization problem of renewable power producer 1. Therefore, problem* (3.16) *can be reformulated by replacing the objective function* (3.16a) *with the right-hand side of* (3.18)*. The resulting problem is a MILP.*

3.2.2 MPEC Applications

Bilevel programs and their reformulation as MILPs are used extensively in this dissertation.

- In Paper D, we model the trading problem of a wind power producer that is a price-maker in the balancing market as a bilevel program. The lower-level problem represents the clearing of an auction-based balancing market. The upper-level problem is the one of a wind power producer optimizing its offer curve in order to maximize revenues from the day-ahead and the balancing markets. Example 3.2 presents a simplified formulation similar to the one in Paper D.
- Paper E models as an MPEC the hierarchical relationship between a virtual power plant operator and the flexible consumers in a demand response framework. In the upper-level problem, the virtual power plant's operator

sets the consumer price. The lower-level problem is the one of a consumer who decides on the optimal consumption schedule on the basis of a utility, where the electricity cost is weighted by the comfort resulting from power consumption.

- A similar approach is used in Paper F, where the price-setting entity in the upper-level problem is a retailer whose objective is the maximization of the profits.

- Paper G considers a two-stage market-clearing problem accounting for the projected costs of the day-ahead dispatch on the real-time system operation in a stochastic programming fashion, see also Section 3.3. The clearing conditions of a traditional day-ahead market auction are then imposed, thus rendering the problem a bilevel one.

- In Paper H, we jointly consider the day-ahead dispatch and reserve determination in a network-constrained auction in a robust optimization framework. As Section 3.4 clarifies, robust optimization aims at determining a solution that is feasible for any realization of uncertain parameters, and optimal in the worst-case instance. In mathematical terms, this translates into multilevel problems of the *min-max* type, which can be cast as MPECs.

3.3 Stochastic Programming

In practice, it is seldom the case that all the parameters of an optimization problem are known with certainty at the time of making a decision. This is particularly true of electricity markets including renewable power generation facilities. Indeed, owing to the structure of the markets described in Chapter 2, some decisions have to be made in advance, e.g., the day-ahead trading decisions for a producer or scheduling decisions for a market or system operator. This section introduces stochastic programming, which is one of the most established frameworks for optimization under uncertainty.

3.3.1 Formulation of a Stochastic Programming Problem

Under the assumption that uncertain parameters take values in a discrete probability space, which is typical of stochastic programming, a two-stage stochastic

(linear) program with recourse writes as:

$$\underset{\mathbf{x},\mathbf{y}_\omega}{\text{Min.}}\ \mathbf{c}^T\mathbf{x} + \sum_\omega \pi_\omega \times \mathbf{q}_\omega^T\mathbf{y}_\omega \tag{3.19a}$$

$$\text{s.t. } \mathbf{A}\mathbf{x} = \mathbf{b}\ , \tag{3.19b}$$

$$\mathbf{T}_\omega\mathbf{x} + \mathbf{W}_\omega\mathbf{y}_\omega = \mathbf{h}_\omega\ , \qquad \forall\omega\ . \tag{3.19c}$$

In model (3.19), the parameters $\mathbf{q}_\omega$, $\mathbf{T}_\omega$, $\mathbf{W}_\omega$ and $\mathbf{h}_\omega$ are uncertain. Model (3.19) accommodates for a discrete number of realizations or scenarios ω of the uncertain parameters, each of which occurs with probability π_ω.

The decision variable $\mathbf{x}$ represents the vector of first-stage or *here and now* decisions, which are made before the realization of the uncertainty. Variables $\mathbf{y}_\omega$ are second-stage or *recourse* decisions, which adapt depending on the realization of the uncertainty. Indeed, the subscript ω indicates that there is a set of such variables for each realization of the uncertain parameters.

Constraints (3.19b) involve only first-stage variables, while (3.19c) link them with the recourse decisions. Naturally, there is one set of constraints of the latter type for each realization of the uncertainty. First-stage variables have associated cost $\mathbf{c}^T\mathbf{x}$, while recourse variables have cost $\mathbf{q}_\omega^T\mathbf{y}_\omega$. The objective function (3.19a) represents therefore the expected value of the cost.

Example 3.4 (Two-stage network-constrained market-clearing) *As an example of the use of stochastic programming in relation with electricity market modeling, we present a two-stage market-clearing model where the day-ahead dispatch represents the first-stage decision, while the recourse decision is the re-dispatch in the balancing market. Such a model was originally presented in a similar form in [PZP10], and constitutes the basis for the model presented in Paper G.*

$$\underset{\mathbf{p},\boldsymbol{\delta},\mathbf{r}_\omega^{\mathrm{U}},\mathbf{r}_\omega^{\mathrm{D}},\boldsymbol{\delta}_\omega^{\mathrm{B}}}{\textit{Min.}}\ \sum_k c_k p_k + \sum_\omega \pi_\omega \sum_k \left(c_k^{\mathrm{U}} r_{k\omega}^{\mathrm{U}} - c_k^{\mathrm{D}} r_{k\omega}^{\mathrm{D}}\right) \tag{3.20a}$$

$$\textit{s.t.} \sum_{k\in\Phi_i^{\mathrm{G}}} p_k - \sum_{j\in\Phi_i^{\mathrm{N}}} B_{ij}(\delta_i - \delta_j) = \sum_{m\in\Phi_i^{\mathrm{L}}} \widehat{l}_m - \sum_{q\in\Phi_i^{\mathrm{W}}} \widehat{w}_q\ , \quad \forall i\ , \tag{3.20b}$$

$$p_k \le P_k\ , \qquad \forall k\ , \tag{3.20c}$$

$$B_{ij}(\delta_i - \delta_j) \le T_{ij}\ , \qquad \forall i,j \in \Phi_i^{\mathrm{N}}\ , \tag{3.20d}$$

$$p_k \ge 0\ , \qquad \forall k\ , \tag{3.20e}$$

$$\begin{aligned}
&\sum_{k\in\Phi_i^{\mathrm{G}}} \left(r_{k\omega}^{\mathrm{U}} - r_{k\omega}^{\mathrm{D}}\right) - \sum_{j\in\Phi_i^{\mathrm{N}}} B_{ij}\left(\delta_{i\omega}^{\mathrm{B}} - \delta_i - \delta_{j\omega}^{\mathrm{B}} + \delta_j\right) \\
&= \sum_{m\in\Phi_i^{\mathrm{L}}} \left(l_{m\omega} - \widehat{l}_m\right) - \sum_{q\in\Phi_i^{\mathrm{W}}} \left(w_{q\omega} - \widehat{w}_q\right) , \qquad \forall i, \omega , \qquad (3.20\mathrm{f}) \\
&p_k + r_{k\omega}^{\mathrm{U}} \leq P_k , \qquad \forall k, \omega , \qquad (3.20\mathrm{g}) \\
&p_k - r_{k\omega}^{\mathrm{U}} \geq 0 , \qquad \forall k, \omega , \qquad (3.20\mathrm{h}) \\
&B_{ij}(\delta_{i\omega}^{\mathrm{B}} - \delta_{j\omega}^{\mathrm{B}}) \leq T_{ij} , \qquad \forall i, j \in \Phi_i^{\mathrm{N}}, \omega , \qquad (3.20\mathrm{i}) \\
&r_{k\omega}^{\mathrm{U}} \geq 0, r_{k\omega}^{\mathrm{D}} \geq 0 , \qquad \forall k, \omega . \qquad (3.20\mathrm{j})
\end{aligned}$$

The first term in the objective function (3.20a) *represents the cost of the day-ahead dispatch. This decision is constrained by* (3.20b)–(3.20e)*, which correspond to the constraints in model* (3.7)*. We remark that the load and renewable power production on the right-hand side of the day-ahead balance equation are forecasts of stochastic values. We indicate this with the symbol* $\widehat{\ }$ *over the parameters.*

Variables $r_{k\omega}^{\mathrm{U}}$ *and* $r_{k\omega}^{\mathrm{D}}$ *represent the redispatch (production increase and decrease, respectively) of producer* k *in scenario* ω *at the balancing stage. These variables are adaptable to the realization of the stochastic load and renewable power production, and are therefore recourse decisions. The second term in the objective function* (3.20a) *represents the expected cost, or benefit in the case of production decrease, of redispatch at the balancing stage.*

The voltage angle at node i *in scenario* ω *at the balancing stage is indicated with* $\delta_{i\omega}^{\mathrm{B}}$*. Furthermore,* $l_{m\omega}$ *and* $w_{q\omega}$ *are the realizations of load and renewable power production. Hence, constraint* (3.20f) *enforces, along with* (3.20b)*, the power balance condition at the balancing stage. Constraints* (3.20g) *and* (3.20h) *ensure a feasible redispatch for each production block* k*. Transmission constraints at the balancing stage are enforced by* (3.20i)*. Constraints* (3.20j) *define nonnegative variables.*

The framework of stochastic programming is naturally extendable to nonlinear programs with an appropriate reformulation of the linear terms and constraints in (3.19) into the more general nonlinear case. A particular instance of interest for this dissertation is that of stochastic MPECs, which is relevant when one or more parameters of the lower-level problem is subject to uncertainty. In this case, then, several lower-level problems should be considered, i.e., one per scenario. The general formulation (3.14) can be extended in order to account

for stochastic parameters as follows:

$$\underset{\mathbf{x}^1,\mathbf{x}^2_\omega,\mathbf{y}_\omega}{\text{Max.}} \ \mathbb{E}\left\{\theta_\omega(\mathbf{x}^1,\mathbf{x}^2_\omega,\mathbf{y}_\omega)\right\} \tag{3.21a}$$

$$\text{s.t. } \boldsymbol{\phi}_\omega(\mathbf{x}^1,\mathbf{x}^2_\omega,\mathbf{y}_\omega) \leq \mathbf{0}\,, \qquad \forall\omega\,, \tag{3.21b}$$

$$\boldsymbol{\psi}_\omega(\mathbf{x}^1,\mathbf{x}^2_\omega,\mathbf{y}_\omega) = \mathbf{0}\,, \qquad \forall\omega\,, \tag{3.21c}$$

$$\mathbf{y}_\omega \in \arg\min_{\mathbf{z}} \left\{ f_\omega(\mathbf{x}^1,\mathbf{x}^2_\omega,\mathbf{z}) \text{ s.t. } \mathbf{g}_\omega(\mathbf{x}^1,\mathbf{x}^2_\omega,\mathbf{z}) \leq \mathbf{0}\,, \mathbf{h}_\omega(\mathbf{x}^1,\mathbf{x}^2_\omega,\mathbf{z}) = \mathbf{0} \right\}\,, \quad \forall\omega\,, \tag{3.21d}$$

where $\mathbf{x}^1$ is the set of upper-level first-stage decision variables, $\mathbf{x}^2_\omega$ the upper-level recourse variables and $\mathbf{y}_\omega$ the decision variables for each scenario ω. It should be remarked that there is one lower-level problem (3.21d) for each scenario, which implies that one set of KKT conditions should be included per scenario.

The reader is referred to [KW94, BL11] for thorough introductions to stochastic programming. Further details on stochastic MPECs are available in [GCF+12].

3.3.2 Applications of Stochastic Programming

Several papers presented in this dissertation make use of stochastic programming models.

- The bilevel model presented in Paper D, which determines the optimal trading strategy of a wind power producer that is a price-maker in the balancing market, is in fact a stochastic MPEC. Indeed, the market-clearing problem at the balancing stage is dependent on the realization of wind power production and system deviation, both of which are stochastic. We model this uncertainty by including the equilibrium conditions of a market-clearing problem for each scenario for these two variables.
- Paper E presents an MPEC where the upper-level problem consists in the minimization of the imbalance for a virtual power plant. The latter depends on the stochastic amount of wind power production, which is modeled by employing scenarios. The problem is formulated in a stochastic programming fashion, aiming at the minimization of the expected imbalance over the scenario set.
- The model in Paper F is a stochastic MPEC. Indeed, the lower-level problem for the consumers involves the optimization of a utility that depends on weather-related variables. Therefore, multiple lower-level problems are considered.

- Paper G presents a stochastic programming model for clearing of day-ahead markets accounting for the cost of actions at the balancing stage (recourse decisions), with the addition of further equilibrium constraints. The basic two-stage market-clearing model, without equilibrium constraints, is introduced in Example 3.4 as an instance of the use of stochastic programming in relation with electricity market modeling. In the case of Paper G, the lower-level problem is deterministic, since the day-ahead market-clearing only depends on the bids submitted by the market players. Therefore, there is only one instance of this problem. On the contrary, the upper-level problem considers the projected cost of the day-ahead decision at the balancing stage, which is minimized in expectation in a stochastic programming fashion.

- Paper C is also related to stochastic programming since it deals with the trading problem of a price-taker wind power producer. However, scenarios are not employed in this work, as there exists an analytical solution to the problem. In practice, the full probability distribution of wind power production is used to determine the optimal solution. A stochastic programming version of the problem would approximate the optimal result obtained.

3.4 Robust Adaptable Optimization

An alternative framework to stochastic programming when dealing with problems of optimization under uncertainty is robust optimization, which is the focus of this section.

3.4.1 Formulation of a Robust Adaptable Optimization Problem

In its original formulation, robust optimization aims at determining a solution to a mathematical program that is feasible under any realization of the stochastic parameters within an uncertainty set and/or optimal in their worst-case realization [BBC11].

In this work, we consider the framework of *robust adaptable optimization*, which is the natural counterpart of stochastic programming with recourse in the framework of robust optimization. A linear problem of robust adaptable optimization

writes as follows:

$$\underset{\mathbf{x}}{\text{Min.}}\ \mathbf{c}^T\mathbf{x} + \underset{\mathbf{q},\mathbf{T},\mathbf{W},\mathbf{h}}{\text{Max.}}\ \underset{\mathbf{y}}{\text{Min.}}\ \mathbf{q}^T\mathbf{y} \tag{3.22a}$$

$$\text{s.t. } \mathbf{T}\mathbf{x} + \mathbf{W}\mathbf{y} = \mathbf{h}\ , \tag{3.22b}$$

$$\text{s.t. } (\mathbf{q},\mathbf{T},\mathbf{W},\mathbf{h}) \in \mathcal{U}\ , \tag{3.22c}$$

$$\text{s.t. } \mathbf{A}\mathbf{x} = \mathbf{b}\ . \tag{3.22d}$$

The multilevel structure of problem (3.22) is typical of problems of robust optimization. The decision variables of the upper-level minimization problem are a set of first-stage decisions, $\mathbf{x}$. Just as in the case of stochastic programming, such variables cannot adapt to the realization of the stochastic parameters $\mathbf{q}$, $\mathbf{T}$, $\mathbf{W}$ and $\mathbf{h}$. The lower-level problem aims at the minimization of the cost of recourse $\mathbf{q}^T\mathbf{y}$, provided that the feasibility constraints (3.22b) are satisfied under the current realization of the uncertainty. It should be noticed, though, that differently from the case of stochastic programming, where there is a set of recourse decisions per scenario, there is only one such set in robust adaptable optimization. This represents the optimal recourse decision in response to the worst-case realization, i.e., the realization of the uncertain parameters $(\mathbf{q},\mathbf{T},\mathbf{W},\mathbf{h})$ in the set $\mathcal{U}$ that yields maximum cost of recourse. This worst-case realization is enforced by the mid-level maximization problem.

Naturally, the choice of a meaningful uncertainty set $\mathcal{U}$ is just as important to robust optimization as the generation of realistic scenarios is to stochastic programming. On the other hand, the structural complexity of robust adaptable optimization problems hinders the use of sophisticated uncertainty sets, as multilevel problems of the type of (3.22) become quickly intractable. In practice polyhedral or elliptical uncertainty sets are employed in the literature on the subject [BBC11].

In the following example we formulate the joint determination of the day-ahead dispatch and reserve as a robust optimization problem. This topic is the focus of Paper H, which we refer to for further detail.

Example 3.5 (Robust day-ahead dispatch and reserve determination) *Let us consider the problem of jointly determining the day-ahead dispatch* $\mathbf{p}$ *and the reserves* $\mathbf{R}^{\mathrm{U}}$ *for up-regulation and* $\mathbf{R}^{\mathrm{D}}$ *for down-regulation. Indicating with* $\mathcal{Q}(\cdot)$ *the cost of the redispatch decision in the worst-case realization of the uncertainty, which is a function of the first-stage decision, the problem writes*

as follows:

$$\underset{\mathbf{p},\mathbf{R}^{\mathrm{U}},\mathbf{R}^{\mathrm{D}},\boldsymbol{\delta}}{\mathit{Min.}} \sum_{k} \left(c_k p_k + C_k^{\mathrm{U}} R_k^{\mathrm{U}} + C_k^{\mathrm{D}} R_k^{\mathrm{D}}\right) + \mathcal{Q}\left(\mathbf{p}, \mathbf{R}^{\mathrm{U}}, \mathbf{R}^{\mathrm{D}}, \boldsymbol{\delta}\right) \tag{3.23a}$$

$$s.t. \sum_{k\in\Phi_i^{\mathrm{G}}} p_k - \sum_{j\in\Phi_i^{\mathrm{N}}} B_{ij}(\delta_i - \delta_j) = \sum_{m\in\Phi_i^{\mathrm{L}}} \widehat{l}_m - \sum_{q\in\Phi_i^{\mathrm{W}}} \widehat{w}_q \;, \quad \forall i \;, \tag{3.23b}$$

$$p_k + R_k^{\mathrm{U}} \leq P_k \;, \qquad \forall k \;, \tag{3.23c}$$

$$p_k - R_k^{\mathrm{D}} \geq 0 \;, \qquad \forall k \;, \tag{3.23d}$$

$$B_{ij}(\delta_i - \delta_j) \leq T_{ij} \;, \qquad \forall i, j \in \Phi_i^{\mathrm{N}} \;, \tag{3.23e}$$

$$R_k^{\mathrm{U}} \geq 0 \;, R_k^{\mathrm{D}} \geq 0 \;, \qquad \forall k \;. \tag{3.23f}$$

The per unit cost associated with reserve are indicated in the objective function (3.23a) *with* C_k^{U} *and* C_k^{D} *for up- and down-regulation, respectively. The production constraints are updated to* (3.23c) *and* (3.23d)*, so as to guarantee that the producer can actually deliver the contracted amount of reserve if necessary.*

The function $\mathcal{Q}\left(\mathbf{p}, \mathbf{R}^{\mathrm{U}}, \mathbf{R}^{\mathrm{D}}, \boldsymbol{\delta}\right)$ *embeds the mid- and lower-level problems, which is explicit in the general formulation* (3.22) *for a robust adaptable optimization problem. This function can be expressed in extended form as follows:*

$$\begin{aligned}
&\mathcal{Q}\big(\mathbf{p}, \mathbf{R}^{\mathrm{U}}, \mathbf{R}^{\mathrm{D}}, \boldsymbol{\delta}\big) \\
&= \underset{(\mathbf{l},\mathbf{w})\in\mathcal{U}}{\mathit{Max.}} \; \underset{\mathbf{r}^{\mathrm{U}},\mathbf{r}^{\mathrm{D}},\boldsymbol{\delta}^{\mathrm{B}}}{\mathit{Min.}} \sum_{k} \left(c_k^{\mathrm{U}} r_k^{\mathrm{U}} - c_k^{\mathrm{D}} r_k^{\mathrm{D}}\right) && \text{(3.24a)} \\
&\qquad s.t. \sum_{k\in\Phi_i^{\mathrm{G}}} \left(r_k^{\mathrm{U}} - r_k^{\mathrm{D}}\right) - \sum_{j\in\Phi_i^{\mathrm{N}}} B_{ij}\left(\delta_i^{\mathrm{B}} - \delta_i - \delta_j^{\mathrm{B}} + \delta_j\right) \\
&\qquad\qquad = \sum_{m\in\Phi_i^{\mathrm{L}}} \left(l_m - \widehat{l}_m\right) - \sum_{q\in\Phi_i^{\mathrm{W}}} \left(w_q - \widehat{w}_q\right) \;, \;\; \forall i \;, && \text{(3.24b)} \\
&\qquad\qquad r_k^{\mathrm{U}} \leq R_k^{\mathrm{U}} \;, \qquad \forall k \;, && \text{(3.24c)} \\
&\qquad\qquad r_k^{\mathrm{D}} \leq R_k^{\mathrm{D}} \;, \qquad \forall k \;, && \text{(3.24d)} \\
&\qquad\qquad B_{ij}(\delta_i^{\mathrm{B}} - \delta_j^{\mathrm{B}}) \leq T_{ij} \;, \qquad \forall i, j \in \Phi_i^{\mathrm{N}} \;, && \text{(3.24e)} \\
&\qquad\qquad r_k^{\mathrm{U}} \geq 0, r_k^{\mathrm{D}} \geq 0 \;, \qquad \forall k \;. && \text{(3.24f)}
\end{aligned}$$

The max-min *problem in* (3.24a) *ensures that the redispatch cost is minimized in the worst-case realization of load and renewable power production in the uncertainty set* $\mathcal{U}$*. Constraints* (3.24c) *and* (3.24d) *enforce that the redispatch is no greater than the amount of reserve contracted at the day-ahead stage.*

3.4.2 Applications of Robust Adaptable Optimization

The only application of robust adaptable optimization in this dissertation is in Paper H. The problem considered in this work is very similar to the one formulated in Example 3.5. The aim is the minimization of the total cost in the day-ahead and balancing markets in the worst-case realization of the uncertain wind power production at different nodes of the network. To solve the resulting three-level *min-max-min* problem, we employ a cutting-plane algorithm [KJ60], which converges to the optimal solution in a finite number of steps.

Chapter 4

Application Results

In this chapter, we gather the highlights of the research presented in Part II of this dissertation. The structure of the chapter is the following.

In Section 4.1, we consider the problem of determining optimal trading strategies for wind power producers. Firstly, the price-taker case is addressed in Section 4.1.1, which discusses results from a simulation based on real data and forecasts for Nord Pool. This work is fully presented in Paper C. Then in Section 4.1.2, we address the trading problem for a producer with the capability of altering the balancing market outcome with its bidding strategy, and summarize the results of the case study presented in Paper D.

Section 4.2 considers a market environment that includes end consumers responsive to dynamic pricing. In Section 4.2.1, we look at the operation problem of a virtual power plant that consists of a wind power production facility and flexible demand, which is controlled by means of a price signal. Then, we consider the joint bidding and pricing model for a retailer trading with an infinite electricity market and providing electricity to flexible consumers in Section 4.2.2. The highlights we present in this section summarize the results of the case studies in Papers E and F.

Finally, Section 4.3 is dedicated to optimal market dispatch with stochastic renewable sources. In Section 4.3.1, we consider the stochastic-programming-

based model to clear the day-ahead market, accounting for the projected costs of regulation in the balancing market, presented in Paper G. Then in Section 4.3.2, we consider the robust optimization model in Paper H, aimed at determining the day-ahead dispatch and the purchase of reserves. Throughout Section 4.3, we present the highlights of the simulations included in Papers G and H, which are based on the IEEE Reliability Test-System [GWA+99].

4.1 Trading Strategies for Stochastic Power Producers

Papers C and D address the problem of optimal trading for a wind power producer in short-term electricity markets. While the case of wind power is specifically addressed, most of the conclusions could easily be extended to other renewables that are stochastic and non-dispatchable, such as solar and wave power. When considering this problem, we make the following two assumptions.

- There is no interdependence between offers for different market periods. This implies that the optimal offer for each time period can be determined independently from the others by making use of a static, single-period model.
- The intra-day market is discarded from the analysis in view of its very low liquidity, as discussed in Section 2.2.2.

Under these two simplifications, we first discuss the results in a price-taker setting in Section 4.1.1. Then, we consider the price-maker case in Section 4.1.2.

4.1.1 Trading Stochastic Production as a Price-Taker

When stochastic power producers offer in short-term electricity markets, they very rarely trade in a single market floor. Being their production uncertain, they most likely need to take corrective measures in the balancing market after having traded in the day-ahead market, so as to align their contracts for delivery with their actual output.

In a price-taker setting, the main driver in the determination of the optimal offer is the difference between the day-ahead and the balancing market prices.

Actually, since these prices are stochastic, we are interested in the expected value of their difference. For example, in a market employing the one-price system for imbalances described in Section 2.2.3, the producer's problem of bidding as a price-taker reduces to a rather trivial arbitrage problem. Indeed, if the producer expects a higher price in the balancing market than in the day-ahead market, then it should not offer at all in the day-ahead market, and sell its whole production in the balancing market. On the other hand, if a lower balancing market price is expected as compared to the day-ahead one, the producer should offer as much as possible in the day-ahead market. Then, it would eventually buy back the electricity it is not able to produce from the balancing market at a lower price.

In Paper C, we consider a two-price balancing market, which constitutes a more interesting case than the one-price system in a price-taker framework. We assume that the price difference between the day-ahead and the balancing market is uncorrelated with the output of the producer, which is reasonable since the producer is a price-taker. Under the assumptions above, it is shown that the optimal day-ahead offer is

$$\widetilde{W}_k^* = F_{W_k}^{-1}\left(\frac{\left|\widehat{\psi}_k^{(\downarrow)}\right|}{\widehat{\psi}_k^{(\uparrow)} + \left|\widehat{\psi}_k^{(\downarrow)}\right|}\right) , \tag{4.1}$$

where $F_{W_k}^{-1}$ is the quantile function for the distribution of stochastic power production, and $\widehat{\psi}_k^{(\downarrow)}$ ($\widehat{\psi}_k^{(\uparrow)}$) is the expectation of the difference between the down (up)-regulation price and the day-ahead price.

In the case study presented in Paper C, we test the strategy (4.1) for a wind power producer in a realistic setting simulating the functioning of the Nord Pool market over a 10 month period. We consider actual data for prices in the period between March and the end of the year 2008. Furthermore, we employ probabilistic forecasts for wind power production, needed to model the quantile function in (4.1), issued according to the method in [PK10]. As far as the market prices are concerned, forecasts from [Jón12] are used.

As a benchmark to test the performance of the optimal offer (4.1), we consider a strategy that is traditionally used by wind power producers participating in the day-ahead market: offering the conditional expectation of the distribution of wind power production. Figure 4.1 illustrates the increase in cumulative revenues per installed MW, as compared to offering the conditional mean over the period considered in the case study. The starred solid line indicates the offer in (4.1). As one can see, this strategy yields a higher revenue compared to the case where the producer offers the conditional mean. The improvement totalls about €100 per MW of installed capacity in the 10 months considered in the

test case.

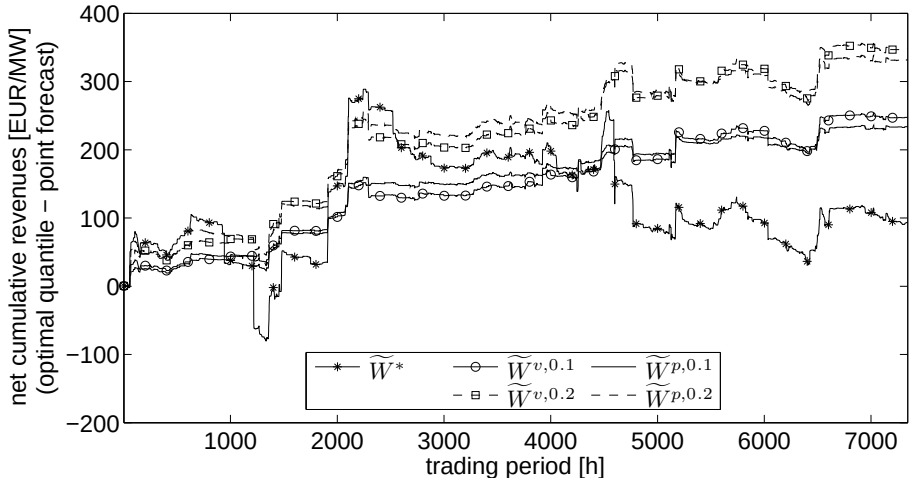

Figure 4.1: Increase in net cumulative revenues for a price-taker producer compared to offering the conditional mean (point forecast) with the strategies proposed in Paper C

Another result in Figure 4.1 that is worth mentioning is that the strategy (4.1) is exposed to the risk of significant losses in single trading periods, which results in the vertical drops of the starred solid line in the figure. As discussed in detail in Paper C, this is due to the price forecasts being uncorrect in those trading periods. This causes the producer, accordingly to (4.1), to take a "wrong" position (either long or short) with a large exposure, e.g., by offering close to zero or to the nominal capacity at the day-ahead market.

To overcome this problem, we propose that the offer (4.1) be constrained so as to limit its deviation from the conditional mean forecast. It should be remarked that the conditional mean forecast is a risk-averse bid by definition, as it minimizes the expected squared deviation of wind power production. We propose two different constraining strategies. In the first one, the offer (4.1) is bounded within a band centered around the conditional mean, and whose diameter is defined as a percentage of the conditional mean itself. In the second constraining strategy, we impose limits in the probability space, by allowing the quantile in (4.1) to deviate by at most 0.1 or 0.2 from the quantile corresponding to the predicted conditional mean. In Figure 4.1, the cumulative improvement in revenues is illustrated with lines with circular and square markers for the former constraining strategy, and with lines without markers for the latter one. Furthermore, we employ solid lines for tighter constraints and dashed lines for

looser ones. As one can see, constraining the bid about the conditional mean reduces the risk of losses stemming from single trading periods, resulting in smoother revenue improvements in the figure. Furthermore, such constrained strategies are not only risk-averse, but they also yield better performance than the strategy (4.1) in the period considered, by reducing the impact of biases in the forecasts.

Further financial results for the producer are included in Table 4.1. The imbalance costs in the second column refer to the opportunity costs of a strategy, compared to bidding with perfect information on the actual realization of wind power production. As one can see, strategy (4.1) reduces the imbalance costs by over 2%. However, this strategy is outperformed by the constrained strategies, which further cut imbalance costs up to roughly 6% with tighter constraints and 8% with looser constraints.

A different view of the strategies presented above is given in Table 4.2, which illustrates their impact on the wind power producer's imbalance. The total producer's deviation in the first column is broken down into two parts. The first one, which appears in the second column in the table, represents deviations that are traded at the day-ahead price in the balancing market. The second part are the imbalances that are traded at the balancing market price. These imbalances are included in the third column, whose header is "penalty", since the producer is worse off with the balancing market price than with the day-ahead one. As discussed in Section 2.2.3, the former type of imbalances are beneficial to the system, since contrarily to the ones of the latter type, they help it restore balance between production and consumption. As one can notice, strategy (4.1) and the strategies employing looser constraints increase the total imbalance of the producer. However, none of the constrained strategies increase significantly the imbalance in the penalized direction as the strategy in (4.1) does. This is another practical reason for preferring a constrained strategy, as system operators often monitor the offers of wind power producers to ensure that their imbalance be not too large.

4.1.2 Trading as a Price-Maker in the Balancing Market

In Paper D, we abandon the price-taker assumption and consider a wind power producer whose offering strategy impacts prices in the balancing market. To this end, we develop a bilevel model based on stochastic MPECs, see Sections 3.2 and 3.3. The upper-level problem in this model represents the offering problem of a wind power producer, while the lower-level one is the balancing-market clearing, which includes stochastic parameters. In this paper, we consider a one-price system for pricing imbalances. This results in a setup similar to the

Strategy	Net revenue per installed MW (€/MW)	Imbalance cost per installed MW (€/MW)	Imbalance cost reduction (%)
Conditional mean	94436.40	4076.51	0.00
Equation (4.1)	94529.96	3982.95	2.30
Constrained (±10% value)	94684.18	3828.74	6.08
Constrained (±20% value)	94784.27	3728.64	8.53
Constrained (±10% probability)	94670.78	3842.13	5.75
Constrained (±20% probability)	94768.55	3744.37	8.15

Table 4.1: Economic results for a price-taker wind power producer in the test-case in Paper C

Strategy	Energy imbalance (h)		
	Total	Day-Ahead price	Penalty
Conditional mean	484.92	277.71	207.21
Equation (4.1)	755.29	498.66	256.62
Constrained (±10% value)	495.91	286.72	209.19
Constrained (±20% value)	519.70	304.85	214.85
Constrained (±10% probability)	488.94	281.93	207.00
Constrained (±20% probability)	514.62	301.74	212.87

Table 4.2: Energy imbalance for a price-taker wind power producer in the test-case in Paper C. Values in hours of operation at nominal capacity

one in Example 3.2, although the lower-level problem models the clearing of the balancing market rather than the day-ahead one. Furthermore, the upper-level problem is extended by allowing the possibility of offering price-quantity curves rather than single quantities.

In order to evaluate the performance of the optimal strategy, we employ three alternative offers for benchmarking, namely, the conditional mean and median forecasts, as well as the zero offer. We remark that, as briefly explained in the previous section, the optimal day-ahead market bid for a price-taker stochastic power producer in a one-price system is either zero or the nominal capacity. In particular, the optimal offer is zero if the expectation of the difference between the day-ahead and the balancing market price is negative, while it is the nominal capacity if it is positive. However, the nominal capacity proves to be highly suboptimal in the cases we study. We refer to Paper D for a comprehensive discussion.

The results we summarize here are obtained through a case study based on the Nord Pool market. Indeed, we model the system deviation and the supply curve of the balancing market using actual market data. As far as wind power is concerned, we employ Beta distributions to model its uncertain production, as proposed in [FGRM05].

By employing the parameters $\alpha = 3.78$ and $\beta = 1.62$ for modeling the distribution of wind power production, and considering an installed capacity of 300 MW, we obtain that the optimal offer is totally inelastic (i.e., there is no price differentiation of the offer) and equal to

$$x = 76.69\,\text{MWh}\,. \tag{4.2}$$

Notice that that such a value is a very low quantile (with proportion 0.01) of the wind power production distribution. However, it is important to remark

that under the price-maker assumption, the optimal offer is neither zero nor the nominal capacity as in the price-taker case.

Table 4.3 shows the expected financial improvement obtained with offer (4.2) as compared to the benchmarks described above. Remarkably, this offer improves the expected revenues by 1.5% as compared to the zero offer, and slightly over 3% with respect to the conditional mean or median.

Profit improvement w.r.t.		
mean (%)	median (%)	zero (%)
3.08	3.25	1.58

Table 4.3: Financial results obtained using the optimal bid for a price-maker wind power producer in the case study in Paper D

Figure 4.2 illustrates how the optimal offering curve changes as a function of the penetration of the producer in the market. These results are obtained in simulations where we change this penetration by rescaling the installed generation capacity of the producer. As one can see in the figure, the offering curve moves to the right as market penetration increases. This is consistent with what one would expect intuitively. Indeed, the prices a producer gets for deviations in a one-price market get closer and closer to the ones of a two-price market as its penetration increases. For example, if the considered producer were the only one causing imbalance, then its deviation would always be of the same sign as the system's, because these two quantities coincide. Therefore, the producer would always receive or pay the balancing market price both in a one-price system (by definition) and in a two-price system (since its deviation is always in the same direction as the system's). As seen in the previous section, the optimal offer yielded by (4.1) in a two-price system is a central quantile of the distribution of wind power production when the expected price difference between day-ahead and up- and down-regulation price are comparable. Therefore, we expect intuitively that the optimal offer of a wind power producer in a one-price market tends to the central quantiles of the predicted output distribution as the penetration of the producer increases. What we see in Figure 4.2 is a transition between a low-penetration case, comparable to a price-taker case in a one-price market where the optimal offer is zero, to a high-penetration case, where the optimal offering curve is closer to the median of the wind power distribution.

A similar sensitivity analysis, performed with respect to the rank correlation of the wind power production with the aggregate deviation from other market participants, yields interesting results. Figure 4.3 shows the optimal offering curve with different values of rank correlation between wind power production

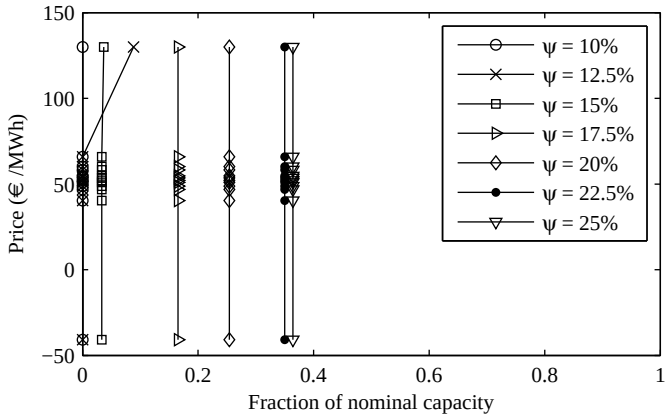

Figure 4.2: Day-ahead offer curves with different levels of market penetration of the price-maker producer in the case study in Paper D

and residual system deviation. We observe that the offering curve shifts to the left as the correlation increases, which matches intuitive reasoning. Indeed, if the wind power production and the system deviation had a rank correlation equal to -1, then offering the median would cause the wind power producer to always have a deviation of a different sign compared to the system's (assuming a symmetric distribution for system deviation). By doing this, the producer would always receive a better price than the day-ahead one for its imbalance. Therefore, from an intuitive point of view, quantiles close to the median would yield a high performance with negative values of correlation. As correlation increases, the offer curve moves to the left-hand side of the figure, indicating that the producer hedges from the penalties for underproducing. In a market with a hockey-stick supply curve, as the one considered in the case study, the penalties for underproducing tend to be higher than the ones for overproducing. This is because the cost of activating additional production units is higher than the cost savings for reducing the production from already dispatched units.

4.2 Optimal Demand-Side Management

Papers E and F focus on problems of demand-side management with dynamic pricing. The problems in both papers are formulated as MPECs, where the lower-level problem is a utility maximization problem of an end consumer exposed to dynamic prices, and flexible as far as the consumption for heating is concerned. The upper-level problems are the one of a virtual power plant operator in Paper E and the one of a retailer acting as an intermediary between the

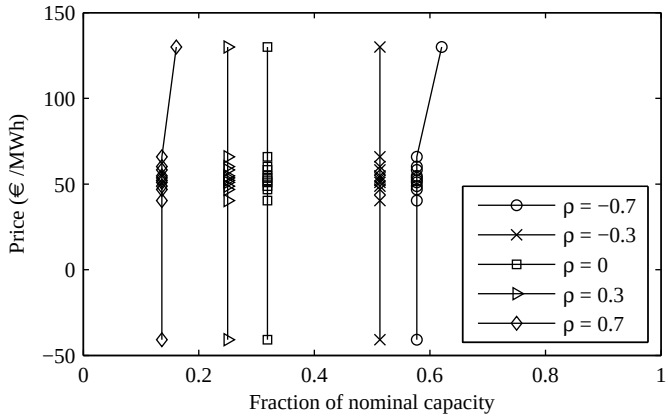

Figure 4.3: Day-ahead offer curves with different levels of correlation between the wind power output of the price-maker producer and the residual system deviation in the case study in Paper D

electricity markets and the end consumers in Paper F.

4.2.1 Managing a Virtual Power Plant

In Paper E, we consider the problem of a virtual power plant (VPP) operator, which owns wind power production facilities and is associated to a number of loads that are flexible in their consumption for heating.

The flexible load receives from the operator of the virtual power plant a dynamic price signal, and solves a utility-maximization problem where the cost of electricity procurement is weighted against a quadratic loss function that penalizes the deviation from a reference temperature. The heating dynamics for the consumer are modeled by using a discrete-time state-space model [Mad07]. This constitutes the lower-level problem. The upper-level problem — the VPP operator's — decides on the optimal dynamic price signal to be sent out to the consumers. Its objective is the minimization of the absolute value of the electricity imbalance caused by the deviation of wind power production with respect to the day-ahead forecast. This is accomplished by shifting the flexible consumption in time through an appropriate price signal. In practice, the VPP operator exploits the flexibility of demand response to absorb fluctuations of stochastic power production, therefore reducing the impact on the system of wind power's limited predictability.

Simulations of the model are presented in Paper E, where we make use of scenarios for wind power production issued according to the method in [PMN+09]. The optimization is carried out in a rolling horizon fashion. First, the price signal is optimized for a certain time horizon. Then, the decision for the first hour is implemented and the horizon is rolled one period forward.

Figure 4.4 shows the dynamics of relevant variables in the simulation during 24 hours by comparing the case with dynamic price to the case with a fixed price equal to €0.2/kWh. As one can notice in Figure 4.4(a), the variable price allows the VPP to smooth out most of the imbalance due to the wind power forecasting errors. The only imbalances that cannot be absorbed by the flexible consumption take place when the load is already zero, see Figure 4.4(b), and cannot be reduced any further to cover the underproduction of wind power with respect to the day-ahead forecast. Furthermore, the imbalance is smoothed out without causing a large difference in the dynamics of the indoor temperature for the end consumer in Figure 4.4(c), i.e., without jeopardizing consumer's comfort. Figure 4.4(d) shows the dynamics of the price, which is bounded between €0.1/kWh and €0.3/kWh. Generally, the day-ahead forecast overestimates the actual wind power production during the considered period. Hence, the VPP operator discourages excessive consumption by feeding the consumer prices in the high end of the range.

Table 4.4 summarizes the results for the day of simulation illustrated in Figure 4.4. Compared to the fixed-price situation, the setup with dynamic price and flexible load reduces imbalances for the VPP by more than half. The consumer discomfort caused by deviations of the temperature from the reference increases only slightly, as we already pointed out in the discussion above. However, in this case the cost for the consumer increases sensibly, owing to the high prices on average to discourage consumption. Under the assumption that the forecasting error is symmetric for wind power, we expect as many periods characterized by overproduction with respect to the forecast, and therefore by low prices, as periods where the wind power plant underproduces. Thus, the increased cost for the consumers during the latter periods, which we highlighted in the example, should be counterbalanced by periods where cost is actually reduced in the long run.

4.2.2 Optimal Strategy for Retailers Supplying Price-Responsive Demand

A bilevel setup similar to the one presented in the previous section is considered in Paper F. The lower-level problem is still the one of a consumer whose electricity demand for heating is flexible, and whose dynamics can be described

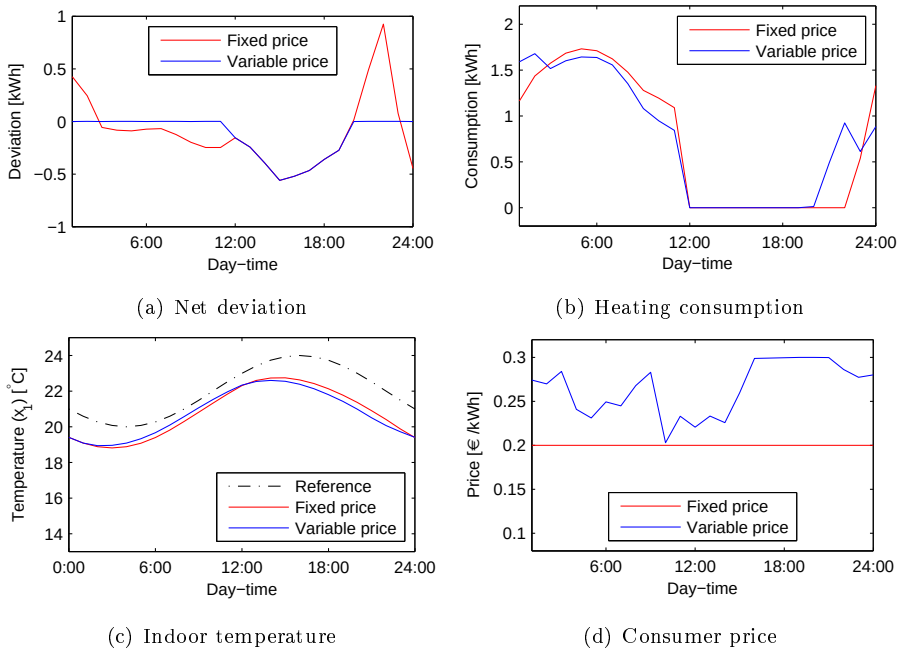

(a) Net deviation

(b) Heating consumption

(c) Indoor temperature

(d) Consumer price

Figure 4.4: Dynamics of relevant quantities during the simulation of management of a virtual power plant in Paper E

by a state-space model. However, in the upper-level problem we now look at a profit-maximizing retailer rather than at a virtual power plant. The retailer acts as an intermediary: it trades in the day-ahead and in the balancing markets, and then provides electricity to its customers. The demand from flexible consumers is influenced by the dynamic price signal, which is a decision variable of the retailer. Furthermore, the retailer decides on the amount of electricity to be purchased in the market at each stage, so as to minimize the cost of providing power to its customers.

The results of a number of simulations are presented in Paper F. The first objective of these simulations is to assess the capability of this setup to shift the load towards periods of low price in the wholesale electricity market. Note that as a result of the market mechanisms illustrated in Section 2.3, prices are lower in periods characterized by high production from renewables. Hence, a shift of a significant part of the load to low-price periods implies a more efficient use of renewables. Figure 4.5 illustrates the price and the consumption dynamics for three load types with different flexibility, defined as the willingness to accept a temperature deviation from a reference. In practice, different levels of flexibil-

	Unit	Fixed price	Variable price
Expected total imbalance	kWh	6.79	2.98
Consumer cost	€	3.57	4.77
Consumer discomfort	(€)	0.11	0.13

Table 4.4: Overall results of the simulations of management of a virtual power plant spanning one day with rolling horizon in the case study in Paper E

ity are enforced by defining different bands for the indoor temperature, within which there is no penalty in the consumer's utility function. In Figure 4.5, the consumer types are presented in order of decreasing flexibility. It should be noticed that the dynamics in this figure are stochastic, since we consider uncertainty in the model by employing scenarios. As one can see, a significant part of the consumption takes place at night, when prices are lower in the wholesale market, indicating that the retailer passes the wholesale market incentive on to the consumer.

Furthermore, we compare the dynamic pricing setup previously discussed to two other pricing schemes which are currently in use: the fixed-price scheme where the consumer price is constant throughout the day, and the time-of-use (TOU) scheme, where the price is higher during peak hours and lower during valley hours. For consistency, we enforce the average dynamic and time-of-use prices be equal to the constant fixed price.

Table 4.5 summarizes some financial results of the simulation for the retailer. As one can notice, the setup with dynamic price yields both the highest revenues from customer payments, and the lowest total costs for the retailer among the three setups considered. In particular, both the procurement costs (i.e., costs under perfect information) and the imbalance penalties (i.e., the opportunity cost for not being able to forecast the consumption perfectly at the day-ahead stage) are minimized through the use of dynamic pricing. As a result, profits are highest under dynamic pricing. The setup with time-of-use price yields the second lowest costs in the wholesale market, indicating a rather efficient use of generation resources compared to the fixed-price case. Finally, the retailer revenues under the time-of-use scheme are lowest. This indicates that this scheme is particularly favorable to flexible consumers. In contrast, the setup with dynamic pricing yields the highest consumer payment as long as the average daily price is constant across the considered price schemes. Hence, further rewards for flexibility, e.g., reducing the average dynamic price, should be thought of for rewarding consumers under this pricing scheme.

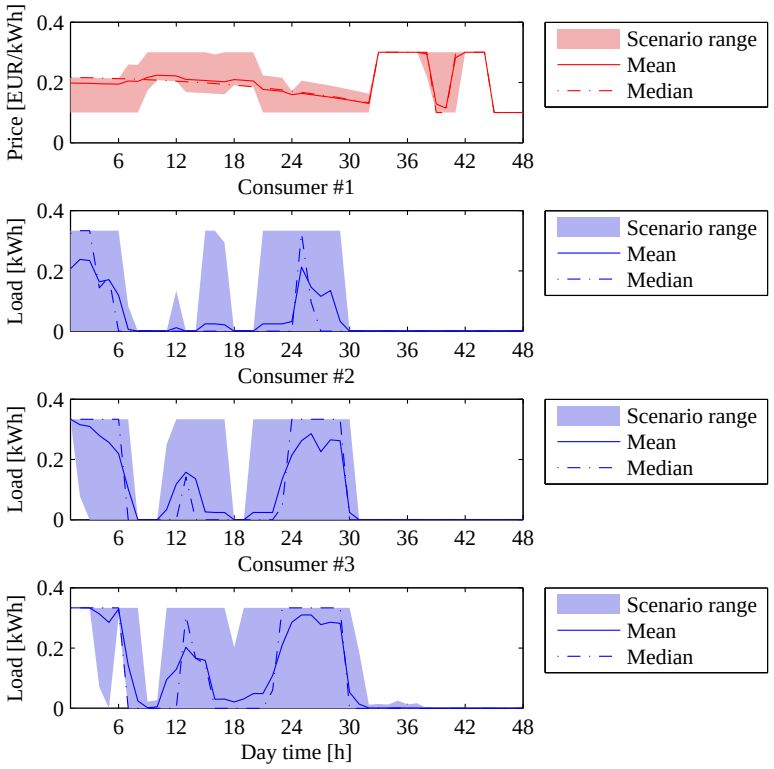

Figure 4.5: Flexible consumption (l) patterns for the consumer types with dynamic price $\widetilde{\pi}$ sent by the retailer in the simulation in Paper F

Table 4.6 sheds light on the impact of different levels of consumer flexibility on the financial results. To this end, we consider three different distributions of the consumers among the three consumer types characterized by different levels of flexibility. As one can notice, the total cost for the consumers as a whole increases as the level of flexibility decreases. In particular, the procurement costs to satisfy the flexible part of the load (i.e., heating) are particularly sensitive, while the costs for the inflexible part of the load (all the other appliances) are more or less stable. This is not only caused by a reduction in consumption, but also by the fact that more flexible consumers pay lower prices to the retailer. Indeed, the average price paid for heating purposes drops sensibly with increasing consumer flexibility.

Retailer performance		Pricing		
		Fixed	TOU	Dynamic
Revenues		3.4205	3.3164	3.5049
Costs	perfect information	1.0970	1.0781	1.0680
	imbalance penalties	0.0096	0.0088	0.0083
	total	1.1067	1.0868	1.0763
Profits		2.3139	2.2296	2.4286

Table 4.5: Market performance of the retailer in the simulations with fixed, time-of-use and dynamic price in Paper F. All the values are averages for the considered scenarios expressed in €

Consumer result index		Unit	Flexibility		
			High	Medium	Low
Costs	flexible load	€	0.5517	0.7180	0.8757
	inflexible load	€	2.7969	2.7868	2.7767
	total	€	3.3486	3.5049	3.6524
Price	flexible load	€/kWh	0.1870	0.1885	0.1921
	inflexible load	€/kWh	0.2060	0.2053	0.2045

Table 4.6: Consumer results in simulations with different demand flexibility in Paper F. All the values are averages for the considered scenarios

4.3 Market Dispatch in Presence of Renewables

Market and system operator's problems are addressed in Papers G and H. The former of these papers addresses the problem of determining an efficient day-ahead dispatch of stochastic producers, accounting for its impact on the balancing operations. In Paper H, we consider the joint determination of the day-ahead and reserve dispatch in presence of renewables in the market.

4.3.1 Improved Day-Ahead Scheduling of Renewables

As shown in [PZP10], there is potential for reducing expected system operation costs if the traditional sequential dispatch of the day-ahead and balancing markets described in Section 2.2.5 is replaced by a two-stage day-ahead dispatch based on principles of stochastic programming, of the like of the model presented in Example 3.4. However, models of this type present some issues of revenue adequacy, as conventional flexible producers recover their costs only in

expectation but not under any realization of the uncertainty. In Paper G, we show that similar improvements in the expected system cost can be achieved by a conventional day-ahead market-clearing if the dispatch of renewable stochastic producers is carefully chosen, instead of being equal to the mean forecast of wind power production, which is still the current practice in many markets worldwide. To determine the optimal dispatch of renewable producers, we propose a bilevel model where uncertainty is handled using stochastic programming. This model is similar to the two-stage one in Example 3.4, with the addition of the equilibrium conditions of a classical day-ahead market-clearing as constraints. Notice that, as we discuss in Paper G, the latter measure ensures revenue adequacy for conventional producers regardless of the realization of stochastic production.

The model is tested on a modified version of the IEEE Reliability Test-System [GWA+99], which includes two wind power producers, and compared both to the sequential day-ahead and balancing market-clearing, and to the two-stage market-clearing presented in [PZP10]. Figure 4.6 illustrates the expected system cost, which aggregates costs at the day-ahead and at the balancing stage, for the three clearing procedures as a function of wind power penetration in the system, in two different cases of correlation between the stochastic production from the two wind power producers in the system. As one can notice, the conventional sequential market-clearing (ConvD) has the worst performance among the three models in expectation. Naturally, the two-stage market-clearing (StochD) yields the lowest cost in expectation, since ConvD is suboptimal and the proposed bilevel model (ImpD) is a constrained version of StochD. However, the performance of ImpD is rather close to the optimal one. In particular, the expected cost is a decreasing function of the penetration of wind power in the system. This is not the case with the conventional sequential dispatch ConvD. Indeed, after a critical point indicated with a dashed vertical line in the figure, the expected cost starts increasing as more wind power capacity is integrated in the system. Remarkably, the proposed market-clearing model (ImpD) is capable of better coping with situations where the renewable stochastic producers are positively correlated with each other.

Table 4.7 summarizes the results of the case study presented in Paper G in terms of profits for some of the flexible conventional producers that provide regulation. As one can see, these producers recover their costs in expectation in the two-stage market-clearing model (StochD), but incur losses in some realizations of the output of stochastic producers. Furthermore, the probability of incurring losses for the units displayed in the table is remarkably high. With the sequential market-clearing (ConvD) and the proposed scheme (ImpD), the conventional producers are guaranteed cost recovery in any realization of the stochastic output of producers in the system. Notice, however, that the model we propose has a more balanced behavior in terms of expected revenues for conventional producers. On the contrary, the conventional dispatch yields very

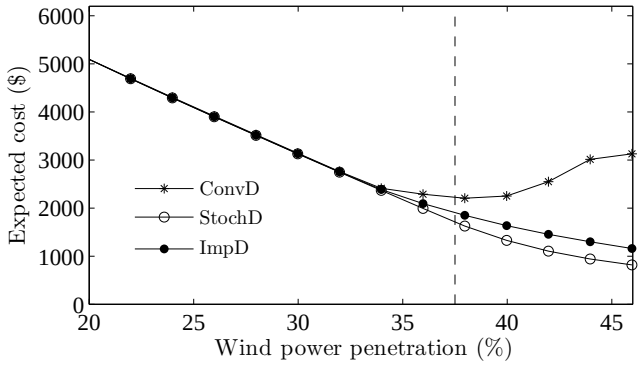

(a) $\rho = 0.35$

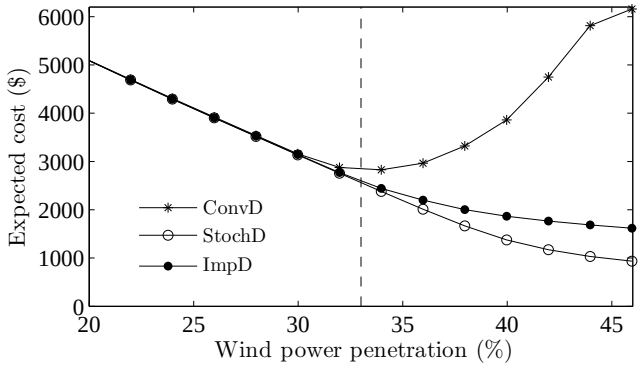

(b) $\rho = 0.75$

Figure 4.6: Impact of the wind power penetration level and spatial correlation on the expected cost of system operation for different day-ahead dispatch models in the application study in Paper G

high returns for the flexible producers, at the expense of the renewable producers, which pay too high regulation costs as a result of the inefficient day-ahead dispatch of the market.

		Unit			
		1	6	11	12
ConvD	Expected profit ($)	379.8	359.7	724.9	389.1
StochD	Expected profit ($)	45.6	48.4	99.7	64.9
	Average losses ($)	−17.4	−10.9	−17.6	−11.5
	Probability profit < 0	0.81	0.71	0.71	0.75
ImpD	Expected profit ($)	170.2	263.7	531.6	178.7

Table 4.7: Highlights of profits for some of the producers that provide regulation in the case study in Paper G, with a wind penetration equal to 38% and a correlation $\rho = 0.35$ between the two wind power producers

4.3.2 Robust Day-Ahead and Reserve Dispatch in Presence of Renewables

The sequential and deterministic manner with which the reserve and the day-ahead markets are cleared in the market organization described in Section 2.2.5 becomes more and more suboptimal as stochastic renewable sources penetrate the market. On the contrary, the joint determination of the amount of reserve capacity and the forward schedule in a stochastic programming framework is advocated in [MCPR09] to increase the efficiency of market operation.

Starting from the assumption that the reserve and dispatch schedules must be jointly robust to the uncertain realization of stochastic production in order to avoid costly load-shedding events, Paper H proposes an approach based on robust adaptable optimization, see Section 3.4. The proposed model builds on the one in Example 3.5. Its objective is the minimization of the total cost incurred in the reserve, day-ahead and balancing market in the worst-case realization

of the uncertain production from wind power generators. We consider general polyhedral uncertainty sets to model the stochastic generation for a number of wind power producers in the grid. In the remainder of this section, we report the highlights of a case study where the proposed model is applied to a modified version of the 24-bus IEEE Reliability Test-System [GWA+99] including six wind power producers. The stochastic programming counterpart of the same problem is considered as a benchmark for discussion.

In Table 4.8, the system cost is reported for both the robust optimization and the stochastic programming approach. The cost incurred at the balancing stage (for redispatch, load-shedding and their total) is reported both in expectation and in the worst-case scenario. To guarantee a fair comparison, the input scenarios to the stochastic programming approach follow a truncated Gaussian distribution, while the model based on robust optimization considers the support of this distribution as the uncertainty set.

Let us now comment the results in Table 4.8. Firstly, the robust optimization approach yields more conservative results than the stochastic programming one in terms of upward reserve. Indeed, the latter must be sufficient to cover the negative deviation, i.e., an underproduction, from wind power producers in any circumstance envisaged in the uncertainty set. On the other hand, the robust optimization approach dispatches no downward reserve, because this is not needed in the worst-case realization of wind power output, which is necessarily an underproduction in cases where there is no cost associated to wind spillage like in the considered example. In expectation, the robust optimization approach is not as efficient as the stochastic programming one, which is optimal and thus achieves the lowest total cost. However, the proposed approach trades off a slight increase in the expected system cost (about 2.8%) with an increased robustness, resulting in a drop in total system cost by over two thirds in the worst-case realization of the uncertainty.

A similar comparison is presented in Table 4.9. This table reports the system cost in a case where the forecast distribution for the uncertainty used in the stochastic programming approach (a truncated Gaussian) is different from the actual one (a uniform distribution with the same support). Since the two distributions share the same support, the dispatch obtained with the robust optimization approach does not change as compared to the one in the previous case. Remarkably, in this case the robust optimization model obtains lower costs in expectation than the stochastic programming one, which is penalized by a relatively large load-shedding cost. These results suggest that the performance of the stochastic programming approach degrades more quickly than the one of its robust counterpart if the scenarios used as input underestimate the probability in the tail of the actual distribution of the uncertainty. However, in the converse case where the scenarios overestimate the weight in the tail of the distribution,

Cost	Robust Optimization		Stochastic Programming	
Dispatch	17 897.52		17 512.07	
Upward reserve	489.72		355.59	
Downward reserve	0		130.28	
Total day-ahead	18 387.25		17 997.95	
	Expectation	Worst-case	Expectation	Worst-case
Redispatch	339.32	2989.46	147.82	2634.55
Load-shedding	0	0	72.83	43 586.85
Total balancing	339.32	2989.46	220.64	46 221.40
Total aggregate	18 726.56	21 376.72	18 218.59	64 219.34

Table 4.8: Comparison of system cost with the robust optimization and the stochastic programming approaches based on a simulation in Paper H. Values in $

stochastic programming may retain lower system cost in expectation. We refer to Paper H for further results.

Cost	Robust Optimization	Stochastic Programming
Dispatch	17 897.52	17 512.07
Upward reserve	489.72	355.59
Downward reserve	0	130.28
Total day-ahead	18 387.25	17 997.95
Redispatch (exp.)	576.75	335.06
Load-shedding (exp.)	0	923.26
Total balancing (exp.)	576.75	1258.32
Total aggregate (exp.)	18 964.00	19 256.27

Table 4.9: Comparison of system cost (only in expectation for the balancing market) with the robust optimization and the stochastic programming approaches with inaccurate prediction of the distribution of the uncertainty, based on a simulation in Paper H. Values in $

Chapter 5

Conclusions and Perspectives

In this dissertation, we address several problems of decision-making under uncertainty for the optimal management of stochastic and non-dispatchable renewables in electricity markets. In particular, we consider both the point of view of market players, i.e., producers, virtual power plant operators and retailers, and the one of market and system operators. By making use of tools of optimization under uncertainty, namely stochastic programming, stochastic bilevel programming and robust optimization, we show that the market value of renewables can be increased through improved decision making.

5.1 Overview of the Contribution

Assuming the point of view of renewable power producers employing stochastic, non-dispatchable sources, in particular wind, we first focus on the determination of optimal short-term trading strategies in Papers C and D. The participation in electricity markets envisages trading in multiple floors with different gate closures, some of them with a substantial advance in time to the delivery of electricity. This, coupled with the uncertain nature of stochastic renewable

sources of electricity, renders the determination of the optimal offering strategy a problem of optimization under uncertainty.

In Paper C, we show that there exists an analytical solution to the trading problem when the producer participates as a price-taker both in the day-ahead and in the balancing markets. Similarly to the *newsvendor* problem [RS64], the optimal solution is a certain quantile of the predicted distribution of the stochastic production, which depends on the expectation of the prices in the two market floors. Through a test-case based on the Nord Pool market, we confirm the theoretical superiority of this quantile-based strategy with respect to the conditional mean forecast, which has been used traditionally by stochastic power producers. However, we show that better financial results are obtained in the test-case by constraining the quantile-based strategy in a band centered about the conditional mean of the output distribution. This result highlights the exposure of the quantile-based bid to large losses stemming from single trading periods, and its suboptimality when the forecasts employed for decision-making are inaccurate. Note that this is a practical problem also typical of stochastic programming.

To render the price-taker assumption unnecessary, we employ the framework of mathematical programming with equilibrium constraints (MPEC) [LPR96]. In Paper D, we consider a similar trading problem, where the impact of the stochastic producer's offer on the balancing market is accounted for by embedding the equilibrium conditions of the clearing problem of this market. Since the latter is stochastic, we consider the optimality conditions for multiple market-clearing problems in a stochastic MPEC [GCF+12]. Because these optimality conditions can be linearized by using binary variables [FM81], this results in a very large combinatorial problem. In Paper D, we show that the model is tractable in a realistic case study. Furthermore, the optimal solution results in significantly improved revenues in expectation for the producer.

The complementary point of view of demand-side management is also addressed in this dissertation. Specifically, we consider how the introduction of dynamic prices for end consumers would impact the strategy of virtual power plant (VPP) operators and retailers trading in the wholesale market, and result in a more efficient use of the resources. We model problems of this type as hierarchical optimization problems, which we cast as MPECs where the upper-level optimization problem, i.e., the VPP operator's or the retailer's, sets a dynamic price signal and the lower-level one, i.e., the consumer's, optimizes the consumption plan.

In Paper E, we consider the case of a VPP operator that owns stochastic power production facilities and supplies consumers that are flexible in their load for heating. The dynamic price signal is employed to control the consumption from

the flexible consumers, with the objective of minimizing the expected value of the imbalance resulting from the stochastic power production. We show that the need to resort to the balancing market is drastically reduced as imbalances can be smoothed out by exploiting the consumers' flexibility. However, models of this type suffer from two drawbacks. The first one is the complexity of MPEC models already discussed above. The second one is the need for a reliable model of the consumers' dynamics and preferences to be used in the lower-level problem. In practice, a big modeling and clustering effort is required for a real-world application of models of this type.

A problem similar to the one described above, and with the same practical drawbacks just mentioned, is considered in Paper F. In this work, however, we consider a profit-maximizing retailer in the upper-level problem instead of a VPP operator. Through a case study, we show that by employing a dynamic price signal to exploit consumer flexibility, the retailer cost for purchasing electricity at the wholesale market is reduced. This fact signals that a more efficient use of the production resources is made. However, we highlight that only the retailer benefits from the increased efficiency, while the consumers are better off with other price schemes than the dynamic one, e.g., a time-of-use tariff.

Finally, this dissertation addresses the challenges that stochastic, non-dispatchable renewable sources pose to the market and system operators. Indeed, traditional deterministic tools for solving the day-ahead energy, and possibly reserve, dispatch problems are increasingly suboptimal as a growing penetration of renewables in the system calls for costlier operations in the balancing market. We consider solutions based on stochastic programming and on robust optimization to tackle problems of this type.

In Paper G, we consider the optimal day-ahead dispatch of stochastic production in a two-stage energy-only market. We build on the two-stage stochastic-programming-based model proposed in [PZP10], which is known to yield the lowest expected cost but also to guarantee cost recovery for the producers and the market operator only in expectation, and not in any realization of the uncertainty. The model we propose aims at the minimization of the expected system cost, comprising the cost at the day-ahead and at the balancing markets, as the one in [PZP10], and includes in an MPEC fashion the optimality conditions of a traditional day-ahead market-clearing, where the dispatch of the stochastic producers is fixed. This guarantees cost recovery in any realization of the uncertain production, while it still retains most of the gains of the stochastic programming approach in [PZP10] compared to the traditional sequential, deterministic procedure for market-clearing currently employed. Among the disadvantages of the proposed model, however, is the additional complexity introduced by embedding the optimality conditions in an MPEC, which have a mixed-integer linear reformulation and therefore result in a combinatorial problem.

Finally in Paper H, we consider the problem of jointly determining the day-ahead energy and reserve dispatch, which is studied using a stochastic programming approach in [MCPR09]. With respect to the latter work, we take an alternative path and formulate the problem in the framework of robust adaptable optimization [BBC11]. This approach is particularly relevant within this context, as the resulting energy and reserve dispatch is immune to the worst-case realization of the uncertain power production, thus resulting in no load-shedding events. We show that the robust solution is slightly suboptimal in comparison with the dispatch obtained from the corresponding stochastic programming model. However, the former is not only better immunized to the worst-case realization of the uncertainty than the latter, but it may also perform better if the actual distribution of the stochastic production is different from the forecast one. Notice that this case is particularly relevant, as modeling accurately the stochastic production from several renewable power producers spread in the network, accounting for their correlation, is a rather challenging task. Furthermore, we experience that the robust optimization model has better computational performance than its stochastic programming counterpart in the case study considered. However, it should be pointed out that the formulation we propose is limited to polyhedral sets for the stochastic power production, as the use of more complex uncertainty sets hinders a straightforward solution of the problem.

5.2 Future Research

The research works presented in this dissertation open the way to future research in different directions.

As far as the problem of trading renewable power is concerned, we can identify a number of improvements to our models. First of all, it would be of great interest to extend the price-maker assumption, which so far is limited to the balancing market, to the day-ahead market as well. The assumption in our model is justified by the larger volumes traded in the day-ahead market than in the balancing market. However, we can envisage situations in the future where single renewable power producers will be able to influence the day-ahead price formation. Furthermore, the inclusion of different market floors in the model, e.g., the intra-day and/or the futures and derivatives markets, would be of great relevance. In particular, the intra-day market is seen as key to a successful large-scale integration of renewables, and a combination of trading in this market and in the financial markets could reduce the risk exposure of renewable power producers. Another direction for future research is modeling trading as a price-maker in a two-price market. This would constitute not only a valuable operational tool for renewable power producers, but also a significant contribu-

tion to the debate on the design of balancing markets. Besides, the inclusion of a network representation in the offering model would be an improvement of particular importance to markets with nodal pricing, which are very popular in the United States. Finally, it would be especially interesting to consider the optimal trading strategy of a portfolio including both renewable and conventional sources. This is of particular relevance nowadays, as the increasing integration of distributed generation and the envisaged development of demand response are promoting the concept of *virtual power plant*.

Needless to say, extensions of the research carried out on demand-side management for virtual power plant operators and retailers in a dynamic-price framework are also possible. A straightforward improvement of the presented models would be the development of more sophisticated descriptions of the consumer behavior, including other sources of flexible consumption than heating. Besides, building algorithms to cluster the large number of consumers associated to a retailer or to a virtual power plant is paramount for the practical use of bilevel models of the type we propose, as these models are computationally expensive. In view of practical applications with short look-ahead time and/or involving a large number of consumers, it would also be especially important to propose alternative models, e.g., based on control theory, to determine appropriate price signals for the consumers. Finally, modeling competition among retailers in a demand response framework with dynamic pricing would be a relevant extension of the presented work. This would be particularly important as future market design might not only render residential consumers price-responsive, but also increase their awareness and market power, as aggregators of consumers may be allowed to negotiate directly with retailers.

The market-clearing models proposed in this dissertation open up several directions of future research as well. First of all, a relevant extension would be the inclusion of different markets in the proposed clearing procedures, e.g., the reserve market, and/or the flexible ramping markets currently under development [AAR+12], which could yield higher efficiency and reliability for the system. Another improvement would be the development of alternative methods to determine the day-ahead dispatch of stochastic producers while reducing the computational burden for the market operator. Indeed, the bilevel model presented suffers the computational problems already mentioned, which complicate its practical application to large-scale problems. Finally, the use of robust optimization in the context of the determination of the day-ahead energy and reserve dispatch opens up interesting research directions. Indeed, this framework requires the definition of uncertainty sets for stochastic renewable production in different sites of the system. Therefore, there is a need to develop stochastic tools to model such sets. Besides, advances are needed to formulate and solve optimization models that allow for more sophisticated uncertainty sets than polyhedral ones, e.g., ellipsoidal sets.

Part II

Papers

Paper A

Impact of Wind Power Generation on European Cross-Border Power Flows

Authors:
Marco Zugno, Pierre Pinson, Henrik Madsen

In press for:
IEEE Transactions on Power Systems.

Impact of Wind Power Generation on European Cross-Border Power Flows

Marco Zugno[1], Pierre Pinson[1], Henrik Madsen[1]

Abstract

A statistical analysis is performed in order to investigate the relationship between wind power production and cross-border power transmission in Europe. A dataset including physical hourly cross-border power exchanges between European countries as dependent variables is used. Principal component analysis is employed in order to reduce the problem dimension. Then, nonlinear relationships between forecast wind power production as well as spot price in Germany, by far the largest wind power producer in Europe, and power flows are modeled using local polynomial regression. We find that both forecast wind power production and spot price in Germany have substantial nonlinear effects on power transmission on a European scale.

A.1 Introduction

Driven by the need to comply with stringent international agreements, which aim at reducing the environmental impact of energy production as well as energy dependence, the deployment of renewable energy in Europe has grown at an unprecedented pace in the recent years. Among renewable sources, wind power plays a central role both for its impressive technological development and for its expansion. Particular features of wind power, like its stochastic and non-dispatchable nature and its very low marginal cost, render it very different from the more conventional sources of energy.

Due to its low marginal cost, wind power production has the consequence of lowering market prices via the so-called "merit-order effect" [1]. This is because wind power enters the energy supply function from the left, or, in an alternative

[1]DTU Informatics, Technical University of Denmark, Richard Petersens Plads, bld. 305, DK-2800 Kgs. Lyngby, Denmark

interpretation, reduces the load and thus shifts the intersection between supply and load to the left, thus pushing more expensive sources of energy out of the production schedule. Simulation with market models in [2] and statistical analysis in [3] confirm the price reduction effect of wind power. The latter work also shows that the driving variable of this mechanism is wind power forecast rather than actual production, since the former one is used when producers bid on the market.

The European transmission network is composed of five different synchronous zones, which in turn gather several interconnected national and international energy markets. These are organized with different rules and characterized by different generation portfolios; furthermore climate conditions vary widely across Europe. In these conditions significant price differentials are likely to develop between areas, and therefore also significant flows of power from areas with low power price to areas where energy is more expensive. Thus by influencing energy prices, wind generation also drives flows of power from areas with temporarily favorable conditions for wind power production to areas with higher price level, be it due to a high demand or an expensive generation mix [4]. Massive investments are planned in order to increase the transmission limits between countries of the EU in the years to come [5].

Among the challenges for a successful integration of high penetration of wind power are the variability of its power output and the limited accuracy of wind power forecasting [6, 7]. Both these problems can be addressed by aggregating the power output of wind farms distributed over a wide region. Indeed due to the lower variability of wind power production in Europe as compared to generation from a single region, more than 20% of the European demand could be covered by wind power without significant changes in the system [8]. Furthermore forecast errors can be drastically reduced by the so-called "smoothing effect" of aggregation, as discussed in [9]. Investigations of this type generally assume infinite transmission capacity, while as [10] points out, the interaction between wind power production and transmission constraints should be accounted for, if these phenomena are to be analyzed at a European scale.

In this context, modeling how wind power production interacts with the flow of energy in large international power systems is particularly appealing. Models of this type are needed when planning investments in new wind power or transmission capacity. From an operational point of view, they can help the process of scheduling cross-border power exchanges.

Power system models have been developed and simulated in the literature in order to study the effect of increasing penetration of wind power on European cross-border flow. Such models are simulated in [10] in order to study the congestion of individual interconnections in different scenarios of wind power

penetration in Europe. A similar intent is pursued in [11], with the focus being on offshore wind power, and in [12], where copulas are employed to simulate wind power production at different locations. Besides, the effect of wind forecast errors on the uncertainty of cross-border flows has been investigated in [13].

As opposed to simulation using market and grid models, this work follows a top-down statistical approach based on historical data, along the lines of the method employed in [14]. Among the advantages of this approach is the relative simplicity, since no detailed modeling of the underlying physical structure of the power system is required. On the other hand, the reliance on historical data implies the impossibility of extrapolating the analysis out of the range of observations. In this paper a method for analyzing the impact of wind-related variables (external variables) on the European cross-border flows (dependent variables) is developed and employed. The focus is directed towards the effect of forecast wind power production in Germany, which, besides being the largest producer of wind energy in Europe, is centrally located and highly interconnected with the neighboring countries. As Germany—along with other countries in Northern Europe—is setting ambitious targets for installed wind power capacity already by 2020 [15] the presented methodology will allow to assess how future deployment of wind power in this important region will affect the European transmission grid, pinpointing its limitations and possible bottlenecks.

The methodology proposed in this work follows three steps. First, Principal Component Analysis (PCA) is employed in order to reduce the size of the problem, which would otherwise require the analysis of a large number of flows. PCA determines the most significant modes of the flow dataset, i.e. the directions in which it shows most of its variation. The dimension reduction is then performed by selecting a reduced set of modes, which account for a large fraction of the variance of the original dataset. At a second stage, local polynomial regression is applied on this basis in order to model the interaction between the external variables and the chosen modes of the flow dataset. The final step consists in mapping the results of the analysis back from the reduced basis to the original space, i.e. the individual cross-border flows.

This paper is structured as follows. The dataset used in this work is briefly introduced in Section A.2, and the choice of the explanatory and dependent variables is motivated. Section A.3 describes the employed methodology. In Section A.4 we discuss the results of the application of this method on the available dataset. Finally, concluding remarks and possible future extensions of this work are provided in Section A.5.

A.2 Dataset

The dataset employed in this work spans a period of 3 years from January 2006 until the end of December 2008. Since during the winter daylight savings only one measurement is available for the duplicated hour, 26301 hourly observations are available in total both for dependent and explanatory variables.

A.2.1 Dependent variables

Physical hourly cross-border power flows between 34 European and bordering extra-European countries form the set of the dependent variables used in this work. This consists of 70 flows in 2006, 72 in 2007 after the addition of the tie-lines connecting Bulgaria-Macedonia and Estonia-Finland, and 74 in 2008 after the addition of the Norway-Netherlands and Greece-Turkey interconnections. Since the analysis to carry out needs data to be available for the whole period for all the interconnections, the set of physical flows is restricted to the original 70 interconnections established as of 2006. Furthermore, data are missing for significant parts of the period 2006–2008 in other two flows. The final dataset is therefore restricted to 68 cross-border interconnections. Given the low number of discarded flows compared to the total, such discard has a limited impact.

Finally, a data cleaning procedure indicated the presence of outliers stemming from phenomena of different nature. Exceptionally high or low values for most European flows were recorded during the UCTE system split on the 4th November 2006, see [16]. Similarly, unusual flows can be observed during the winter switch from daylight savings to solar time for most interconnections. Finally, a small number of local, single-hour spikes involving few adjacent flows is observed, possibly stemming from smaller technical failures. Such limited number of outliers is removed from the dataset leaving 26281 hourly observations.

A.2.2 Explanatory variables

For the reasons mentioned in Section A.1 the focus of the analysis is directed towards wind power production in Germany. As [3] states, the driving variable to be considered when analyzing the effect of wind power is the production forecast rather than the actual production. Indeed the former is used when bidding wind power at the spot market, where the price is settled. Since both wind power forecasts and load affect the spot price, it is of interest to analyze their combined effect on the cross-border flow of power. Therefore the first

explanatory variable to be considered in the analysis is the forecast wind power penetration

$$\widehat{r}_t = \frac{\widehat{W}_t}{L_t} \,, \tag{A.1}$$

where $\widehat{W}_t$ is the wind power production forecast and L_t the load, both aggregated for Germany as a whole. Both these variables are available in the considered dataset for the whole 2006–2008 period. It should be noticed that wind power in Germany developed constantly in the considered period. Indeed, the installed capacity grew from 18.4 GW at the beginning of 2006 to 23.9 GW at the end of 2008 [17]. Nevertheless, the impact on this study is limited owing to the fact that wind power penetration is employed rather than a scaling of the production with respect to the total installed capacity.

An alternative approach is the direct use of the spot price in Germany as an explanatory variable. The effect of wind power is then considered in an indirect way, under the assumption that wind power forecast, or penetration, is negatively correlated with the spot price, as shown in [3]. Although the core of the analysis presented in this paper considers the wind power penetration as explanatory variable, we provide an example using the electricity price in Section A.4.2.

The time series of spot prices in the German electricity market (EEX) is characterized by sparse spikes reaching out to around €2500/MWh. As a way to solve this issue, among other benefits, logarithmic transformation is commonly employed when dealing with price time series, see e.g. [18]. The time series of logarithmic prices can be generated through the transformation

$$P_t^l = \log\left(1 + P_t\right) \,. \tag{A.2}$$

This way the distance between the sparse high prices is shrunk, while the relative distance between the denser low prices is increased. As a side effect, handling negative prices is not possible under the logarithmic transformation. In the dataset, 15 prices at the end of the year 2008 turned out to be negative. These values are discarded from the dataset, which is therefore further reduced to 26266 observations. Alternatively, a shifted log transformation [19] could be employed without requiring the exclusion of negative prices.

A.3 Methodology

Although the study of a power network could be performed by independently analyzing each single flowgate, several reasons point at other options. First,

studying a wide power system like the European one would require the analysis of a large number of flows, with negative consequences on the dimensionality of the problem. Furthermore, due to the net structure of power systems several flows can be highly correlated due to e.g. loop flows. This means that part of the analysis carried out by independently considering each interconnection would be redundant. On top of that, noise can render less visible the object of the investigation. As Section A.3.1 explains, PCA is used here in order to overcome these issues.

Once a reduced set of principal components is indicated by PCA, statistical regression is employed on the reduced basis in order to model the dependence structure between flows and external variables. As power systems are complex and nonlinear, their study requires nonlinear regression techniques. Local polynomial regression was successfully applied in [14] to perform an analysis similar to the one in this work, though only considering the Austrian power system. The same technique, which is introduced in Section A.3.2, is used in this work. The reader interested in a deeper presentation of local polynomial regression is referred to [20].

A.3.1 Principal component analysis

PCA is a technique that is often used when dealing with multivariate data in order to reduce the problem dimension, see [21]. Problem simplification is obtained by selecting a reduced basis of orthogonal variables, which account for most of the variance in the dataset. Let us denote with the vector $\mathbf{X_t}$ the values of the N physical hourly cross-border flows at time t. Let us also assume that T hourly values are available for each interconnection. The centered version $\widetilde{\mathbf{X}}_\mathbf{t}$ of the multivariate time-series of the power flows is given by

$$\widetilde{\mathbf{X}}_\mathbf{t} = \mathbf{X_t} - \bar{\mathbf{X}} \,, \tag{A.3}$$

where $\bar{\mathbf{X}}$ is the vector of the mean values of the N flows. The covariance matrix $\mathbf{C}$ of the flows can be computed as

$$\mathbf{C} = \frac{1}{T} \sum_{t=1}^{T} \widetilde{\mathbf{X}}_\mathbf{t} \widetilde{\mathbf{X}}_\mathbf{t}^T \,. \tag{A.4}$$

The eigenvectors of the covariance matrix $\mathbf{C}$ form a new orthogonal basis for the flow dataset. In practice, such eigenvectors represent modes of the dataset, i.e. groups of flows that often exhibit a similar behavior. By ordering the eigenvectors so that the corresponding eigenvalues are arranged in a decreasing fashion, one ensures that the higher the ranking of a vector in the new basis,

the higher the fraction of total variance of the dataset it explains. This is a trivial result of the fact that these fractions and the eigenvalues are linearly proportional.

The principal components are obtained by selecting the first n eigenvectors in the new ordered basis. Although the choice of n is arbitrary, there are several criteria for this selection, e.g. the method of the average eigenvalue and the scree graph method, which are discussed in [21]. The latter method, which basically consists in a graphical discrimination between small and large eigenvalues, has been used in this work. As a consequence of this selection, only the n directions (or modes) of the flow space with the largest variance are retained in the analysis, while the remaining $N - n$ are discarded. This is done since the modes with larger variance carry most of the statistical information while the ones with smaller variance can often be associated with noise.

Let us denote with $\mathbf{Y_i}, i = 1, \ldots, n$ the principal components of the dataset. These form a reduced orthonormal basis for the original flows, and one can always write the centered flow observations $\widetilde{\mathbf{X}}_\mathbf{t}$ as a linear combination of the PCs $\mathbf{Y_i}$'s plus an error term ϵ_t, which has zero mean and finite variance

$$\widetilde{\mathbf{X}}_\mathbf{t} = \sum_{i=1}^{n} \alpha_{i,t} \mathbf{Y_i} + \epsilon_t \qquad \forall t \,, \tag{A.5}$$

In other words, we achieve a similar statistical representation of the original flow dataset through linear projection from the reduced space of the PCs. Generally speaking, the higher the fraction of the original variance is retained with the chosen PCs, the more accurate such representation will be. More precisely, it is to be underlined that the variance is a full description of the statistical information contained in a dataset only under the assumption of joint normality. When the original variables (flows) do not follow a multivariate normal distribution, the comparison between the variance of the original dataset and the variance of its projection on the PC space is an indicator of the amount of the retained statistical information up to moments of order 2. In the case that higher order moments of the residuals are large in comparison to the original signal, alternatives to PCA should be considered, e.g. Independent Component Analysis (ICA) [22].

The advantage of using PCA is now clearly visible, as it is possible to represent every multivariate flow observation $\widetilde{\mathbf{X}}_\mathbf{t}$, which is N-dimensional, with a set of n coefficients $\alpha_{i,t}$, where $n < N$.

It should be pointed out that PCA is often carried out on centered and standardized variables, i.e. by diagonalizing the correlation matrix $\mathbf{R}$ rather than the covariance matrix $\mathbf{C}$. The choice of using the covariance matrix is motivated

by the fact that in this way the information on the magnitude of the flows is not lost in the division $r_{ij} = c_{ij}/(\sigma_{\widetilde{X}_i}\sigma_{\widetilde{X}_j})$. This is clearly an advantage in this case as all the dependent variables (flows) are measured in the same unit, and, as Section A.4 underlines, this choice allows a more intuitive interpretation of the principal components. Furthermore, as [23] points out, carrying out PCA on the covariance matrix can better isolate the strongest variations in a dataset with uniform units.

Finally, it is important to remark that data might present significant trends when longer datasets (i.e., spanning several years) are employed. For example, an increase in demand could introduce slow variations in power flows. In that case, simply centering the multivariate flow dataset as in (A.3) might reveal itself inadequate to remove such trends. To this end, one might filter the dataset of power flows so that low-frequency dynamics are discarded from the analysis.

A.3.2 Local polynomial regression

The model of Eq. (A.5), representing the power flows as a linear combination of the principal components of the dataset, can be modified in order to account for the effect of explanatory variables $\mathbf{u_t}$, e.g. the forecast wind power penetration $\widehat{r}_t$ and the transformed electricity price P_t^l. This is done by allowing the coefficients α_i of the principal components to vary as functions of $\mathbf{u_t}$

$$\widetilde{\mathbf{X}}_\mathbf{t} = \sum_{i=1}^{n} \alpha_i(\mathbf{u_t})\mathbf{Y_i} + \epsilon_t \qquad \forall t \; . \tag{A.6}$$

In this work local polynomial regression, see e.g. [20], is employed in order to study the functional forms of the $\alpha_i(\mathbf{u_t})$ coefficients. This technique allows to fit a curve or a surface (depending on whether $\mathbf{u_t}$ is formed by one or more explanatory variables) to these relationships by locally approximating them as low-order polynomials. Although in principle $\mathbf{u_t}$ could be of any dimension m, for practical applications this vector should be sized reasonably. For example it is not possible to visualize the coefficients $\alpha_i(\mathbf{u_t})$ if $m > 2$. Furthermore, the computational time increases with the dimension of this vector.

The first step of the technique consists in the definition of a grid in the space of the explanatory variable $\mathbf{u}$. The grid is formed here by choosing l equally spaced quantiles in each dimension of $\mathbf{u}$. Let us indicate with $\mathbf{u}_i$ the time series of the i-th explanatory variable, sorted in increasing order. We are interested in the quantiles with the following probabilities

$$p_k = \frac{k}{l} - \frac{1}{2l} \qquad k = 1, \ldots, l \; . \tag{A.7}$$

Let us define $h_k = Tp_k + 1/2$, where T is the sample size. If h_k is an integer, the k-th quantile u_i^k is the h_k-th point in the sorted sequence $\mathbf{u}_i$. Otherwise, it can be estimated with the following linear interpolation

$$u_i^k = u_{i,\lfloor h_k \rfloor} + (h_k - \lfloor h_k \rfloor)\left(u_{i,\lfloor h_k \rfloor + 1} - u_{i,\lfloor h_k \rfloor}\right) \ , \tag{A.8}$$

where the second subscript on the u's indexes a certain element of the vector $\mathbf{u}_i$.

A grid is then formed by considering the l^m combinations of points $(u_1^{k_1}, u_2^{k_2}, \ldots, u_m^{k_m})$ where $k_i = 1, 2, \ldots, l$ for $i = 1, 2, \ldots, m$. Alternatively, equally spaced u_i^k could be used with no consequences on the remainder of the methodology presented here.

Weighted least-squares regression is then performed locally at each point of the grid. A set of q data points, where $1 \leq q \leq T$, is used for regression. These points, called *neighbors*, are the q closest points to the considered point of the grid. Naturally the neighbors selection procedure requires that a suitable metric ρ is defined on the explanatory variable space. Hereafter the Euclidean distance is adopted, after variables measured in different units are normalized. The ratio $h = q/T \leq 1$ between the considered number of neighbors and the total number of data points is referred to as *bandwidth*. High bandwidths increase the smoothness of the regression, with the trade-off of an increased bias of the regressed model. In this work a bandwidth $h = 0.2$ is used.

A weight function has to be defined in order to assign higher importance to the observations $(\widetilde{\mathbf{X}}_\mathbf{t}, \mathbf{u}_t)$, whose values of the explanatory variables are the closest neighbors of the grid point. Among the many possibilities, a weight function based on the tricube function is chosen here

$$w(z) = \begin{cases} (1 - z^3)^3 & 0 \leq z < 1 \ , \\ 0 & \text{otherwise} \ . \end{cases} \tag{A.9}$$

One should notice that $w(z)$ is non-increasing for positive z. Let us name $\mathbf{u}_\#^j$ the j-th point of the grid and with $\overline{\mathbf{u}}^j$ its q-th furthest neighbor. Since $\rho(\overline{\mathbf{u}}^j, \mathbf{u}_\#^j)$ is at a maximum in the considered neighborhood, the weight function

$$f^j(\mathbf{u}) = w\left(\frac{\rho(\mathbf{u}, \mathbf{u}_\#^j)}{\rho(\overline{\mathbf{u}}^j, \mathbf{u}_\#^j)}\right) \tag{A.10}$$

is well defined. Indeed it assigns non-increasing weights to points with increasing distance from $\mathbf{u}_\#^j$. A weight of 1 is assigned to the grid point $\mathbf{u}_\#^j$, while $\overline{\mathbf{u}}^j$ and all the points outside the neighborhood have 0 weight.

Weighted least squares regression, see [24], is employed locally for each point $\mathbf{u}_{\#}^{j}$ of the grid. Each observation $(\widetilde{\mathbf{X}}_\mathbf{t}, \mathbf{u}_t)$ is weighted according to the weight function in (A.10). The output of weighted least squares regression is a local model for $\alpha_i(\mathbf{u_t})$, approximated as a first order polynomial of the explanatory variables. The model is determined according to a weighted least squares criterion, which ensures that the modeling error ϵ_t is minimized in a consistent way.

After this procedure is carried out for all the points in the grid, a curve or surface $\widehat{\alpha}_i(\mathbf{u_t})$ is fitted from the individual local approximations. Such a fit models the behavior of the coefficients $\alpha_i(\mathbf{u_t})$ of the principal components in the whole space of interest as functions of the explanatory variables. Conclusions could be drawn directly from the shape of the regression surface of the $\alpha_i(\mathbf{u_t})$'s, provided that the principal components can be easily interpreted. As an alternative, one can choose to map the analysis back to the original space of the non-centered flows, obtaining the models $\widehat{\mathbf{X}}(\mathbf{u}_t)$

$$\widehat{\mathbf{X}}(\mathbf{u}_t) = \sum_{i=1}^{n} \widehat{\alpha}_i(\mathbf{u}_t)\mathbf{Y_i} + \bar{\mathbf{X}}_\mathbf{t} \ . \tag{A.11}$$

This way regression curves or surfaces are obtained for each individual flow in the dataset.

A.4 Results

This section presents the results obtained from the application of the method proposed in Section A.3 to the dataset described in Section A.2. Clearly, analyses of this type depend heavily on the availability and on the quality of large datasets, which are not always publicly available. Although datasets for power flows, wind power production and load are available for certain electricity markets, e.g., PJM [25] and the European markets [26], the collection of such datasets require the coordination of a number of entities so as to ensure consistency in terms of sampling frequency, sampling time and time-span. Obviously, this is a limitation for the readers willing to perform a similar study, but unable to interact with the entities owning the data.

A.4.1 Principal component analysis

The results of PCA applied to the dataset of the cross-border flows show that it is possible to express most of the original variance with a limited number of

principal components (PCs). By using the scree-graph method, see [21], the 8 PCs with highest variance are selected. The criterion used ensures that further inclusion of PCs would not increase sensibly the cumulative fraction of variance explained by the set.

Table A.1 summarizes the characteristics of the selected components. Its second column reports the fraction of total dataset variance explained by each of the PCs individually, while the third column shows the cumulative fraction of variance jointly explained by selecting the first i PCs. It is seen that almost 2/3 of the total variance are explained by the first 4 PCs. Furthermore, the selected set of 8 PCs explains 82.11% of the original variance, despite the dramatic reduction in size of the problem from the original 68 flows to 8 modes. In

Table A.1: Individual and cumulative fraction of variance explained by the i-th principal component and by the principal components up to the i-th one respectively

Principal component	Individual fraction of variance [%]	Cumulative fraction of variance [%]
1	28.89	28.89
2	18.83	47.73
3	10.55	58.28
4	7.69	65.97
5	5.53	71.50
6	4.83	76.32
7	2.97	79.29
8	2.81	82.11

relation to the discussion on the non-normality assumption in Section A.3.1, it is stressed that different statistical descriptions, such as the comparison of the interquantile ranges of the flows and their residuals, showed a similar behavior as the one illustrated in Table A.1 for the variance.

The analysis of the structure of the PCs gives further insight into the characteristics of the European power system. Indeed when PCA is carried out on the covariance matrix, see the discussion in Section A.3.1, the structure of the PCs often offers a physical interpretation. Let us denote with $\mathbf{Y_i}$ the i-th PC. It is a vector of 68 elements

$$\mathbf{Y_i} = [Y_{i,1} \dots Y_{i,68}]^T \ , \tag{A.12}$$

where $Y_{i,j}$ represents the weight of the j-th individual flow in the i-th PC. Large weights of the same sign on a PC show that the corresponding flows tend to

deviate from their mean in the same direction; conversely they tend to deviate in opposite directions if their weights have different signs.

Fig. A.1 shows the structure of the first PC as an example. In this illustration the widths of the arrows in the map of Europe are scaled, so that each of them is proportional to the weight $Y_{1,j}$ of the respective j-th cross-border flow in the first PC. As one can see, the main contribution to this first PC is given by the simultaneous flow of power directly from Switzerland to Germany, directly from France to Germany and by the flow from France to Germany through Belgium and the Netherlands. The fact that this mode alone explains almost 30% of the variation of the dataset signals the importance of the power flow between France and Germany on a European scale.

The second and third PC, not shown here for the sake of brevity, offer interesting interpretations, too. The second PC is mainly composed of power flowing from Germany to the Nordic region, and internally in Scandinavia from Sweden to Norway. A possible interpretation could be that cheap power is flowing from continental Europe to Norway so that water can be kept stored in the Norwegian hydro dams, or the other way around when continental Europe imports power from Norway. A second significant pattern in this principal component, although less important, is the flow of power through Switzerland in the North to South direction. Furthermore, the main trend in the third PC is the flow of power towards Italy from France, both directly and through Switzerland, and from Germany, through Switzerland and to a lesser extent Austria.

A.4.2 Regression curves for principal components

Regression curves or surfaces modeling the behavior of the $\alpha_i(\mathbf{u}_t)$ coefficients in (A.6) as functions of the multivariate input $\mathbf{u}_t$ are readily obtained by using local polynomial regression.

Fig. A.2 shows the curve modeling the behavior of the $\alpha_1(\widehat{r}_t)$ coefficient as a function of wind power penetration in Germany. The curve clearly represents the mean trend of the relationship between the two variables, and not a deterministic model of them. Therefore one should expect observations to be spread around this curve, due to their stochasticity and dependency on other variables not accounted by the model. Nevertheless one can draw some intuitive conclusions from this mean trend, also as a result of the interpretability of the first principal component. In Section A.4.1 it is underlined how the main trend in this mode is the power flow from France and Switzerland to Germany. As one can see in Fig. A.2, the corresponding coefficient tends to decrease rather sensibly when wind power penetration in Germany increases. The implication is that the

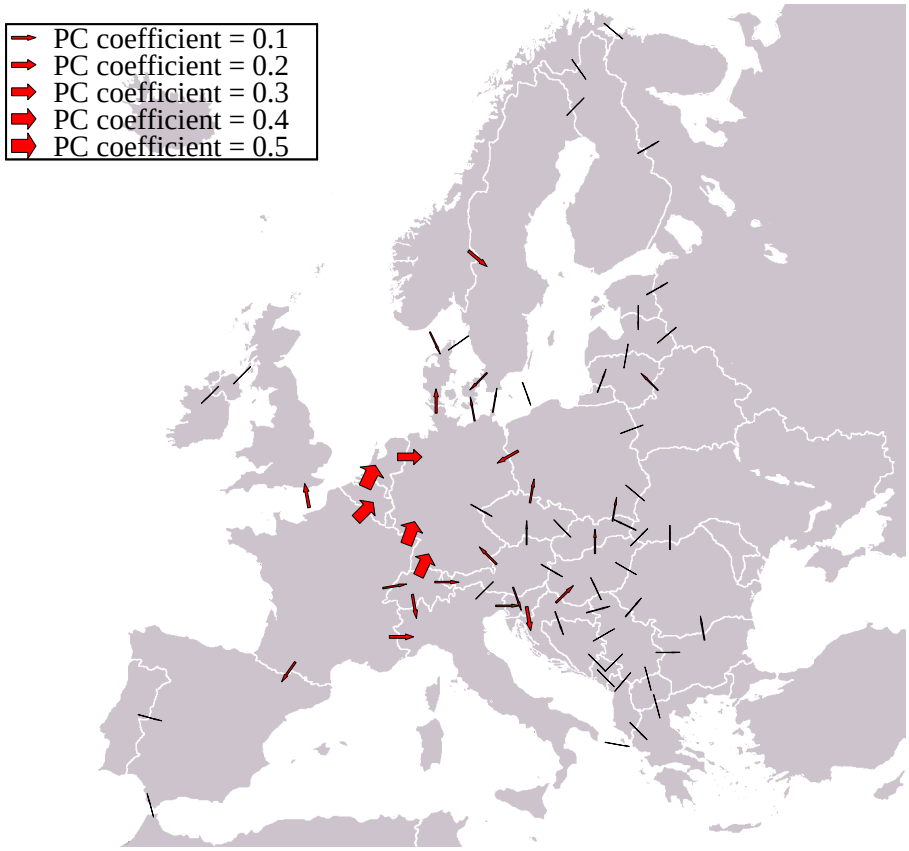

Figure A.1: Map of Europe showing the weight of each single centered physical flow $\tilde{\mathbf{X}}_\mathbf{i}$ in the first principal component $\mathbf{Y_1}$. The width of the lines in the figure is proportional to the coefficient of the respective flow in $\mathbf{Y_1}$

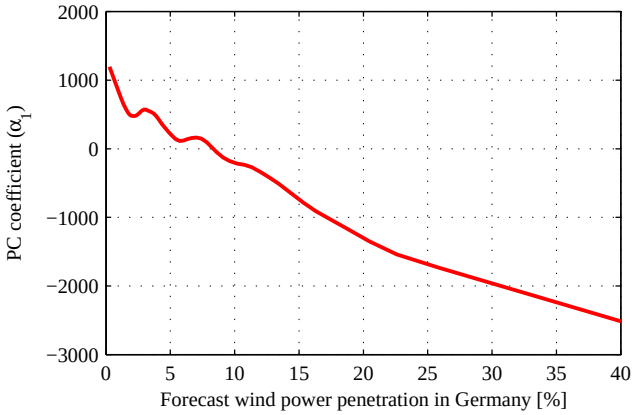

Figure A.2: Regression on the coefficient $\alpha_1(\mathbf{u}_t)$ of the first principal component relative to wind power penetration in Germany

higher $\widehat{r}_t$ in Germany, the lower its import of power[2].

Similar conclusions can be drawn from the regression on the coefficients of the other PCs, which are not shown here. For instance, the value of α_2 rises as $\widehat{r}_t$ increases, indicating an increased flow of power from Germany to the Nordic region and, less markedly, to Switzerland.

Regression curves modeling the behavior of the PC coefficients as a function of the logarithmic spot price in Germany can be obtained in exactly the same fashion. Fig. A.3 shows the α_2 coefficient modeled as a function of this independent variable. The results can again be interpreted quite intuitively. Indeed, the regression curve shows that high values of flow from Germany to Scandinavia are in average achieved with low spot price level at the EEX market. The coefficient then decreases as prices rise in Germany, and its sign changes when $\log(1 + P_t)$ approaches 4.

The approach is easily extendable to the case where the independent variable $\mathbf{u}_t$ is multivariate. Fig. A.4 shows the regression surface modeling $\alpha_1(\mathbf{u}_t)$ as a function of $\mathbf{u}_t = [\widehat{r}_t, h_t]$, where h_t is the day-time. The latter variable appears to influence the coefficient, too, as higher flow values are obtained during hours where consumption peaks. Not surprisingly the decreasing trend relative to

[2]It is to be noted that at this time only qualitative conclusions can be drawn. For example, one cannot distinguish when Germany is importing or exporting. Therefore, the statement could be rephrased to "the higher $\widehat{r}_t$ in Germany, the higher its export of power".

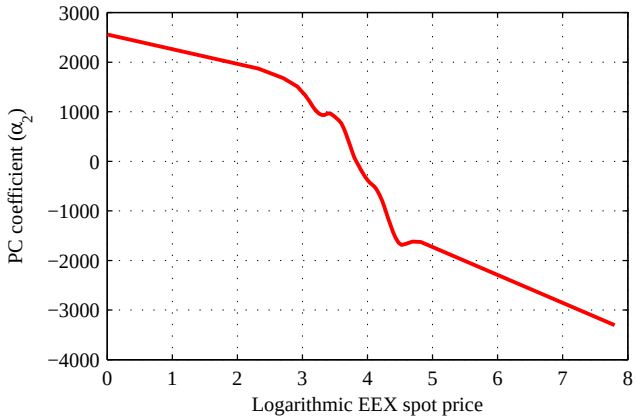

Figure A.3: Regression on the coefficient $\alpha_2(\mathbf{u}_t)$ of the first principal component relative to the logarithm of spot price in Germany

wind power penetration is confirmed at every hour of the day.

A.4.3 Regression curves for power flows

So far only intuitive conclusions based on the structure of the PCs have been drawn, since the regression was carried out on their coefficients α_i. By applying (A.11) it is possible to perform similar analyses on the space of interest, i.e. the original space of power flows. Indeed regression curves or surfaces for the coefficients sum up to curves and surfaces for each single flow.

Fig. A.5 shows the regression for the flow between the Danish DK1 area, i.e. the Jutland peninsula and the Funen island, and Norway (NO). The surface models the relationship between this flow and wind power penetration in Germany as well as day-time. It is seen that, as wind power penetration increases, DK1 passes from importing power from Norway to exporting power. Therefore the statistical model confirms the intuitive economic reasoning according to which the flexible Norwegian hydro plants withhold their production when energy prices are low due to significant wind power penetration, and increase their production when prices are high.

Models for the total net power flow of a country or control area can be determined as the signed sum of the models for individual flows. This can help

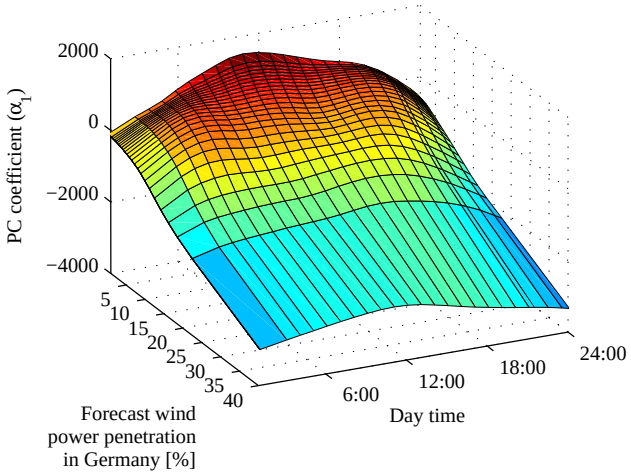

Figure A.4: Regression on the coefficient $\alpha_2(\mathbf{u}_t)$ of the first principal component relative to wind power penetration in Germany and day-time

shed some light on the behavior of individual power systems as a reaction to increased wind power production. Fig. A.6 shows the example of the Austrian power system. It is seen that Austria is on average a net power exporter for low levels of wind power penetration in Germany, while it is a net importer with high wind power penetration. This is partly caused by the flexibility of the Austrian generation portfolio, which is largely dominated by hydro plants. Once more, the statistical model shows how the market pushes hydro power producers to provide arbitrage services as wind power production increases the volatility of market prices.

A.4.4 Sensitivity of the Results to the Presence of Trends

As mentioned in the last paragraph of Section A.3.1, the presence of trends in the dataset might be an important practical issue when performing analyses based on PCA. Indeed, in the latter methodology, defined in Section A.3.1, the dataset is centered by subtracting the mean. When considering long datasets spanning several years, low frequency dynamics ought to be removed from the dataset by employing a low-pass filter.

Some relevant figures for the considered period 2006–2008 in Germany are reported in Table A.2. Such table is useful to get a preliminary assessment of the presence and of the magnitude of trends. Notably, despite a constant increase in

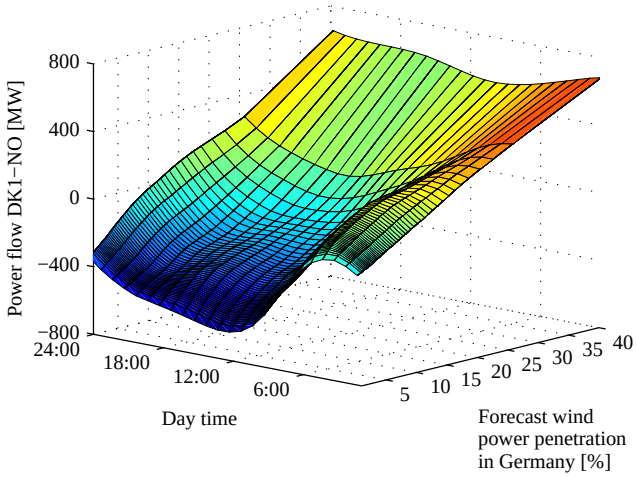

Figure A.5: Regression curve modeling the relationship between the power flow from the continental part of Denmark (the Jutland peninsula and the Funen island, area code DK1) and Norway (NO) as function of wind power penetration in Germany and day-time

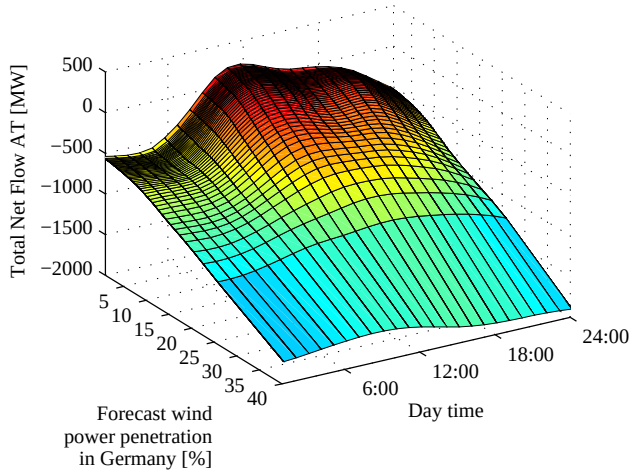

Figure A.6: Regression curve modeling the relationship between the net power flow of Austria as function of wind power penetration in Germany and day-time

installed wind power capacity in the period, the total annual wind power output in Germany declined between 2007 and 2008. Besides, the growth in electricity demand almost stopped between these two years. As a result, the ratio between these two quantities is not monotonic in the considered period.

Table A.2: Total annual wind energy production, total annual load and their ratio in Germany during the period 2006–2008

Quantity	2006	2007	2008
Total wind energy production [TWh]	34.31	42.36	41.67
Total load [TWh]	489.03	496.59	497.61
Ratio	0.0702	0.0853	0.0837

Table A.2 shows no steady, slow-dynamics increase in the ratio between total demand and wind power production, as one may expect intuitively in light of the constant increase in installed wind power capacity. However, the significant swings in total annual wind power production, e.g., between 2006 and 2007, might still impact the analysis. The remainder of this section discusses this impact through a detailed analysis of the models performed on a year-to-year basis.

A measure to validate the models (A.11) obtained for the flows is the Normalized Root Mean Squared Error (NRMSE), which can be calculated for each interconnection j as follows:

$$\mathrm{NRMSE}_j = \frac{\sqrt{\frac{\sum_{t=1}^{T}\left(\widehat{X}_j(\mathbf{u}_t)-X_{j,t}\right)^2}{T}}}{\max_t\{X_{j,t}\}-\min_t\{X_{j,t}\}}\,. \tag{A.13}$$

The value in the numerator in (A.13) is the Root Mean Squared Error (RMSE), i.e., the average squared deviation of the flow model $\widehat{X}_j(\mathbf{u}_t)$ from the actual observations. The term in the denominator is a scaling factor normalizing all the flows to the range of their observations.

In order to assess the impact of trends in the dataset, NRMSE is calculated for each flow in the dataset, first by employing data for the whole period 2006–2008, then considering data for one single year at a time. This can be done simply by modifying the time indices in the sum in (A.13). It should be remarked that the dominating principal components obtained in these studies are consistent throughout the years.

The results of this analysis are shown in Fig. A.7. The average value of NRMSE across the flows is roughly 15-20%. More interestingly, NRMSE seems to be

rather stable across the considered years for each interconnection. This indicates that the impact of trends in the dataset is not so critical for the application considered. Indeed if this were the case, one would expect that the performance of the models would swing significantly across subsets of the dataset.

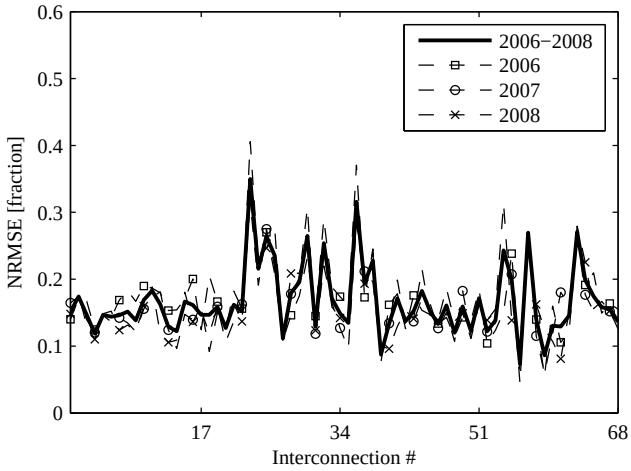

Figure A.7: Normalized Root Mean Squared Error (NRMSE) for every interconnection for the whole 2006–2008 period, and for each year in the period individually

A.4.5 Regional Analysis

The models shown up to this point consent an analysis of the effect of explanatory variables on each individual flow or country. We now group the results obtained for individual interconnections in different geographical regions: North, South, West and East of Germany.

Table A.3 reports the average value of the models for the flows obtained for Northern Europe for values of wind power penetration in Germany from 0% to 25% with step increases of 5%. Spline interpolation of the models at the desired wind power penetration levels was required, due to the definition of the grid in the explanatory variable space, which is based on quantiles. For the sake of consistency, all the flows are directed in the South to North direction (so that negative flows indicate flow of power southwards). The pattern emerging from the analysis is quite clear. At low levels of wind power penetration, Germany is importing power from the Nordic countries through any available in-

Table A.3: Modeled average cross-border flows North of Germany as functions of German wind power penetration

Average Flow	Wind Power Penetration [%]					
[MWh/h]	0	5	10	15	20	25
DE-DK1	-803	-485	-410	-465	-372	-199
DE-DK2	-276	-86	-39	-63	-24	55
DE-SE	-276	-102	-46	-61	-13	67
DK1-NO	-636	-255	-119	-83	40	179
DK1-SE	-228	-54	14	23	64	116
DK2-SE	-510	-117	44	76	210	356

terconnections, where power flows in the North to South direction indeed. This North-South flow tends to drop, though, as wind power penetration increases in Germany. For example, the average flow in the two interconnections between Denmark and Sweden is reversed at a penetration as low as 10%, also due to a likely increased production from the Danish wind turbine fleet. The same trend is seen for all the flows shown in Table A.3. When penetration reaches 25%, power is flowing in the South to North direction in all the interconnections except the one between Germany and DK1, where the percentage of installed wind power on the total production capacity is even higher than in Northern Germany.

Let us now consider the flows directed southwards from Germany, included in Table A.4. It is clear that the higher the wind power penetration in Germany, the more this country exports to its direct neighbors to the South: Switzerland and Austria. As opposed to the situation in the Nordic region, the trend seems to stop at the direct neighbors. Indeed, there is no clear pattern in the interconnection between Switzerland and Italy, which is somewhat stable at 3000 MWh/h. Furthermore, although the power flow between Austria and Italy increases, this trend is marginal due to the low capacity of this line. A possible explanation for this phenomenon is the high installed hydro power capacity in Switzerland and Austria, which confers extra flexibility to their power systems in comparison to e.g. Denmark, which is similarly located in the middle between Germany and the Nordic region. Finally, it appears that there is a loop-flow in the power transit from Germany to Switzerland through Austria, as the flow from the last to the second country is positively correlated with German wind power penetration.

Clear trends emerge as well from the analysis of power flows to the West of Germany in Table A.5. At null wind power penetration in Germany, the Netherlands imports power both from this country and from France through Belgium. When

Table A.4: Modeled average cross-border flows South of Germany as functions of German wind power penetration

Average Flow [MWh/h]	Wind Power Penetration [%] 0	5	10	15	20	25
DE-CH	759	1390	1733	2096	2435	2680
CH-IT	3064	2715	2917	3206	3277	3213
DE-AT	212	423	565	728	930	1136
AT-CH	422	545	618	697	774	836
AT-IT	158	156	161	166	168	168

Table A.5: Modeled average cross-border flows West of Germany as functions of German wind power penetration

Average Flow [MWh/h]	Wind Power Penetration [%] 0	5	10	15	20	25
DE-NL	1583	2131	2316	2498	2580	2582
NL-BE	-352	132	313	568	810	953
BE-FR	-1284	-852	-685	-452	-173	55
DE-FR	-1919	-1571	-1510	-1368	-1175	-1029
DE-CH	759	1390	1733	2096	2435	2680
FR-CH	463	760	916	996	1084	1174

penetration reaches 5%, the Netherlands only import power from Germany on average, as the direction of the flow to Belgium is reversed. In the same fashion, the French export of power to Belgium drops, even turning into a slight import when wind power penetration reaches 25% in Germany. This country imports power from France in all the cases shown in Table A.5, but this import is gradually halved from about 2000 MWh/h to 1000 MWh/h at the extreme columns in the table. This fact disproves the belief that there is a loop flow carrying power from the North to the South of Germany through France, at least on a country level. According to Table A.5, the loop flow appears to be a bit souther than that. Indeed the power flow from France to Switzerland appears to increase as German wind power penetration rises, while at the same time the direct import of Switzerland from Germany is heightened, as we already commented on earlier.

The situation in Eastern Europe is summarized in Table A.6. The trends in this region are more complex, also due to the huge number of cross-border flows. Proceeding in the analysis from North to South, we see that there is an increasing power export from Germany to Poland as wind power penetration

Table A.6: Modeled average cross-border flows East of Germany as functions of German wind power penetration

Average Flow [MWh/h]	Wind Power Penetration [%] 0	5	10	15	20	25
DE-PL	414	414	473	582	660	700
PL-CZ	779	819	885	951	947	888
PL-SK	312	330	375	425	452	451
CZ-DE	877	1033	1026	958	902	852
CZ-AT	589	655	720	799	848	874
CZ-SK	784	680	736	834	865	850
SK-HU	801	897	987	1078	1137	1163
HU-HR	488	614	686	759	826	873
HR-SI	113	381	474	531	597	641
SI-IT	365	477	525	561	577	575
SI-AT	-176	-44	-23	-19	19	68

rises in the former country. Nevertheless, most of the extra power imported by Poland is exported in turn to Slovakia and the Czech Republic. The latter country, a net exporter of energy on average, sees an increasing part of its export shifting to Austria and, to a lesser extent, to Slovakia from Germany, as wind power penetration rises in this country. The increased power imported from North by Slovakia is then exported in the South direction through Hungary and Croatia to Slovenia. Finally it is seen that Slovenia imports less and less power from Austria, and exports more and more power to Italy as the German wind power penetration increases.

A.5 Conclusion

In this work a statistical method for analyzing the impact of wind power in Germany on European cross-border power flows is presented and applied.

The problem dimension is successfully reduced by applying Principal Component Analysis (PCA). Besides, PCA indicates the most important modes of physical power flow in the European system. These modes are the flows carrying power from France to Germany, both directly and through Belgium and the Netherlands, the flow from Germany to Scandinavia and the one from Germany in the South direction. This confirms the centrality of Germany in the study of the European power system.

Local polynomial regression is employed on the PCs both with respect to forecast wind power penetration and spot price in Germany. It is shown that both the external variables have a remarkable impact on the flows. Indeed an increase in forecast wind power penetration causes a fall in the German import of power (or rise in the export), while rising spot prices have the opposite effect. Furthermore, especially in the case of EEX spot price, non-linearities are evident in these relationships.

From a global perspective, it is seen that variations of wind power penetration in Germany have significant effects on power flows in Europe. Indeed import and export patterns between countries change significantly, and loop flows originate. Furthermore, while some of the interconnections benefit from an increasing forecast wind power penetration in Germany, i.e. the ones linking the main average exporters to Germany (France and, at least at low wind power levels, Scandinavia), the stress on other interconnections, e.g. the ones linking Germany to the South of Europe, increases as more and more wind power is produced in Germany. Analyses like the one presented in this paper can contribute to the state-of-the-art by quantitatively assessing such global phenomena, whose understanding is currently limited to a qualitative or intuitive level.

Clearly, the study presented in this paper could be performed thanks to the availability of datasets for wind power production, consumption and power flows, which is in general not straightforward, with the notable exceptions of the PJM market [25] and ENTSO-E [26]. It is hoped that in the near future, convinced by the results of data-driven research studies like this one, TSOs and market operators will strengthen their effort to make more and more datasets of this type available to researchers worldwide.

Possible applications of the methodology proposed in this paper are related to both long- and short-term problems. Long-term problems that could benefit from analyses of this type include decisions on investment in new wind power capacity and in grid expansion. As far as the short-term problems are concerned, this methodology could support the process of scheduling cross-border flows as well as the assessment of risk in interconnected power systems.

The described methodology has been employed for analysis only. In the future though, such a modeling approach could also be used in connection with power system models or forecasting tools. Such tools would have to be calibrated with the results of data-driven analysis, as the one shown in this paper, for simulating European power flows as a function of appropriate explanatory variables, which could include the nominal power capacity of a certain country, market prices, etc.

Acknowledgment

The authors gratefully acknowledge Austrian Power Grid AG (APG) for the support through the project "Impact of Stochastic Generation on EU Cross-border Flows". The European Network of Transmission System Operators for Electricity (ENTSO-E) is also acknowledged for its role in providing the dataset. Furthermore, we would like to thank the Editor of this Journal and three anonymous referees for providing constructive comments that undoubtedly contributed to improving the quality of this manuscript. Finally, we thank Peter Meibom for his valuable comments on this work.

References A

[1] P. Morthorst, S. Ray, J. Munksgaard, and A. F. Sinner, "Wind energy and electricity prices," tech. rep., European Wind Energy Association, 2010. http://www.ewea.org/fileadmin/ewea_documents/documents/publications/reports/MeritOrder.pdf.

[2] P. Giabardo, M. Zugno, P. Pinson, and H. Madsen, "Feedback, competition and stochasticity in a day ahead electricity market," *Energy Economics*, vol. 32, no. 2, pp. 292–301, 2010.

[3] T. Jónsson, P. Pinson, and H. Madsen, "On the market impact of wind energy forecasts," *Energy Economics*, vol. 32, no. 2, pp. 313–320, 2010.

[4] H. Abildgaard, D. Klaar, B. Kriszak, J. Rodriguez, and W. Winter, "European Wind Integration Study (EWIS) – Reference study towards a successful integration of wind power into European electricity grids," in *Proceedings of CIGRE Session*, (Paris, France), 2008.

[5] "ENTSO-E pilot ten years network development plan," tech. rep., ENTSO-E, 2010. https://www.entsoe.eu/fileadmin/user_upload/_library/SDC/TYNDP/TYNDP-final_document.pdf.

[6] A. Costa, A. Crespo, J. Navarro, G. Lizcano, H. Madsen, and E. Feitosa, "A review on the young history of the wind power short-term prediction," *Renewable and Sustainable Energy Reviews*, vol. 12, no. 6, pp. 1725–1744, 2008.

[7] G. Giebel, R. Brownsword, G. Kariniotakis, M. Denhard, and C. Draxl, "The state-of-the-art in short-term prediction of wind power : A literature overview, 2nd edition," tech. rep., ANEMOS.plus, 2011. http://www.prediktor.dk/referenc.htm.

[8] G. Giebel, "A variance analysis of the capacity displaced by wind energy in europe," *Wind Energy*, vol. 10, no. 1, pp. 69–79, 2007.

[9] U. Focken, M. Lange, K. Mönnich, H.-P. Waldl, H. G. Beyer, and A. Luig, "Short-term prediction of the aggregated power output of wind farms–a statistical analysis of the reduction of the prediction error by spatial smoothing effects," *Journal of Wind Engineering and Industrial Aerodynamics*, vol. 90, no. 3, pp. 231–246, 2002.

[10] F. van Hulle, P. Kreutzkamp, and S. Uski-Joutsenvuo, "Enhancing cross border exchange to facilitate wind power integration at European scale," in *Proceedings of German Wind Energy Conference (DEWEC)*, (Bremen, Germany), nov 2008.

[11] J. Tande, M. Korpås, L. Warland, K. Uhlen, and F. van Hulle, "Impact of TradeWind offshore wind power capacity scenarios on power flows in the European HV network," in *Proceedings of the 7th International Wind Integration Workshop*, (Madrid, Spain), may 2008.

[12] S. Hagspiel, A. Papaemannouil, M. Schmid, and G. Andersson, "Copula-based modeling of stochastic wind power in Europe and implications for the Swiss power grid," *Applied Energy*, vol. 96, pp. 33–44, 2012.

[13] N. A. Cutululis, P. Sørensen, G. Giebel, M. Korpås, and L. Warland, "Uncertainty on predicted cross border flows caused by wind forecast errors," in *Proceedings of the 7th International Wind Integration Workshop*, (Madrid, Spain), may 2008.

[14] B. Klöckl and P. Pinson, "Effects of increasing wind power penetration on the physical operation of large electricity market systems," in *Integration of Wide-Scale Renewable Resources Into the Power Delivery System, CIGRE/IEEE PES Joint Symposium*, 2009.

[15] "Energy concept for an environmentally sound, reliable and affordable energy supply," tech. rep., Federal Ministry of Economics and Technology (BMWi), 2010. `http://www.bmwi.de/English/Navigation/Service/publications,did=367764.html`.

[16] "Final report system disturbance on 4 November 2006," tech. rep., UCTE, 2007. `https://www.entsoe.eu/resources/publications/former-associations/ucte/other-reports/`.

[17] DEWI, "Statistics archive." Online, 2012. `http://www.dewi.de/dewi/index.php?id=47&L=%5C%5C%5C%27`.

[18] A. León and A. Rubia, *Modelling prices in competitive electricity markets*, ch. 8, pp. 177–189. Wiley & Sons, 2004.

[19] R. Weron, *Modeling and Forecasting Electricity Loads and Prices–A statistical Approach*, ch. 4. Wiley, 2006.

[20] W. Cleveland and S. Devlin, "Locally weighted regression: An approach to regression analysis by local fitting," *Journal of the American Statistal Association*, vol. 83, no. 403, pp. 596–610, 1988.

[21] A. C. Rencher, *Multivariate statistical inference and applications*, ch. 9. Wiley-Interscience, 1998.

[22] A. Hyvärinen, J. Karhunen, and O. Erkki, *Independent Component Analysis*. Wiley, 2001.

[23] D. S. Wilks, *Statistical methods in the atmospheric sciences, 2nd edition*, vol. 91 of *International Geophysics*, ch. 11, pp. 469–471. Elsevier Academic Press, 2006.

[24] H. Madsen, *Time series analysis*, ch. 3. Chapman & Hall/CRC, 2008.

[25] PJM Electricity Market. Website, 2012. `http://www.pjm.com/home.aspx`.

[26] ENTSO-E. Website, 2012. `http://www.entsoe.net/default.aspx`.

Paper B

Statistical Analysis of the Impact of Wind Power on Market Quantities and Power Flows

Authors:
Pierre Pinson, Tryggvi Jónsson, Marco Zugno, Juan Miguel Morales, Henrik Madsen

Presented at:
IEEE Power and Energy Society General Meeting 2012

Statistical Analysis of the Impact of Wind Power on Market Quantities and Power Flows

Pierre Pinson[1], Tryggvi Jónsson[2], Marco Zugno[1], Juan Miguel Morales[3], Henrik Madsen[1]

Abstract

In view of the increasing penetration of wind power in a number of power systems and markets worldwide, we discuss some of the impacts that wind energy may have on market quantities and cross-border power flows. These impacts are uncovered through statistical analyses of actual market and flow data in Europe. Due to the dimensionality and nonlinearity of these effects, the necessary concepts of dimension reduction using Principal Component Analysis (PCA), as well as nonlinear regression are described. Example application results are given for European cross-border flows, as well as for the impact of load and wind power forecasts on Danish and German electricity markets.

B.1 Introduction

Wind power capacities are rapidly expanding in a number of countries, maybe most noticeably in Europe, the US and China. This is facilitated by direct and indirect incentives, for instance in the form of feed-in tariffs or of prioritization in electricity pools. Both variability and limited predictability of that renewable energy source will yield a radical shift in the paradigms of power systems management. The parallel development of other forms of renewable energy e.g. solar and wave, may contribute to dampen or inversely magnify the undesirable effects of wind power on the physical operation of power systems as well as market characteristics. A recent status of the deployment of renewable energy capacities worldwide is available in [1].

[1]DTU Informatics, Technical University of Denmark, Richard Petersens Plads, bld. 305, DK-2800 Kgs. Lyngby, Denmark

[2]ENFOR A/S, Lyngsø Allé 3, DK-2970 Hørsholm, Denmark

[3]Centre for Electric Power and Energy, Technical University of Denmark, Elektrovej, bld. 325, DK-2800 Kgs. Lyngby, Denmark

Electricity network and markets were designed based on a long history of dealing with various forms of dispatchable generation, for which the concepts of unit commitment, economic dispatch, contingency analysis made sense in view of the technical characteristics of the physical units. The increasing penetration of wind power challenges these practices, owing to its impact on market quantities and cross-border flows. As an illustrative example, the impact of wind power predictability is now regularly accounted for in network expansion and future offshore grid studies [2, 3]. It is of utmost importance to properly characterize and model the effects of wind on markets and power flows before we may be able to project ourselves in the future with scenarios of substantial renewable energy penetration. For the example of Denmark, the objective is to have 50% of the electricity consumption met by wind energy by 2025 [4]. This has triggered a number of technical and economical analyses focused on market value, investment and power flows, as in [5] for instance. Note that game-changers may also appear, most likely in the form of various forms of demand-side management [6].

Both meteorological and economical effects are at the roots of this impact: *(i)* wind power generation over a region is directly influenced by the geographical coverage of weather systems, while *(ii)* wind energy has a direct consequence on market quantities due to the so-called merit-order effect which places wind at the very left of the market supply curves. Complex network effects then add on to yield the final power flows. In view of the complexity brought in by all these combined aspects, system studies of the effect of wind on market quantities and power flows may necessitate relying on crude simplifications and on simulations. Recent examples of these detailed system studies partly based on simulations include [7] for the case of the UK system in 2020 and [8] concentrating on the Swiss power system at the horizon 2030. Toy model simulations can actually highlight some of the effects of wind on electricity markets, as in [9]. Simplified system and toy models may however mask some of the effects that are aimed at being uncovered. This is the reason why inversely, statistical *ex-post* analyses of some of the key variables can already give a fair picture, without looking at a complete modeling of all meteorological, market and network effects. Example statistical analyses of market quantities were for instance performed in [10, 11] and [12] for the case of the Danish and Spanish electricity markets, respectively.

In this paper, we review the methodological aspects necessary for the statistical analysis of the impact of wind power on market quantities and power flows (Section B.2). Especially, we insist on the nonlinear nature of this impact, and on its potential nonstationarity. In parallel, owing to the potentially large dimensions of datasets to be analysed, we also discuss dimension reduction (based on Principal Component Analysis) that may prove necessary when looking at power flows over the whole electricity network of a region. Subsequently, an example application to the case of the Nord Pool (Western Denmark control zone - DK1) and EEX (Germany) markets considered in Section B.3. Similarly

in Section B.4, we look at the case of power flows related to the Austrian control block, and of cross-border power flows over the whole ENTSO-E (European Network of Transmission System Operators for Electricity) system. The paper finally ends in Section B.5 with conclusions, implications of the findings, as well as perspectives for future work.

B.2 Methodological aspects

In this Section we review some statistical modeling concepts necessary for the various applications covered in the following, that is, the impact of wind on both market quantities and power flows. These concepts include nonlinear regression based on local polynomial models, as well as PCA for dimension reduction.

B.2.1 Nonlinear regression with local polynomial models

Whatever the variables of interest, the set of observations consists of time-series of measurements. We denote by $\{y_t\}$, $t = 1, \ldots, T$, the observed time-series for the response variable, and by $\mathbf{x}_t^\top = [x_t^1 \ldots x_t^i \ldots x_t^m]$ the vector of m explanatory variables at time t. In a practical setup, the response variable may be the day-ahead electricity price or the overall system balance of a TSO's network, and generated wind power the explanatory variable for instance.

The relationship between explanatory and response variables is written in the form of a general regression model,

$$y_t \;=\; \theta(\mathbf{x}_t) + \epsilon_t, \qquad t = 1, \ldots, T. \tag{B.1}$$

The noise term $\{\epsilon_t\}$, $i = 1, \ldots, T$, is a sequence of independent and identically distributed (i.i.d.) random variables with unknown distribution F. It is assumed that F has a zero mean and a finite variance σ_ϵ^2. In general, it is assumed that both $\mathbf{x}$- and y-values can be normalized. Therefore, they are all contained in the unit interval, while $\epsilon_t \in [-1, 1]$, $\forall t$.

Based on the concept of local polynomial regression, it is assumed that θ may be locally approximated by k-order polynomials. Most common instances of local polynomial regression include kernel smoothing ($k = 0$) and local linear regression ($k = 1$). Note that in practice, the curse of dimensionality imposes that the dimension of $\mathbf{x}$ has to be low, say less than 3 (for a discussion on that issue, see [13, pp. 83-84]).

θ is approximated at a number of fitting points, chosen based on a rule of thumb or after consideration of the data distribution. Let us focus on a single fitting point $\tilde{\mathbf{x}} = [\tilde{\mathbf{x}}^1, \ldots, \tilde{\mathbf{x}}^m]$ only. The k-order local polynomial approximation $\mathbf{z}_t$ of the vector of explanatory variables $\mathbf{x}_t$ is given by:

$$\mathbf{z}_t^\top = \mathbf{p}_k^\top(\mathbf{x}_t). \tag{B.2}$$

For instance if $k = 1$, $\mathbf{p}_1(\mathbf{x}_t) = [1 \;\; \mathbf{x}_t]$.

In parallel, write $\underline{\boldsymbol{\theta}}$ the vector of local coefficients at $\tilde{\mathbf{x}}$, so that locally at $\tilde{\mathbf{x}}$ one obtains the following linear model

$$y_t = \mathbf{z}_t^\top \underline{\boldsymbol{\theta}}, \quad t = 1, \ldots, T, \tag{B.3}$$

which is then fitted by minimizing a weighted loss of the form

$$\hat{\underline{\boldsymbol{\theta}}} = \arg\min_{\underline{\boldsymbol{\theta}}} \sum_{t=1}^{T} w_t \rho(y_t - \mathbf{z}_t^\top \underline{\boldsymbol{\theta}}) \tag{B.4}$$

with the w_t weights assigned by a Kernel function, i.e.

$$w_t = K(\mathbf{x}_t, \tilde{\mathbf{x}}) \;\; = \;\; \prod_i \omega\left(\frac{|x_t^i - \tilde{x}^i|_i}{h^i}\right). \tag{B.5}$$

In the above, $|.|_i$ denotes a chosen distance on the i-th dimension of $\mathbf{x}$ (typically the Euclidean distance), and $\mathbf{h} = [h^1 \;\; \ldots \;\; h^m]$ is the bandwidth for that particular fitting point $\tilde{\mathbf{x}}$. As an example, ω can be defined as a tricube function,

$$\omega(v) = \begin{cases} (1 - v^3)^3, & v \in [0, 1] \\ 0 \qquad\quad , & v > 1 \end{cases}, \tag{B.6}$$

as introduced and discussed in e.g. [14]. This type of estimation procedure may also be made adaptive in order to account for smooth temporal changes in the regression, if aiming at accounting for seasonal variations in the effects of interest for instance. The weights in Eq. (B.4) would then include a time decay, e.g. in the form of exponential forgetting, in order to gradually discount older observations.

For the fitting of these local linear models, the type of regression will decide upon the loss function to be minimized. In the case where the mean effect is to be modelled, they are to be fitted using weighted least-squares. ρ then takes the form of a quadratic loss function, such that

$$\rho(\epsilon) = \epsilon^2/2. \tag{B.7}$$

If aiming to perform quantile regression instead, for a given nominal proportion τ, $\tau \in [0,1]$, one chooses an asymmetric piecewise linear loss function ρ_τ as

$$\rho_\tau(\epsilon) = \begin{cases} (\tau-1)\epsilon, & \epsilon < 0 \\ \tau\epsilon & , \ \epsilon > 0 \end{cases} . \tag{B.8}$$

For an overview of the theory and application of quantile regression, we refer to [15].

Finally when the local coefficients are calculated at all fitting points, the complete coefficient functions $\hat{\boldsymbol{\theta}}(\mathbf{x})$ can be obtained by linear or spline interpolation of the local coefficients. This will be illustrated in the example applications below.

B.2.2 Generalization to higher dimensions using Principal Component Analysis (PCA)

The case of a single response variable was considered so far only. This setup may be suitable if looking at the impact of one or more variables (say, wind and load) on day-ahead market prices. If concentrating however on the effect of wind power on a set of variables over a network e.g. power flows, the dimension n of the response variable will be greater than 1, and potentially very large. The model of Eq. (B.1) therefore needs to be generalized as

$$\mathbf{y}_t \ = \ \theta(\mathbf{x}_t) + \epsilon_t, \qquad t = 1, \ldots, T, \tag{B.9}$$

where $\mathbf{y}_t = [y_t^1 \ \ldots \ y_t^n]$ is now a multivariate response.

In order to ease the estimation of the coefficient functions θ, a first necessary step consists in reducing the dimension of the problem. This is done here in a PCA framework, by summarizing the information from the n-dimensional response in a q-dimensional basis of Principal Components (PCs), $q << n$. These PCs are chosen so that they maximize their ability to explain the variance of the original multivariate response. For an overview of PCA, of the properties of the PCs, and more generally of multivariate data analysis, we refer to [16]. A more applied introduction focused on atmospheric sciences can be found in [17]. In the power systems literature, PCA for dimension reduction was for instance employed in [18] for studying spatially distributed wind power generation in Ireland.

Before to apply the PCA itself, the multivariate response is first centred and normalized. The benefits of such preprocessing are discussed in [17]. Subsequently,

finding the PCs for the multivariate response $\mathbf{y}$ is performed by diagonalizing the covariance matrix of the data,

$$\mathbf{R}_y = \frac{1}{T}\sum_{t=1}^{T} \mathbf{y}_t \mathbf{y}_t^\top. \tag{B.10}$$

After diagonalizing, the PCs are obtained as the eigenvectors of $\mathbf{R}_y$ with the largest corresponding eigenvalues. The number of PCs to be selected is decided upon through graphical and/or numerical methods [16]. The ratio of the sum of the selected eigenvalues over that for all eigenvalues gives the share of the variance in the response data explained by these PCs. In the following we will use the average eigenvalue method for PC selection, as in [19]. We denote by $\tilde{\mathbf{y}}_j$, $j = 1, \ldots, q$ the obtained PCs ($q << n$). All observed values $\mathbf{y}_t$ for the response variables can consequently be written as a linear combination of the PCs,

$$\mathbf{y}_t = \sum_{j=1}^{q} \alpha_t^j \tilde{\mathbf{y}}_j + \nu_t, \quad \forall t, \tag{B.11}$$

with an additional random noise ν_t originating from the unexplained variance in the data. A projection operator $\mathbf{P}$ can then be introduced, permitting to project the original response into the space spanned by the PCs,

$$\mathbf{P} = [\tilde{\mathbf{y}}_1 \ \ldots \ \tilde{\mathbf{y}}_q]. \tag{B.12}$$

$\mathbf{P}$ allows projecting standardized response values $\mathbf{y}_t$ in the basis defined by the principal components, since Eq. (B.11) can be rewritten as

$$\mathbf{y}_t = \mathbf{P}^\top \boldsymbol{\alpha}_t + \nu_t, \quad \forall t, \tag{B.13}$$

with $\boldsymbol{\alpha}_t = [\alpha_t^1 \ \ldots \ \alpha_t^q]$.

Finally by combining the models of Eqs. (B.9) and (B.11), one obtains

$$\mathbf{y}_t = \sum_{j=1}^{q} \theta(\mathbf{x}_t)\tilde{\mathbf{y}}_j + \varepsilon_t, \qquad t = 1, \ldots, T, \tag{B.14}$$

where the noise ε_t combines the original noise from the regression model with the additional one coming from the PCA decomposition. In other words in the basis formed by the PCs, the coefficients $\boldsymbol{\alpha}_t$ are replaced by coefficient functions of the explanatory variables $\mathbf{x}$ similar to that of Eq. (B.1). These coefficient functions can be estimated in the same fashion as in Section B.2.1.

B.3 Application to electricity market quantities

A first and highly relevant application to the methodology presented for uncovering the nonlinear effect of wind power on some response variable consists in looking at the effect of wind power on prices in electricity markets. This effect was first looked at in [10], which attempted to find a linear relationship between observed wind power generation and prices in the Nord Pool day-ahead market in Western Denmark. Since then, [11] argued that *(i)* the relationship of interest is actually between day-ahead prices and the predicted values for load and wind power, while *(ii)* such a relationship is most surely nonlinear. These aspects are discussed below, after introducing the set of available data.

B.3.1 Available data

For this study of the impact of wind power on electricity market quantities, focus is given to two markets highly penetrated by wind energy, namely the Nord Pool and EEX ones. More precisely, the Western Denmark area of the Nord Pool (often referred to as DK1) is looked at since corresponding to the control zone with the highest wind power penetration (more than 20% of the energy consumption met by wind energy). Long records of market quantities (day-ahead and imbalance prices, imbalance sign, etc.) are available for those markets.

In parallel in both cases, relevant forecast and measured data are freely available at the websites of the corresponding network operators. Energinet.dk is the TSO in Denmark. In Germany, only the wind information at the control zones of RWE, Eon and Vattenfall is considered, since accounting for most of the wind capacities. Overall, the data include day-ahead wind power forecasts, as well as measured wind power generation and load. We simulate the availability of load forecasts by adding noise to the measurements, with a variance consistent to reported accuracy of load forecasts for a country today (between 2 and 4% Mean Average Percent Error - MAPE).

Overall, the data for the Danish test case cover a period from the 1^{st} of January 2008 to the 13^{th} February 2008, while those for Germany are for the two years of 2006-2007.

B.3.2 Sample results focused on day-ahead prices

We follow the argument of [11] such that the predicted values for the load and the wind power generation are those that impact the day-ahead prices in these electricity markets. This argument is directly motivated by their clearing mechanism based on bids that are in turn based on predictions.

We first work with a single explanatory variable only, the predicted wind power penetration, defined as the ratio of wind power and load forecasts. It represents the foreseen share of wind in the day-ahead electricity mix at the time of market clearing and for each time unit over the following day. The response variable is the corresponding day-ahead price for every time unit. The scatter plots representing the empirical relationship between these explanatory and response variables in the Nord Pool and EEX markets are gathered in Fig. B.1.

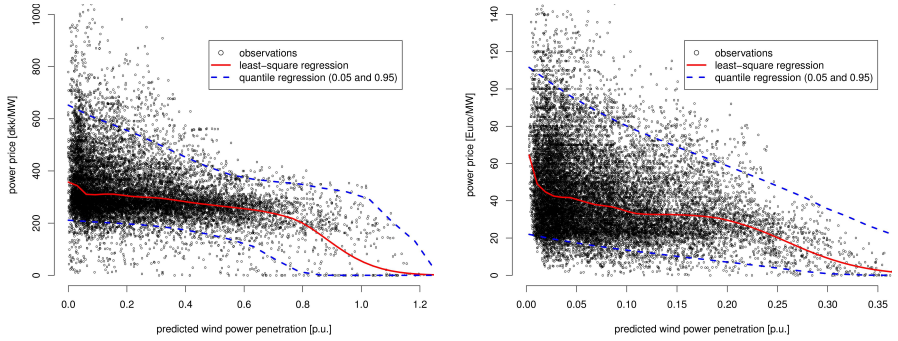

(a) Nord Pool, Western Denmark area (DK1) - 1.1.2008 to 13.2.2010

(b) EEX - 1.1.2006 to 31.12.2007

Figure B.1: The relationship between predicted wind power penetration and the day-ahead market prices in the Nord Pool and EEX day-ahead markets.

Local polynomial regression is employed for characterizing the evolution of day-ahead prices as a function of predicted wind power penetration. On the one hand, the least-square fitting gives the mean trend, while on the other hand quantile regression with nominal proportions $\tau = 0.05$ and $\tau = 0.95$ yields prediction intervals with a 90% nominal coverage rate. Note that for this response variable the data are log-transformed before fitting the regression models, even though the results are presented in the original space of the variable. We use 30 fitting points, with a nearest-neighbour bandwidths covering local neighborhoods corresponding to 10% of the data.

The mean trend is qualitatively similar for both markets, with day-ahead prices

decreasing with increasing predicted wind power penetration, even though there may be some quantitative differences. Maybe the most important one is that the day-ahead price appears to tend more rapidly towards 0 in the EEX market, already at around 35% predicted wind power generation, while it is only the case in Denmark when this explanatory variable gets closer to 100% penetration. The bands given by quantile regression also illustrate how the price variability and convergence towards 0 differ for the two markets.

To further detail the dependence between day-ahead prices and predicted load and wind power generation, the local polynomial regression approach is upgraded so that both predicted variables are simultaneously seen as explanatory ones ($m = 2$). We use 20 fitting points for each variable (leading to a total of 400 fitting points), with a nearest-neighbour bandwidths covering local neighborhoods corresponding to 20% of the data. The resulting smooth surface is depicted in Fig. B.2 for DK1 and for least-square regression only. It confirms the joint role of predicted load and wind power: the former induces an upward pressure on prices, while the latter pushes them back down, the impact of wind being greater at lower load values.

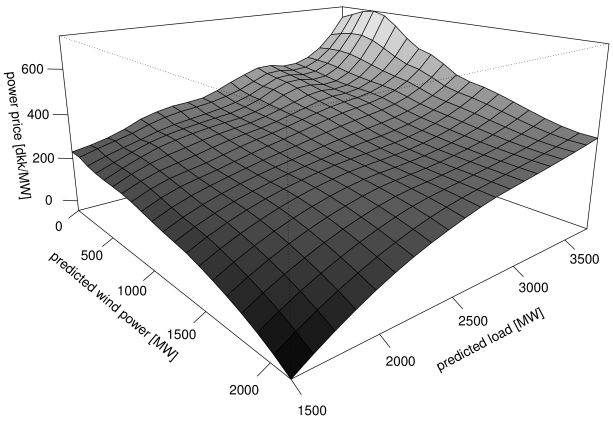

Figure B.2: The relationship between predicted wind power generation, predicted load, and the day-ahead market prices in the Nord Pool day-ahead market, Western Denmark area (DK1), 1.1.2008 to 13.2.2010.

Similar analysis may be performed for other market quantities and other markets, with focus on the various moments of their distributions. The uncovered dependencies may then be used as additional knowledge for the building of relevant forecast methodologies of market quantities. Example recent works in that direction include [20] focusing on the prediction of day-ahead prices accounting

for wind power predictions, and [21] looking at the specific case of imbalance sign characterization and prediction.

B.4 Application to power flows

A second relevant application of the statistical approaches described in the present paper relates to the analysis of power flows within and over one or more control zones. The results we gather and discuss in the following are based on some of the data and work of [22] for the analysis of power flows related to the Austrian control block, and of [19] for the analysis of cross-border power flows over the whole ENTSO-E system. For confidentiality reasons, some of the results may not be detailed.

B.4.1 Example focus on the Austrian control block

The underlying motivation of the work performed in [22] was to perform an *ex-post* analysis of available power flow data within Austria, as well as of cross-border power flows, in relation with some of the publicly available data from EEX and the German TSOs. These data basically are the same than those considered in Section B.3.2, i.e. wind power forecasts, wind power and load measurements, as well as all market quantities. They cover the period of 2006-2007. A basic question to be answered is how much the German wind power and market influence the power flows experienced by the Austrian TSO.

The Austrian control block is operated by the TSO APG (Austrian Power Grid), for an installed generation capacity of more than 19 GW (12 GW in hydro power units), while the maximum load is less than 10 GW. This control zone is physically linked to six different control blocks and a total of nine control zones. Two independent analyses were performed focused on *(i)* all the cross-border flows, and *(ii)* the power flows over 23 400kV-systems throughout Austria, in order to uncover the impact of German wind and market quantities on all these power flows. Dimension reduction was necessary in the latter case: most of the variance in the power flows of the 23 400kV-systems could be explained with 4 PCs only.

Let us give here a set of results focusing on the impact of predicted wind power penetration in Germany and of day-ahead prices in the EEX market on the APG net balance. This contrasts with the more detailed analysis of individual cross-border and 400kV-systems power flows which can be found in [22]. The

APG net balance is calculated as the sum of all power export minus the sum of all import at a given time. It is expressed here in MW. Fig. B.3 gathers the scatter plots for that analysis, while depicting the regression curves for the mean effect (least-square regression), as well as 90% prediction intervals defined by the quantile regression curves with nominal proportions of 0.05 and 0.95.

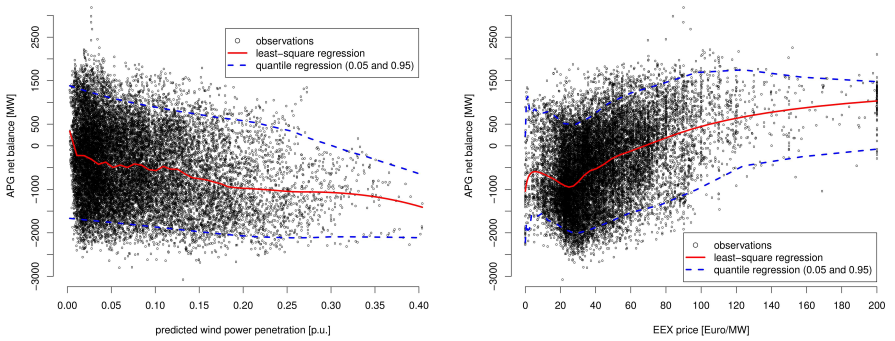

(a) Predicted wind power penetration in Germany

(b) EEX day-ahead prices

Figure B.3: The impact of predicted wind power penetration in Germany and the EEX day-ahead prices on the APG net balance over 2006-2007.

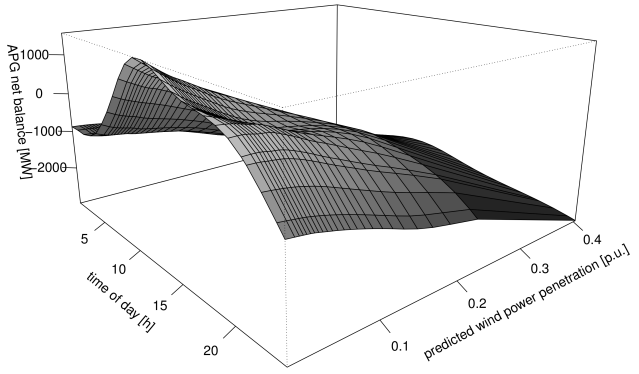

Figure B.4: The impact of predicted wind power penetration in Germany on the APG net balance over 2006-2007, as function of the time of the day.

The plots in Fig. B.3 reveals that the Austrian control block tends to export

more as the EEX price gets higher, but also to import more as the predicted wind power penetration in Germany is greater. Actually the mean trend is that Austria only imports when there is almost no wind power penetration in Germany. One also observes that obviously these are trends only, with large intervals around this mean trend, showing that other effects are to be accounted for. For instance, it may be crucial to account for daily and seasonal variations in the power flow patterns. This is illustrated by Fig. B.4 which depicts the mean impact of predicted wind power penetration in Germany on the total balance of the APG control block, also as a function of the time of the day. It shows how Austria has a typical cycle of importing at night and exporting during the day, when there is no or almost no wind power penetration in Germany. As this wind power penetration increases, even though there still are variations over the day, the Austrian control block tends be in an import situation at any hour of the day. In general, we have observed that it is highly beneficial to account for potential diurnal and seasonal variations in our analysis of power flows.

B.4.2 General results related to ENTSO-E system

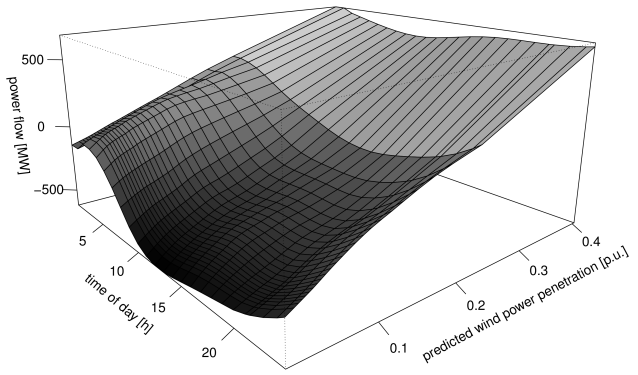

Figure B.5: The impact of predicted wind power penetration in Germany on cross-border power flows between DK1 and Norway over 2006-2008.

The type of study performed for the Austrian control block was generalized to the whole ENTSO-E system. The dataset there consists of hourly cross-border power flows between 34 European and bordering extra-European countries, over a 3 year period covering 2006 to 2008. After quality check, the study is restricted to 68 cross-border interconnections. The overall question studied is similar to the

above section, i.e. related to the impact of German wind and market quantities on the whole set of European cross-border flows. The analysis performed is fully covered by [19].

For this dataset, 8 PCs were deemed enough to represent the overall dynamics of the cross-border power flows over the ENTSO-E system, explaining 82% of the original variance in the data. Local polynomial models were then used on the PCs, conditioned by the predicted wind power penetration in Germany, EEX day-ahead prices, as well as the time of the day.

Out of the extensive analysis covered, let us show an illustrative example results in Fig. B.5, which depicts the impact of predicted wind power penetration in Germany on cross-border power flows between DK1 and Norway over 2006-2008. As wind power penetration is predicted to be greater in Germany, the situation switches from DK1 importing power from Norway to exporting. Consistent behaviour was observed at the interconnection between DK1 and Germany. This is in line with intuitive economic reasoning, such that an hydro-dominated control zone like the Norwegian one tend to withhold production when energy prices are low due to significant wind power penetration, and inversely increase production when prices are high. This result is in fact similar to that of Fig. B.4 for the case of Norway. A noticeable difference though is that Austria is directly interconnected to the German network, while it is not the case of Norway. Overall in view of the work of [19], the data available today permits to quantify how much German wind and market quantities impact cross-border flows over the whole ENTSO-E system. The identified PCs may be seen as modes of propagation of power flows, which are more of less stimulated depending on various explanatory variables. This analysis may be refined in the future by also accounting for wind and market-related variables in other countries as well.

B.5 Conclusions

The effect of wind power generation on electricity markets and power flows is recognized but not always understood and quantified. Owing to the potential complexity of modelling all meteorological, economical and network aspects involved, we suggest that an interesting alternative to full system studies consists in performing statistical *ex-post* analyses of the datasets available at market and network operators. When acknowledging the potentially nonlinear and nonstationary impact of wind power on these quantities, the regression techniques (and related estimation concepts) come fairly natural. Also the issue of the dimensionality of the dataset involved may be dealt with based on statistical dimension reduction techniques e.g. the PCA approach employed here.

It is not possible to cover in a single paper all the analyses that could be performed based on the datasets available. We have therefore pointed at further reading for more extensive studies. Overall, it appears that load and wind power forecast have a significant impact on today's market quantities. This impact can be characterized as nonlinear and nonstationary, and quantified through appropriate statistical regression techniques. Similarly, these variables, or the market price used as a proxy, highly influence power flows within and between control zones. This effect was evidenced and modeled for the case of the APG control block, as well as for the all interconnectors of the ENTSO-E system. Note that the impact of forecast errors should also be thoroughly studied, as they are known to induce unscheduled power exchanges.

Here only the effect of some explanatory variables e.g. predicted wind power generation, on market quantities and power flows was considered. Interestingly, the time dimension could also be accounted for in a straightforward manner by generalizing the methodological concepts presented in a time-varying regression framework. This would then permit to *(i)* assess the way uncovered effects evolved over the past years, for instance as a function of installed wind capacities, and *(ii)* tentatively predict what the future effects of more substantial renewable energy penetration levels on electricity markets and power flows may be. Obviously, these predictions would be based on stationarity assumptions, which would be very weak in view of the non-negligible changes to be expected in market and power systems operations in the foreseeable future.

Such a statistical approach should be considered as part of, or jointly with, other system studies. They can provide valuable insight to TSOs and policy makers, while allowing market participants to refine their forecasting and participation strategies. Note that importantly, it is the spatio-temporal dynamics of all types of renewable energy sources that should be seen as explanatory variables in the future, in view of the future plans for deployment of renewable energy capacities.

Acknowledgment

This work was partly supported by the European Cost Action "WIRE: Weather Intelligence for Renewable Energies" (ES1002), and by the Austrian Power Grid through the project "Impact of Stochastic Generation on EU Cross-border Flows". The European Network of Transmission System Operators for Electricity (ENTSO-E), APG, Energinet.dk and Nord Pool A/S are also acknowledged for their role in providing the dataset.

References B

[1] REN11, "Renewable 2011 — Global status report," tech. rep., Renewable Energy Policy Network for the 21st Century, 2011. `http://www.ren21.net`.

[2] T. Trötscher and M. Korpås, "A framework to determine optimal offshore grid structures for wind power integration and power exchange," *Wind Energy*, vol. 14, no. 8, pp. 977–992, 2011.

[3] J. O. G. Tande, M. Korpås, L. Warland, K. Uhlen, and F. Van Hulle, "Impact of TradeWind offshore wind power capacity scenarios on power flows in the European HV network," in *7th International Workshop on Large-Scale Integration of Wind Power and on Transmission Networks for Offshore Wind Farms, Madrid, Spain, May*, 2008.

[4] EA Energy Analyses, "50% wind power in Denmark by 2025 — English summary," tech. rep., EA Energy Analyses, Copenhagen, Denmark, 2007. `http://www.ea-energianalyse.dk/reports`.

[5] H. H. Lindbo, "50% wind in Denmark 2025 — A technical economical analysis." *IEA workshop* (technical presentation), 2007.

[6] G. Strbac, "Demand side management: Benefits and challenges," *Energy Policy*, vol. 36, no. 12, pp. 4419–4426, 2008.

[7] A. Gerber, M. Qadrdan, M. Chaudry, J. Ekanayake, and N. Jenkins, "A 2020 GB transmission network study using dispersed wind farm power output," *Renewable Energy*, vol. 37, no. 1, pp. 124–132, 2012.

[8] S. Hagspiel, A. Papaemannouil, M. Schmid, and G. Andersson, "Copula-based modeling of stochastic wind power in Europe and implications for the Swiss power grid," *Applied Energy*, 2011.

[9] P. Giabardo, M. Zugno, P. Pinson, and H. Madsen, "Feedback, competition and stochasticity in a day ahead electricity market," *Energy Economics*, vol. 32, no. 2, pp. 292–301, 2010.

[10] P. E. Morthorst, "Wind power and the conditions at a liberalized power market," *Wind Energy*, vol. 6, no. 3, pp. 297–308, 2003.

[11] T. Jónsson, P. Pinson, and H. Madsen, "On the market impact of wind energy forecasts," *Energy Economics*, vol. 32, no. 2, pp. 313–320, 2010.

[12] L. Gelabert, X. Labandeira, and P. Linares, "An ex-post analysis of the effect of renewables and cogeneration on Spanish electricity prices," *Energy Economics*, vol. 33, pp. 59–65, 2011.

[13] T. J. Hastie and R. J. Tibshirani, *Generalized Additive Models*, vol. 43. Chapman & Hall/CRC, 1990.

[14] W. S. Cleveland and S. J. Devlin, "Locally weighted regression: An approach to regression analysis by local fitting," *Journal of the American Statistical Association*, vol. 83, no. 403, pp. 596–610, 1988.

[15] R. Koenker, *Quantile Regression*, vol. 38. Cambridge University Press, 2005.

[16] J. M. Lattin, J. D. Carroll, and P. E. Green, *Analyzing Multivariate Data*. Thomson Brooks/Cole Pacific Grove, CA, 2003.

[17] D. S. Wilks, *Statistical methods in the atmospheric sciences*, vol. 100. Academic press, 2011.

[18] D. J. Burke and M. J. O'Malley, "A study of principal component analysis applied to spatially distributed wind power," *IEEE Transactions on Power Systems*, vol. 26, no. 4, pp. 2084–2092, 2011.

[19] M. Zugno, P. Pinson, and H. Madsen, "Impact of wind power generation on european cross-border power flows," *IEEE Transactions on Power Systems*, 2013. (submitted).

[20] T. Jónsson, P. Pinson, H. A. Nielsen, H. Madsen, and T. S. Nielsen, "Forecasting electricity spot prices accounting for wind power predictions," *IEEE Transactions on Sustainable Energy*, vol. 4, no. 1, pp. 210–218, 2013.

[21] T. Jónsson, P. Pinson, H. A. Nielsen, and H. Madsen, "Electricity market imbalance sign prediction through conditional Holt-Winters models," *Energy Economics*, 2013.

[22] B. Klöckl and P. Pinson, "Effects of increasing wind power penetration on the physical operation of large electricity market systems," in *Integration of Wide-Scale Renewable Resources Into the Power Delivery System, 2009 CIGRE/IEEE PES Joint Symposium*, pp. 1–6, IEEE, 2009.

Paper C

Trading Wind Energy on the Basis of Probabilistic Forecasts both of Wind Generation and of Market Quantities

Authors:
Marco Zugno, Tryggvi Jónsson, Pierre Pinson

Published in:
Wind Energy (2012), DOI: 10.1002/we.1531

Trading Wind Energy on the Basis of Probabilistic Forecasts both of Wind Generation and of Market Quantities

Marco Zugno[1], Tryggvi Jónsson[2], Pierre Pinson[1]

Abstract

Wind power is not easily predictable and non-dispatchable. Nevertheless, wind power producers are increasingly urged to participate in electricity market auctions in the same manner as conventional power producers. The aim of this paper is to propose an operational strategy for trading wind energy in liberalised electricity markets and to assess its performance. At first the so-called optimal quantile strategy is revisited. It is proved that without market power, i.e. under the price-taker assumption, this strategy maximises expected market revenues. Forecasts of wind power production, of day-ahead and real-time market prices and of the system imbalance are inputs to this strategy. Subsequently, constraining of the bid that maximises the expected revenues is proposed as a way to overcome the strategy's disregard of practical limitations and, at the same time, of risk. Two constraining techniques are introduced: constraining in the decision space and in the probability space. Finally, the trade of a wind power producer is simulated in a test-case for the Eastern Danish (DK-2) price area of the Nordic Power Exchange (Nord Pool) during a 10 month period in 2008. The results of the test-case show the financial benefits of the aforementioned strategy as well as the consequent interaction with the electricity market. This study will support a demonstration in the framework of the EU project ANEMOS.plus.

[1]DTU Informatics, Technical University of Denmark, Richard Petersens Plads, bld. 305, DK-2800 Kgs. Lyngby, Denmark
[2]ENFOR A/S, Lyngsø Allé 3, DK-2970 Hørsholm, Denmark

Nomenclature

Main symbols

ρ_k	Wind power producer revenues at trading period k
W_k	Wind power production at trading period k
π_k	Market price at trading period k
C_k	Negative wind power producer revenues due to imbalance at trading period k
ψ_k	Unit regulation costs for positive and negative imbalances at trading period k
$W^{(max)}$	Installed wind power capacity
r_k	Quantile of wind power distribution at trading period k
P_k	Probability of imbalance direction at trading period k
a_v	Parameter determining the width of the bound to the optimal bid in the decision space
a_p	Parameter determining the width of the bound to the optimal bid in the probability space

Superscripts

$^{(S)}$	Referring to the day-ahead market
$^{(\uparrow/\downarrow)}$	Referring to the real-time market
$^{(\uparrow)}$	Referring to up-regulation in the real-time market
$^{(\downarrow)}$	Referring to down-regulation in the real-time market
*	Optimal
$\tilde{}$	Contracted at the day-ahead market
$\hat{}$	Forecast

C.1 Introduction

In liberalised electricity markets, competition stands as the fundamental mechanism ensuring the efficient operation of the system. Competition is implemented through the establishment of a market (or multiple markets operating under different rules and gate-closures) where energy is traded. Bids for sale and purchase are collected by the market operators, which are responsible for optimally scheduling the dispatch of energy and allocating sufficient power reserve. The

backbone of most liberalised electricity markets are the day-ahead markets, often referred to as *spot* markets (in Europe) or *forward* markets (in the U.S.), on which most of the trading takes place. Typically these markets offer a platform for trading energy to be delivered/withdrawn within a certain period during the upcoming day. The minimum period length is referred to as *trading period* in this paper; every contract covers one or more trading periods.

Although most renewables are not easily predictable and non-dispatchable, renewable power producers are increasingly urged to participate in electricity markets in the same manner as producers of conventional energy. Here we specifically concentrate on wind energy, which has been the most rapidly growing renewable energy source over the last decade. Our developments and conclusions could however be similarly applied for other types of non-dispatchable renewables e.g.solar energy.

Wind power generation is the typical example of a stochastic and non-dispatchable renewable energy source. Although the possibility of curtailing power exists, it is not economically sound as long as the electricity price (including potential subsidies) remains positive. As a result, trading wind energy in a day-ahead electricity market requires forecasts of wind power production, which can be performed only with limited accuracy, as discussed in [1]. Reviews of the state of the art of wind power forecasting methods and operational tools can be found in [2, 3, 4], while [5] discusses their application in electricity markets.

Differences between contracted and actual energy production (e.g.due to forecasting errors) have to be settled on the intra-day and/or the real-time markets. Due to shorter lead-time from gate closure to delivery, these markets might reduce the revenues of producers that cause imbalance, as more flexible market players are called to equilibrate the system – generally at higher costs. Joint operation of wind and hydro power has recently emerged as a way to reduce imbalance costs among other benefits, see for instance [6] or [7]. However, this solution is only conceivable for market participants having both energy sources in their portfolio. For other producers, the most practical option for imbalance settlement is to rely on the market. Although it is sometimes possible to adjust contracts through existing intra-day markets, the volumes exchanged there are generally low, as illustrated by [8] for the main European electricity markets. Producers are therefore most often forced to rely on the real-time market, where bids for regulation are activated by the TSO close to real-time, and producers are charged for their imbalances, which are determined post-delivery. Hence, the only way for them to reduce imbalance costs is to bid optimally into the day-ahead market, so that the risk of facing losses on the real-time market is minimised. This bid is optimised conditioned upon the information available at the time of contracting, both in terms of future wind power production and market prices.

The penalties faced by electricity producers in the real-time market are generally asymmetric, in some cases even single sided, i.e. they are only to be paid by the producers that increase the overall imbalance with their own. This incites market participants whose portfolio includes a stochastic component to be more strategic in their approach to bidding, see [9]. Indeed it can be analytically shown that under these conditions the optimal day-ahead market bid for a wind energy producer is a certain quantile of the distribution of wind power generation, see for instance [10, 11, 12]. This optimal quantile is a dynamic function of the day-ahead and the imbalance prices, which are not known a priori. Market experience shows that such optimal bids might significantly differ from the point forecasts of wind power production (consisting of the conditional expectation for each lead time). In practice, however, point forecasts are still commonly used when contracting wind power in the day-ahead market. A more theoretical discussion about quantile forecasts being optimal bids in electricity markets can be found in [13].

The existing literature has already described and analysed a number of strategies for trading wind power in the day-ahead market, with different approaches with regards to the uncertainty in production and in market prices. As a basic approach, some authors consider that traditional point forecasts of wind power generation may be used for analysing the value of wind energy in electricity markets, e.g.[14, 15, 16]. Furthermore, [17] models wind generation uncertainty through Markov probability tables and chooses, in a discrete decision space, the bid that minimises the expected costs. Alternatively, [18] suggests the construction of a utility cost function to model the financial risk of wind power producers participating in the market, using persistence forecasting of wind power and average values as price forecasts. The stochastic optimisation algorithm described in [19] uses scenarios of wind power production as input along with historical imbalance prices. Besides, [12] makes use of probabilistic forecasts of wind power and yearly or quarterly average values of imbalance prices in order to determine the optimal quantile bid, in a fashion resembling that of [10]. The same strategy is implemented in [20], using probabilistic forecasts and measured data for wind speed and yearly averages as estimates of the day-ahead and real-time prices. Finally, [21] proposes a linear programming technique for optimising the trade of wind energy in day-ahead, intra-day and real-time markets. The uncertainty in both wind power production and market prices is modelled through simple ARIMA/ARMA models. All these works and strategies either only account for uncertainty in wind power generation but disregard uncertainty in the market quantities, or include both but make use of simple forecasting methods.

In this work, we revisit the quantile strategy described in [10] and [12] and generalise it by considering stochastic rather than deterministic market prices. State-of-the-art probabilistic forecasts both of wind power generation and of market quantities are considered as input. These market quantities include the

regulation sign, which can be down-regulation, up-regulation or no regulation, as well as the unit regulation costs. This strategy is formulated in Section C.2 as a stochastic optimisation problem, which aims at the maximisation of the expected revenues (or utility) of the market participant. This approach is hereafter referred to as Expected Utility Maximisation (EUM). Having the maximisation of the expected value of the revenues as the objective, such an approach directly relates to a long-term optimisation of the market performance of the wind power producer. It is also shown through an example that, due to the uncertainties involved and potentially large forecast errors, such a strategy may occasionally lead to severe losses from a single contract. For instance this might occur when the regulation sign forecast wrongly assigns a high probability to an imbalance direction that is not realised. It is proposed in Section C.3 to constrain the EUM bid in terms of deviations from the point forecasts, either in the quantity space or in the probability space. The two constraining methods are proposed with two different ranges of the allowed interval in the decision space. The motivation for this constraining is twofold. From a practical perspective, constraining the bid is beneficial, because system operators are reluctant to allow large deviations from the point forecasts. This is because efficient system planning requires market bids to closely reflect the actual delivery of energy. Moreover, since point forecasts have been used as operational bids since wind energy started to be traded on electricity markets, such point forecasts act as anchors in the mind of the operators. From a different point of view, this work shows that by setting a constraint on the allowed deviation from the point forecast, the trader can reduce the impact of forecasting errors and increase its risk-aversion. Next, in Section C.4, the participation of a wind power portfolio in the Nord Pool market (Eastern Denmark price area) over a period of 10 months in 2008 is considered in order to evaluate the actual performance of the aforementioned trading strategies. To our knowledge a test-case of such length, combining state-of-the-art forecasts of wind power production, day-ahead and imbalance prices, as well as observed wind production and market data, has never been performed. The results of the exercise show the possibility for wind power producers to significantly reduce their imbalance costs and control the risk of dramatic losses.

The contribution of this paper to the state-of-the-art on the subject is threefold. First of all, the derivation of the optimal quantile strategy is extended to the case where market prices are stochastic. Owing to this formulation, probabilistic forecasts both of wind power production and of market quantities are needed by the decision maker. Secondly, we introduce constraining of the bid as a way to account for issues related to the practical implementability of the strategy and, in parallel, risk-aversion. Finally, we present a realistic test-case simulating wind power trading, and we assess the market value of state-of-the art probabilistic forecasts of wind power production and of market quantities.

The derivation of the optimal quantile strategy presented in this paper is valid under the price-taker assumption, i.e.the wind power producer cannot influence market prices with its bid. Therefore, the aim of this work is to propose operational strategies and to assess the market value of forecasts under this hypothesis. In future markets with increasing penetration of wind power this assumption might not hold, since wind power producers might impact the total system imbalance and therefore influence the price formation mechanisms with their trading strategy. By introducing the constraining of the bid, this issue is partly addressed, since constrained strategies result in lower imbalance and, therefore, limit the impact on prices. The derivations and the results presented in this paper thus constitute a valuable starting point and a reference for further research on the subject, where the dependence structure between wind power production and market prices is taken into account.

The work presented here will support and serve as the basis for a real-world demonstration of stochastic approaches to wind power participation in electricity markets in the framework of the EU project ANEMOS.plus.

C.2 The Expected Utility Maximisation (EUM) bidding strategy

This section is devoted to the introduction of the strategy maximising the expected utility of a wind power producer participating at both the day-ahead and the real-time energy markets. At first, the strategy is derived in Section C.2.1. Then, the forecasts needed in order to decide on the optimal bid are described in Section C.2.2. Finally, possible shortcomings of the strategy are discussed based on a test-case in Section C.2.3.

C.2.1 Derivation of the EUM strategy

In electricity day-ahead markets, power producers have to indicate the amount of energy they are willing to deliver at any trading period through a bid submitted to the market operator. Bids are collected with a certain lead-time to the physical delivery of energy. For example, at the Nord Pool day-ahead market the deadline for submission is at noon on the day prior to delivery. Let $\widetilde{W}_k$ denote the amount of energy contracted in the day-ahead market and let W_k be the stochastic production of wind energy, both for the k-th trading period. The power producer will then have to correct the stochastic imbalance $W_k - \widetilde{W}_k$ on the real-time market. This is because the possibility of trading on the intra-day

market is disregarded, due to its general illiquidity. Hence, the total revenues of the generator, ρ_k, can be expressed as the sum of the revenues, $\rho_k^{(S)}$ and $\rho_k^{(\uparrow/\downarrow)}$, obtained at the day-ahead and the real-time market respectively

$$\rho_k = \rho_k^{(S)} + \rho_k^{(\uparrow/\downarrow)} \tag{C.1}$$

The revenues at the day-ahead market can be determined as the multiplication of the contracted energy $\widetilde{W}_k$ with the day-ahead market price $\pi_k^{(S)}$

$$\rho_k^{(S)} = \pi_k^{(S)} \widetilde{W}_k \tag{C.2}$$

The real-time market revenues are positive if $W_k > \widetilde{W}_k$ (energy surplus to be sold) and negative if $W_k < \widetilde{W}_k$ (energy deficit to be purchased)

$$\rho_k^{(\uparrow/\downarrow)} = \begin{cases} \pi_k^{(\downarrow)}(W_k - \widetilde{W}_k), & W_k \geq \widetilde{W}_k \\ \pi_k^{(\uparrow)}(W_k - \widetilde{W}_k), & W_k < \widetilde{W}_k \end{cases} \tag{C.3}$$

In this expression, $\pi_k^{(\downarrow)}(\pi_k^{(\uparrow)})$ represents the unit down(up)-regulation price which is paid to (by) an overproducing (underproducing) generator. At Nord Pool real-time prices are restricted such that

$$\begin{aligned} \pi_k^{(\downarrow)} &\leq \pi_k^{(S)} \\ \pi_k^{(\uparrow)} &\geq \pi_k^{(S)} \end{aligned} \tag{C.4}$$

at all times. Then depending on the total imbalance of the system, the inequality sign is substituted by an equality sign in at least one of the two inequalities in Equation (C.4). More specifically, let the net system imbalance be denoted as

$$(\widetilde{G}_k - G_k) - (\widetilde{L}_k - L_k) \tag{C.5}$$

where $\widetilde{G}_k$ and G_k denote the total (i.e.summed over all the producers dispatched at the day-ahead market) energy production, contracted and realised respectively, for the k-th trading period. Similarly, $\widetilde{L}_k$ and L_k represent the contracted and realised consumption, respectively, for the consumers and the retailers scheduled at the day-ahead market. Notice that when the quantity in Equation (C.5) is different from zero, real-time bids have to be activated in order to restore energy balance. During hours of power surplus, i.e. when the net system imbalance in Equation (C.5) is < 0, the following holds for the prices

$$\begin{aligned} \pi_k^{(\downarrow)} &\leq \pi_k^{(S)} \\ \pi_k^{(\uparrow)} &= \pi_k^{(S)} \end{aligned} \tag{C.6}$$

This situation is commonly referred to as down-regulation. Conversely during hours of power deficit (when the system net imbalance in Equation (C.5) is > 0),

commonly termed up-regulation, it holds that

$$\begin{aligned} \pi_k^{(\downarrow)} &= \pi_k^{(S)} \\ \pi_k^{(\uparrow)} &\geq \pi_k^{(S)} \end{aligned} \tag{C.7}$$

Finally during hours of perfect balance between load and production then

$$\pi_k^{(S)} = \pi_k^{(\downarrow)} = \pi_k^{(\uparrow)} \tag{C.8}$$

In this way, only the producers contributing to the overall system imbalance risk being penalised, while the ones acting to reduce it receive the day-ahead price for their realised production, when transactions on both the day-ahead and the real-time markets are combined. The rationale behind this choice of market design is that producers should not be allowed to profit from their imbalances. However, it should be pointed out that there are exceptions to this. For instance, the Dutch APX electricity market is just one example of a market where energy imbalance can actually be rewarded.

Now Equation (C.1) can be reformulated as:

$$\rho_k = \pi_k^{(S)} W_k + C_k^{(\uparrow/\downarrow)}. \tag{C.9}$$

Assuming that the wind power producer is a price-taker individually, which is reasonable if it does not hold a significant share of the total production, the term $\pi_k^{(S)} W_k$ in Equation (C.9) is independent of its decision. That is, neither the day-ahead price $\pi_k^{(S)}$ nor the wind power production W_k are influenced by the bidding policy adopted in the day-ahead market. This implies that curtailment is not considered as an option, for the reasons discussed in Section C.1. The term $\pi_k^{(S)} W_k$ represents the revenues that the producer could achieve if it had perfect information on its future wind power production (i.e. if contracted power and wind power production are equal: $\widetilde{W}_k = W_k$). The second term in Equation (C.9) can be made explicit as

$$C_k^{(\uparrow/\downarrow)} = \begin{cases} \psi_k^{(\downarrow)}(W_k - \widetilde{W}_k), & W_k \geq \widetilde{W}_k \\ \psi_k^{(\uparrow)}(W_k - \widetilde{W}_k), & W_k < \widetilde{W}_k \end{cases} \tag{C.10}$$

where the variables $\psi_k^{(\downarrow)}$ and $\psi_k^{(\uparrow)}$ represent the unit regulation costs for positive and negative imbalances at the real-time market, and are given by

$$\psi_k^{(\downarrow)} = \pi_k^{(\downarrow)} - \pi_k^{(S)} \tag{C.11}$$

$$\psi_k^{(\uparrow)} = \pi_k^{(\uparrow)} - \pi_k^{(S)} \tag{C.12}$$

The quantity in Equation (C.10) therefore accounts for negative revenues, which represent the losses for the producer contracting $\widetilde{W}_k$ at the day-ahead market

in comparison to the case of perfect information. At Nord Pool it holds that $C_k^{(\uparrow/\downarrow)} \leq 0$ at all times. Elsewhere (e.g.APX in the Netherlands), $C_k^{(\uparrow/\downarrow)} > 0$ might occur. Regarding the latter case, economists argue that although situations where producers can gain from their imbalance are possible, this cannot be exploited in the sense of strategic bidding. The argument is that the expectation $\mathbb{E}\left\{C_k^{(\uparrow/\downarrow)}|\chi\right\}$ of the losses given the information available at the moment of bidding is negative. As a consequence, the producers are expected to suffer losses from their imbalance in the long run, although in some trading periods they might be able to gain from it. Interested readers are referred to [22] for a detailed discussion.

As one can see from Equations (C.4), (C.11) and (C.12), at Nord Pool $\psi_k^{(\downarrow)} \leq 0$ and $\psi_k^{(\uparrow)} \geq 0$, and they are equal to zero in the cases of up- and down-regulation respectively. It should also be noted that both the unit regulation costs in Equations (C.11) and (C.12) are stochastic variables as the day-ahead price and the imbalance prices are not known in advance by the power producer.

It is assumed from now on that the wind power producer is *rational* (see e.g. [23] for a conceptual introduction) and that its objective is the maximisation of the expected value of its total revenues. The set of bids $\widetilde{\mathbf{W}}^*$ maximising the total revenues is

$$\widetilde{\mathbf{W}}^* = \arg\max_{\widetilde{\mathbf{W}}} \mathbb{E}\left\{\sum_{k=i_{TP}}^{f_{TP}} \rho_k\right\} \tag{C.13}$$

where i_{TP} and f_{TP} are the shortest and the longest lead-times considered in the optimisation, respectively. Here the commonly accepted assumption of independence of decisions for different trading periods is followed. However it may be argued that market dynamics should be accounted for, see for instance [24, 25, 26]. Under the assumption of time-independent decisions over time, the maximisation of the sum of the revenues over time is equal to the maximisation of the revenues obtained at each single k. The optimal bid at the day-ahead market is then

$$\widetilde{W}_k^* = \arg\max_{\widetilde{W}_k} \mathbb{E}\left\{\rho_k\right\} \tag{C.14}$$

Since the first term in Equation (C.9) is not dependent on the decision on the day-ahead market, the maximisation of the expected revenues in Equation (C.14) is equivalent to the maximisation of the expectation of the regulation costs, which are non-positive

$$\widetilde{W}_k^* = \arg\max_{\widetilde{W}_k} \mathbb{E}\left\{C_k^{(\uparrow/\downarrow)}\right\} \tag{C.15}$$

The problem in Equation (C.15) is a variant of the well known linear terminal loss problem (also called the newsvendor problem), see for instance [27], in which the imbalance costs to be borne by the decision maker are stochastic, asymmetric and piecewise linear. Under the assumption that the unit up- and down-regulation costs are independent of the power producer's imbalance, these stochastic costs can be replaced by *certainty equivalents* in the optimisation problem. Assuming that the considered wind power producer is relatively small, such a simplification seems quite reasonable as the producer is a price-taker. Nevertheless, it is clear that some variables could influence wind power production and real-time costs at the same time. This could be the case of e.g. weather related variables in a relatively small power system. This issue goes beyond the scope of this article, but it certainly calls for future research in modelling variables influencing both prices and wind power production.

According to the theory of certainty equivalents, see [27], the rational decision maker can determine the optimal decision without taking into account the whole distribution function of the unit costs. Instead an equivalent problem is solved, in which the stochastic unit costs are substituted by certain deterministic functions of the unit costs themselves. It is proved below that maximising $C_k^{(\uparrow/\downarrow)}$ in Equation (C.10) is equivalent to maximising the expectation of the following function with deterministic unit costs

$$\overline{C}_k^{(\uparrow/\downarrow)} = \begin{cases} \widehat{\psi}_k^{(\downarrow)}(W_k - \widetilde{W}_k) & W_k \geq \widetilde{W}_k \\ \widehat{\psi}_k^{(\uparrow)}(W_k - \widetilde{W}_k) & W_k < \widetilde{W}_k \end{cases} \tag{C.16}$$

where $\widehat{\psi}_k^{(\downarrow)}$ and $\widehat{\psi}_k^{(\uparrow)}$ denote the expected values of the unit regulation costs $\psi_k^{(\downarrow)}$ and $\psi_k^{(\uparrow)}$. The expectation of the imbalance costs in Equation (C.10) can be expanded as

$$\begin{aligned} \mathbb{E}\left\{C_k^{(\downarrow/\uparrow)}\right\} = &\int_0^{+\infty} \int_0^{\widetilde{W}_k} \psi_k^{(\uparrow)}(W_k - \widetilde{W}_k) dP_{W_k} dP_{\psi_k^{(\uparrow)}} \\ &+ \int_{-\infty}^{0} \int_{\widetilde{W}_k}^{W^{(max)}} \psi_k^{(\downarrow)}(W_k - \widetilde{W}_k) dP_{W_k} dP_{\psi_k^{(\downarrow)}} \end{aligned} \tag{C.17}$$

where $W^{(max)}$ is the installed capacity of the wind power producer. Still assuming independence between the unit regulation costs and wind power production the integrations can be separated so that one gets to

$$\begin{aligned} \mathbb{E}\left\{C_k^{(\downarrow/\uparrow)}\right\} = &\int_0^{+\infty} \psi_k^{(\uparrow)} dP_{\psi_k^{(\uparrow)}} \int_0^{\widetilde{W}_k} (W_k - \widetilde{W}_k) dP_{W_k} \\ &+ \int_{-\infty}^{0} \psi_k^{(\downarrow)} dP_{\psi_k^{(\downarrow)}} \int_{\widetilde{W}_k}^{W^{(max)}} (W_k - \widetilde{W}_k) dP_{W_k} \end{aligned} \tag{C.18}$$

This is by definition equal to

$$\begin{aligned}\mathbb{E}\left\{C_k^{(\downarrow/\uparrow)}\right\} =& \widehat{\psi}_k^{(\uparrow)} \int_0^{\widetilde{W}_k} (W_k - \widetilde{W}_k) dP_{W_k} \\ &+ \widehat{\psi}_k^{(\downarrow)} \int_{\widetilde{W}_k}^{W^{(max)}} (W_k - \widetilde{W}_k) dP_{W_k}\end{aligned} \tag{C.19}$$

which is equal to the expected value of the equivalent loss in Equation (C.16).

The problem of maximising the expectation of the utility in Equation (C.16) is a standard linear terminal loss problem, which can then be treated as the general case in [27]. The proof is omitted here and only the expression for the Expected Utility Maximisation (EUM) bid is given

$$\widetilde{W}_k^* = F_{W_k}^{-1}\left(\frac{\left|\widehat{\psi}_k^{(\downarrow)}\right|}{\widehat{\psi}_k^{(\uparrow)} + \left|\widehat{\psi}_k^{(\downarrow)}\right|}\right) \tag{C.20}$$

where F_{W_k} is the cumulative distribution function of the wind power production W_k. Therefore, the EUM bid $\widetilde{W}_k$ is a quantile of the distribution of the stochastic variable W_k corresponding to the probability given by the fraction

$$\widetilde{r}_k^* = \frac{\left|\widehat{\psi}_k^{(\downarrow)}\right|}{\widehat{\psi}_k^{(\uparrow)} + \left|\widehat{\psi}_k^{(\downarrow)}\right|} \tag{C.21}$$

C.2.2 Input forecasts to the EUM strategy

From the treatment in Section C.2.1 it follows that the determination of the optimal bid requires forecasts of both wind power production and imbalance costs.

As far as wind power production is concerned, a probabilistic forecast is needed, as the distribution F_{W_k} of the generation W_k appears in Equation (C.20). Here the non-parametric probabilistic tool described in [28] and [29] is considered. This tool provides the user with a set of forecast quantiles of the wind power distribution for each trading period. Let us denote the α-quantile of wind power production at time k with $q_{W_k}(\alpha)$, such that

$$F_{W_k}\left(q_{W_k}(\alpha)\right) = \alpha \tag{C.22}$$

The provided forecasts are then

$$\widehat{q}_{W_k}(\alpha) = \mathbb{E}\left\{q_{W_k}(\alpha) | M, \boldsymbol{\theta}, \chi_t\right\} \tag{C.23}$$

for different values $\alpha \in [0, 1]$. The expectation on the right side of Equation (C.23) is conditioned on the choice of the model M, on its estimated parameters $\boldsymbol{\theta}$ and on the information χ_t available at the time t when the forecast is issued. It holds trivially that $t < k$. In the example of Nord Pool t might be 11am (one hour before the deadline for bidding), while k could be any of the hours in the following day. From now on the condition on the expectation is discarded in order to lighten the notation. However, the reader should keep this in mind whenever a forecast is defined. An example of quantile forecast can be seen in Figure C.1. The complete forecast of the function F_{W_k} can then be obtained

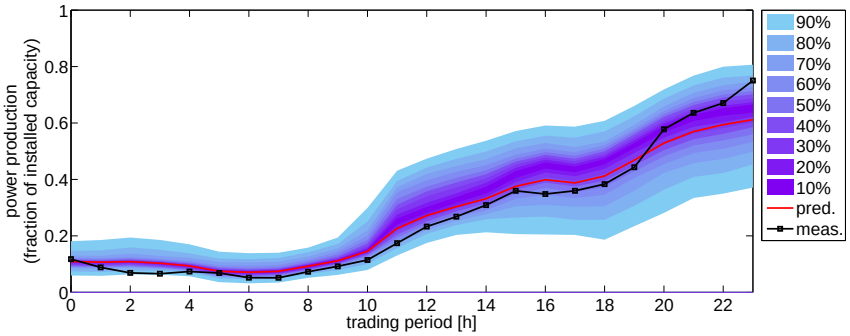

Figure C.1: Example of probabilistic forecast of production for a wind power portfolio in Eastern Denmark. The forecast was issued on the previous day at 11am.

from the set of forecast quantiles $\widehat{q}_{W_k}(\alpha)$ by linear interpolation.

The expected values of the regulation costs $\widehat{\psi}_k^{(\downarrow)}$ and $\widehat{\psi}_k^{(\uparrow)}$ need to be forecast as well. Methods for forecasting the day-ahead market price $\pi_k^{(S)}$, as well as the unit imbalance costs $\psi_k^{(\downarrow)}$ and $\psi_k^{(\uparrow)}$, conditioned upon the regulation sign[3], are described in [30]. The following forecasts are therefore available

$$\widehat{\pi}_k^{(S)} = \mathbb{E}\left\{\pi_k^{(S)}\right\} \tag{C.24}$$

$$\widehat{\psi}^{(\downarrow)}_{k|\psi_k^{(\downarrow)}<0} = \mathbb{E}\left\{\psi_k^{(\downarrow)} | \psi_k^{(\downarrow)} < 0\right\} \tag{C.25}$$

$$\widehat{\psi}^{(\uparrow)}_{k|\psi_k^{(\uparrow)}>0} = \mathbb{E}\left\{\psi_k^{(\uparrow)} | \psi_k^{(\uparrow)} > 0\right\} \tag{C.26}$$

[30] also presents a method for estimating conditional posterior probabilities of

[3] In [30] a given hour is defined as up-regulation hour if $\psi_k^{(\uparrow)} > 0$ and a down-regulation hour if $\psi_k^{(\downarrow)} < 0$.

imbalance in each direction being penalised at any given time k, defined as

$$P_k^{(\downarrow)} = P\left\{\psi_k^{(\downarrow)} < 0\right\} \tag{C.27}$$

$$P_k^{(\uparrow)} = P\left\{\psi_k^{(\uparrow)} > 0\right\} \tag{C.28}$$

From a pure trading perspective this is equivalent to predicting the sign of the actual imbalance as the trader is indifferent to imbalances he/she is not penalised for. The models for $\widehat{\psi}^{(\downarrow)}_{k|\psi_k^{(\downarrow)}<0}$, $\widehat{\psi}^{(\uparrow)}_{k|\psi_k^{(\uparrow)}>0}$ and $\widehat{P}_k^{(\uparrow/\downarrow)}$ are all conditional Holt-Winters models with a diurnal seasonality. For the penalty forecasts, the models are conditioned upon the forecast system load and the forecast spot price for the area, while the direction probability model is conditioned upon the forecast wind power penetration (i.e. the ratio between the forecast wind power production in the whole system and the forecast system load).

An example of forecasts of the regulation signs is shown in Figure C.2. It should be noticed that the two probabilities in the figure do not sum to 1. Indeed, the probability of no regulation $P_k^{(0)}$ might also be positive, and at any time k it holds

$$P_k^{(\uparrow)} + P_k^{(\downarrow)} + P_k^{(0)} = 1 \tag{C.29}$$

The expected values $\widehat{\psi}_k^{(\downarrow)}$ and $\widehat{\psi}_k^{(\uparrow)}$ can then be determined according to the

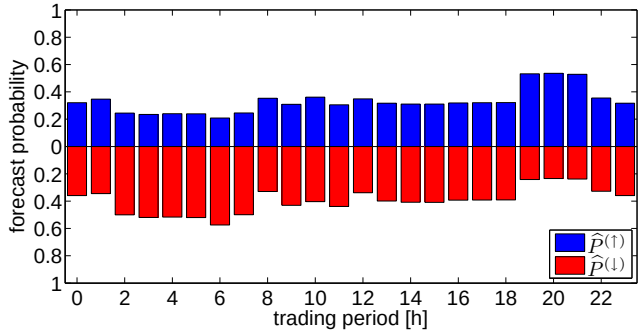

Figure C.2: Example of forecast probabilities of up ($\widehat{P}^{(\uparrow)}$) and down ($\widehat{P}^{(\downarrow)}$) regulation in DK-2.

law of total expectation

$$\widehat{\psi}_k^{(\downarrow)} = \widehat{\psi}^{(\downarrow)}_{k|\psi_k^{(\downarrow)}<0}\widehat{P}_k^{(\downarrow)} + \widehat{\psi}^{(\downarrow)}_{k|\psi_k^{(\downarrow)}=0}(1-\widehat{P}_k^{(\downarrow)}) = \widehat{\psi}^{(\downarrow)}_{k|\psi_k^{(\downarrow)}<0}\widehat{P}_k^{(\downarrow)} \tag{C.30}$$

$$\widehat{\psi}_k^{(\uparrow)} = \widehat{\psi}^{(\uparrow)}_{k|\psi_k^{(\uparrow)}>0}\widehat{P}_k^{(\uparrow)} + \widehat{\psi}^{(\uparrow)}_{k|\psi_k^{(\uparrow)}=0}(1-\widehat{P}_k^{(\uparrow)}) = \widehat{\psi}^{(\downarrow)}_{k|\psi_k^{(\uparrow)}>0}\widehat{P}_k^{(\uparrow)} \tag{C.31}$$

In the cases when both $\widehat{\psi}_k^{(\downarrow)}$ and $\widehat{\psi}_k^{(\uparrow)}$ are zero the ratio in Equation (C.21) is not defined. In these cases the producer might bid the median, corresponding to the 0.5 quantile, which maximises the expected market revenues in the general case where the forecast penalties in the two regulation directions are equal. Figure C.3 plots an example of forecast, $\widetilde{r}_k^*$, and measured, r_k, ratios in Equation (C.21) for a power producer in Eastern Denmark participating in Nord Pool. The resulting bid maximising the expected revenues is shown in Figure C.4.

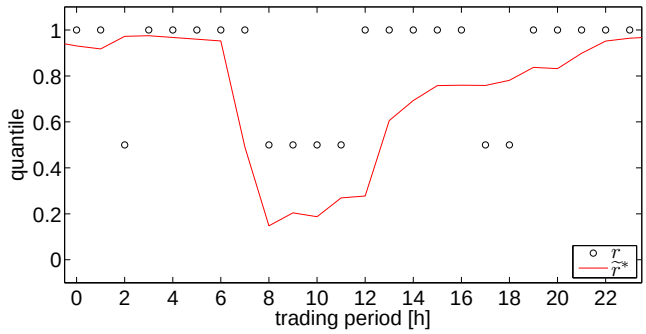

Figure C.3: Optimal forecast ($\widetilde{r}^*$) and measured (r) ratios for a wind power portfolio in DK-2 on a selected day.

As one can see from the scale employed on the y-axis of the figure, the bid is shown as a fraction of the total installed capacity. The point forecast, which is currently the reference for wind power producers participating in day-ahead markets, is also shown for comparison.

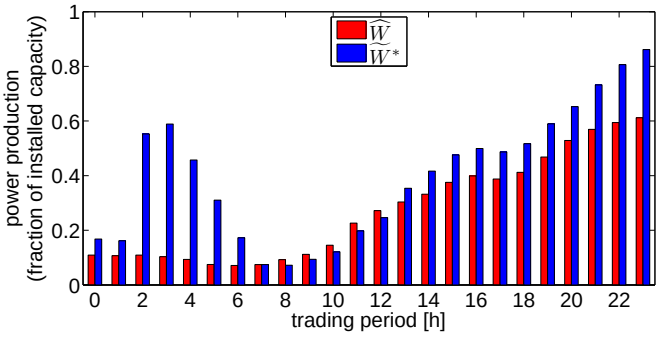

Figure C.4: Example of point forecast ($\widehat{W}$) and EUM bid ($\widetilde{W}^*$) for a wind power portfolio in DK-2.

C.2.3 Testing the EUM bid

This section presents the setup and the results obtained in a test-case simulating energy trading in Nord Pool. Its aim is to assess the performance of the EUM bidding strategy compared to the traditional point forecast bidding. Afterwards, the main drawbacks of the EUM strategy are discussed, along with the reasons motivating the introduction of more risk-averse strategies, which are presented in Section C.3.

In this test-case, the DK-2 (Denmark East) market area has been considered as the geographic location of the wind power plants of a virtual power producer. Data and forecast availability motivate the choice of a 10-month period of simulation, spanning from the 1st March 2008 to the 31st December 2008. The size of the producer is not defined, and all the results are scaled to its installed capacity. It is assumed, though, that the producer is a price-taker, i.e.that changes in its bidding policy do not influence the market. This implies that its size is small relatively to the total installed capacity in the region.

The data set used consists of measured wind power production, point and probabilistic forecasts of wind power production, observed regulation costs and the market forecasts previously described. All data refer to the DK-2 market area and have a temporal resolution of 1 hour. Based on point forecasts issued by WPPT, see [31, 32], probabilistic wind power forecasts are obtained by the method described in [29] and [28] while market forecasts have been obtained as outlined in [30]. All observations used are publicly available on `www.energinet.dk`.

For the sake of performing a realistic test-case, the forecasts of wind power production, of day-ahead and real-time market prices and of imbalance direction probabilities used in this study were issued before 11am of the previous day. Because the day-ahead gate closure at NordPool is noon, these forecasts are precisely the information available for producers bidding on the day-ahead market.

Table C.1 shows the economic results of the wind power producer in both the cases of point forecast bidding and of EUM bid. The third column represents the reduction in the imbalance costs in Equation (C.10) with respect to the case of point forecast bidding. Imbalance cost reduction is a relevant index for assessing the quality of a bidding strategy for wind power producers. Indeed, there is a "fatal" part, i.e.which could be achieved no matter how bad a bidding strategy is employed, that is implicitly included in the total producer profits. For example, a producer could at least earn its realised wind power production times the down-regulation price just by never participating at the

day-ahead market. On the contrary, imbalance costs represent what the wind power producer can actually improve by employing a more advanced strategy. Furthermore, the imbalance cost reduction with respect to a reference bid, the point forecast in this example, provides with an upper bound for performance improvement, i.e.the 100% reduction that would be achieved by bidding with perfect information. The value of imbalance cost reduction in the first row is trivially 0, while one can notice that the improvement obtained with the EUM is 2.3%.

Strategy	Net revenue per installed MW (€/MW)	Imbalance cost per installed MW (€/MW)	Imbalance cost reduction (%)	Price per MWh (€/MWh)
Point forecast	94436.40	4076.51	0.00	54.48
EUM	94529.96	3982.95	2.30	54.54

Table C.1: Economic results for the wind power producer in the test-case performed from the 1st March 2008 to the 31st December 2008 with real market data and forecasts issued for the DK-2 market area.

Figure C.5 shows the subtraction of the cumulative revenues obtained with the EUM strategy and the cumulative revenues obtained with the point forecast bid for each trading period in the test-case. The difference in revenues is positive overall, meaning that the EUM bid is outperforming the point forecast bid in the long run. On the other hand, the performance of the EUM bid appears to be rather volatile and characterised by steep drops, for instance around the 1200th and the 4500th hours in the figure. This suggests that the producer adopting the EUM strategy is exposed to the risk of significant losses stemming from a single contract. It can be shown that the losses are due to inaccurate forecasts of the regulation costs or sign. What the EUM aims at is, essentially, to set the day-ahead market bid on the "safe" side of the decision space, i.e. on the imbalance direction that will not be penalised at the real-time market and paid at the day-ahead price $\pi_k^{(S)}$. As Figure C.3 shows, by doing this the optimal ratio $\widetilde{r}_k^*$, and therefore the EUM strategy, results in being somewhat "extreme". In fact, when the forecasts indicate that one regulation direction is far more likely than another, $\widetilde{r}_k^*$ tends to the extreme values 0 or 1, as shown in the early and late hours of the day in Figure C.3. Figure C.4 shows that this yields a bid that is significantly different from the point forecast during these hours. Generally situations where the EUM bid is close to the nominal capacity or zero are not rare. Hence the producer is in the situation of probably having a great imbalance in the forecast "safe" regulation direction. In the case that the forecasts leading to $\widetilde{r}_k^*$ are correct, the imbalance is paid at the day-ahead price $\pi_k^{(S)}$, with no loss for the producer. On the other hand, if the forecast turns out to be incorrect the producer will have to pay regulation costs for a high

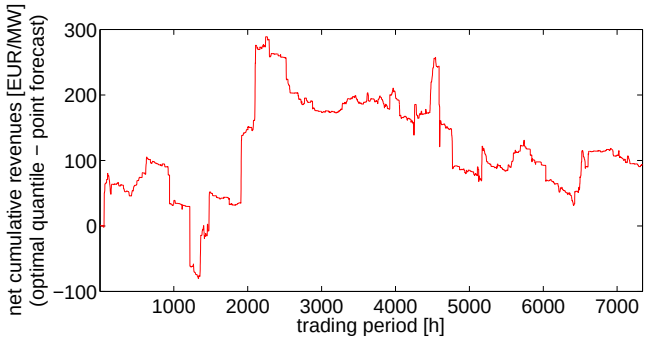

Figure C.5: Subtraction of the cumulative revenues per installed MW using the EUM bid and the cumulative revenues using the point forecast. Its positive value signals an improvement in the performance.

amount of energy, resulting in one of the significant losses shown in Figure C.5. Furthermore, the wind power producer using the EUM strategy can be expected to incur large imbalances, which are unwanted by the TSO. This casts doubt on the possibility of using the EUM strategy in practice.

C.3 Constraining the EUM bid

As an extension to the EUM strategy, a parameter for constraining the bid is introduced in this section as a way to reduce the expected imbalance level. There are several motivations for doing this. As Section C.2 discussed, the EUM bid is often quite far from the point forecast. On the other hand market authorities require that the energy bid be representative of the actual (or forecast) production of a generator. Hence an excessive deviation of the bid from the expected production could be seen as a way to take advantage of the market and thus it could be penalised. Secondly, a strategy causing high imbalance levels might influence the price formation mechanism, especially with respect to the regulation prices. If this happens, the price-taker assumption is violated and, therefore, the model of the market becomes inconsistent.

As a matter of fact, the point forecast bid is a robust decision when the producer is seeking to minimise the impact on the system imbalance. Indeed, the point forecast commonly minimises the expectation of the squared deviation from the

energy production W_k

$$\widehat{W}_k = \arg\min_x \mathbb{E}\left\{(x - W_k)^2\right\} \tag{C.32}$$

It should be pointed out, though, that different criteria could be employed [33]. The most commonly used least-squares criterion only makes the point forecast optimal in the sense of minimising imbalance volumes (in squared values), with no economic considerations. Therefore, a compromise between the EUM bid and the point forecast could reconcile revenue maximisation with practical implementability of the strategy, with respect both to monitoring of the bid by the TSO and to potential violations of the price-taker assumption. Moreover, seeking a compromise between these two strategies is intuitively related to the reduction of risk. Indeed, as discussed above, the EUM strategy is exposed to the risk of large losses under price-forecasting errors. By trying to render the bid less extreme, i.e. closer to the point forecast, the producer would reduce the amount of regulating power, and therefore losses, in these cases. This will be illustrated in the test-case in Section C.4. Finally, energy traders are somehow bound to the point forecast, which has traditionally been bid on the day-ahead market and has proved to be reliable over the years. For this reason it is desirable for an operational strategy not to deviate too much from it.

The main idea in this section is that the bid should somehow be bounded to some values around the point forecast. In this way extreme bid values - and hence extreme losses - are avoided. Constraints can be imposed in the decision space, so that the bid $\widetilde{W}_k^*$ is limited within a certain interval $[\underline{W}_k, \overline{W}_k]$. The mathematical formulation is described in Section C.3.1. As an alternative, the limit can be imposed in the probability space so that the optimal ratio $\widetilde{r}_k^*$ is limited in a similar interval $[\underline{r}_k, \overline{r}_k]$. This is introduced in Section C.3.2.

C.3.1 Constraints in the decision space

In this section we propose the determination of the allowed interval for the bid as a function of the expected value of wind power production $\widehat{W}_k$.

The allowed interval of the decision space is centred around the point forecast

$$\widehat{W}_k = \mathbb{E}\left\{W_k\right\} \tag{C.33}$$

and has radius equal to a certain percentage of this value itself. Two values for the radius are used in the application case-study, i.e. 10% and 20% of $\widehat{W}_k$. Naturally the larger the allowed interval the more risk-neutral the strategy. The suggested bid in this case can be determined as

$$\widetilde{W}_k^{v,a_v} = \min\left\{\max\left\{\widetilde{W}_k^*, \widehat{W}_k \cdot (1 - a_v)\right\}, \widehat{W}_k \cdot (1 + a_v)\right\} \tag{C.34}$$

where a_v is to be set to either 0.1 or 0.2. Figures C.6(a) and C.6(b) show the EUM bid and the point forecast $\widehat{W}_k$ along with the allowed intervals with $a_v = 0.1$ and $a_v = 0.2$.

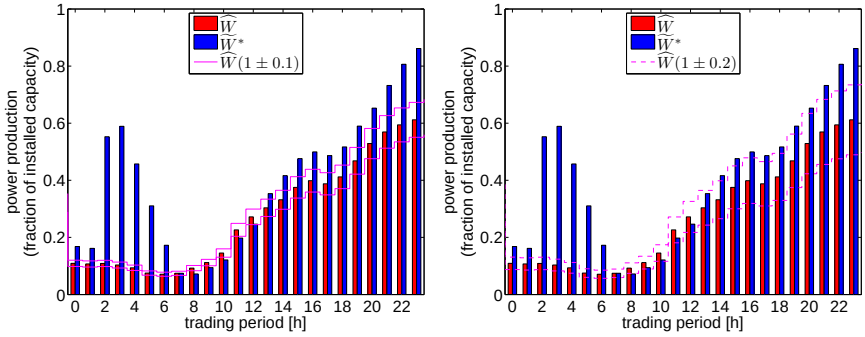

(a) Constraints in value ($a_v = 0.1$) (b) Constraints in value ($a_v = 0.2$)

Figure C.6: Point forecast ($\widehat{W}$), EUM bid ($\widetilde{W}^*$) and allowed interval with constraints on the decision space.

C.3.2 Constraints in the probability space

In the second method proposed here, the ratio $\widehat{r}_k^*$ in Equation (C.21) is allowed to span a certain interval in the probability space. This interval is centred around the value of the cumulative distribution at the point forecast $\widehat{W}_k$

$$\widehat{r}_k = F_{W_k}\left(\widehat{W}_k\right) \tag{C.35}$$

The radius of the interval is then to be set to a certain fraction of the probability space. In this work the radii 0.1 and 0.2 are used. The constrained bid can then be determined as

$$\widetilde{W}_k^{p,a_p} = {F_{W_k}}^{-1}\left(\min\left\{\max\left\{\widehat{r}_k^*, \widehat{r}_k - a_p\right\}, \widehat{r}_k + a_p\right\}\right) \tag{C.36}$$

where a_p is to be set to 0.1 or 0.2 according to the desired risk aversion of the bid. Figures C.7(a) and C.7(b) show the EUM bid and the point forecast $\widehat{W}_k$ along with the allowed intervals with $a_p = 0.1$ and $a_p = 0.2$.

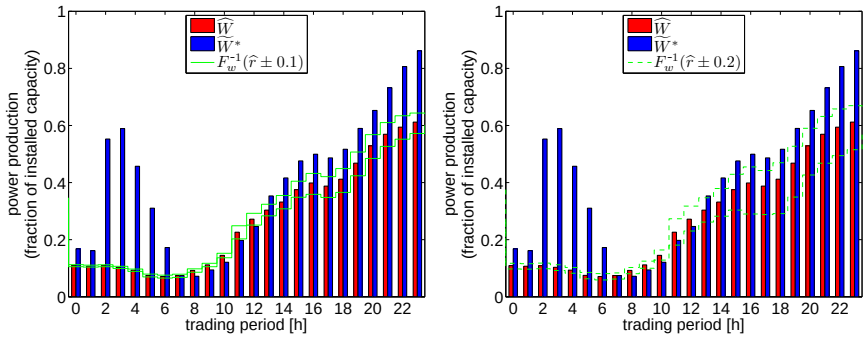

(a) Constraints in probability ($a_p = 0.1$) (b) Constraints in probability ($a_p = 0.2$)

Figure C.7: Point forecast ($\widehat{W}$), EUM bid ($\widetilde{W}^*$) and allowed interval with constraints on the probability space.

C.4 Test case results

In this section we discuss the results of a test-case simulating the strategies presented above in a realistic market situation. The setup of the test-case is the same as described in Section C.2.3. Section C.4.1 discusses the performance of the bidding strategies from the point of view of the producer and its economic result, while Section C.4.2 discusses the implications of the proposed strategies from a system point of view.

C.4.1 Economic advantage of the strategies

The main economic results for the power producer are shown in Table C.2. This shows the total revenues of the producer and its imbalance losses per MW of installed capacity, the percentage reduction in imbalance losses obtained by the strategy compared to the case of point forecast bidding and the average price per MWh paid to the producer.

As one can see, the constrained strategies introduced in the previous section produce better results than the plain EUM one. The reduction in imbalance costs amounts to around 6% when the constraint limit is set to 10% (both in value and in probability) and to around 8.5% when it is set to 20%. A slightly better performance is obtained by constraining in value than in probability. As far as the last column of Table C.2 is concerned it should be mentioned that with perfect information on wind power production the energy would have been

sold at an average price of €56.83 in the considered period.

The improved profits obtained with these strategies, compared to that of using the point forecast bidding, are illustrated in Figure C.8. Indeed, this figure displays the difference between the cumulative revenues obtained by using the EUM strategy and its constrained versions and the revenues obtained by bidding the point forecast. All the cumulative revenues in this plot are expressed in € per MW of installed wind power capacity. It can be seen how the EUM bid ($\widetilde{W}$) is the least efficient strategy, apart from the point forecast bidding. The constrained strategies, besides performing better than the EUM, are also less exposed to significant isolated losses.

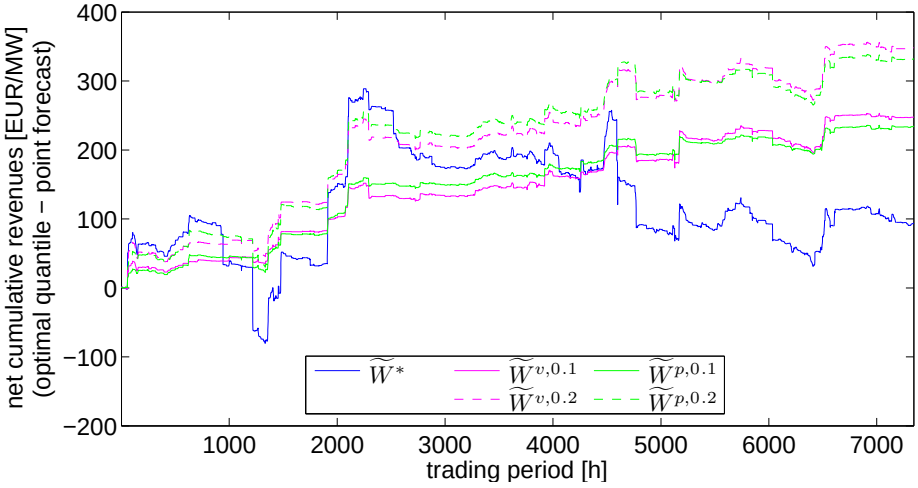

Figure C.8: Improvement of the cumulative revenues for the strategies described in Sections C.2 and C.3 with respect to the point forecast bidding strategy.

In view of the results above, there is clearly a relationship between range of the constraint and net revenues. Intuitively, there is also a relationship with risk, since as pointed out in Section C.3 an increase in the allowed bid range results in a higher risk of a large imbalance, and therefore a higher risk of large losses. In principle, the full joint probability distribution of wind power production and market prices should be employed in order to assess risk quantitatively. An *a posteriori* approach is followed here, in that risk is assessed by analysing the realised standard deviation of the hourly imbalance losses.

Figures C.9(a) and C.9(b) show the imbalance cost reduction obtained in the test-case as a function of the parameters a_v and a_p. The trend is increasing in

Strategy	Net revenue per installed MW (€/MW)	Imbalance cost per installed MW (€/MW)	Imbalance cost reduction (%)	Price per MWh (€/MWh)
Point forecast	94436.40	4076.51	0.00	54.48
EUM	94529.96	3982.95	2.30	54.54
Constrained (±10% value)	94684.18	3828.74	6.08	54.63
Constrained (±20% value)	94784.27	3728.64	8.53	54.68
Constrained (±10% probability)	94670.78	3842.13	5.75	54.62
Constrained (±20% probability)	94768.55	3744.37	8.15	54.67

Table C.2: Economic results for the wind power producer in the test-case.

both cases up to a certain value of the parameter (approximately 0.6 and 0.2 for a_v and a_p respectively). Increasing the constraining parameter further beyond these critical values results in less profits. This is because the distribution of the producer's hourly revenues is bounded on the upper side by $\pi_k^{(s)} W_k$. By allowing larger deviations from the point forecasts, this maximum value of the revenues is reached during more and more trading periods. In this way the rate of growth of the revenues slows down, as fewer trading periods offer possible improvements. Meanwhile, when forecasts are not perfect the risk of losses increases. When the critical level of the constraining parameter is reached, the increased losses exceed the revenue growth, resulting in the negative slopes on the right sides of Figures C.9(a) and C.9(b). This decline is only stopped when the allowed bid interval is large enough to contain the optimal quantiles for all trading periods, as in the flat part of the curve on the right side of Figure C.9(b). At that point the constrained strategy is in practice equal to the original EUM strategy.

The empirical standard deviation of the hourly imbalance losses is plotted in Figure C.9(c) and C.9(d). As one can see in Figure C.9(d), the EUM strategy (to which the constrained strategy converges when the constraining parameter a_p is just above 0.6) is the riskiest strategy, since it incurs the highest standard deviation of hourly losses. Strategies with lower values of the constraining parameters are subject to lower risk, but the trend is not monotonic all the way down to the point forecast (achieved with $a_v = a_p = 0$). The latter strategy would in fact be very risk-averse in case of equal penalties for up- and down-regulation. In a realistic case with different penalties, the most risk-averse constrained strategy is obtained for a value a_v slightly lower than the one delivering best revenues, while the value a_p that delivers the highest revenues is to a good approximation the one that is minimising the standard deviation of the losses.

Furthermore, Table C.2 and Figures C.9(a) and C.9(b) indicate that the EUM strategy does not achieve the best performance among the considered strategies in the simulated market period. One would expect that a 10-month period is long enough for considering the incidence of isolated losses on the cumulative revenues negligible, so that the EUM strategy achieves the optimal performance. On the contrary, this study seems to suggest that the EUM strategy is not optimal in practice. Indeed, even from a theoretical point of view the EUM bid is optimal only under the assumption that probabilistic forecasts of wind power production and of market prices are correct. In practice, errors in the probabilistic forecasts might cause the loss of optimality that is observable in this test-case. On the other hand the constrained strategies seem to limit the negative effects of forecast errors both by reducing the risk of losses stemming from single hourly-contracts and by achieving a better performance in the long run.

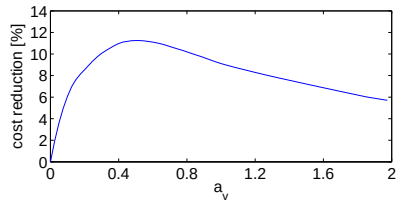

(a) Imbalance loss reduction with constraints in value

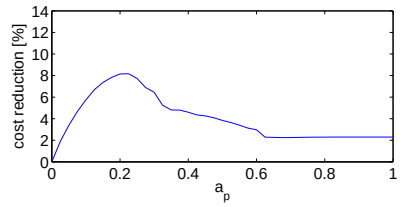

(b) Imbalance loss reduction with constraints in probability

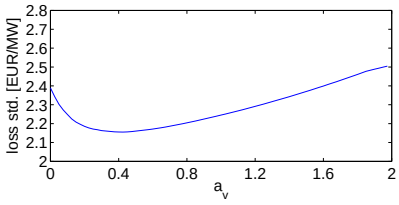

(c) Imbalance loss standard deviation with constraints in value

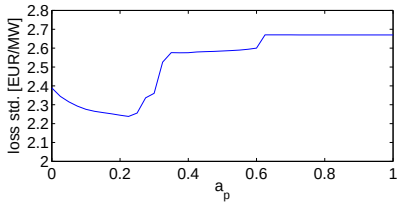

(d) Imbalance loss standard deviation with constraints in probability

Figure C.9: Producer's imbalance loss reduction and standard deviation in the test-case as a function of constraining parameter.

C.4.2 Interaction with the system

This section sheds some light on the effects of the strategies presented in Sections C.2 and C.3 in terms of energy imbalance introduced in the system.

Table C.3 shows the simulation results in terms of imbalance direction. The first three columns show the energy imbalance brought to the system by the wind producer in the considered 10 months, in total and divided between positive, i.e. producer being long (second column), and negative imbalance, i.e. producer being short (third column). All the values are expressed in hours of operation at nominal capacity, i.e.they are obtained by dividing the total energy imbalance (MWh) over the simulation by the installed capacity (MW). It can be seen that the more risk-neutral the strategy, the higher the overall energy imbalance. In this sense, the EUM strategy appears to have an extreme behaviour, pushing the total imbalance from less than 500 hours of operation, obtained with the point forecast bid, to over 700 hours. The four constrained strategies appear to have a limited effect on the overall imbalance. The strategies with tighter bounds ($\pm$ 10% in value and $\pm$ 0.1 in probability) cause only a negligible increase, while when the ones with the less restrictive bounds ($\pm$ 20 % in value and $\pm$ 0.2 in probability) are used the total imbalance rises by 35 hours at most.

Furthermore, an evaluation of the second and the third columns shows that generally more advanced strategies tend to bid above the actual production. This means that the producer is more often short rather than long. In fact, one can see that the difference between the values in the second and the third columns, which is almost zero with the point forecast bidding, tends to spread markedly when other strategies are used. This result might at a first sight look counterintuitive, since penalties are on average higher for up-regulation than for down-regulation. Nevertheless other factors, i.e.skewness of wind power production distribution, have an influence on this. According to expectations, the prevalence of up-regulation power is more evident when less risk-averse strategies are used.

The fourth and the fifth columns of Table C.3 show the percentage of market hours during which the producer is long and short respectively. It can be seen that the variation in number of regulation hours, despite the significant variation in the imbalance volumes, is at most 1.5%. This indicates that the proposed strategies change the volumes of the energy imbalance but not the general trend in the number of up- or down-regulation periods. Finally, the last two columns show the maximum value of energy imbalance, again expressed in hours of operation at nominal capacity, during a single hour. Interestingly only the row corresponding to the EUM bid shows a considerable increase, which underlines the fact that constraining the EUM bid is an effective method to limit the maximum value of imbalance.

Table C.4 looks at the producer's imbalance from a different perspective. This table separates the results for the imbalance into two components: the component opposite to the overall system imbalance, which is paid at the day-ahead market price and is shown in the second and the fourth columns, and the component in the same direction, which is paid at the day-ahead price minus the imbalance cost and is shown in the third and fifth columns. While in the case of the EUM bid the third column shows a significant increase, its values are roughly unchanged with the tighter constraints and slightly increased with the looser ones. In turn, the second column increases by a significant amount in most cases. These two facts indicate that the increase in energy imbalance caused by the use of more advanced strategies, which has been discussed above, actually involves only the direction in which the producer is not penalised, i.e. the one paid at the day-ahead price. There are two implications of this. On one hand, part of the energy imbalance is shifted to the opposite direction with respect to the system imbalance (second column in Table C.4), thus contributing to restoring the overall balance – yet on a marginal level due to the price-taker assumption. In other words, the proposed constrained strategies are able to better "read" the feedback signal sent by the regulation prices and adapt to it, thus reducing the system imbalance. On the other hand, the variation in imbalance could become significant if the proposed strategies become common practice

Strategy	Energy imbalance (h) Total	> 0	< 0	Imbalance hours (%) > 0	< 0	Max value (h/h) > 0	< 0
Point forecast	484.92	235.94	248.98	45.45	54.47	0.54	0.70
EUM	755.29	269.93	485.35	46.28	53.72	0.66	0.89
Constrained ($\pm$10% value)	495.91	236.48	259.43	44.26	55.73	0.56	0.68
Constrained ($\pm$20% value)	519.70	244.82	274.88	44.06	55.91	0.58	0.68
Constrained ($\pm$10% probability)	488.94	237.82	251.12	46.09	53.91	0.57	0.68
Constrained ($\pm$20% probability)	514.62	245.98	268.64	46.60	53.40	0.59	0.68

Table C.3: Energy imbalance of the wind power producer in the test-case.

for producers. As a result, this could influence the formation of the regulation prices as well as possibly change the direction of the system imbalance. While it has been shown that the trading behaviour of wind power producers is capable of affecting day-ahead prices at NordPool even at the current level of market penetration, see [34, 35], the relationship with the real-time market penalties, which are the quantities that ultimately determine the optimal bid in Equation (C.20), has not been investigated yet. In the event that the trading strategies presented above become common practice, they might influence the real-time penalties and no longer be optimal, and could possibly destabilise the system. Then, the market power of wind power producers should be accounted for if efficient bidding strategies are to be designed for producers with a large total capacity or for combined producers. This can be achieved by modelling energy markets as closed-loop systems, see for instance [25, 26].

C.5 Conclusions

In this work, the optimal quantile strategy for trading wind power in liberalised energy market is revisited. It is shown that this strategy maximises the expected value of the market revenues (utility), under the assumption that the wind power producer is a price-taker, i.e. its market strategy is not capable of influencing price formation. The use of the Expected Utility Maximisation (EUM) strategy in practice requires probabilistic forecasts of wind power production, point forecasts of day-ahead and real-time market prices and of the imbalance sign probabilities. All these forecasts can be provided by state-of-the-art forecasting techniques.

An evaluation of the EUM strategy in a realistic test-case in Nord Pool highlights both its improved performance and its risk-neutral nature. The former is underlined by a 2.3% reduction of the imbalance costs. As far as the latter is concerned, the test-case shows that this strategy is exposed to a number of significant losses that take place in short periods of time. These losses are caused by the use of inaccurate forecasts which cause the bid to differ significantly from the actual wind power production.

Constraining of the bid is then introduced in two different versions: with constraints in the decision space and in the probability space. The main idea is that bounding the bid to a certain interval around the point forecast can help reduce the distance of the bid from the actual wind power production. This heuristic can solve some issues, associated with the control of market authorities of the producer's bid as well as with its influence on the price formation mechanism. Indeed, constrained strategies generally reduce the imbalance introduced

Strategy	Energy imbalance (h)			Imbalance hours (%)	
	Total	Day-Ahead price	Penalty	Day-Ahead price	Penalty
Point forecast	484.92	277.71	207.21	62.81	37.19
EUM	755.29	498.66	256.62	65.14	34.86
Constrained (±10% value)	495.91	286.72	209.19	63.16	36.84
Constrained (±20% value)	519.70	304.85	214.85	63.59	36.41
Constrained (±10% probability)	488.94	281.93	207.00	62.72	37.28
Constrained (±20% probability)	514.62	301.74	212.87	63.39	36.61

Table C.4: Energy imbalance of the wind power producer in the test-case.

by the wind power producer in the system, thus lowering the potential impact on real-time prices and the sub-optimality of the strategy in a price-maker market environment. Moreover, the risk of incurring high regulation costs is also reduced by using constrained strategies.

Furthermore, the test-case is extended in order to assess the performance of the constrained strategies. The results of the simulation show that the constrained strategies outperform both the point forecast and the EUM strategies. The latter fact shows that constraining the EUM bid is also an effective way for reducing the impact of forecast errors on long-term revenues. At a second stage in the test-case, the interactions between a producer employing this strategy and the overall system are analysed. It is shown that only the EUM bid causes a significant increase in the total energy imbalance compared to the point forecast bid. The constrained strategies increase the amount of regulated energy at most by about 10% in the case of less restrictive bounds, while the increase is negligible when the strategies with tighter bounds are adopted. Moreover, it is pointed out that this increase in the regulated power involves only the component in the opposite direction compared to the overall system imbalance. As a result, the constrained strategies might be able to reduce the overall imbalance, thus marginally benefiting the system, at least as long as they do not become common practice.

We underline that the obtained results hold as long as the wind power producer does not own a significant share of the overall production capacity. When this hypothesis is not true, the power producer cannot be considered a price-taker. It is expected that in this case the performance of the proposed strategies decreases. In addition, the assertion that these strategies may be beneficial to the system by reducing the overall imbalance might prove incorrect. This is because such a large producer -or many smaller producers using the same bidding policy- might change the direction of the system imbalance, thus contributing positively to it rather than reducing it. For these reasons, an interesting future development of this work could be to study the relationship between the bid of a large wind power producer and the formation of the regulation prices in the real-time market. This could then lead to the formulation of optimal bidding strategies of practical use for large wind power producers, as well as more stable from a system point of view.

Similarly, modelling explanatory variables influencing wind power production and energy market prices at the same time is of clear interest for future research. This would account for the situation where a high penetration of wind power in the system is able to influence the prices, although the considered wind power producer is too small to have any sort of market power on its own.

Besides, trading on the intra-day market could also be included in the problem

under the assumption of sufficient liquidity of this market. As shown in [21], this trading floor gives market participants further possibilities for reducing the risk of losses. Indeed, producers can employ forecasts with a shorter lead-time (typically one hour) with clear advantages in terms of accuracy. Therefore, an assessment of the advantages both for the producers and the system obtained by increasing the liquidity of balancing markets would be particularly interesting.

Finally, another direction for further research could be to account for the dynamic aspects of the market. In this way the assumption of independence of decisions in different trading periods would be overcome. The dynamic view of the market could include, for instance, modelling competition among producers as well as the market participation of mixed portfolios. In the latter case a typical situation could be the coupling of wind power with hydro power or energy storage, both of which allow for shifts in the trade of power between different trading periods. This research could lead to the determination of more advanced bidding strategies in competitive market environments, possibly for producers with a diversified portfolio of energy sources.

Acknowledgement

The work presented has been partly supported by the European Commission, which is hereby greatly acknowledged, under the Anemos.plus project (ENK6-CT2006-038692). The authors would also like to give credit to DONG Energy, ENFOR, Nord Pool and Energinet.dk for their role in providing the data used in this work. In particular, the authors would like to thank Torben S. Nielsen and Henrik Aa. Nielsen from ENFOR, as well as John Tøfting, Jes Smed and Lars Kruse from DONG Energy for the constructive discussions that enhanced the level of this research. Finally, we express our gratitude to the Editor of this journal and to the three anonymous referees for providing insightful comments and suggestions for improving this manuscript.

References C

[1] H. Madsen, P. Pinson, G. Kariniotakis, H. A. Nielsen, and T. S. Nielsen, "Standardizing the performance evaluation of short-term wind power prediction models," *Wind Engineering*, vol. 29, no. 6, pp. 475–489, 2005.

[2] G. Giebel, G. Kariniotakis, and R. Brownsword, "The state of the art in short-term prediction of wind power – a literature overview," tech. rep., EU project ANEMOS, Deliverable Report D-1.1, available online: http://www.anemos-project.eu, 2003.

[3] A. Costa, A. Crespo, J. Navarro, G. Lizcano, H. Madsen, and E. Feitosa, "A review on the young history of the wind power short-term prediction," *Renewable and Sustainable Energy Reviews*, vol. 12, no. 6, pp. 1725–1744, 2008.

[4] C. Monteiro, R. Bessa, V. Miranda, A. Botterud, J. Wang, and G. Conzelmann, "Wind power forecasting: State-of-the-art 2009," Tech. Rep. ANL/DIS-10-1, Argonne National Laboratory, 2009.

[5] A. Botterud, J. Wang, V. Miranda, and R. J. Bessa, "Wind power forecasting in U.S. electricity markets," *The Electricity Journal*, vol. 23, no. 3, pp. 71–82, 2010.

[6] J. L. Angarita, J. Usaola, and J. Martínez-Crespo, "Combined hydro-wind generation bids in a pool-based electricity market," *Electric Power Systems Research*, vol. 79, no. 7, pp. 1038–1046, 2009.

[7] F. P. Montero and J. J. Perez, "Pump up the volume: Using hydro storage to support wind integration," *Renewable Energy World*, vol. 12, no. 5, pp. 80–88, 2009.

[8] C. Weber, "Adequate intraday market design to enable the integration of wind energy into the European power systems," *Energy Policy*, vol. 38, no. 7, pp. 3155–3163, 2010.

[9] K. Skytte, "The regulating power market on the Nordic power exchange Nord Pool: an econometric analysis," *Energy Economics*, vol. 21, no. 4, pp. 295–308, 1999.

[10] J. B. Bremnes, "Probabilistic wind power forecasts using local quantile regression," *Wind Energy*, vol. 7, no. 1, pp. 47–54, 2004.

[11] U. Linnet, "Tools supporting wind energy trade in deregulated markets," Master's thesis, Technical University of Denmark, 2005.

[12] P. Pinson, C. Chevalier, and G. Kariniotakis, "Trading wind generation from short-term probabilistic forecasts of wind power," *IEEE Transactions on Power Systems*, vol. 22, no. 3, pp. 1148–1156, 2007.

[13] T. Gneiting, "Quantiles as optimal point forecasts," *International Journal of Forecasting*, vol. 27, no. 2, pp. 197–207, 2011.

[14] J. L. Angarita-Márquez, C. A. Hernandez-Aramburo, and J. Usaola-Garcia, "Analysis of a wind farm's revenue in the British and Spanish markets," *Energy Policy*, vol. 35, no. 10, pp. 5051–5059, 2007.

[15] R. Barthelmie, F. Murray, and S. Pryor, "The economic benefit of short-term forecasting for wind energy in the UK electricity market," *Energy Policy*, vol. 36, no. 5, pp. 1687–1696, 2008.

[16] J. Chang, B. C. Ummels, W. G. van Sark, H. P. den Rooijen, and W. L. Kling, "Economic evaluation of offshore wind power in the liberalized Dutch power market," *Wind Energy*, vol. 12, no. 5, pp. 507–523, 2009.

[17] G. Bathurst, J. Weatherill, and G. Strbac, "Trading wind generation in short-term energy markets," *IEEE Transactions on Power Systems*, vol. 17, no. 3, pp. 782–789, 2002.

[18] S. Galloway, G. Bell, G. Burt, J. McDonald, and T. Siewerski, "Managing the risk of trading wind energy in a competitive market," *Generation, Transmission and Distribution, IEE Proceedings*, vol. 153, no. 1, pp. 106–114, 2006.

[19] J. Matevosyan and L. Söder, "Minimization of imbalance cost trading wind power on the short-term power market," *IEEE Transactions on Power Systems*, vol. 21, no. 3, pp. 1396–1404, 2006.

[20] M. Gibescu, W. L. Kling, and E. W. Van Zwet, "Bidding and regulating strategies in a dual imbalance pricing system: case study for a Dutch wind producer," *International Journal of Energy Technology and Policy*, vol. 6, no. 3, pp. 240–253, 2008.

[21] J. M. Morales, A. J. Conejo, and J. Pérez-Ruiz, "Short-term trading for a wind power producer," *IEEE Transactions on Power Systems*, vol. 25, no. 1, pp. 554–564, 2010.

[22] A. Boogert and D. Dupont, "On the effectiveness of the anti-gaming policy between the day-ahead and real-time electricity markets in the Netherlands," *Energy Economics*, vol. 27, no. 5, pp. 752–770, 2005.

[23] K. Binmore, *Game theory: a very short introduction.* Oxford University Press, 2008.

[24] F. Alvarado, "The stability of power system markets," *IEEE Transactions on Power Systems*, vol. 14, no. 2, pp. 505–511, 1999.

[25] Y. Liu, *Network and temporal effects on strategic bidding in electricity markets.* PhD thesis, University of Hong Kong, 2006.

[26] P. Giabardo, M. Zugno, P. Pinson, and H. Madsen, "Feedback, competition and stochasticity in a day ahead electricity market," *Energy Economics*, vol. 32, no. 2, pp. 292–301, 2010.

[27] H. Raiffa and R. Schlaifer, *Applied statistical decision theory.* Division of Research – Harvard Business school, 1964.

[28] P. Pinson, *Estimation of the uncertainty in wind power forecasting.* PhD thesis, Ecole des Mines de Paris, France, 2006.

[29] P. Pinson and G. Kariniotakis, "Conditional prediction intervals of wind power generation," *IEEE Transactions on Power Systems*, vol. 25, no. 4, pp. 1845–1856, 2010.

[30] T. Jónsson, "Forecasting of electricity prices accounting for wind power predictions," Master's thesis, Technical University of Denmark, 2008.

[31] T. S. Nielsen, *Online prediction and control in nonlinear stochastic systems.* PhD thesis, Technical University of Denmark, 2002.

[32] "ENFOR's website," June 2011. `http://www.enfor.dk`.

[33] R. Bessa, V. Miranda, A. Botterud, and J. Wang, "'Good' or 'bad' wind power forecasts: A relative concept," *Wind Energy*, vol. 14, no. 5, pp. 625–636, 2011.

[34] T. Jónsson, P. Pinson, and H. Madsen, "On the market impact of wind energy forecasts," *Energy Economics*, vol. 32, no. 2, pp. 313–320, 2010.

[35] T. Jónsson, M. Zugno, H. Madsen, and P. Pinson, "On the market impact of wind power (forecasts) – An overview of the effects of large-scale integration of wind power on the electricity market," in *IAEE's 33rd International Conference*, (Rio de Janeiro, Brazil), 2010.

Paper D

Pool Strategy for a Price-Maker Wind Power Producer

Authors:
Marco Zugno, Juan Miguel Morales, Pierre Pinson, Henrik Madsen

In press for:
IEEE Transactions on Power Systems, DOI: 10.1109/TPWRS.2013.2252633

Pool Strategy for a Price-Maker Wind Power Producer

Marco Zugno[1], Juan Miguel Morales[2], Pierre Pinson[1], Henrik Madsen[1]

Abstract

We consider the problem of a wind power producer trading energy in short-term electricity markets. The producer is a price-taker in the day-ahead market, but a price-maker in the balancing market, and aims at optimizing its expected revenues from these market floors. The problem is formulated as a Mathematical Program with Equilibrium Constraints (MPEC) and cast as a Mixed-Integer Linear Program (MILP), which can be solved employing off-the-shelf optimization software. The optimal bid is shown to deliver significantly improved performance compared to traditional bids such as the forecast conditional mean or median of wind power distribution. Finally, sensitivity analyses are carried out to assess the impact on the offering strategy of the producer's penetration in the market, of the correlation between wind power production and residual system deviation, and of the shape of the forecast distribution of wind power production.

D.1 Nomenclature

D.1.1 Sets

k Index for up-regulation block offered at the balancing market, from 1 to N_K

j Index for down-regulation block offered at the balancing market, from 1 to N_J

ω Index for scenario, from 1 to N_Ω

[1]DTU Informatics, Technical University of Denmark, Richard Petersens Plads, bld. 305, DK-2800 Kgs. Lyngby, Denmark

[2]Centre for Electric Power and Energy, Technical University of Denmark, Elektrovej, bld. 325, DK-2800 Kgs. Lyngby, Denmark

D.1.2 Constants

c_k Offered cost for up-regulation block k

b_j Offered benefit for down-regulation block j

C_k Production limit for up-regulation block k

C_j Consumption limit for down-regulation block j

w_ω Own wind power production in scenario ω

δ_ω Residual system deviation in scenario ω

$\lambda_\omega^{\mathrm{DA}}$ Day-ahead market price in scenario ω

C^{W} Installed capacity for wind power producer

D.1.3 Lower-Level Variables

$p_{k\omega}$ Up-regulation from block k in scenario ω

$p_{j\omega}$ Down-regulation from block j in scenario ω

$\lambda_\omega^{\mathrm{B}}$ Balancing market price in scenario ω

$\mu_{k\omega}^{\mathrm{S}}$ Dual variable for capacity constraint at the balancing market for block k in scenario ω

$\mu_{j\omega}^{\mathrm{D}}$ Dual variable for capacity constraint at the balancing market for block j in scenario ω

D.1.4 Upper-Level Variables

x_ω Wind power producer's offer in scenario ω

D.2 Introduction

In the recent years, the deployment of wind power into power systems worldwide has increased with impressive pace. In part this expansion has been supported by national governments in the form of market incentives, which resulted in wind power having a competitive advantage with respect to conventional sources of

energy. In many cases, wind power producers are granted a fixed feed-in tariff or a minimum price for their production, so as to hedge them from the price fluctuations of electricity markets. Furthermore, they are often relieved of their balance responsibility, which means that the Transmission System Operators (TSOs) bear the costs for the deviations of actual production from the generation schedule, which wind power producers inevitably incur.

As the cost per produced MWh of wind power constantly decreases, wind power producers are forced to participate in electricity markets in the same way as conventional power generators. However, wind generation is characterized by peculiar features that distinguish it from most of the other electricity sources. First of all, it is stochastic, and thus can be forecast only with a certain degree of accuracy [1]. Furthermore, it is non-dispatchable. These features imply that deviations of the actual production from the schedule must be covered by back-up plants.

On the other hand, electricity markets were conceived at a time when the large-scale penetration of wind power was not foreseen. Therefore, their design is better suited to traditional power plants, which are dispatchable and may need a certain time-lag between the submission of production plans and the actual delivery of power. In modern electricity markets, most of the energy trade takes place in so-called *day-ahead* markets, with an advance in time typically in the range between 12–36 hours. Participants are then allowed to contract changes to their day-ahead schedules either in *intra-day* or *balancing* markets. However, prices in such markets may involve penalties and are generally less attractive and more volatile than in the day-ahead market.

In view of the several market floors and of the uncertainty involved, both in production and in market quantities, the problem of determining the optimal bid for a wind power producer is a multi-stage, stochastic optimization problem.

So far the state-of-the-art of research on the topic has focused on the problem of trading wind power as a price-taker. Considering the day-ahead and the balancing market stages only, it can be shown that the optimal day-ahead bid for a price-taker wind power producer is a certain quantile of the forecast wind power distribution, which is a function of the market prices, see [2], as well as [3] and [4] for the case with stochastic market prices. Such quantile-based approach is used to evaluate the performance of wind power forecasts in [5] and [6], both of which employ historical averages of market prices. Furthermore, the performance of this approach is analyzed in [4] in a realistic test-case using state-of-the-art forecasts of both wind production and market prices. Another analytical approach is proposed in [7], where the optimal bid is chosen in a discrete decision space, and the uncertainty in wind power production is modeled using probability tables. Furthermore, an approach based on utility-functions is presented in [8]

along with the use of persistence forecasting of wind power production and historical values for market prices. The stochastic programming approach is also popular. In [9], wind power production is modeled using scenarios, and historical averages of prices are used. Furthermore, [10] deals with the participation of wind power producers in multiple market stages (day-ahead, intra-day and balancing). Recently, [3] and [11] have shown further analytical results on the problem of trading wind as a price-taker.

To our knowledge, there are no attempts in the literature to study the optimal bidding for a wind power producer in a price-maker setting. However, the problem is becoming increasingly interesting as, due to its growing penetration into power systems, wind power is more and more capable of influencing market prices [12].

This work models the market participation of a wind power producer that is a price-maker[3] in the balancing market in the framework of *Mathematical Programs with Equilibrium Constraints* (MPECs) [13]. Because a much larger volume is traded in the day-ahead market, we assume that the wind power producer is a price-taker at that stage. Therefore, we can employ scenarios for the day-ahead market price, as well as for wind power production and residual system deviation. We also assume that bids are independent between different trading periods, and therefore consider a single time period in our formulation. The output of the optimization model consists of the optimal day-ahead offer and the balancing market prices for any realization of wind power production and system deviation. Since producers are allowed to bid supply curves in the day-ahead market, the optimal offer is a non-decreasing curve relating quantities of energy to the corresponding minimum accepted prices.

The structure of this paper is the following. Section D.3 introduces the setup of the problem. Then, the mathematical formulation is described in detail in Section D.4. Results from a series of case studies are presented in Section D.5. Finally, Section D.6 concludes the paper.

D.3 Problem Description

This section introduces the electricity market framework considered and the setup of the problem as a bilevel model.

[3]We define a producer to be a price-maker when it is capable of impacting the market result through its offer in a broad sense, not necessarily only by marking up its price offer above the marginal cost of production

D.3.1 Market Framework

In this work, we consider the short-term trade of electricity in the *day-ahead* and the *balancing* market. In the day-ahead market, wind power producers sell production for each trading period of the following day with a certain advance in time to the actual delivery, typically in the range between 12–36 hours. Since at the time of offering the actual wind power production is uncertain, producers must settle the excess or deficit of production by trading at the balancing market. Notice that *intra-day* markets are not considered in this work. This simplification is realistic since these markets have generally low liquidity [14].

Furthermore, we consider a *one-price* balancing market, i.e., all deviations are settled at a unique price, determined according to the marginal pricing rule. The so-called *two-price* or *dual-price* settlement of imbalances, where the day-ahead market price is applied to unwanted deviations in the opposite direction to the overall system imbalance, while the marginal price at the balancing stage is applied to all the other deviations, is not considered in this work. We remark that considering a two-price balancing market in this framework would be possible with some modifications, either by modeling the switch between day-ahead and marginal price with binary variables, or by employing supply curves dependent on the realization of the system deviation. The former option would come at the expense of a higher computational complexity, the latter of an increased modeling burden. We underline that, while some markets (e.g., a part of the Nordic countries in Nord Pool [15] and the Iberian MIBEL [16] in Europe) employ the two-price system for imbalances, there are a number of markets where the one-price scheme is adopted (e.g., Norway [15], the Dutch APX [17] and the German EEX [18] markets).

D.3.2 Bilevel Setup

The setup of the problem is sketched in Fig. D.1. The Wind Power Producer (WPP) seeks to maximize its total revenues from the day-ahead and the balancing market. Since we assume that the wind power producer is a price-taker at the day-ahead stage, but a price-maker at the balancing market, only the clearing of the latter market is explicitly included in the producer's optimization problem. This is because the day-ahead price is not influenced by the decision of the wind power producer and therefore, it can be modeled exogenously with a discrete number of scenarios. On the contrary, there is a dependence between the balancing market clearing and the optimization problem of the wind power producer. Indeed, the balancing market is cleared with knowledge on the bid of the wind power producer; in turn, the latter optimizes its offer on the basis of

the anticipation of the balancing market price, given its offer and a forecast of its production and of the residual system deviation.

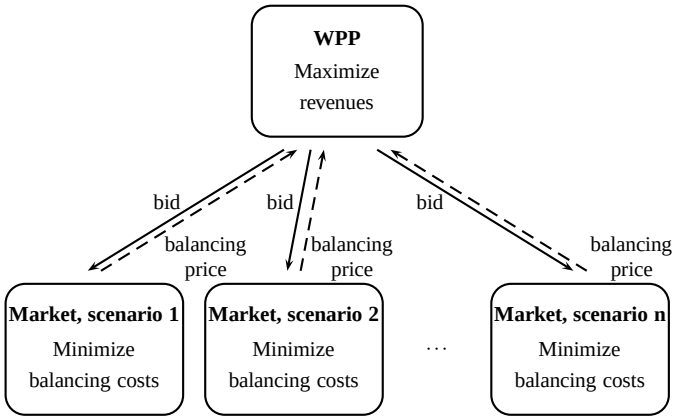

Figure D.1: Sketch of the problem setup

Since we model the uncertainty in future wind power production and residual system deviation with scenarios, we need to solve a balancing market clearing problem for each scenario. Such problem yields, for the particular realization of the uncertainties considered, the optimal dispatch of regulating power and the balancing market price, which enters the upper-level optimization problem (i.e., the producer's one). In the upper-level objective function, the market outcome corresponding to a certain scenario is weighted by the corresponding scenario probability.

Notice that we model exogenously the market participation of players other than the considered wind power producer through scenarios for the residual system deviation. In other words, we make use of a statistical tool able to forecast the aggregate imbalance from other wind power producers, possibly bidding strategically, and the load. However, if production forecasts for all the other wind power producers are available, competition should be modeled through an *Equilibrium Program with Equilibrium Constraints (EPEC)* [19]. We leave this complex topic for future research.

D.4 Mathematical Formulation

The bilevel optimization scheme outlined in Section D.3.2 corresponds to a stochastic formulation of an MPEC. We first formulate the problem in the gen-

eral framework of stochastic MPECs in Section D.4.1. Then, we present the formulation of the lower-level problems in Section D.4.2, and of the upper-level one in Section D.4.3.

D.4.1 Stochastic MPEC Formulation

The problem at hand has a bilevel structure where several (lower-level) optimization problems are nested in another (upper-level) one. This can be formulated as a stochastic MPEC as follows.

$$\text{Max.} \quad f(\mathbf{x}, \boldsymbol{\lambda}^{\mathrm{B}}) \tag{D.1a}$$

$$\text{s.t.} \quad h(\mathbf{x}, \boldsymbol{\lambda}^{\mathrm{B}}) \leq 0 \,, \tag{D.1b}$$

$$\left(\mathbf{p}_1, \lambda_1^{\mathrm{B}}, \boldsymbol{\mu}_1\right) \in \underset{\mathbf{y} \in F_1(\mathbf{x})}{\arg\min} \left\{ g_1(\mathbf{x}, \mathbf{y}) \right\} \,, \tag{D.1c}$$

$$\left(\mathbf{p}_2, \lambda_2^{\mathrm{B}}, \boldsymbol{\mu}_2\right) \in \underset{\mathbf{y} \in F_2(\mathbf{x})}{\arg\min} \left\{ g_2(\mathbf{x}, \mathbf{y}) \right\} \,, \tag{D.1d}$$

$$\vdots$$

$$\left(\mathbf{p}_{N_\Omega}, \lambda_{N_\Omega}^{\mathrm{B}}, \boldsymbol{\mu}_{N_\Omega}\right) \in \underset{\mathbf{y} \in F_{N_\Omega}(\mathbf{x})}{\arg\min} \left\{ g_{N_\Omega}(\mathbf{x}, \mathbf{y}) \right\} \,. \tag{D.1e}$$

The upper-level problem consists in the maximization of the objective function $f(\mathbf{x}, \boldsymbol{\lambda}^{\mathrm{B}})$ in (D.1a) subject to the feasibility constraint (D.1b), and further constrained by the optimality conditions of the lower-level problems (D.1c)–(D.1e). For a risk-neutral wind power producer, the objective function $f(\mathbf{x}, \boldsymbol{\lambda}^{\mathrm{B}})$ is the expected value of the total revenues in the day-ahead and balancing markets, given the information available at the time of bidding. The decision variables of the upper-level problem are the bid $\mathbf{x}$ in the day-ahead market, as well as the variables of the lower-level problems.

The lower-level problems are represented by (D.1c)–(D.1e) for all scenarios $\omega = 1, 2, \ldots, N_\Omega$. Such problems aim at the minimization of the objective functions $g_\omega(\mathbf{x}, \mathbf{y})$, provided that the decision vector $\mathbf{y}$ is included in the feasible sets $F_\omega(\mathbf{x})$. As we will see in the following section, the objective function of this problem represents the system balancing costs in the realization ω of the uncertainty, which are minimized in the balancing market. The clearing of this market results in the dispatch of balancing power $\mathbf{p}_\omega$, primal variable of the lower-level problem, as well as in the dual variables $\lambda_\omega^{\mathrm{B}}$ and $\boldsymbol{\mu}_\omega$. Notice that, as the remainder of the section will clarify, we are particularly interested in the value of $\lambda_\omega^{\mathrm{B}}$. Indeed, this variable indicates the balancing market price in scenario ω, which enters the upper-level optimization problem. Notice also that

the lower-level problems are parameterized in the wind power producer's offer in the day-ahead market $\mathbf{x}$, which enters such problems as a constant.

Formulation (D.1) is not suitable for being solved directly by an optimization solver, owing to the nested optimization of the lower-level problems in (D.1c)–(D.1e). However, such optimization problems can be replaced by their Karush-Kuhn-Tucker (KKT) conditions, for which a mixed-integer linear formulation exists, under reasonably mild assumptions. Indeed, KKT conditions are necessary and sufficient for optimality if the lower-level problems are convex and their constraints satisfy some regularity conditions [20]. If this holds, bilevel problem (D.1) can be reformulated as a single-level optimization problem. We derive this formulation explicitly in the remainder of this section.

D.4.2 Lower-Level Problem

The solution to the problem below for each scenario ω clears the balancing market.

$$\underset{p_{k\omega},p_{j\omega}}{\text{Min.}} \quad \sum_{k=1}^{N_K} c_k p_{k\omega} - \sum_{j=1}^{N_J} b_j p_{j\omega} \tag{D.2a}$$

$$\text{s.t.} \quad \sum_{k=1}^{N_K} p_{k\omega} - \sum_{j=1}^{N_J} p_{j\omega} = -(w_\omega - x_\omega) - \delta_\omega \ : \lambda_\omega^{\mathrm{B}} \ , \tag{D.2b}$$

$$-p_{k\omega} \geq -C_k \ : \mu_{k\omega}^{\mathrm{S}} \qquad \forall k \ , \tag{D.2c}$$

$$-p_{j\omega} \geq -C_j \ : \mu_{j\omega}^{\mathrm{D}} \qquad \forall j \ , \tag{D.2d}$$

$$p_{k\omega}, p_{j\omega} \geq 0 \qquad \forall k, j \ . \tag{D.2e}$$

The decision variables $p_{k\omega}$ and $p_{j\omega}$ represent the dispatch of up- and down-regulation power, respectively, from block offers k and j. The parameter c_k is the price offer (per unit cost) associated with the deployment of supply power from block k. Similarly, b_j is the per unit benefit associated with the power production decrease (down-regulation) from block j. Therefore, objective (D.2a) is the balancing cost in scenario ω. The balance of supply and demand is enforced by (D.2b). Indeed, the terms on the right-hand side of the equation are, after a change in sign, the sum of the deviation from the wind power producer (actual production w_ω minus day-ahead bid x_ω) and from all the other market participants (δ_ω). Notice that the residual system deviation and the producer's own imbalance are to be considered as a *perfectly inelastic* demand (or supply) of power, which must be met at any market price. Consequently, these two terms do not appear in the objective function (D.2a), while their sum is enforced to be equal to the power output of flexible generators at the

balancing stage through (D.2b). Equations (D.2c) and (D.2d) ensure that the dispatch of regulating power is not greater than the capacities C_k and C_j, which are the sizes of the block offers in the balancing market. Finally, non-negativity of the power dispatch is enforced by (D.2e). Notice that the dual variables of the problem are indicated after each constraint preceded by a colon. Variable $\lambda_\omega^{\mathrm{B}}$ is of particular importance, as it indicates the marginal cost of production, which is the balancing market price in a one-price imbalance settlement.

As one can notice, problem (D.2) is linear and thus it can be equivalently represented by the following set of KKT conditions [20]

$$0 \leq p_{k\omega} \perp c_k - \lambda_\omega^{\mathrm{B}} + \mu_{k\omega}^{\mathrm{S}} \geq 0 \qquad \forall k\,, \tag{D.3a}$$

$$0 \leq p_{j\omega} \perp -b_j + \lambda_\omega^{\mathrm{B}} + \mu_{j\omega}^{\mathrm{D}} \geq 0 \qquad \forall j\,, \tag{D.3b}$$

$$\sum_{k=1}^{N_K} p_{k\omega} - \sum_{j=1}^{N_J} p_{j\omega} = -(w_\omega - x_\omega) - \delta_\omega\,, \tag{D.3c}$$

$$0 \leq \mu_{k\omega}^{\mathrm{S}} \perp C_k - p_{k\omega} \geq 0 \qquad \forall k\,, \tag{D.3d}$$

$$0 \leq \mu_{j\omega}^{\mathrm{D}} \perp C_j - p_{j\omega} \geq 0 \qquad \forall j\,, \tag{D.3e}$$

where the $\perp$ operator separating two inequalities implies that at least one of them holds strictly. Conditions (D.3a) and (D.3b) are stationarity conditions; the inequalities on the right-hand side define, along with the non-negativity definitions on the left-hand side of (D.3d) and (D.3e), the feasible space of the dual problem. Conditions (D.3d) and (D.3e) are complementarity slackness conditions; the inequalities on the right-hand side define, along with (D.3c) and the non-negativity definitions on the left-hand side of (D.3a) and (D.3b), the primal feasible space.

Since the $\perp$ operator is equivalent to requiring that the multiplication between two linear expressions be equal to 0, the KKT conditions (D.3) include nonlinearities. However, it is possible to linearize such conditions by employing binary variables [21], yielding the following set of optimality conditions

$$0 \leq c_k - \lambda_\omega^{\mathrm{B}} + \mu_{k\omega}^{\mathrm{S}} \leq M_1^{\mathrm{SS}} z_{k\omega}^{\mathrm{S1}} \qquad \forall k\,, \tag{D.4a}$$

$$0 \leq p_{k\omega} \leq M_2^{\mathrm{SS}} \left(1 - z_{k\omega}^{\mathrm{S1}}\right) \qquad \forall k\,, \tag{D.4b}$$

$$0 \leq -b_j + \lambda_\omega^{\mathrm{B}} + \mu_{j\omega}^{\mathrm{D}} \leq M_1^{\mathrm{SD}} z_{j\omega}^{\mathrm{D1}} \qquad \forall j\,, \tag{D.4c}$$

$$0 \leq p_{j\omega} \leq M_2^{\mathrm{SD}} \left(1 - z_{j\omega}^{\mathrm{D1}}\right) \qquad \forall j\,, \tag{D.4d}$$

$$\sum_{k=1}^{N_K} p_{k\omega} - \sum_{j=1}^{N_J} p_{j\omega} = -(w_\omega - x_\omega) - \delta_\omega\,, \tag{D.4e}$$

$$0 \leq C_k - p_{k\omega} \leq M_1^{\mathrm{S}} z_{k\omega}^{\mathrm{S2}} \qquad \forall k\,, \tag{D.4f}$$

$$0 \leq \mu_{k\omega}^{\mathrm{S}} \leq M_2^{\mathrm{S}} \left(1 - z_{k\omega}^{\mathrm{S2}}\right) \qquad \forall k\,, \tag{D.4g}$$

$$0 \leq C_j - p_{j\omega} \leq M_1^{\mathrm{D}} z_{j\omega}^{\mathrm{D2}} \qquad \forall j\ , \tag{D.4h}$$

$$0 \leq \mu_{j\omega}^{\mathrm{D}} \leq M_2^{\mathrm{D}} \left(1 - z_{j\omega}^{\mathrm{D2}}\right) \qquad \forall j\ , \tag{D.4i}$$

$$z_{k\omega}^{\mathrm{S1}}, z_{j\omega}^{\mathrm{D1}}, z_{k\omega}^{\mathrm{S2}}, z_{j\omega}^{\mathrm{D2}} \in \{0,1\} \qquad \forall k, j\ , \tag{D.4j}$$

where the M constants are large enough to guarantee that the inequalities are never binding when the right-hand side is different from 0. Notice that, as long as such assumption holds and in view of the binary variable definitions in (D.4j), we have that constraints (D.4a) and (D.4b) are equivalent to (D.3a); (D.4c) and (D.4d) to (D.3b); (D.4f) and (D.4g) to (D.3d); (D.4h) and (D.4i) to (D.3e). Each balancing market clearing problem, i.e., for every scenario, can be replaced by its KKT conditions (D.4).

Furthermore, for reasons that will become apparent later in this section, it is interesting to notice that the dual of the lower-level problem (D.2) is, for every scenario ω,

$$\underset{\mu_{k\omega}^{\mathrm{S}}, \mu_{j\omega}^{\mathrm{D}}, \lambda_{\omega}^{\mathrm{B}}}{\mathrm{Max.}} \quad -\lambda_{\omega}^{\mathrm{B}} \left[(w_\omega - x_\omega) + \delta_\omega\right] - \sum_{k=1}^{N_K} C_k \mu_{k\omega}^{\mathrm{S}} - \sum_{j=1}^{N_J} C_j \mu_{j\omega}^{\mathrm{D}} \tag{D.5a}$$

$$\text{s.t. } \lambda_{\omega}^{\mathrm{B}} - \mu_{k\omega}^{\mathrm{S}} \leq c_k \qquad \forall k\ , \tag{D.5b}$$

$$-\lambda_{\omega}^{\mathrm{B}} - \mu_{j\omega}^{\mathrm{D}} \leq -b_j \qquad \forall j\ , \tag{D.5c}$$

$$\mu_{k\omega}^{\mathrm{S}}, \mu_{j\omega}^{\mathrm{D}} \geq 0 \qquad \forall k, j\ . \tag{D.5d}$$

The optimal objective function values of (D.5) and (D.2) are equal.

Finally, we stress that the network is not considered in this balancing market clearing model. This simplification, however, is justified in a European context, since the vast majority of European electricity markets employ zonal pricing.

D.4.3 Upper-Level Problem

In a one-price system, all deviations from the day-ahead schedule are settled at the marginal cost, i.e., the dual $\lambda_{\omega}^{\mathrm{B}}$ of the balance equation (D.2b) at the balancing market. Hence, the optimization problem of a wind power producer writes as

$$\underset{\substack{x_\omega,\, p_{k\omega},\, p_{j\omega},\\ \lambda_{\omega}^{\mathrm{B}},\, \mu_{k\omega}^{\mathrm{S}},\, \mu_{j\omega}^{\mathrm{D}}}}{\mathrm{Max.}} \quad \mathbb{E}\left\{\lambda_{\omega}^{\mathrm{DA}} x_\omega + \lambda_{\omega}^{\mathrm{B}} \left(w_\omega - x_\omega\right)\right\} \tag{D.6a}$$

$$\text{s.t. } 0 \leq x_\omega \leq C^{\mathrm{W}} \qquad \forall \omega\ , \tag{D.6b}$$

$$x_\omega = x_{\omega'} \qquad \omega, \omega' \in \Omega_i, \forall i\ , \tag{D.6c}$$

$$x_\omega \leq x_{\omega'} \qquad \omega \in \Omega_i, \omega' \in \Omega_j, i < j \ , \tag{D.6d}$$

KKT conditions of the lower-level problems .

The objective function (D.6a) is the expectation of the sum of two terms. The first term represents the revenues in the day-ahead market in scenario ω, since it is given by the multiplication of the day-ahead market price $\lambda_\omega^{\mathrm{DA}}$ with the offer x_ω in the same market. In an analogous fashion, the second term represents the revenues at the balancing stage in scenario ω. Therefore, the objective function is the expected total revenues at the two market floors. Notice that, since the wind power producer is a price-taker in the day-ahead market, $\lambda_\omega^{\mathrm{DA}}$ is a parameter and not an optimization variable. Furthermore, since the cleared day-ahead price is disclosed prior to the realization of the stochastic production and the residual system deviation in real-time, scenarios for the day-ahead price can be considered as first-stage scenarios, while the other scenarios can be regarded as second-stage. This implies that the scenario set Ω can be partitioned in a number of subsets Ω_i, across which the day-ahead price is constant, i.e.,

$$\lambda_\omega^{\mathrm{DA}} = \lambda_{\omega'}^{\mathrm{DA}}, \ \forall \omega, \omega' \in \Omega_i, \ \forall i \ . \tag{D.7}$$

Furthermore, since the order of the partitions Ω_i is arbitrary, we assume that they are sorted so that the corresponding day-ahead price is increasing, i.e.,

$$\lambda_\omega^{\mathrm{DA}} \leq \lambda_{\omega'}^{\mathrm{DA}}, \ \forall \omega \in \Omega_i, \forall \omega' \in \Omega_j, i < j \ . \tag{D.8}$$

Constraint (D.6b) enforces that the bid of the wind power producer be included in the range between 0 and the installed capacity C^{W}. Furthermore, market practices usually allow producers to submit bids in the form of non-decreasing supply curves, i.e., price-quantity pairs indicating how much energy the producer is willing to deliver at a certain day-ahead price. Constraints (D.6c) and (D.6d) together ensure that the wind power producer's offer is consistent with such practices, based on the partitioning of the scenario set Ω imposed by (D.7) and (D.8). Equation (D.6c) is a *non-anticipativity* constraint, which imposes that a single quantity is offered for every first-stage scenario (realization of the day-ahead price). Constraint (D.6d) enforces that the offer curve is non-decreasing.

The problem is complicated by the bilinear terms $\lambda_\omega^{\mathrm{B}} x_\omega$ in the objective function (D.6a), which can be linearized by applying the strong duality theorem on the lower-level (market-clearing) problem. At optimality, the objective value of

the primal (D.2) and the dual (D.5) problems are equal, i.e.,

$$\begin{aligned}\sum_{k=1}^{N_K} c_k p_{k\omega} - \sum_{j=1}^{N_J} b_j p_{j\omega} = &- \lambda_\omega^{\mathrm{B}} \left[(w_\omega - x_\omega) + \delta_\omega\right] \\ &- \sum_{k=1}^{N_K} C_k \mu_{k\omega}^{\mathrm{S}} - \sum_{j=1}^{N_J} C_j \mu_{j\omega}^{\mathrm{D}} \ .\end{aligned} \tag{D.9}$$

We can therefore reformulate the term inside the expectation operator in (D.6a) as follows

$$\begin{aligned}\lambda_\omega^{\mathrm{B}} \left(w_\omega - x_\omega\right) = &- \sum_{k=1}^{N_K} \left(C_k \mu_{k\omega}^{\mathrm{S}} + c_k p_{k\omega}\right) \\ &+ \sum_{j=1}^{N_J} \left(-C_j \mu_{j\omega}^{\mathrm{D}} + b_j p_{j\omega}\right) - \lambda_\omega^{\mathrm{B}} \delta_\omega \ ,\end{aligned} \tag{D.10}$$

where the expression on the right-hand side is linear.

The final optimization problem, incorporating the linearization of the bilinear terms in (D.10) and of the KKT conditions of the lower-level problem in (D.4), as well as using a finite number of scenarios for describing the uncertainty, so that the expectation operator in (D.6a) reduces to a sum weighted by probabilities, writes as

$$\begin{aligned}\underset{\Theta}{\text{Max.}} \quad & \sum_{\omega=1}^{N_\Omega} \pi_\omega \Bigg\{ \lambda_\omega^{\mathrm{DA}} x_\omega - \sum_{k=1}^{N_K} \left(C_k \mu_{k\omega}^{\mathrm{S}} + c_k p_{k\omega}\right) \\ & + \sum_{j=1}^{N_J} \left(-C_j \mu_{j\omega}^{\mathrm{D}} + b_j p_{j\omega}\right) - \lambda_\omega^{\mathrm{B}} \delta_\omega \Bigg\} \\ \text{s.t.} \quad & \text{(D.6b)–(D.6d)} \ , \\ & \text{(D.4a)–(D.4j)} \qquad \forall \omega \ .\end{aligned} \tag{D.11a}$$

The set of decision variables includes variable x_ω of the upper-level problem, the variables of the primal and the dual lower-level problems, as well as the binary variables needed for the linearization of the complementarity conditions, i.e.,

$$\begin{aligned}\Theta = \big\{ & x_\omega, p_{k\omega}, p_{j\omega}, \lambda_\omega^{\mathrm{B}}, \mu_{k\omega}^{\mathrm{S}}, \mu_{j\omega}^{\mathrm{D}}, \\ & z_{k\omega}^{\mathrm{S1}}, z_{j\omega}^{\mathrm{D1}}, z_{k\omega}^{\mathrm{S2}}, z_{j\omega}^{\mathrm{D2}}, \ \forall k, j, \omega \big\} \ .\end{aligned} \tag{D.12}$$

Notice that model (D.11) is a Mixed-Integer Linear Problem (MILP), which can be solved employing off-the-shelf optimization software.

D.5 Application Studies

This section describes a series of studies on the application of the presented model in a realistic setup. At first, the models employed in the examples for random variables are described in Section D.5.1. Then, results obtained in a single example are commented on in Section D.5.2. Finally, Sections D.5.3, D.5.4 and D.5.5 present the results of sensitivity analyses assessing the impact of the producer's market penetration, of the correlation between its output and the residual system deviation, and of the shape of the forecast wind power probability density function, respectively.

D.5.1 Modeling the Uncertainty

The uncertainties in the system, i.e., day-ahead price, wind power production and system deviation, are modeled using a discrete set of scenarios. It is assumed that the first-stage variable (day-ahead price) is independent of the second-stage ones (wind power production and residual system deviation). This basically means that we can build the scenario tree by generating first-stage and second-stage scenarios independently, and associating a copy of the second-stage scenarios to each first-stage scenario. Note that this assumption implies no loss of generality for the proposed method, since it could be overcome by employing a scenario generation method accounting for the possible dependency structure between first-stage and second-stage variables. We underline that this could be achieved without increasing the size of the optimization problem, and therefore, it is merely an issue linked to the scenario generation method, which is out of the scope of this paper. Finally, we point out that this independence assumption might be not valid in practice in markets with high penetration of wind power production, especially as far as the relationship between the day-ahead price and the forecast wind power distribution is concerned [12]. In this regard, however, we would like to underline that this simplification does not result in an overestimation of the economic improvement obtained with the proposed offering model, but quite the opposite. In fact, neglecting the possible correlation between these variables would result in conservative performance results in comparison to more "traditional" trading strategies (e.g., offering the forecast mean or a certain quantile), which do not allow differentiated offers on the basis of the realization of the day-ahead price, as the proposed method does.

Day-ahead price scenarios were generated by random sampling from the probabilistic forecast of the spot price in Nord Pool for the 12th trading period of the 7th September 2011. The probabilistic forecast is obtained by employing the semi-parametric approach extensively described in [22]. That method com-

bines a nonparametric description of the central part of predictive distributions based on quantile regression for quantiles with nominal proportion between 5% and 95%, and a parametric (exponential) description of the distribution tails. The quantile regression models use the predicted conditional expectations of day-ahead price and load as input. The parameters in the quantile regression models are adaptively estimated using the method of [23], while the parameters for the exponential tails are estimated once and for all under the maximum likelihood criterion.

As far as the second-stage variables are concerned, we employ Beta distributions to model wind power generation, as advocated in [24]. In practical applications it would be desirable to make use of a state-of-the-art forecasting tool employing a non-parametric model for the distribution of wind power production [25]. However, Beta distributions are sufficiently realistic to the purpose of this paper. Furthermore, notice that this assumption implies no loss of generality, as drawing scenarios from a non-parametric distribution would result in no additional complexity for the proposed optimization method.

For the residual system deviation we consider a Student's t-distribution, which provides a good fit for the hourly data for net system deviation in Western Denmark (DK-1 area price in Nord Pool) during the year 2011, which are available at [26]. A histogram of the actual data and an illustration of the parametric fit are provided in Fig. D.2. Once again, in a practical application it would be desirable to employ a state-of-the-art probabilistic model to describe this stochastic variable, possibly getting rid of the stationarity assumption implicit in our approach.

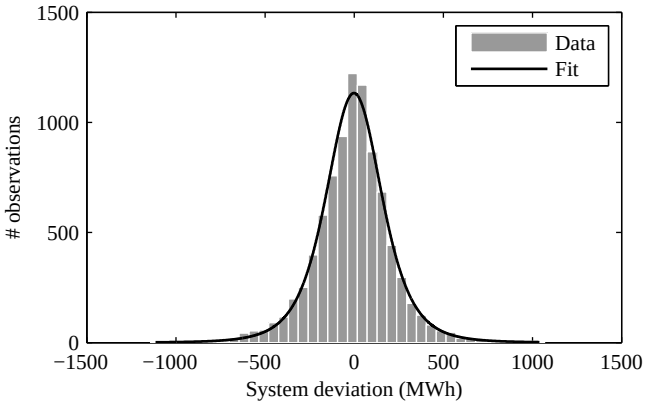

Figure D.2: Histogram for system deviation in Western Denmark (DK-1 price area of Nord Pool) during 2011, and fit using a Student's t distribution

The parameters employed for these distributions are shown in Table D.1. Furthermore, notice that when sampling scenarios for the system deviation from the Beta distribution, we discarded scenarios lower (greater) than the 0.001 (0.999) quantile. This is done because arbitrarily low (or high) values of system deviation could be sampled, which is not realistic and could potentially destabilize the results of the analysis. Furthermore, it should be noticed that the standard deviation of the Student's t-distribution used for the residual system imbalance is 217.57 MWh, which is comparable to the installed wind power capacity $C^{\mathrm{W}} = 300\,\mathrm{MW}$ owned by the producer. On the contrary, the total installed capacity in Denmark is approximately 14 GW. These two figures are in line with the assumption that the producer is a price-taker at the day-ahead market, where a significant share of the total installed capacity is supposed to participate, and a price-maker at the balancing market, whose trading volume corresponds to the total system imbalance.

Table D.1: Information on stochastic input parameters

Stochastic variable	Distribution type	Parameters	# scenarios original	# scenarios reduced
λ^{DA}	non-parametric	-	10 000	12
w	Beta	$\alpha = 3.78$ $\beta = 1.62$ $C^{\mathrm{W}} = 300$	10 000	100
δ	Student's t	$\mu = -0.96$ $\sigma = 161.14$ $\nu = 4.43$	10 000	100

As one can see in Table D.1, 10 000 scenarios were generated independently for each stochastic variable. In order to impose different rank correlation levels between wind power production and system deviation, we employed the method in [27]: first, we generated two random permutations of 10 000 Normal scores; then, we imposed the desired correlation (notice that Pearson and Spearman correlation almost coincide for Gaussian variables) by multiplying the permutations by the Cholesky factor of the desired rank correlation matrix; finally, we reordered the random samples for wind power production and system deviation according to the order of this product.

After this, we made use of the fast-forward scenario reduction technique [28] to decrease the number of first-stage and second-stage scenarios to 12 and 100, respectively. This procedure is based on a heuristic that iteratively adds scenarios to a reduced set, so as to minimize the maximum mutual distance between elements. Then, probabilities of the reduced scenarios are determined by assigning

the probability of each scenario in the original set to the closest element in the reduced set.

The last variables to be set are the ones characterizing the bids of participants at the balancing market, i.e., the per unit costs (benefits) of offered production increase (decrease), c_k (b_j), and the size of the respective blocks C_k (C_j). Data of individual bids at the balancing market are hardly available, owing to the confidentiality policies of market and transmission system operators. However, Nord Pool Spot publishes historical supply curves for the day-ahead Scandinavian market [29].

We employed the supply curve for the 12th trading period on the 7th September 2011 and the scenarios generated for the day-ahead price in Nord Pool for the same day and time to build bids for up- and down-regulation. First of all, we halved the capacity of the day-ahead bids in order to account for the fact that not all the generators trading in the day-ahead market are participating at the balancing market. This results in the marginal cost curve illustrated in Fig. D.3. Assuming that all the producers whose marginal cost is below the day-ahead

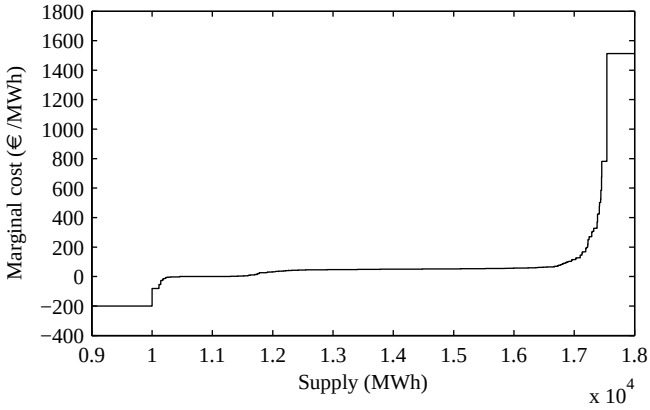

Figure D.3: Marginal cost curve at the balancing market

price scenario are dispatched at the day-ahead market, and the ones whose cost is above such price are not, we consider that down-regulation (production decrease from schedule) is supplied by the former participants and up-regulation by the latter ones. This way, we obtain a set of balancing market bids that is dependent on the first-stage scenario, i.e., the realization of the day-ahead price. In total we employed $N_K + N_J = 159$ offer blocks in the case study, with variable total numbers of up- and down-regulation blocks depending on the level of the day-ahead price, as a result of the splitting of the curve explained above.

Notice that, despite we derive the bids from a supply curve, demand could provide regulation as well at the balancing market by increasing or decreasing the scheduled consumption.

D.5.2 Results with Optimal Bidding

In the first case study, we employ the dataset generated as described in the previous section and impose a correlation $\rho = 0.3$ between the out-turn of the wind power producer and the residual system deviation using the method in [27], which is briefly sketched in Section D.5.1.

Defining the producer's penetration in the balancing market, ψ, as the ratio between the standard deviation of the wind power distribution and its sum with the standard deviation of the residual system imbalance, we obtain

$$\psi = \frac{\sigma_w}{\sigma_w + \sigma_\delta} = 19.88\,\% \,. \tag{D.13}$$

Notice that this definition of penetration is only one among several possible ones. However, as clarified later, it is intuitive as an increase in ψ is obtained by scaling up the wind power producer's capacity, and scaling down the total system deviation.

In this case, a totally price-insensitive day-ahead offer is optimal, consisting of the following optimal quantity

$$x = 76.69\,\text{MWh} \,. \tag{D.14}$$

First of all, it seems that the possibility of offering a curve does not lead to improved market results in this case, as the producer prefers a single quantity bid. We link this feature to the choice of a mostly convex supply curve, see Fig. D.3. Indeed, for increasing prices, the penalty given by the price spread between the day-ahead and the balancing markets tends to be higher for a "short" producer (i.e., producing less than the day-ahead offer). This implies that the higher the day-ahead price, the lower the optimal bid for the producer. However, this is not possible since constraint (D.6d) enforces that the bid curve be not decreasing.

Second, the optimal quantity bid in (D.14) appears to be a rather low quantile of the wind power distribution. Indeed, it lays just below the lowest scenario for wind power production. However, notice that this bid is far from being trivial. Indeed, for a price-taker wind power producer in a market with one-price settlement of imbalances, the optimal bid would be either 0 or the nominal capacity,

depending on whether the expectation of the balancing price is higher or lower than the day-ahead price [3]. Besides, wind power producers often bid the forecast conditional mean of wind power distribution in practice, which is perceived as a "safe" strategy. Among the reasons for this is the fact that there is a well established literature on point forecasting for wind power production, and the fact that point forecasts have been used for years since wind generation became a contributor to the electricity generation mix in power systems. Furthermore, point forecasts such as the conditional mean are recognized as risk-averse, as it minimizes the expected squared deviation from actual production [4]. Remarkably, none of these possible offers are optimal.

Table D.2 reports the main financial results obtained by bidding the optimal quantity (D.14). The first and second columns represent the improvement in average market revenues as compared to the strategies of offering the conditional mean and median of wind power distribution in the day-ahead market. The third column, instead, compares with the case where the actual production is traded exclusively at the balancing market. Notice that the nominal capacity offer is not included in the table, as this offer is far from being optimal with a hockey-stick supply curve such as the one depicted in Fig. D.3.

The improvement is above 3% as compared to bidding the mean or the median, and above 1.5% better than with a null day-ahead bid. The last column reports the average energy price (€54.26/MWh) obtained by averaging the ratio between revenues and wind power production over the scenario set.

Table D.2: Financial results obtained using the optimal bid

Profit improvement w.r.t.			Average price
mean (%)	median (%)	zero (%)	(€/MWh)
3.08	3.25	1.58	54.26

Finally, it should be noticed that, while the offer in (D.14) is aimed at maximizing the expected revenues, no account is taken of the possible impact on the producer's imbalance. Indeed, this offer results in an expected average imbalance (in absolute value) equal to 122.06 MWh. On the other hand, a known result is that the expected absolute value of the imbalance is minimized by offering the forecast median, which in this case would yield an expected imbalance of 44.82 MWh. We refer the reader to [4] for further discussion on the topic as well as for quantitative results obtained in a price-taker setting.

The optimization described above was performed using CPLEX 12 in GAMS. The model size is reported in Table D.3. The algorithm converged in 1680 s

on a laptop equipped with a 4-core processor clocking at 2.66 GHz. Despite the model size, the problem was solved relatively fast. In this respect, it is worth mentioning that the algorithm was warm-started by setting the binary variables to the values resulting from the market-clearing procedure when the wind power producer's offer is set to the mean of the scenario set for production at any price level. Notice that the latter problem is an LP, and therefore solves rather quickly.

Table D.3: Reduced model size in CPLEX

	Size
Rows	57 353
Columns	35 748
Non-zeros	150 797
Binaries	17 885

D.5.3 Sensitivity Analysis: Market Penetration

As mentioned in the previous section, we expect the optimal bid for a small wind power producer to be either 0 or the nominal capacity when the latter quantity is small compared to the residual system deviation. On the contrary, in the idealized situation where the producer is the only participant incurring deviations from the day-ahead schedule, we would expect that the optimal bid be close to the median of the conditional wind power distribution. This is because the resulting balancing market price would always be less favorable than the day-ahead market price. In the cases in between these two extremes, we expect the bid to have an intermediate behavior.

Different levels of penetration ψ, as defined in (D.13), of the wind power producer in the balancing market can be obtained simply by scaling the wind power production (D.15) and the residual system deviation (D.16), so as to satisfy (D.17). Since there is one degree of freedom left, we can choose the scaling factors A and B that leave unchanged the sum between the installed wind power capacity and the maximum absolute value of system deviation, as enforced by (D.18).

$$w^i_\omega = A w_\omega \ , \tag{D.15}$$

$$\delta^i_\omega = B \delta_\omega \ , \tag{D.16}$$

$$\psi^i = \frac{\sigma_{w^i}}{\sigma_{w^i} + \sigma_{\delta^i}} = \frac{A\sigma_w}{A\sigma_w + B\sigma_\delta} \ , \tag{D.17}$$

$$AC^{\mathrm{W}} + \max_{\omega} \left\{ \left| \delta_{\omega}^{i} \right| \right\} = C^{\mathrm{W}} + \max_{\omega} \left\{ |\delta_{\omega}| \right\} \ . \tag{D.18}$$

This makes comparisons more consistent, since we can expect similar prices with similar total deviation levels in the balancing market. We consider penetration levels spanning from 10% to 25% with an interval of 2.5%.

Fig. D.4 shows the optimal bids obtained for the penetration levels mentioned above. As one can notice, the optimal offer in the day-ahead market is 0 with the lowest value of penetration $\psi = 10\%$. Then, the curve tends to increase with the value of ψ, as we expected from our intuitive analysis.

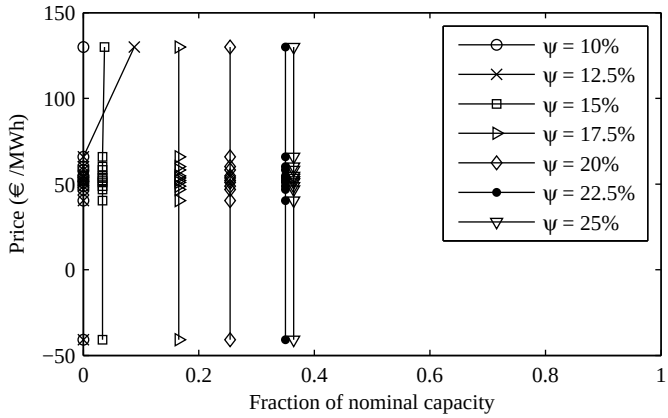

Figure D.4: Day-ahead offer curves with different levels of market penetration of the producer

The main financial results are summarized in Table D.4. It is important to notice that, as ψ increases, the improvement obtained using the optimal bid versus the conditional mean and median drops from over 7% to about 2%. On the contrary, the improvement compared to the zero day-ahead offer rises from 0% to around 2.5%. Finally, the average price obtained decreases by €3.5/MWh. This result is also in line with the expectations, since an increasing penetration implies that the total imbalance will tend to be in general of the same sign as the producer's deviation, thus leading to less favorable prices.

D.5.4 Sensitivity Analysis: Correlation

For the study in this section, we reorder the second-stage scenarios so as to impose a rank correlation level of -0.7, -0.3, 0, 0.3 and 0.7, using the method

Table D.4: Financial results with different levels of market penetration of the producer

Producer penetration (%)	Profit improvement w.r.t. mean (%)	median (%)	zero (%)	Average price (€/MWh)
10	7.34	7.58	0.00	56.90
12.5	5.97	6.20	0.03	56.10
15	4.56	4.79	0.16	55.34
17.5	3.63	3.81	1.26	54.68
20	3.05	3.23	1.58	54.24
22.5	2.53	2.70	2.18	53.76
25	1.96	2.13	2.53	53.40

in [27], which is sketched in Section D.5.1.

The optimal offering curves are depicted in Fig. D.5. As it appears, there is a decreasing trend in the day-ahead offer, which drops from roughly 170 MWh ($\rho = -0.7$) to about 40 MWh ($\rho = 0.7$). Apparently, the producer takes better advantage of the negative correlation with the residual system deviation by bidding closer to its median. Indeed, such a bid implies that the producer's deviation is more frequently of opposite sign compared to the system imbalance, and will therefore result in more favorable balancing market prices. With increasing correlation, a low bid better hedges the producer from the highest balancing prices, which occurs when the system is short of power.

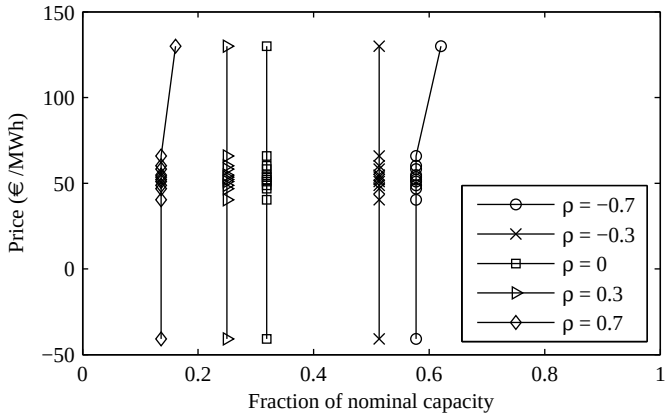

Figure D.5: Day-ahead offer curves with different levels of correlation between the wind power output of the producer and the residual system deviation

Table D.5 reports the main financial results in this sensitivity study. The higher the correlation, the larger the improvement with respect to bidding the median. Contrarily, the improvement with respect to the zero day-ahead bid drops. Finally, the average price diminishes with increasing correlation, which is an intuitive result, since a high correlation between own and system deviations implies less favorable prices in the balancing market.

Table D.5: Financial results with different levels of correlation between the wind power output of the producer and the residual system deviation

Correlation	Improvement w.r.t.			Average price
	mean (%)	median (%)	zero bid (%)	(€/MWh)
-0.7	0.19	0.27	4.72	54.84
-0.3	0.69	0.95	3.57	54.47
0	1.89	2.59	2.33	54.36
0.3	3.08	3.25	1.58	54.26
0.7	7.43	8.05	0.13	52.93

D.5.5 Sensitivity Analysis: Distribution Shape

In this section, we consider different Beta distributions modeling the forecast probability density function (pdf) of wind power production. To this end, we consider four different values ($[1.89, 3.78, 5.67, 7.56]$) for the parameter α of the Beta distribution, and four different values ($[1.62, 3.24, 4.86, 6.48]$) for β. To assess the effect of a changing distribution on the performance of the proposed strategy, we consider the 16 possible combinations of these parameter values.

The considered parameter space covers a wide range of cases of wind power production. Qualitatively speaking, the chosen parameters give rise to pdfs with low mean and positive skewness when $\alpha < \beta$, with mean around half the installed wind power capacity and skewness close to 0 when $\alpha \approx \beta$, and to distributions with high mean and negative skewness when $\alpha > \beta$. Fig. D.6 illustrates three examples of Beta distributions, one for each group described above, obtained with parameter values employed in the simulation.

To analyze the performance improvement brought by the proposed optimal strategy, we test it against two usual benchmarks for day-ahead market offer: the zero-offer and the conditional mean of wind power distribution.

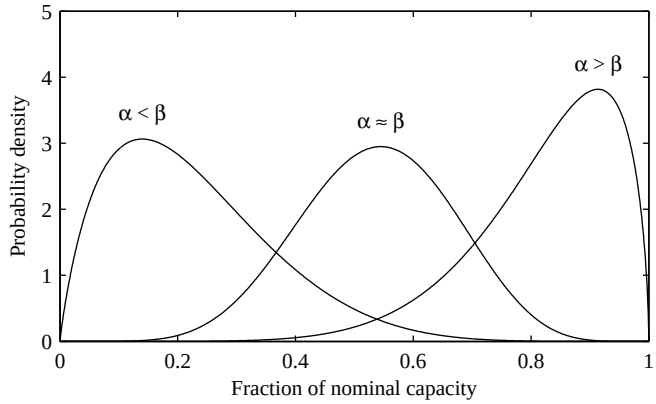

Figure D.6: Examples of Beta distributions as parameters change: $\alpha = 1.89$ and $\beta = 6.48$ result in the low-mean distribution, $\alpha = 7.56$ and $\beta = 6.48$ in the mid-mean distribution, $\alpha = 7.56$ and $\beta = 1.62$ in the high-mean distribution

In Fig. D.7, the improvement in expected profit with respect to the zero offer is shown as a surface for the 16 combinations of the α and β parameters of the Beta distribution considered. As one can notice, the improvement lies between 0 and 3%, which is consistent with the magnitude of the improvement observed in the previous studies. Remarkably, the zero-offer is basically optimal for low values of α and high values of β, which result in low-mean Beta distributions. Furthermore, there is a rather visible increasing trend of the performance improvement toward the right-hand side of the figure, where we find gradually higher values of α and lower values of β. Indeed, the combinations of parameters located on the right corner of the figure result in distributions with the highest mean and most negative skewness. Intuitively, it is reasonable that the zero offer becomes less and less efficient as the power distribution shifts closer to the installed capacity.

Fig. D.8 illustrates the improvement with respect to offering the forecast conditional mean of wind power production. Once again, the magnitude of the improvement is consistent with the results obtained so far. Besides, there is a trend specular to the one observed in Fig D.7. Indeed, the performance improvement decreases as we move from the left to the right-hand side of the figure. This trend highlights that, with combinations of α and β yielding distributions with high mean and negative skewness, the margin for improvement of the optimal strategy compared to offering the conditional mean decreases.

Finally, let us point out that the surfaces in Figs. D.7 and D.8 are obtained

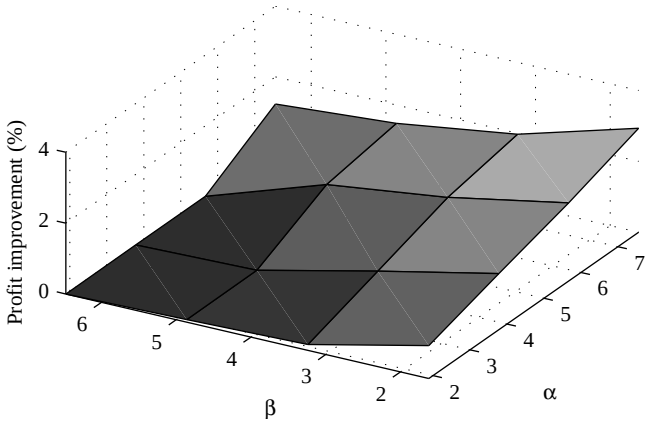

Figure D.7: Profit improvement with respect to offering zero as a function of the parameters α and β of forecast wind power distribution

from a single simulation per set of parameter values. These surfaces correspond to one of the potential realizations from a stochastic process, the stochasticity coming from how representative these particular sets of scenarios may be. If one wanted to have a full (though very costly) picture of the potential variations in these surfaces, one would have to repeat the simulations several times in a Monte Carlo fashion, therefore obtaining their empirical probabilistic description

D.6 Conclusion

This paper considers the optimization problem of a wind power producer being a price-taker at the day-ahead market, but a price-maker at the balancing market. We model this problem as a Mathematical Program with Equilibrium Constraints (MPEC) and cast it as a Mixed-Integer Linear Program (MILP). Uncertainty in day-ahead price, wind power production, and system deviation is modeled by employing scenarios.

Through a case study built from Nord Pool, the Scandinavian electricity market, and considering a one-price settlement of imbalances, we show that the optimal day-ahead bid is different from the zero and the nominal capacity offer, as well as from the forecast conditional mean and median of wind power distribution. This result is non trivial, since for a price-taker producer the optimal bid is either zero or the nominal capacity. The improvement in expected revenues with respect to these strategies amounts to between 1.5% and 3%.

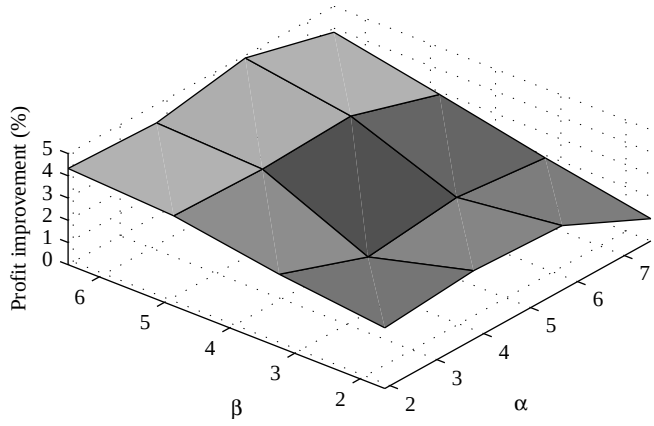

Figure D.8: Profit improvement with respect to offering the forecast mean as a function of the parameters α and β of forecast wind power distribution

Furthermore, we assess the impact of the producer's market penetration, correlation with the system imbalance and shape of forecast distribution of power production. We find that the optimal offer in the day-ahead market is increasing with market penetration and decreasing with correlation. Besides, the average market value of the energy traded by the wind power producer is a decreasing function of both parameters. Finally, we show a consistent performance improvement up to 5% with respect to offering zero or the mean at the day-ahead market, under a number of different distributions of forecast wind power production.

This work opens up several directions for future research. First of all, it would be interesting to assess the impact of market design on the optimal offering strategy and on the market results for the wind power producer, by modeling e.g., the two-price imbalance settlement. This would shed light on the current debate on the optimal design of balancing markets. Furthermore, the model could be extended so as to allow trading in the intraday market. Besides, considering the offering problem of a wind power producer that is a price-maker at all market stages would be a relevant extension. Modeling the electricity network could be another important upgrade of the model presented. Another topic of research consists in devising a method to solve this problem by using decomposition techniques, capable of exploiting its structure. Finally, modeling competition between wind power producers in the framework of *Equilibrium Problems with Equilibrium Constraints* (EPECs) would be particularly interesting.

Acknowledgment

Juan M. Morales, Pierre Pinson and Henrik Madsen are partly funded by the iPower platform project, supported by DSF (Det Strategiske Forskningsråd) and RTI (Rådet for Teknologi og Innovation), which are hereby acknowledged. Furthermore, we thank Tryggvi Jónsson from DTU Compute for providing the day-ahead price scenarios. The authors are grateful to Edmar de Almeida from the Federal University of Rio de Janeiro (UFRJ) and Yannick Perez from University Paris-Sud 11 for their valuable comments on this work. Finally, we thank five anonymous referees and an editor for a constructive discussion that certainly increased the value of this paper.

References D

[1] H. Madsen, P. Pinson, G. Kariniotakis, H. A. Nielsen, and T. S. Nielsen, "Standardizing the performance evaluation of short-term wind power prediction models," *Wind Engineering*, vol. 29, no. 6, pp. 475–489, 2005.

[2] J. B. Bremnes, "Probabilistic wind power forecasts using local quantile regression," *Wind Energy*, vol. 7, no. 1, pp. 47–54, 2004.

[3] C. J. Dent, J. W. Bialek, and B. F. Hobbs, "Opportunity cost bidding by wind generators in forward markets: Analytical results," *IEEE Transactions on Power Systems*, vol. 26, no. 3, pp. 1600–1608, 2011.

[4] M. Zugno, T. Jónsson, and P. Pinson, "Trading wind energy on the basis of probabilistic forecasts both of wind generation and of market quantities," *Wind Energy*, vol. In Press, 2012.

[5] P. Pinson, C. Chevalier, and G. Kariniotakis, "Trading wind generation from short-term probabilistic forecasts of wind power," *IEEE Transactions on Power Systems*, vol. 22, no. 3, pp. 1148–1156, 2007.

[6] M. Gibescu, W. L. Kling, and E. W. Van Zwet, "Bidding and regulating strategies in a dual imbalance pricing system: Case study for a Dutch wind producer," *International Journal of Energy Technology and Policy*, vol. 6, no. 3, pp. 240–253, 2008.

[7] G. Bathurst, J. Weatherill, and G. Strbac, "Trading wind generation in short-term energy markets," *IEEE Transactions on Power Systems*, vol. 17, no. 3, pp. 782–789, 2002.

[8] S. Galloway, G. Bell, G. Burt, J. McDonald, and T. Siewerski, "Managing the risk of trading wind energy in a competitive market," *IEE Proceedings—Generation, Transmission and Distribution*, vol. 153, no. 1, pp. 106–114, 2006.

[9] J. Matevosyan and L. Söder, "Minimization of imbalance cost trading wind power on the short-term power market," *IEEE Transactions on Power Systems*, vol. 21, no. 3, pp. 1396–1404, 2006.

[10] J. M. Morales, A. J. Conejo, and J. Pérez-Ruiz, "Short-term trading for a wind power producer," *IEEE Transactions on Power Systems*, vol. 25, no. 1, pp. 554–564, 2010.

[11] E. Y. Bitar, R. Rajagopal, P. P. Khargonekar, K. Poolla, and P. Varaiya, "Bringing wind energy to market," *IEEE Transactions on Power Systems*, vol. 27, no. 3, pp. 1225–1235, 2012.

[12] T. Jónsson, P. Pinson, and H. Madsen, "On the market impact of wind energy forecasts," *Energy Economics*, vol. 32, no. 2, pp. 313–320, 2010.

[13] Z.-Q. Luo, J.-S. Pang, and D. Ralph, *Mathematical Programs with Equilibrium Constraints*. Cambridge University Press, 1996.

[14] C. Weber, "Adequate intraday market design to enable the integration of wind energy into the European power systems," *Energy Policy*, vol. 38, no. 7, pp. 3155–3163, 2010.

[15] Nord Pool Spot, "Transmission system operators (TSOs)," 2013. (last access: January).

[16] Red Eléctrica de España, "Operación del sistema eléctrico," 2013. (last access: January), in Spanish.

[17] TenneT, "The imbalance pricing system," 2013. (last access: January).

[18] German transmission system operators, "Internet platform for tendering control reserve," 2013. (last access: January).

[19] S. A. Gabriel, A. J. Conejo, J. D. Fuller, B. F. Hobbs, and C. Ruiz, *Complementarity Modeling in Energy Markets*, vol. 180 of *International Series in Operations Research & Management Science*, ch. 7, pp. 263–322. New York: Springer, 2012.

[20] D. Luenberger, *Linear and Nonlinear Programming*. Addison-Wesley Publishing Company, 1984.

[21] J. Fortuny-Amat and B. McCarl, "A representation and economic interpretation of a two-level programming problem," *Journal of the Operational Research Society*, vol. 32, no. 9, pp. 783–792, 1981.

[22] T. Jónsson, *Forecasting and decision-making in electricity markets with focus on wind energy*. PhD thesis, Technical University of Denmark, 2012.

[23] J. K. Møller, H. A. Nielsen, and H. Madsen, "Time-adaptive quantile regression," *Computational Statistics & Data Analysis*, vol. 52, no. 3, pp. 1292–1303, 2008.

[24] A. Fabbri, T. Gomez San Román, J. Rivier Abbad, and V. H. Méndez Quezada, "Assessment of the cost associated with wind generation prediction errors in a liberalized electricity market," *IEEE Transactions on Power Systems*, vol. 20, no. 3, pp. 1440–1446, 2005.

[25] P. Pinson and G. Kariniotakis, "Conditional prediction intervals of wind power generation," *IEEE Transactions on Power Systems*, vol. 25, no. 4, pp. 1845–1856, 2010.

[26] Energinet.dk, "Website," August 2012. `http://energinet.dk/EN/El/Engrosmarked/Udtraek-af-markedsdata/Sider/default.aspx`.

[27] R. L. Iman and W. J. Conover, "A distribution-free approach to inducing rank correlation among input variables," *Communications in Statistics—Simulation and Computation*, vol. 11, no. 3, pp. 311–334, 1982.

[28] N. Gröwe-Kuska, H. Heitsch, and W. Römisch, "Scenario reduction and scenario tree construction for power management problems," in *Power Management Problems, IEEE Bologna Power Tech Proceedings*, 2003.

[29] Nord Pool Spot, "Website," August 2012. `http://nordpoolspot.com/Market-data1/Downloads/Elspot-System-price-curves/Elspot-System-price-curve/`.

Paper E

Modeling Demand Response in Electricity Retail Markets as a Stackelberg Game

Authors:
Marco Zugno, Juan Miguel Morales, Pierre Pinson, Henrik Madsen

Presented at:
12th IAEE European Energy Economics Conference (2012)

Modeling Demand Response in Electricity Retail Markets as a Stackelberg Game

Marco Zugno[1], Juan Miguel Morales[2], Pierre Pinson[1], Henrik Madsen[1]

Abstract

We model the retail market with dynamic pricing as a Stackelberg game where both retailers (leaders) and flexible consumers (followers) solve an economic cost-minimization problem. The electricity retailer optimizes an economic objective over a daily horizon by setting an hourly price-sequence, which is then communicated to the end-consumers. In turn, on the basis of such price sequence, consumers optimize a utility function that accounts both for energy procurement costs and for the benefit loss resulting from deferring consumption. The game is formulated as a Mathematical Problem with Equilibrium Constraints (MPEC) and cast as a Mixed Integer Linear Program (MILP), which can be solved using off-the-shelf optimization software. In an illustrative example, we consider a retailer associated with both flexible demand and wind power production. Such an example shows the efficiency of dynamic pricing as a way to control the load for minimizing the imbalances due to wind power, assesses the overall economic results for the retailer and the consumers as well as the dynamic properties of consumer flexibility.

E.1 Introduction

The increasing political pressure to reduce the environmental impact of electricity generation is causing a massive deployment of production capacity from unpredictable and intermittent renewable energy sources, such as wind and solar. Facilitating the integration of such sources in electricity markets is therefore seen as of primary importance.

[1]DTU Informatics, Technical University of Denmark, Richard Petersens Plads, bld. 305, DK-2800 Kgs. Lyngby, Denmark

[2]Centre for Electric Power and Energy, Technical University of Denmark, Elektrovej, bld. 325, DK-2800 Kgs. Lyngby, Denmark

Power markets nowadays are still designed according to the principle of *demand-following supply*, which dictates that the energy generation portfolio of the system should be flexible enough to always match the load. Given the non-dispatchable nature of wind and solar power, which cannot guarantee a certain production level in all meteorological conditions, a reliable power system operation needs the backup from dispatchable, conventional sources. Obviously, this fact limits the share of renewable generation capacity that can be integrated in a power system.

One of the key factors for easing the large-scale integration of renewables is demand response. Indeed, its efficient deployment can bring about a shift in power markets, by endowing them with a *supply-following demand* whose flexibility can be exploited to match the variable output of renewable sources. Several initiatives have been proposed in order to involve both large and small consumers in the provision of demand flexibility, including most notably load shedding programmes, time-of-use and real-time tariffs for consumers [1]. Although large consumers are already allowed in many European countries to provide demand response, e.g. by participating at power exchanges or at load shedding programmes, the development of initiatives to involve small consumers are still at an experimental stage.

In order to involve small consumers in demand response, many advocate the use of dynamic price signals. Several questions, though, are still unanswered, including quantifying the potential of dynamic pricing for peak-shaving, load-shifting and reduction of imbalance costs, its impact on the social welfare and the redistribution of the welfare surplus to the players involved.

In this work, we model the retail market with dynamic pricing as a Stackelberg game [2] where both retailers (leaders) and flexible consumers (followers) solve an economic cost-minimization problem. The electricity retailer optimizes an economic objective over a daily horizon by setting an hourly price-sequence, which is then communicated to the end-consumers. In turn, on the basis of such a price sequence, consumers optimize a utility function that accounts both for energy procurement costs and for the benefit loss resulting from deferring consumption. We consider that consumers are flexible in their consumption for heating, and model heating dynamics using state-space models similar to [3].

This paper is structured as follows. Section E.2 illustrates the conceptual framework from a high-level perspective. The mathematical formulation of such framework is then presented in Section E.3. An illustrative example enlightening the main features of the model is introduced in Section E.4. Finally, Section E.5 concludes the paper.

E.2 Conceptual framework

This section illustrates the general concept behind the model presented in this paper, which is a Stackelberg (or leader-follower) game. The structure of such a game is represented as a block diagram in Figure E.1. A leader, in this case

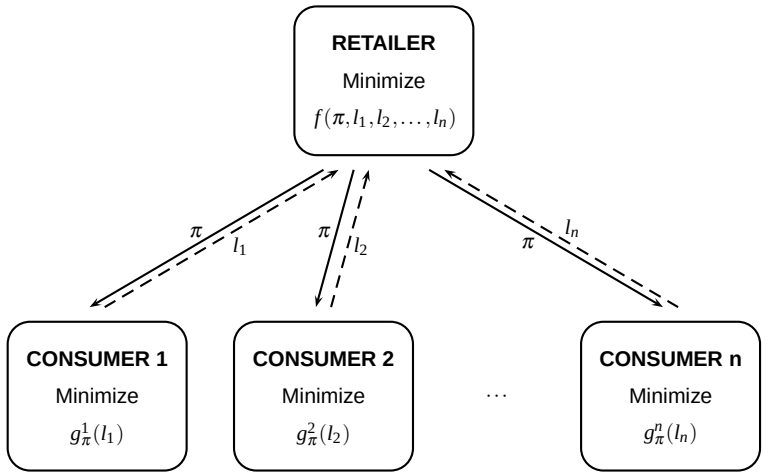

Figure E.1: Conceptual framework for modeling demand response as a bilevel program. Solid arrows indicate exchange of information, while dashed arrows represent inferences on the consumer behavior

the retailer, minimizes its objective function $f(\pi, l_1, l_2, \ldots, l_n)$. For the sake of generality of this section we will leave the definition of the objective function, which is most likely of economical nature, to Section E.3.2. As the notation tells explicitly, though, such objective function directly depends on the price π, which is a decision variable of the leader. Furthermore, the objective function f depends on the demand $l_i, i = 1, 2, \ldots, n$ from the n consumers (followers) associated to the leader.

Obviously, the consumptions l_i are ultimately decisions of the consumers. In a demand response framework with variable price, consumers would have to solve optimization problems where the minimization of the cost of electricity procurement is weighted against the loss of comfort implied by possible anticipations or delays in energy consumption. For example considering the electricity consumption for heating, the objective function $g_\pi^i(l_i)$ for consumer i would sum the cost of electricity to a penalty for the deviation of the indoor temperature from a certain reference [4]. Such an optimization problem includes the consumption l_i as decision variable, and is parameterized in the price π decided by the retailer. This problem would then be solved directly by the consumer's smart appliances,

once the price signal π is broadcast by the leader.

The solid lines in Figure E.1 indicate that there is a direct information exchange when the price schedule is sent from the leader to the follower. The dashed lines indicate that the followers do not directly communicate their consumption schedule to the leader. Nevertheless, the leader can infer the followers' consumption schedule given the price signal π on the basis of a model of the consumers.

As a final remark in this section, we point out that the leader of the Stackelberg game need not necessarily be a retailer, but any market entity setting the dynamic consumer price. In different demand response frameworks, the leader could be the Transmission System Operator (TSO), a Distribution System Operator (DSO) or an aggregator of consumers [5]. Obviously, such leaders would have different objective functions, but the bilevel structure of the problem would remain practically unchanged.

E.3 Mathematical formulation

The Stackelberg game sketched in Section E.2 can be formulated rigorously in the framework of *Mathematical Programs with Equilibrium Constraints* (MPEC) [6]. Such games have a bilevel structure where one or more (lower-level) optimization problems are nested in another (upper-level) one. This can be formulated as

$$\begin{aligned}
\text{Min.} \quad & f(\pi, l_1, l_2, \ldots, l_n)\,, && \text{(E.1a)}\\
\text{s.t.} \quad & h(\pi, l_1, l_2, \ldots, l_n) \leq 0\,, && \text{(E.1b)}\\
& l_1 \in \arg\min \left\{ g_\pi^1(l_1) \text{ s.t. } m_\pi^1(l_1) \leq 0 \right\}, && \text{(E.1c)}\\
& l_2 \in \arg\min \left\{ g_\pi^2(l_2) \text{ s.t. } m_\pi^2(l_2) \leq 0 \right\}, && \text{(E.1d)}\\
& \qquad\qquad \vdots \\
& l_n \in \arg\min \left\{ g_\pi^n(l_n) \text{ s.t. } m_\pi^n(l_n) \leq 0 \right\}. && \text{(E.1e)}
\end{aligned}$$

Notice that this formulation employs the same notation as Figure E.1. The lower-level problems are represented by (E.1c)–(E.1e), which include the feasibility constraints $m_\pi^i(l_i) \leq 0$, besides the objective functions $g_\pi^i(l_i)$. The upper-level problem consists in the minimization of the objective function $f(\pi, l_1, \ldots, l_n)$ in (E.1a) subject to the feasibility constraint (E.1b), and further constrained by the optimality of the lower-level problems.

Despite its clarity, formulation (E.1) cannot be translated directly into a com-

putationally manageable optimization problem, owing to the nested optimization of the lower-level problems in (E.1c)–(E.1e). Fortunately though, such optimization problems can be replaced by their Karush-Kuhn-Tucker (KKT) conditions under reasonably mild assumptions. Indeed, KKT conditions are necessary and sufficient for optimality if the lower-level problems are convex and their constraints satisfy some regularity conditions [7]. If this holds, the bilevel problem (E.1) can be reformulated as the following single-level program

$$\begin{aligned}
\text{Min.} \quad & f(\pi, l_1, l_2, \ldots, l_n)\,, && \text{(E.2a)}\\
\text{s.t.} \quad & h(\pi, l_1, l_2, \ldots, l_n) \leq 0\,, && \text{(E.2b)}\\
& \text{KKT conditions of problem for Consumer 1}\,, && \text{(E.2c)}\\
& \text{KKT conditions of problem for Consumer 2}\,, && \text{(E.2d)}\\
& \qquad\vdots\\
& \text{KKT conditions of problem for Consumer n}\,. && \text{(E.2e)}
\end{aligned}$$

In the remainder of this section, we will formulate problem (E.2) explicitly and deal with the nonlinearities in the KKT conditions.

E.3.1 Lower-level problem

As previously mentioned, we focus on the flexibility of the load due to heating. Therefore, the consumer (lower-level) problem is the optimal scheduling of electricity consumption for heating. Similarly to [3], we model the heat dynamics of buildings using state space models [8]. Furthermore, the objective function is defined as the sum over all the T time periods considered in the optimization horizon of the cost of purchasing electricity plus a quadratic penalty for deviations of the temperature from a certain reference fixed a priori. This results in the following problem

$$\begin{aligned}
\text{Min.} \quad & g_\pi(l) = \sum_{t=1}^{T} c(x_{1,t} - \bar{x}_{1,t})^2 + \pi_t l_t\,, && && && \text{(E.3a)}\\
\text{s.t.} \quad & x_{1,t} = a_{11}x_{1,t-1} + a_{12}x_{2,t-1} && : \lambda_{1,t} && t = 1, \ldots, T\,, && \text{(E.3b)}\\
& x_{2,t} = a_{22}x_{2,t-1} + b l_t && : \lambda_{2,t} && t = 1, \ldots, T\,, && \text{(E.3c)}\\
& l_t \geq 0 && : \mu_t && t = 1, \ldots, T\,. && \text{(E.3d)}
\end{aligned}$$

The objective function in (E.3a) comprises two terms: a quadratic penalty for deviations of the indoor temperature (i.e. the first state $x_{1,t}$) from the reference $\bar{x}_{1,t}$, multiplied by the parameter c, and the cost of purchasing electricity $\pi_t l_t$.

The objective function is parameterized in the decision variable π_t of the upper-level problem. Constraints (E.3b) and (E.3c) are the state updates of the model for heat dynamics. The second state $x_{2,t}$ is determined in (E.3c) as a function of its value at the previous step and the electricity consumption. In turn, the indoor temperature $x_{1,t}$ depends in (E.3b) on the previous values of x_1 and x_2, but not directly on the consumption. Finally (E.3d) enforces the nonnegativity of the consumption. In principle, an upper bound could be imposed as well, but this is not necessary in this case since the tuning of the parameters discourages too high consumption levels. We finally point out that the symbols after the colons in (E.3b)–(E.3d) are the dual variables associated with the relative constraints.

We remark that the optimization model (E.3) is akin to the one in [4]. An important difference, though, is the quadratic penalty for deviations from a point reference, rather than the penalty for deviations out of a reference band in [4]. The latter objective function would indeed result in a degenerate lower-level problem with multiple solutions. As a consequence, there would be a multiplicity of Stackelberg solutions [9], while the optimization model (E.2) would only determine (one of) the strong Stackelberg solution(s) [6].

Since the optimization problem (E.3) is a convex minimization problem with linear constraints, the KKT conditions are necessary and sufficient for optimality [7]. Therefore, problem (E.3) is equivalent to the following set of conditions

$$2c(x_{1,t} - \bar{x}_{1,t}) + \lambda_{1,t} - a_{11}\lambda_{1,t+1} = 0 \qquad t = 1, 2, \ldots, T-1\,, \tag{E.4a}$$
$$2c(x_{1,T} - \bar{x}_{1,T}) + \lambda_{1,T} = 0\,, \tag{E.4b}$$
$$\lambda_{2,t} - a_{12}\lambda_{1,t+1} - a_{22}\lambda_{2,t+1} = 0 \qquad t = 1, 2, \ldots, T-1\,, \tag{E.4c}$$
$$\lambda_{2,T} = 0\,, \tag{E.4d}$$
$$\pi_t - b\lambda_{2,t} - \mu_t = 0 \qquad t = 1, \ldots, T\,, \tag{E.4e}$$
$$x_{1,t} = a_{11}x_{1,t-1} + a_{12}x_{2,t-1} \qquad t = 1, \ldots, T\,, \tag{E.4f}$$
$$x_{2,t} = a_{22}x_{2,t-1} + bl_t \qquad t = 1, \ldots, T\,, \tag{E.4g}$$
$$0 \leq \mu_t \perp l_t \geq 0 \qquad t = 1, \ldots, T\,. \tag{E.4h}$$

Such conditions include the stationarity conditions (E.4a)–(E.4e) for the Lagrangian of problem (E.3) taken with respect to $x_{1,t}$ ($t = 1, 2, \ldots, T-1$), $x_{1,T}$, $x_{2,t}$ ($t = 1, 2, \ldots, T-1$), $x_{2,T}$ and l_t ($t = 1, 2, \ldots, T$), respectively. Furthermore, the set (E.4) includes the constraints of the primal and of the dual of problem (E.3), as well as the complementarity conditions (E.4h) relative to the inequality constraints (E.3d). The latter condition implies that both l_t and μ_t are nonnegative and at least one of them is zero at any time.

Although (E.4h) is a nonlinear constraint, it can be equivalently recast as the

following set of mixed-integer linear constraints [10]

$$l_t \geq 0 \qquad t = 1, 2, \ldots, T, \tag{E.5a}$$
$$l_t \leq i_t M_l \qquad t = 1, 2, \ldots, T, \tag{E.5b}$$
$$\mu_t \geq 0 \qquad t = 1, 2, \ldots, T, \tag{E.5c}$$
$$\mu_t \leq (1 - i_t) M_\mu \qquad t = 1, 2, \ldots, T, \tag{E.5d}$$
$$i_t \in \{0, 1\} \qquad t = 1, 2, \ldots, T, \tag{E.5e}$$

where M_l and M_μ are "large enough" constants, which ensure that constraints (E.5b) and (E.5d) are never binding when the right-hand side is different from 0. Notice that with this reformulation, the nonlinearity of (E.4h) has been traded with the integrality of the conditions (E.5).

The values used for the parameters in problem (E.3) are listed in Table E.1. Although such values are arbitrary in this work, they are chosen so that they

Parameter	Value	Unit
c	0.003	€°C^{-2}
$\bar{x}_{1,t}$	$22 + 2\cos\left(\frac{3}{4}\pi + \frac{2\pi t}{24}\right)$	°C
a_{11}	0.9	-
a_{12}	0.07	-
a_{22}	0.95	-
b	2	°C kW^{-1}h^{-1}

Table E.1: Values of the parameters in the consumer problem (E.3)

produce realistic results. Our focus here is on the properties on the model, therefore we refer the reader interested in a realistic estimation of models for heat dynamics to [3]. The temperature reference is chosen so that it has a daily period with its peak during the afternoon. The c constant is chosen so that the results are sensible in a realistic range of electricity prices. In principle, one could imagine that the producers of heating systems would provide a number of such realistic constants to be chosen by the consumer.

An example of the interaction between prices and consumer behavior can be seen in Figure E.2. This figure illustrates the evolution of the indoor temperature $x_{1,t}$ during an entire day when the consumer receives a constant price schedule. The results for three different price levels are shown: $\pi_t =$€0.1/kWh, $\pi_t =$€ 0.2/kWh and $\pi_t =$€0.3/kWh. As one can notice, the heating system never follows precisely the schedule, but there is always a negative difference. This is due to the fact that the cost of electricity is positive, while the penalty for deviations is quadratic, the combination of which makes it optimal to follow the reference at a certain distance from below. Furthermore, if the price is increased

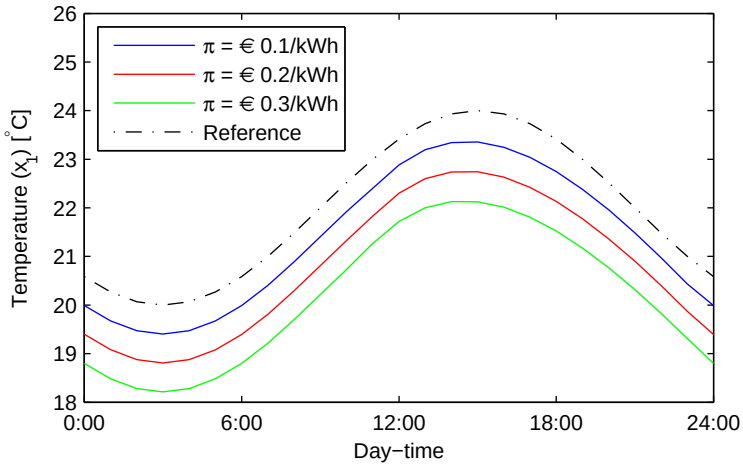

Figure E.2: Reference following for the consumer problem at difference price levels

the consumer is less reluctant to deviate from the reference and accepts a lower temperature.

E.3.2 Upper-level problem

While the structure of the lower-level problem is well defined—the minimization of a cost function for the consumer based on the heat dynamics of buildings—different configurations of the upper-level problem could be thought of, depending on whom the leader of the Stackelberg game is.

In this work, we analyze the case of a retailer equipped with a wind power production facility and a flexible load. To keep the analysis of the problem as simple as possible, we consider only one consumer, although in principle more consumers could be included. It is assumed that the retailer participates at a spot market, and that it has to provide the market operator with a schedule for the hourly load consumption during the following day with a certain advance in time. This is currently the case in NordPool, the Scandinavian electricity market, where retailers have to purchase every day at noon their expected consumption for each hour of the following day.

For the sake of simplicity, we focus on the use of demand response for reducing the imbalance costs due to the deviations of wind power production from its day-

ahead forecast. We assume that the day-ahead schedule s_t for power delivery at hour t of the following day is given by the difference of the day-ahead prognoses of wind out-turn $\widehat{w}_t$ and of consumption $\widehat{l}_t$

$$s_t = \widehat{w}_t - \widehat{l}_t \,. \tag{E.6}$$

We remark that s_t could be both positive or negative, indicating a power delivery to or withdrawal from the grid, respectively. As far as the prognosis for wind power production is concerned, we assume without loss of generality that the retailer uses point forecasts issued before the time of bidding on the spot market. This bidding strategy is still rather common among wind power producers [11]. Besides, the consumption forecast can be determined by solving the consumer problem (E.3) with a constant price signal. In this work, we consider the range of prices between €0.1/kWh and €0.3/kWh. Therefore, a reasonable choice when determining the day-ahead load prognosis is a constant price signal of $\widehat{\pi}_t$ =€0.2/kWh, $\forall t$. This gives the retailer room for adjusting the consumer price later in both directions.

At the real-time stage, the net power withdrawal or delivery will differ from the schedule s_t, owing to the unpredictability of wind power production. Since the level of uncertainty decreases with shorter lead times, we can expect that the forecasts available one hour ahead are less uncertain than the day-ahead ones. Therefore, the retailer has the possibility of smoothing out the forecast errors by sending the consumers a price signal that encourages them to absorb such deviations.

In stochastic programming, it is customary to represent uncertainty with a discrete number of scenarios. We will index the scenarios using the subscript ω. Each scenario is associated with its probability p_ω and with a specific realization of wind power production $w_{t\omega}$, which is the only stochastic variable we consider here. Figure E.3 shows 10 scenarios for wind power out-turn with a 36-hour horizon, along with the corresponding day-ahead point forecast. Both point forecasts and scenarios are generated using time series models following the method proposed in [12]. As one can see in the plot, the hour-ahead information is in the form of a scenario fan, i.e. the first predictions coincide for all the scenarios and represents the current (known) wind power production. This implies that there is perfect information on the current wind power out-turn. In practical situations where decisions are not made exactly in real-time, though very close, the scenarios would differ also at the first time period.

For every scenario ω and time-period t, the net deviation from the schedule is given by

$$d_{t\omega} = w_{t\omega} - l_t - s_t \,, \tag{E.7}$$

where l_t is the actual consumption from the consumers associated with the

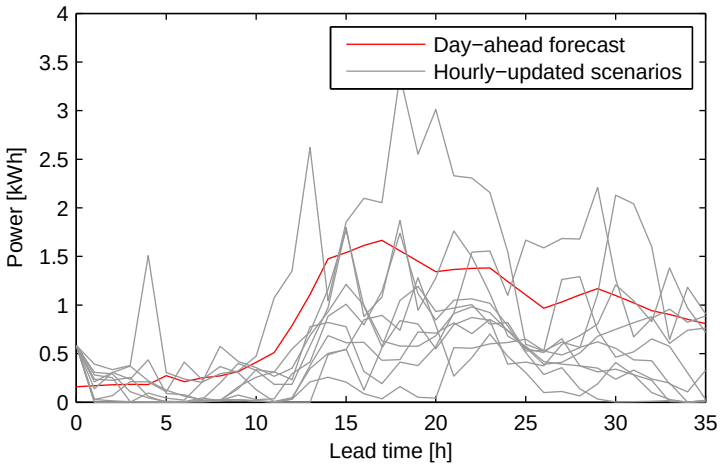

Figure E.3: Example of day-ahead forecast compared to the relative hour-ahead scenarios

retailer. In many electricity markets, deviations from the day-ahead schedule are penalized and in general unwanted, as they require the system operators to take costly corrective measures (e.g. the activation of power reserves). Resembling the operation of a virtual power plant, we aim at minimizing the absolute value of the deviation from the day-ahead schedule (or power imbalance). In order to include the absolute value in a linear optimization model, we split the imbalance into its positive and negative parts, d_t^+ and d_t^- respectively, which are defined as follows

$$d_t^+ = \begin{cases} d_t, & d_t \geq 0\,, \\ 0, & d_t < 0\,, \end{cases} \qquad d_t^- = \begin{cases} 0, & d_t \geq 0\,, \\ d_t, & d_t < 0\,. \end{cases} \tag{E.8}$$

Notice that if the objective function is the minimization of the absolute value of the deviations, it is not necessary to enforce the piecewise definition (E.8). Indeed, it is easy to verify that, for any optimization problem including the following

$$\begin{aligned} \text{Min.} \quad & d_{t\omega}^+ - d_{t\omega}^-\,, && \text{(E.9a)} \\ \text{s.t.} \quad & d_{t\omega}^+ \geq w_{t\omega} - l_t - s_t\,, && \text{(E.9b)} \\ & d_{t\omega}^- \leq w_{t\omega} - l_t - s_t\,, && \text{(E.9c)} \\ & d_{t\omega}^+ \geq 0, d_{t\omega}^- \leq 0 && \text{(E.9d)} \end{aligned}$$

the optimum is unchanged if (E.9b), (E.9c) and (E.9d) are replaced by the piecewise definitions (E.8).

The final formulation of the problem is then readily given by

$$\text{Min.} \quad \sum_{\omega=1}^{N_\omega} p_\omega \left(\sum_{t=1}^{T} d_{t\omega}^{+} - d_{t\omega}^{-} \right) \tag{E.10a}$$

$$\text{s.t.} \quad d_{t\omega}^{+} \geq w_{t\omega} - l_t - s_t \qquad \forall t, \omega \tag{E.10b}$$

$$d_{t\omega}^{-} \leq w_{t\omega} - l_t - s_t \qquad \forall t, \omega \tag{E.10c}$$

$$d_{t\omega}^{+} \geq 0, d_{t\omega}^{-} \leq 0 \qquad \forall t, \omega \tag{E.10d}$$

$$0.1 \leq \pi_t \leq 0.3 \qquad \forall t \tag{E.10e}$$

$$\{\text{(E.4a)–(E.4g)}, \text{(E.5a)–(E.5e)}\} \text{ for every consumer}$$

The objective function (E.10a) is the expectation of the sum over all the T time periods in the horizon of the absolute value of power imbalance. Compared to the constraints of model (E.9), the optimization problem (E.10) includes (E.10e), which enforces that the price is never higher than €0.3/kWh nor lower than €0.1/kWh. This ensures that the consumer will not be asked to give up too much comfort for balancing the operation of the virtual power plant. Finally, the KKT conditions guaranteeing optimality of the lower-level problem are also included. We remark that problem (E.10) is a MILP, which can be solved by employing off-the-shelf optimization software.

After the optimization problem (E.10) is solved, the retailer sends the optimal price signal π_t to the consumers for all the time periods included in the horizon. The process is then repeated iteratively rolling the optimization horizon forward. As a result, only the first price in the signal is actually charged to the consumer at any iteration of this rolling process.

E.4 Illustrative example

This section illustrates an example where the model presented in Section E.3 is simulated over one day. In total 24 optimizations are run, one for every hour of the day, employing a rolling horizon. At each hour the wind power scenarios are updated for the entire horizon, and the initial conditions are set to the corresponding output values at the previous step of the procedure.

Figure E.4 illustrates the dynamics of relevant variables during the simulation. The reader should keep in mind that only realized values are used to produce these plots, i.e. the evolutions are obtained by concatenating the first value of each variable at each step of the rolling procedure. The indoor temperature for the consumer is shown in Figure E.4(a). As one can see, the temperature dynamics with variable price is similar to the one with fixed price. In general

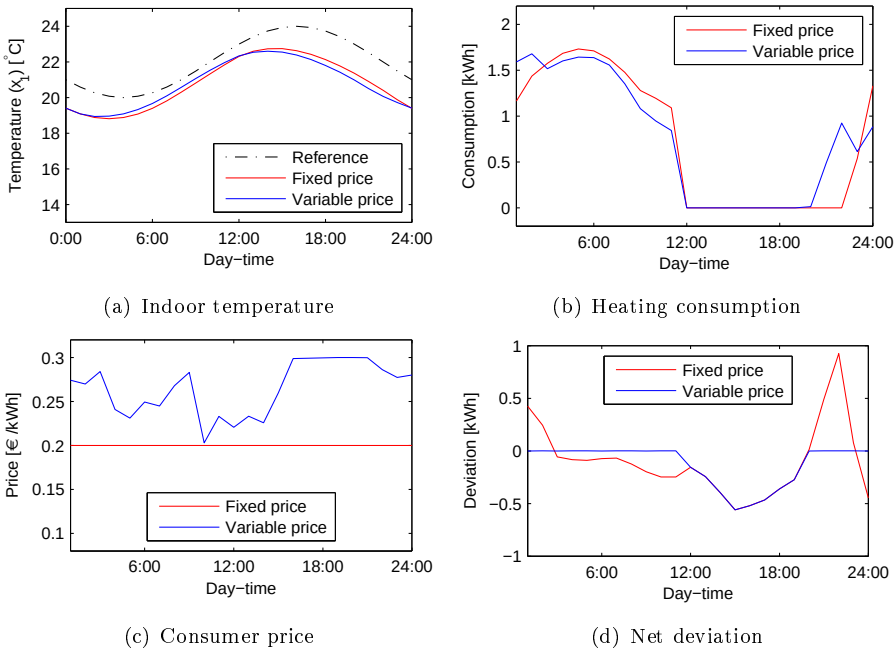

(a) Indoor temperature

(b) Heating consumption

(c) Consumer price

(d) Net deviation

Figure E.4: Dynamics of relevant quantities during hourly simulations spanning one day with rolling horizon

the difference between the two dynamics is rather small, and appears to consist in a small time lag. Figures E.4(b) and E.4(d) deserve to be analyzed jointly. The former one illustrates the dynamics of the consumption in the variable price and the fixed price cases, while the latter shows the power imbalance at each time step. It should be noticed that the power imbalance in the fixed price case is entirely caused by the deviation of wind power production with respect to the day-ahead forecast. By comparing Figures E.4(b) and E.4(d), we notice that the differences in consumption are driven by the wind power imbalances. Indeed, such imbalances are absorbed when possible by deviations in the load induced by the variable price. The only period when the wind power imbalances cannot be absorbed is between 12:00 and 19:00, when the consumption is already null (and therefore cannot be reduced any further) and the wind power deviation is negative (underproduction). Finally, we remark that the wind power imbalance (equivalent to the deviation in the fixed price case in Figure E.4(d)) is mostly negative during the considered day, i.e. the wind plants are underproducing. To reduce such imbalances, there is a need to cut the consumption. This is achieved by sending a dynamic price signal higher than the fixed price, see Figure E.4(c).

Overall results are included in Table E.2. As one can see, the use of dynamic

	Unit	Fixed price	Variable price
Expected total imbalance	kWh	6.79	2.98
Consumer cost	€	3.57	4.77
Consumer discomfort	(€)	0.11	0.13

Table E.2: Overall results of hourly simulations spanning one day with rolling horizon

pricing allows the retailer to cut over half of the power imbalances it would incur using a fixed price. These cost savings, though, are not passed on to the consumers. Indeed, owing to the higher prices, they are charged a total cost larger by roughly one third in the case of dynamic pricing. In general, one would expect that the wind power forecasts are unbiased, i.e. that the error in the long run has zero mean. As a result, the hours where the consumers are charged higher prices should be equally likely than hours where the price is lower. Nevertheless, there is a need to further reward consumer flexibility in order to encourage their participation in demand response programs. Finally, the third row in Table E.2 shows the consumer discomfort, i.e. the sum of the quadratic penalties in the objective function (E.3a). As one could expect, there is a slight increase when dynamic pricing is used, indicating that the consumer is giving up a marginal fraction of her/his comfort for ensuring the balance of the system.

The dynamics of a similar simulation are shown in Figure E.5. In this exam-

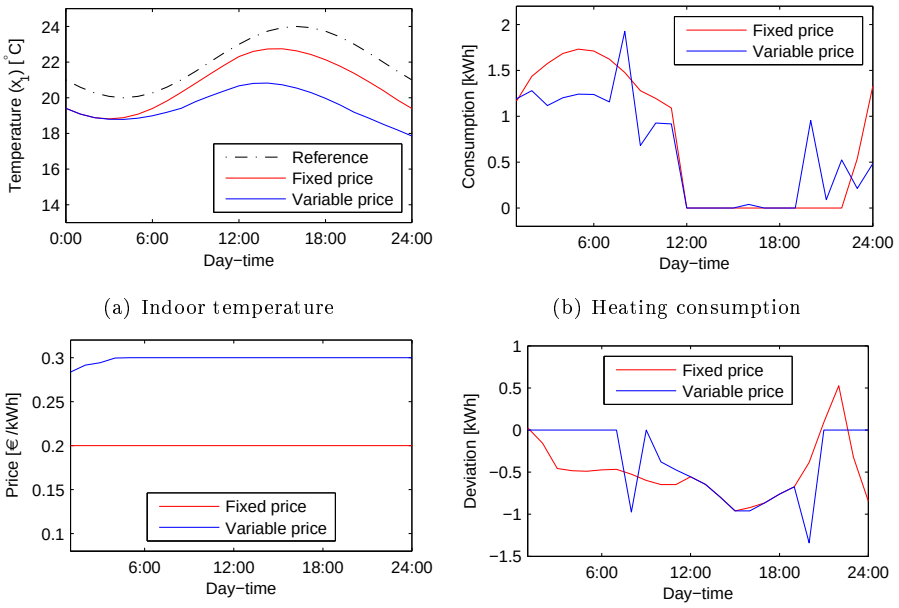

(a) Indoor temperature

(b) Heating consumption

(c) Consumer price

(d) Net deviation

Figure E.5: Dynamics of relevant quantities during hourly simulations spanning one day. The wind power forecasts are biased and overestimate the actual production

ple, a biased day-ahead forecast of wind power production is used. Such bias is introduced by adding 0.4 kWh to the point forecast, which constantly overestimates the wind out-turn as a result. This can be seen in the red line in Figure E.5(d), which is negative except for the 22nd hour of the day. Owing to the constant negative imbalance of wind power production, the dynamic price rapidly shoots up to the upper limit (€0.3 /kWh). The system is working under considerable stress: for example, the indoor temperature with dynamic pricing in Figure E.5(a) is roughly 2°C lower compared to the temperature with fixed price. The quadratic penalty in the objective function makes it difficult to deviate further from the reference temperature. In other words, the "storage" capacity of the heating system is fully used. As a consequence, as one can see in Figure E.5(d), the system can hardly absorb imbalances after the 8th hour in the simulation.

E.5 Conclusion

In this work, we introduced a bilevel framework for modeling demand response. We consider consumer flexibility for heating, and set up a lower-level problem where consumers solve an economic cost minimization problem, once they are given a price schedule as input. Then, such a problem is incorporated as a set of Karush-Kuhn-Tucker equilibrium conditions in an upper-level problem. The framework is general, and different upper-level problems can be thought of considering different market players.

We describe an illustrative example where the upper-level problem is the one of a retailer equipped with a wind power production facility, whose objective is the minimization of the trading imbalances owing to the wind uncertainties. This can be thought of as a virtual power plant operational problem.

The results of the example show that dynamic pricing provides an effective signal for smoothing out the retailer's trading imbalances. The benefits for the consumers, though, are not always clear. Indeed, overestimation of wind power production at the day-ahead stage results in higher consumer prices, which result in both increased costs and reduced comfort. Furthermore, the heating flexibility has dynamic properties that makes it akin to an energy storage. When wind power forecasts are constantly biased, the capacity of the consumers to absorb deviations is rapidly exhausted.

Further results, where the retailer's participation at the day-ahead and real-time markets are optimized simultaneously are available in [13].

References E

[1] J. Torriti, M. G. Hassan, and M. Leach, "Demand response experience in Europe: policies, programmes and implementation," *Energy*, vol. 35, no. 4, pp. 1575–1583, 2010.

[2] H. von Stackelberg, *Market Structure and Equilibrium*. Springer Berlin Heidelberg, 2011.

[3] H. Madsen and J. Holst, "Estimation of continuous-time models for the heat dynamics of a building," *Energy and Buildings*, vol. 22, no. 1, pp. 67–79, 1995.

[4] R. Halvgaard, N. K. Poulsen, H. Madsen, and J. B. Jørgensen, "Economic model predictive control for building climate control in a smart grid," in *IEEE PES Conference on Innovative Smart Grid Technologies (ISGT)*, (Washington, USA), 2012.

[5] D. T. Nguyen, M. Negnevitsky, and M. de Groot, "Pool-based demand response exchange – concept and modeling," *IEEE Transactions on Power Systems*, vol. 26, no. 3, pp. 1677–1685, 2011.

[6] Z.-Q. Luo, J.-S. Pang, and D. Ralph, *Mathematical Programs with Equilibrium Constraints*. Cambridge University Press, 1996.

[7] D. Luenberger, *Linear and Nonlinear Programming*. Addison-Wesley Publishing Company, 1984.

[8] H. Madsen, *Time Series Analysis*. Chapman & Hall/CRC, 2007.

[9] P. Loridan and J. Morgan, "Weak via strong Stackelberg problems: New results," *Journal of Global Optimization*, vol. 8, pp. 263–287, 1996.

[10] J. Fortuny-Amat and B. McCarl, "A representation and economic interpretation of a two-level programming problem," *Journal of the Operational Research Society*, vol. 32, no. 9, pp. 783–792, 1981.

[11] R. J. Barthelmie, F. Murray, and S. C. Pryor, "The economic benefit of short-term forecasting for wind energy in the UK electricity market," *Energy Policy*, vol. 36, no. 5, pp. 1687–1696, 2008.

[12] P. Pinson, G. Papaefthymiou, B. Klockl, H. Nielsen, and H. Madsen, "From probabilistic forecasts to statistical scenarios of short-term wind power production," *Wind Energy*, vol. 12, no. 1, pp. 51–62, 2009.

[13] M. Zugno, J. M. Morales, P. Pinson, and H. Madsen, "A bilevel model for energy retailers participation in a demand response market environment," *Energy Economics*, 2012. Submitted.

Paper F

A Bilevel Model for Electricity Retailers' Participation in a Demand Response Market Environment

Authors:
Marco Zugno, Juan Miguel Morales, Pierre Pinson, Henrik Madsen

Published in:
Energy Economics, 36: 182–197, 2013.

A Bilevel Model for Electricity Retailers' Participation in a Demand Response Market Environment

Marco Zugno[1], Juan Miguel Morales[2], Pierre Pinson[1], Henrik Madsen[1]

Abstract

Demand response programmes are seen as one of the contributing solutions to the challenges posed to power systems by the large-scale integration of renewable power sources, mostly due to their intermittent and stochastic nature. Among demand response programmes, real-time pricing schemes for small consumers are believed to have significant potential for peak-shaving and load-shifting, thus relieving the power system while reducing costs and risk for energy retailers. This paper proposes a game theoretical model accounting for the Stackelberg relationship between retailers (leaders) and consumers (followers) in a dynamic price environment. Both players in the game solve an economic optimisation problem subject to stochasticity in prices, weather-related variables and must-serve load. The model allows the determination of the dynamic price-signal delivering maximum retailer profit, and the optimal load pattern for consumers under this pricing. The bilevel program is reformulated as a single-level MILP, which can be solved using commercial off-the-shelf optimisation software. In an illustrative example, we simulate and compare the dynamic pricing scheme with fixed and time-of-use pricing. We find that the dynamic pricing scheme is the most effective in achieving load-shifting, thus reducing retailer costs for energy procurement and regulation in the wholesale market. Additionally, the redistribution of the saved costs between retailers and consumers is investigated, showing that real-time pricing is less convenient than fixed and time-of-use price for consumers. This implies that careful design of the retail market is needed. Finally, we carry out a sensitivity analysis to analyse the effect of different levels of consumer flexibility.

[1]DTU Informatics, Technical University of Denmark, Richard Petersens Plads, bld. 305, DK-2800 Kgs. Lyngby, Denmark

[2]Centre for Electric Power and Energy, Technical University of Denmark, Elektrovej, bld. 325, DK-2800 Kgs. Lyngby, Denmark

Nomenclature

Sets

T	Time periods in the optimisation horizon
Ω_2	Space of second-stage stochastic variables
Ω_3	Space of third-stage stochastic variables

Indices

t	Index of Program Time Unit (PTU)	$t \in \{1, 2, \dots N_T\}$
ω_2	Scenario index for second-stage stochastic variable	$\omega_2 \in \{1, 2, \dots N_{\Omega_2}\}$
ω_3	Scenario index for third-stage stochastic variable	$\omega_3 \in \{1, 2, \dots N_{\Omega_3}\}$

Random variables

T^a_{t,ω_2}	Ambient temperature
π^s_{t,ω_2}	Energy price at the spot market
$\pi^{\uparrow}_{t,\omega_2}$	Up-regulation price at the real-time market
$\pi^{\downarrow}_{t,\omega_2}$	Down-regulation price at the real-time market
l^i_{t,ω_3}	Consumption from inflexible (must-serve) load
$\psi^{\uparrow}_{t,\omega_2}$	Up-regulation penalty at the real-time market
$\psi^{\downarrow}_{t,\omega_2}$	Down-regulation penalty at the real-time market

Decision variables

E^s_t	Energy contracted at the spot market
$\widetilde{\pi}_{t,\omega_2}$	Dynamic real-time price charged to the end-consumer
l_{t,ω_2}	Energy purchased by the consumer
$\Delta E^{\uparrow}_{t,\omega_2,\omega_3}$	Up-regulation energy purchased at the real-time market
$\Delta E^{\downarrow}_{t,\omega_2,\omega_3}$	Down-regulation energy sold at the real-time market
T^r_{t,ω_2}	Indoor temperature in the consumer building model
T^f_{t,ω_2}	Floor temperature in the consumer building model
T^w_{t,ω_2}	Water temperature in the consumer building model
v_{t,ω_2}	Deviation from the comfort band for indoor temperature

Parameters

$\underline{\pi}$	Minimum dynamic price charged to the end-consumer
$\overline{\pi}$	Maximum dynamic price charged to the end-consumer
π^{AVG}	Average daily dynamic price charged to the end-consumer
ρ	Penalty for deviation from the comfort band for indoor temperature
$\underline{l}$	Minimum flexible consumption for the end-consumer
$\overline{l}$	Maximum flexible consumption for the end-consumer
$\underline{T^r}_t$	Lower bound of the comfort band for indoor temperature
$\overline{T^r}_t$	Upper bound of the comfort band for indoor temperature

F.1 Introduction

Favoured by ambitious international agreements and national plans, integration of renewable power sources is expected to constantly rise in the years to come in most industrialised countries. Several among the currently or potentially deployable renewable sources, namely wind, solar, tidal and wave, are characterised by an intermittent and stochastic nature. This will pose problems to the operation and management of future power systems, as supply must match demand at all times. Furthermore security of supply will become an issue as the capacity margin is lower during peak-demand hours with low intermittent generation. Finally price volatility is also destined to increase, since it is known that intermittent renewables have an impact on market prices under the current demand conditions [1, 2].

As a way to cope with these issues, many propose a revolution of power systems from a structure where supply follows demand to one where demand follows supply. This can be achieved in practice by adopting measures facilitating *demand response*, such as load shedding programmes, time-of-use or real-time based consumer tariffs. While large industrial consumers can participate in spot markets and are already involved in load shedding programmes in many countries, little has been done yet to allow the participation of small end-consumers in demand response programmes, at least within a European context [3]. Nevertheless, demand response is receiving increasing attention from governments and policy makers.

In line with this increasing governmental consideration, demand response is being studied intensively by researchers. Several setups have been proposed involving different stakeholders, namely transmission system operators (TSOs), distributing companies (DISCOs) and retailers. In parallel different advantages of demand response have been stressed, in particular the ability to enhance

power system security, and the possibility of reducing electricity procurement costs and, at the same time, market risk.

The TSO's perspective on the demand-response problem attracted a fair share of interest since centralising the management of demand response may have a number of advantages. On the one hand, specific stochastic unit commitments approaches were introduced, permitting to account for demand-side reserve bids submitted by an aggregator on the day-ahead market [4], or jointly accounting for wind power generation and demand response based on a linear inverse demand function [5]. On the other hand, different economic dispatch models aiming at integrating demand response and wind power were reviewed and compared in [6] and [7], respectively. These are based on a model using multi-directional information exchange where the TSO chooses a price sequence based on communicated production schedules and corresponding load response to that price sequence.

In parallel in view of their potential leading role in the optimal management of demand response, the DISCOs point of view was extensively studied with a blend of load shedding and control-based proposals. Indeed, it may be that DISCOs operating distributed generation and with the capability of interrupting load consider the possibility of optimising their overall operating costs, as in [8]. They may alternatively design optimal bidding strategies with the additional flexibility such that a certain number of load interruptions is allowed by contract as agreed on with the consumers [9]. In a different paradigm focused on the consumption dynamics, the idea of using price signals for controlling a part of the load has recently appeared, based e.g.on statistical models for the forecasting of the conditional load response to varying prices [10], or conversely on the optimisation problem of a load exposed to dynamic market prices [11]. Finally as a more global approach involving DISCOs, retailers (which are purchasers of demand response) as well as aggregations of consumers (sellers), specific market designs may be proposed as in [12], the configuration of which should arguably allow maximising social welfare.

In contrast to these proposals mainly focused on TSOs and DISCOs point of views, we take an original path focused on the joint consideration of the economic optimisation problems of a set of consumers and of their electricity-supplying retailer. In this setup, the retailer naturally acts as a buffer between already existing electricity markets and newly-enabled flexible end-consumers. We assume that consumers respond to a dynamic price signal sent by the retailer by shifting part of their consumption to low-price periods, thus minimising the cost of electricity procurement. The fact that the consumption schedule is decided after the communication of the price signal by the retailer implies that there is a leader-follower structure typical of *Stackelberg games*, which were introduced in the original version of the work later translated in [13]. For simplicity only

the load used for heating purposes is considered as flexible, i.e.it can be shifted in time, although this assumption is not binding. In practice consumer flexibility in time is modelled by using a discrete-time state-space model; the reader not familiar with state space models is referred to [14]. In turn the retailer is also subject to an economic problem, in that it acts as an intermediary by purchasing at wholesale (day-ahead and real-time) markets and selling back to the consumers.

The novelty of this approach is fourfold. First of all, it jointly considers the optimisation problem of consumers, consisting of the maximisation of a utility function minus the electricity procurement costs, integrating it into the retailer problem, which is purely economic. Using a game theoretic approach, completely novel compared to the state-of-the-art reviewed above, we are able to capture the conflicting economic interests of the retailer and their end-consumers. Under the assumption that the introduction of real-time prices makes the consumers rational, we quantify the cost/benefit improvement for both the stakeholders involved. Secondly, by incorporating the consumer optimisation problem in the model, our analysis is based on a realistic cost function rather than resorting to models that arbitrarily choose demand elasticities or consumer benefit functions, as in [4], [5] [8] and [12]. Thirdly, by using a state-space model for consumer preferences within a game-theoretic approach, we rigorously account for the dynamics of demand response, which are often either heuristically approached, see [6] and [7], or simply discarded by making use of static elastic demand as in [4], [5], [8] and [12]. Last but not least, we consider a two-market settlement rather than a single one [6, 7, 4, 5, 9, 10, 11, 12]. This allows us to quantify the advantages of demand response both with respect to peak-shaving(-shifting) and to the reduction of costs due to imbalances (deviations) of real-time consumption from the day-ahead prognosis.

The paper is structured as follows. Section F.2 introduces the mathematical formulation of the retailer and the consumer problems separately. Then, the bilevel problem is linearised and formulated as a single-level optimisation program in Section F.3. Section F.4 discusses the results of an illustrative example. Finally, conclusions are drawn in Section F.5.

F.2 Formulation of retailer and consumer optimisation problems

We consider the economic optimisation problem of an energy retailer, which acts as an intermediary between energy wholesalers and end-consumers. Energy is purchased at the wholesale market and, in turn, it is sold to the consumers, who

face an economic optimisation problem aimed at minimising the cost of their consumption.

Needless to say, the retailer business can only be profitable if the electricity price charged to the consumers $\widetilde{\pi}$ is greater than the purchase (spot) price π^s. This price surcharge is justified by the risk that retailers take when entering into a contract with consumers. Indeed retailers must purchase energy in advance on the wholesale market, at a stochastic price π^s, and sell it to the consumers at a price $\widetilde{\pi}$ that is often regulated and/or fixed. Furthermore they might incur penalties when the aggregate consumption from their customers, which is stochastic, deviates from the schedule resulting from the wholesale market clearing process. The most striking example of the risk faced by retailers is undoubtedly the Californian energy crisis in 2000-2001, where several utilities went bankrupt as a result of soaring wholesale prices and regulated retail rates, see [15].

In this model we specifically focus on the interaction between the retailer and a partially flexible consumer, who can decide on the allocation of its heating consumption based on an hourly price schedule communicated by the retailer as well as on weather forecasts (e.g.of the outdoor temperature). The problem exhibits a bilevel structure, where the retailer determines the price schedule delivering the optimal profits (upper-level problem), while the consumer, based on this price schedule, optimises its flexible consumption (lower-level problem). In game theory, hierarchical optimisation problems of this type are usually referred to as Stackelberg games and can be formulated mathematically in the framework of bilevel programs, which are special instances of *Mathematical Programs with Equilibrium Constraints* (MPECs). The interested reader is referred to [16] for a complete treatment of the subject.

In the following, we adopt the general formulation of a bilevel program

$$\begin{array}{ll} \text{Maximize} & \phi(\mathbf{x},\mathbf{y}) \\ \text{s.t.} & (\mathbf{x},\mathbf{y}) \in Z \\ & \mathbf{y} \in \mathcal{S}(\mathbf{x}) = \arg\min_{\mathbf{y}} \{\theta(\mathbf{x},\mathbf{y}) : \mathbf{y} \in C(\mathbf{x})\} \end{array} \tag{F.1}$$

where $\mathbf{x} \in \mathbb{R}^n$ is the vector of decision variables of the upper-level problem, $\mathbf{y} \in \mathbb{R}^m$ the one of the lower-level problem, $\phi(\mathbf{x},\mathbf{y}) : \mathbb{R}^{n+m} \to \mathbb{R}$ and $\theta(\mathbf{x},\mathbf{y}) : \mathbb{R}^{n+m} \to \mathbb{R}$ the objective functions of the upper- and the lower-level problems respectively, Z is the joint feasible region of the upper-level problem and $C(\mathbf{x})$ the feasible region of the lower-level problem induced by $\mathbf{x}$.

From the discussion above, it is clear that the financial risk of the retailer stems from multiple stochastic variables: spot and regulation market prices, weather-

related variables that influence heating consumption, fluctuations of the inflexible (must-serve) part of the load as well as inaccuracies in modelling consumer behaviour. The specific market design allows the players (retailers and consumers) to make decisions both day-ahead and real-time. Furthermore energy imbalances are settled ex-post, i.e.after their realisation and the calculation of market prices. Decisions made at the later stages benefit from updated information on the stochastic processes that influence the system, either in the form of more accurate forecasts thanks to a shorter look-ahead time or of realised values of random variables. Specifically, we consider the following situation for the three aforementioned stages:

day-ahead The retailer decides on the amount E^s_t of energy purchased at the spot market for every Program Time Unit (PTU) t in the optimisation horizon, based on forecast scenarios of the spot market price π^s_{t,ω_2}, of the up- and down-regulation prices, $\pi^{\uparrow}_{t,\omega_2}$ and $\pi^{\downarrow}_{t,\omega_2}$ respectively, of the ambient temperature T^a_{t,ω_2}, of the inflexible load l^i_{t,ω_3} and on its model of consumer behaviour.

real-time The retailer decides on the price schedule $\widetilde{\pi}_{t,\omega_2}$ to be sent out to the consumers for every PTU in the optimisation horizon, given the certain realisation of the spot price π^s_t and the contracted purchase at the spot market E^s_t. At the same time the consumer optimises its heating consumption schedule l_{t,ω_2} based on the price signal received from the retailer and on the realisation of the ambient temperature T^a_{t,ω_2}, which is assumed to be known at this point. This is a simplification of the more realistic, yet intractable, situation where more accurate forecasts are available in real-time than day-ahead, which would result in an exponentially growing scenario-tree.

ex-post The realisation of the inflexible part of the load l^i_{t,ω_3} becomes known, allowing the calculation of the up- and down-regulation imbalances $\Delta E^{\uparrow}_{t,\omega_2,\omega_3}$ and $\Delta E^{\downarrow}_{t,\omega_2,\omega_3}$, respectively. These imbalances are purchased and sold at the up- and down- regulation price, $\pi^{\uparrow}_{t,\omega_2}$ and $\pi^{\downarrow}_{t,\omega_2}$ respectively, determining the net profit for the retailer.

The proposed model is therefore a stochastic bilevel optimisation model with second- and third-stage recourse. The two levels of the model capture the hierarchical relationship between the retailer and the consumer. The three stages allow us to discriminate between uncertain factors being revealed before real-time operation and those disclosed on an ex-post basis. The remainder of the section is dedicated to the introduction of the upper-level (retailer) and the lower-level (consumer) problems.

F.2.1 Retailer problem

The objective function of the retailer is the maximisation of the expected market profits, with respect to both the second- and third-stage stochastic variables, given by

$$\begin{aligned}\phi(\mathbf{x},\mathbf{y}) = \mathbb{E}_{\Omega_2,\Omega_3}\Bigg\{ \sum_{t=1}^{N_T} \widetilde{\pi}_{t,\omega_2}(l_{t,\omega_2} + l^i_{t,\omega_3}) - \pi^s_{t,\omega_2} E^s_t \\ - \pi^{\uparrow}_{t,\omega_2}\Delta E^{\uparrow}_{t,\omega_2,\omega_3} + \pi^{\downarrow}_{t,\omega_2}\Delta E^{\downarrow}_{t,\omega_2,\omega_3} \Bigg\}\end{aligned} \tag{F.2}$$

where $\mathbf{x} = \left\{\widetilde{\pi}_{t,\omega_2}, E^s_t, \Delta E^{\uparrow}_{t,\omega_2,\omega_3}, \Delta E^{\downarrow}_{t,\omega_2,\omega_3}\right\}$ is the retailer's set of decision variables and $\mathbf{y} \supseteq \{l_{t,\omega_2}\}$ is the consumer's one.

The objective function above is the sum of four terms. The first one represents the revenues from charging the price $\widetilde{\pi}_{t,\omega_2}$ to both the flexible and the inflexible load of the consumer, l_{t,ω_2} and l^i_{t,ω_3} respectively. The second term is the cost of purchasing the energy E^s_t at the spot market price π^s_{t,ω_2}. Finally the last two terms represent the cost (profit) of purchasing (selling) up(down)-regulation power $\Delta E^{\uparrow}_{t,\omega_2,\omega_3}$ ($\Delta E^{\downarrow}_{t,\omega_2,\omega_3}$) at the regulation price $\pi^{\uparrow}_{t,\omega_2}$ ($\pi^{\downarrow}_{t,\omega_2}$), where up- and down-regulation are defined as

$$\Delta E^{\uparrow}_{t,\omega_2,\omega_3} = \begin{cases} l_{t,\omega_2} + l^i_{t,\omega_3} - E^s_t, & l_{t,\omega_2} + l^i_{t,\omega_3} - E^s_t \geq 0 \\ 0, & \text{otherwise} \end{cases} \tag{F.3}$$

$$\Delta E^{\downarrow}_{t,\omega_2,\omega_3} = \begin{cases} E^s_t - l_{t,\omega_2} - l^i_{t,\omega_3}, & l_{t,\omega_2} + l^i_{t,\omega_3} - E^s \leq 0 \\ 0, & \text{otherwise} \end{cases} \tag{F.4}$$

The piecewise definitions (F.3) and (F.4) of the up- and down-regulations are necessary only in a two-price market, i.e.if $\pi^{\uparrow} \neq \pi^{\downarrow}$. On the contrary the problem formulation for a single-price real-time market (i.e.a market where $\pi^{\uparrow} = \pi^{\downarrow}$) requires only one variable definition for the imbalance, without piecewise splits. Although we consider here a two-price market for regulation, the model can be easily adapted to the single-price market case, which is simpler to treat owing to the linearity of the definition of the imbalances.

Due to the fact that the model provides no possibility for consumers to switch to a different retailer, i.e.market competition is not modelled, the retailer could increase the end-consumer price possibly up to infinity in order to maximise its profits. On the other hand the process of retailer-switching is rather slow as compared to the optimisation horizon considered here, which makes it hard to consider competition directly in the model. Still, in order to enforce market

competitiveness of retailer prices, we choose to introduce constraints that model possible future contracts between retailers and price-responsive consumers. We make the assumption that the two parties will agree on certain characteristics of a variable electricity price, i.e.minimum, maximum and average value during the day, just as today they agree on a fixed rate. In mathematical terms, this assumption implies the following constraints on the consumer-price

$$\widetilde{\pi}_{t,\omega_2} \geq \underline{\pi}, \quad \forall t \in T, \forall \omega_2 \in \Omega_2 \tag{F.5}$$

$$\widetilde{\pi}_{t,\omega_2} \leq \overline{\pi}, \quad \forall t \in T, \forall \omega_2 \in \Omega_2 \tag{F.6}$$

$$\frac{1}{24} \sum_{t=1+24i}^{(1+i)24} \widetilde{\pi}_{t,\omega_2} = \pi^{AVG}, \quad i = 0, 1, \ldots, \frac{|T|}{24} - 1, \forall \omega_2 \in \Omega_2 \tag{F.7}$$

Constraints (F.5) and (F.6) ensure that the price charged to the demand is always contained within the range $[\underline{\pi}, \overline{\pi}]$. Constraint (F.7) enforces that by contract the dynamic price signal must have a fixed daily average. Notice that the latter constraint is necessary in order to ensure a sufficient number of low-price periods. In absence of this constraint, the retailer would in principle be allowed to always charge the maximum price to the consumer when not faced by high regulation prices. Finally, we underline that constraints (F.5)–(F.7) consent a straightforward comparison between retailers in a competitive market, based on few meaningful parameters such as the average hourly price and its maximum and minimum values, i.e. the price level and its volatility.

Following the general formulation of a bilevel program (F.1), we write the retailer problem as

$$\begin{aligned} &\underset{\mathbf{x}, \mathbf{y}_{\omega_2}}{\text{Maximize}} && \phi(\mathbf{x}, \mathbf{y}_{\omega_2}) \\ &\text{s.t.} && \text{(F.3)–(F.7)} \\ & && \mathbf{y}_{\omega_2} \in \mathcal{S}_{\omega_2}(\mathbf{x}), \forall \omega_2 \in \Omega_2 \end{aligned} \tag{F.8a}$$

Equation (F.8a) enforces that the schedule for flexible load consumption is part of (one of) the solution(s) $\mathcal{S}_{\omega_2}(\mathbf{x})$ of the lower-level optimisation problem for any realisation of the second stage variables $\omega_2 \in \Omega_2$. In practice each consumption schedule l_{t,ω_2} solves a different optimisation problem parameterised in ω_2.

Furthermore, it should be noticed that the objective function in (F.2) has two nonlinearities. The first one is introduced by the piecewise linear definition of the imbalances (F.3) and (F.4); the second one by the bilinear products $\widetilde{\pi}_{t,\omega_2} l_{t,\omega_2}$ in (F.2). The former nonlinearity can be worked around through a reformulation of the problem, the latter by enforcing the strong duality theorem, see [17], on the lower-level (consumer) problem. The description of the linearisation is left to Section F.3, while the next section introduces the consumer (lower-level) problem.

F.2.2 Consumer problem

We consider a flexible demand response environment, where the consumer can optimise its future consumption based on a dynamic price schedule communicated by the retailer. We assume here that only the load l_{t,ω_2} necessary for heating is flexible, and treat the remaining, inflexible part of the load l^i_{t,ω_3} as a third-stage stochastic variable. We remark that this limitation to heating load is not critical and other sources of consumer flexibility could be considered. In a similar fashion one could consider more general models akin to the one in [11].

Just like the retailer, the end-consumer faces an economic problem, too. With a flexible price, he/she will minimise the cost of the electricity needed for heating by shifting as much consumption as possible to low-price periods, without giving up *too much* on the comfort, i.e.on the indoor temperature of the building. We therefore model the objective of the consumer as a utility function trading-off the cost of electricity procurement and the discomfort for deviating from the reference temperature band.

Two different formulations of the economic optimisation problem of the heating system of a building are introduced in this section. First, a linear programming (LP) formulation is introduced. Then, its equivalent Karush-Kuhn-Tucker (KKT) system is presented.

F.2.2.1 LP formulation of the consumer problem

Based on the work in [18] we consider a three-state, discrete-time state space model for the heating dynamics of a building. The three states of the system are the indoor temperature T^r_{t,ω_2}, the floor T^f_{t,ω_2} temperature and the temperature T^w_{t,ω_2} inside a water tank directly connected to a heat pump. The only input is the electricity consumption l_{t,ω_2}, while the outdoor temperature T^a_{t,ω_2} is a stochastic disturbance. We stress that solar irradiation, an additional disturbance in [18] is discarded here for the sake of simplicity. Using a matrix formulation, the state space model writes

$$\begin{bmatrix} T^r_{t,\omega_2} \\ T^f_{t,\omega_2} \\ T^w_{t,\omega_2} \end{bmatrix} = \mathbf{A} \begin{bmatrix} T^r_{t-1,\omega_2} \\ T^f_{t-1,\omega_2} \\ T^w_{t-1,\omega_2} \end{bmatrix} + \mathbf{B} l_{t-1,\omega_2} + \mathbf{E} T^a_{t-1,\omega_2} \tag{F.9}$$

where all the matrices are constants. The output of interest is clearly the indoor temperature T^r_{t,ω_2}, as this is the only variable influencing the consumer comfort. In the following optimisation model, adapted from [18], the deviation of the output from a reference band $[\underline{T}^r_t \quad \overline{T}^r_t]$ is linearly penalised in the objective

function, where it is summed to the cost of electricity consumption.

$$\underset{\mathbf{y}}{\text{Minimize}} \quad \theta_{\omega_2}(\mathbf{x},\mathbf{y}) = \sum_{t=1}^{N_T} \widetilde{\pi}_{t,\omega_2} l_{t,\omega_2} + \rho v_{t,\omega_2} \tag{F.10a}$$

s.t.

$$T^r_{t,\omega_2} = a_{11}T^r_{t-1,\omega_2} + a_{12}T^f_{t-1,\omega_2} + a_{13}T^w_{t-1,\omega_2} + b_1 l_{t-1,\omega_2} + e_1 T^a_{t-1,\omega_2} \qquad (\mu^r_{t,\omega_2}) \tag{F.10b}$$

$$T^f_{t,\omega_2} = a_{21}T^r_{t-1,\omega_2} + a_{22}T^f_{t-1,\omega_2} + a_{23}T^w_{t-1,\omega_2} + b_2 l_{t-1,\omega_2} + e_2 T^a_{t-1,\omega_2} \qquad (\mu^f_{t,\omega_2}) \tag{F.10c}$$

$$T^w_{t,\omega_2} = a_{31}T^r_{t-1,\omega_2} + a_{32}T^f_{t-1,\omega_2} + a_{33}T^w_{t-1,\omega_2} + b_3 l_{t-1,\omega_2} + e_3 T^a_{t-1,\omega_2} \qquad (\mu^w_{t,\omega_2}) \tag{F.10d}$$

$$l_{t,\omega_2} \geq \underline{l} \qquad (\underline{\lambda}_{t,\omega_2}) \tag{F.10e}$$

$$l_{t,\omega_2} \leq \overline{l} \qquad (\overline{\lambda}_{t,\omega_2}) \tag{F.10f}$$

$$T^r_{t,\omega_2} + v_{t,\omega_2} \geq \underline{T}^r_t \qquad (\underline{\epsilon}_{t,\omega_2}) \tag{F.10g}$$

$$T^r_{t,\omega_2} - v_{t,\omega_2} \leq \overline{T}^r_t \qquad (\overline{\epsilon}_{t,\omega_2}) \tag{F.10h}$$

$$v_{t,\omega_2} \geq 0 \tag{F.10i}$$

The consumer's set of decision variables is $\mathbf{y} = \left\{ l_{t,\omega_2}, v_{t,\omega_2}, T^r_{t,\omega_2}, T^f_{t,\omega_2}, T^w_{t,\omega_2} \right\}$, while $\mu^r_{t,\omega_2}, \mu^f_{t,\omega_2}, \mu^w_{t,\omega_2}, \underline{\lambda}_{t,\omega_2}, \overline{\lambda}_{t,\omega_2}, \underline{\epsilon}_{t,\omega_2}, \overline{\epsilon}_{t,\omega_2}$ are the dual variables associated with constraints (F.10b)–(F.10h). The state space model (F.9) translates into constraints (F.10b), (F.10c) and (F.10d). Inequalities (F.10e) and (F.10f) set the lower and upper limit for electricity consumption, respectively. Variable v_{t,ω_2} represents the absolute value of deviations of the indoor temperature out of the reference band $\left[\underline{T}^r_t \quad \overline{T}^r_t\right]$ through (F.10g)–(F.10i). Positive values of this variable are penalised in the objective function, where they are summed with weight ρ to the cost of electricity over the time horizon N_T.

It is stressed that since the dynamic electricity price $\widetilde{\pi}_{t,\omega_2}$ enters the consumer problem as a constant vector (it is only a variable in the retailer problem), model (F.10) is a linear program. Incidentally, we remark that in this model the retailer must provide the consumer with a price forecast for a certain time-horizon, which resembles the assumption in [6].

Finally, we point out that the objective function (F.10a) with a linear penalisation of the temperature deviations from a reference band is only one of the possible utility functions for the consumer. However, it has certain characteristics that make it appealing, e.g. its simplicity, and the fact that, as we show in what follows, it leads to a reformulation of the bilevel model as a Mixed-Integer Linear Program (MILP). More sophisticated consumer problems could involve varying

upper and lower bounds for the indoor temperature in (F.10g) and (F.10h), defined as linear functions of the consumer price $\widetilde{\pi}_{t,\omega_2}$, or quadratic penalties for deviations from a reference, which closely relates to Linear Quadratic Regulator (LQR) problems in control theory, see [19]. Such extensions of the model are left for future research.

F.2.2.2 KKT formulation of the consumer problem

In this section we present the formulation of the consumer problem given by its Karush-Kuhn-Tucker conditions. The equivalence of the KKT formulation and the one in Section F.2.2.1 is guaranteed by the linearity of the latter one, which implies that solutions of the optimisation problem are also solution of the KKT system of equations and vice versa, see [20].

We begin by stating the stationarity conditions with respect to the decision variables $\mathbf{y} = \left\{ l_{t,\omega_2}, v_{t,\omega_2}, T^r_{t,\omega_2}, T^f_{t,\omega_2}, T^w_{t,\omega_2} \right\}$

$$\begin{cases} \widetilde{\pi}_{t,\omega_2} - b_1\mu^r_{t+1,\omega_2} - b_2\mu^f_{t+1,\omega_2} - b_3\mu^w_{t+1,\omega_2} + \underline{\lambda}_{t,\omega_2} + \overline{\lambda}_{t,\omega_2} = 0, & t < N_T \\ \widetilde{\pi}_{t,\omega_2} + \underline{\lambda}_{t,\omega_2} + \overline{\lambda}_{t,\omega_2} = 0, & t = N_T \end{cases} \tag{F.11}$$

$$0 \leq v_{t,\omega_2} \perp \rho + \underline{\epsilon}_{t,\omega_2} - \overline{\epsilon}_{t,\omega_2} \geq 0 \tag{F.12}$$

$$\begin{cases} \mu^r_{t,\omega_2} - a_{11}\mu^r_{t+1,\omega_2} - a_{21}\mu^f_{t+1,\omega_2} - a_{31}\mu^w_{t+1,\omega_2} + \underline{\epsilon}_{t,\omega_2} + \overline{\epsilon}_{t,\omega_2} = 0, & t < N_T \\ \mu^r_{t,\omega_2} + \underline{\epsilon}_{t,\omega_2} + \overline{\epsilon}_{t,\omega_2} = 0, & t = N_T \end{cases} \tag{F.13}$$

$$\begin{cases} -a_{12}\mu^r_{t+1,\omega_2} + \mu^f_{t,\omega_2} - a_{22}\mu^f_{t+1,\omega_2} - a_{32}\mu^w_{t+1,\omega_2} = 0, & t < N_T \\ \mu^f_{t,\omega_2} = 0, & t = N_T \end{cases} \tag{F.14}$$

$$\begin{cases} -a_{13}\mu^r_{t+1,\omega_2} - a_{23}\mu^f_{t+1,\omega_2} + \mu^w_{t,\omega_2} - a_{33}\mu^w_{t+1,\omega_2} = 0, & t < N_T \\ \mu^w_{t,\omega_2} = 0, & t = N_T \end{cases} \tag{F.15}$$

It should be noticed that the stationarity conditions with respect to the variables appearing in the state-update equations (F.10b)–(F.10d) have a different formulation at the final step N_T of the optimisation horizon. This is because only one state-update equation includes them, rather than two in the general case, as there is no equation imposing the evolution of the state from N_T to N_{T+1}.

The KKT system is completed by the (equality and inequality) constraints already included in Model (F.10), along with the complementary slackness condi-

tions associated with the inequality constraints, i.e.

$$T^r_{t,\omega_2} = a_{11}T^r_{t-1,\omega_2} + a_{12}T^f_{t-1,\omega_2} + a_{13}T^w_{t-1,\omega_2} + b_1 l_{t-1,\omega_2} + e_1 T^a_{t-1,\omega_2} \quad \text{(F.16)}$$

$$T^f_{t,\omega_2} = a_{21}T^r_{t-1,\omega_2} + a_{22}T^f_{t-1,\omega_2} + a_{23}T^w_{t-1,\omega_2} + b_2 l_{t-1,\omega_2} + e_2 T^a_{t-1,\omega_2} \quad \text{(F.17)}$$

$$T^w_{t,\omega_2} = a_{31}T^r_{t-1,\omega_2} + a_{32}T^f_{t-1,\omega_2} + a_{33}T^w_{t-1,\omega_2} + b_3 l_{t-1,\omega_2} + e_3 T^a_{t-1,\omega_2} \quad \text{(F.18)}$$

$$0 \geq \underline{\lambda}_{t,\omega_2} \perp l_{t,\omega_2} - \underline{l} \geq 0 \quad \text{(F.19)}$$

$$0 \leq \overline{\lambda}_{t,\omega_2} \perp l_{t,\omega_2} - \overline{l} \leq 0 \quad \text{(F.20)}$$

$$0 \geq \underline{\epsilon}_{t,\omega_2} \perp T^r_{t,\omega_2} + v_{t,\omega_2} - \underline{T}^r_t \geq 0 \quad \text{(F.21)}$$

$$0 \leq \overline{\epsilon}_{t,\omega_2} \perp T^r_{t,\omega_2} - v_{t,\omega_2} - \overline{T}^r_t \leq 0 \quad \text{(F.22)}$$

We underline that the system of KKT conditions is linear, with the exception of the complementarity conditions (F.12) and (F.19)–(F.22). In order to linearise these conditions we make use of the Fortuny-Amat linearisation [21]; for example (F.12) can be substituted by the following constraints

$$\rho + \underline{\epsilon}_{t,\omega_2} - \overline{\epsilon}_{t,\omega_2} \geq 0 \quad \text{(F.23)}$$

$$v_{t,\omega_2} \geq 0 \quad \text{(F.24)}$$

$$\rho + \underline{\epsilon}_{t,\omega_2} - \overline{\epsilon}_{t,\omega_2} \leq z_{t,\omega_2} M^1 \quad \text{(F.25)}$$

$$v_{t,\omega_2} \leq (1 - z_{t,\omega_2}) M^1 \quad \text{(F.26)}$$

$$z_{t,\omega_2} \in \{0, 1\} \quad \text{(F.27)}$$

where M^1 is a sufficiently large constant. The complementary slackness conditions (F.19)–(F.22) can be linearised using the same strategy. Therefore we end up with a (integer linear) system of KKT conditions equivalent to model (F.10). As a trade-off for introducing additional complexity (i.e.integer variables), we can simply concatenate the KKT system as additional constraints of the upper-level problem. This puts the bilevel problem in a tractable formulation. One is finally left with the necessary linearisation of the objective function (F.2) of the retailer.

F.3 Linearisation and bilevel formulation of the problem

As pointed out in Section F.2.1 there are two nonlinearities in the objective function (F.2) of the upper-level problem. The first one stems from the piecewise definition of negative and positive energy imbalances in (F.3) and (F.4), and can be linearised through a reformulation of the problem. The second nonlinearity

can be overcome by exploiting the strong duality theorem on the lower-level problem. The remainder of this section deals with the linearisation of these terms, and with the presentation of the final formulation of the bilevel problem as a single-level optimisation program.

F.3.1 Reformulation of the energy imbalance

In order to reformulate the problem, let us first define the market penalties for up- and down-regulation

$$\psi^{\uparrow}_{t,\omega_2} = \pi^{\uparrow}_{t,\omega_2} - \pi^{s}_{t,\omega_2} \geq 0 \tag{F.28}$$

$$\psi^{\downarrow}_{t,\omega_2} = \pi^{s}_{t,\omega_2} - \pi^{\downarrow}_{t,\omega_2} \geq 0 \tag{F.29}$$

These values represent the additional cost (or missed revenue) per MWh incurred by the retailer in comparison to the case where it has perfect information on its stochastic consumption. In the latter case, the retailer is charged the spot price for all its consumption. In the former, more realistic, case the retailer will need to adjust its bid on the real-time market, where it is charged $\pi^{\uparrow}_{t,\omega_2} = \pi^{s}_{t,\omega_2} + \psi^{\uparrow}_{t,\omega_2}$ for any additional consumed MWh, and paid $\pi^{\downarrow}_{t,\omega_2} = \pi^{s}_{t,\omega_2} - \psi^{\downarrow}_{t,\omega_2}$ for any MWh consumed less than the schedule cleared at the spot market. Clearly $\psi^{\uparrow}_{t,\omega_2}$ and $\psi^{\downarrow}_{t,\omega_2}$ can be interpreted as the per-unit penalty for imperfect information on future consumption.

Using the market penalties defined above, the objective function (F.2) can be

reformulated as follows

$$\begin{aligned}
\phi(\mathbf{x},\mathbf{y}) &= \mathbb{E}_{\Omega_2,\Omega_3}\Bigg\{\sum_{t=1}^{N_T}\widetilde{\pi}_{t,\omega_2}(l_{t,\omega_2}+l^i_{t,\omega_3})-\pi^s_{t,\omega_2}E^s_t \\
&\quad -(\pi^s_{t,\omega_2}+\psi^{\uparrow}_{t,\omega_2})\Delta E^{\uparrow}_{t,\omega_2,\omega_3}+(\pi^s_{t,\omega_2}-\psi^{\downarrow}_{t,\omega_2})\Delta E^{\downarrow}_{t,\omega_2,\omega_3}\Bigg\} = \\
&= \mathbb{E}_{\Omega_2,\Omega_3}\Bigg\{\sum_{t=1}^{N_T}\widetilde{\pi}_{t,\omega_2}(l_{t,\omega_2}+l^i_{t,\omega_3})-\pi^s_{t,\omega_2}\left(E^s_t+\Delta E^{\uparrow}_{t,\omega_2,\omega_3}-\Delta E^{\downarrow}_{t,\omega_2,\omega_3}\right) \\
&\quad -\psi^{\uparrow}_{t,\omega_2}\Delta E^{\uparrow}_{t,\omega_2,\omega_3}-\psi^{\downarrow}_{t,\omega_2}\Delta E^{\downarrow}_{t,\omega_2,\omega_3}\Bigg\} \\
&= \mathbb{E}_{\Omega_2,\Omega_3}\Bigg\{\sum_{t=1}^{N_T}\widetilde{\pi}_{t,\omega_2}(l_{t,\omega_2}+l^i_{t,\omega_3})-\pi^s_{t,\omega_2}(l_{t,\omega_2}+l^i_{t,\omega_3}) \\
&\quad -\psi^{\uparrow}_{t,\omega_2}\Delta E^{\uparrow}_{t,\omega_2,\omega_3}-\psi^{\downarrow}_{t,\omega_2}\Delta E^{\downarrow}_{t,\omega_2,\omega_3}\Bigg\}
\end{aligned} \tag{F.30}$$

where the last line is obtained by noticing that $l_{t,\omega_2}+l^i_{t,\omega_3}=E^s_t+\Delta E^{\uparrow}_{t,\omega_2,\omega_3}-\Delta E^{\downarrow}_{t,\omega_2,\omega_3}$ holds at any time, which is a result of the definitions in (F.3) and (F.4).

We can now formulate the retailer optimisation problem exploiting the objective function reformulation (F.30)

$$\begin{aligned}
&\underset{\mathbf{x}}{\text{Maximize}} && \phi(\mathbf{x},\mathbf{y}) \text{ in (F.30)} && \\
&\text{s.t.} && \Delta E^{\uparrow}_{t,\omega_2,\omega_3}\geq l_{t,\omega_2}+l^i_{t,\omega_3}-E^s_t && \text{(F.31a)}\\
&&& \Delta E^{\downarrow}_{t,\omega_2,\omega_3}\geq E^s_t-l_{t,\omega_2}-l^i_{t,\omega_3} && \text{(F.31b)}\\
&&& \Delta E^{\uparrow}_{t,\omega_2,\omega_3},\Delta E^{\downarrow}_{t,\omega_2,\omega_3}\geq 0 && \text{(F.31c)}\\
&&& \text{(F.5)–(F.7), (F.8a)} &&
\end{aligned}$$

First, it should be emphasised that the maximisation of (F.2) with the imbalance definitions in (F.3)–(F.4) is equivalent to the maximisation of (F.30) subject to constraints (F.31a)–(F.31c). The latter is a relaxed, yet linear, formulation of the former optimisation problem with a larger feasible space, where the variables $\Delta E^{\uparrow}_{t,\omega_2,\omega_3}$ and $\Delta E^{\downarrow}_{t,\omega_2,\omega_3}$ are allowed to assume greater values than the actual up- and down-regulations. The equivalence of the two optimisation problems is readily proved by noticing that, as long as $\psi^{\uparrow}_{t,\omega_2},\psi^{\downarrow}_{t,\omega_2}>0$, all the additional feasible points of (F.31a)–(F.31c) have a strictly worse objective than at least one feasible point of (F.3)–(F.4), i.e.the one with the minimal

absolute imbalance allowed. In other words, there is no interest for the retailer in artificially pushing up the values of $\Delta E^{\uparrow}_{t,\omega_2,\omega_3}$ and $\Delta E^{\downarrow}_{t,\omega_2,\omega_3}$, as this would contribute negatively to the objective function without any advantages. With similar arguments, it can be shown that $\Delta E^{\uparrow}_{t,\omega_2,\omega_3}$ and $\Delta E^{\downarrow}_{t,\omega_2,\omega_3}$ could assume greater values than the actual up- and down-regulation, but without influencing the other variables, in the case where at least one between $\psi^{\uparrow}_{t,\omega_2}$ and $\psi^{\downarrow}_{t,\omega_2}$ is zero. The actual imbalances can still be calculated by applying (F.3) and (F.4) to the optimal solution of (F.31).

It is also remarked that the reformulation presented in this section is only needed in a two-price real-time market. Under the single-price market structure, there is no need for a piecewise definition of the imbalances (F.3) and (F.4).

F.3.2 Linearisation of bilinear terms

The only nonlinearity still present in objective function (F.30) consists in the bilinear terms $\widetilde{\pi}_{t,\omega_2} l_{t,\omega_2}$. Optimisation problems including bilinear terms are often solved by approximation techniques. For example, [22] makes use of binary expansion on one of the variables involved in the bilinear term, while a piecewise linear approximation is employed in [23]. Using the same approach as in [24], we show that this problem allows for an exact linearisation of these terms. By employing the strong duality theorem, see [17], on the lower-level model (F.10) we enforce that primal and dual objectives are equal at optimality. This implies that

$$\begin{aligned}
\sum_{t=1}^{N_T} \widetilde{\pi}_{t,\omega_2} l_{t,\omega_2} + \rho v_{t,\omega_2} = &-\mu^r_{1,\omega_2} \left(a_{11} T^r_{0,\omega_2} + a_{12} T^f_{0,\omega_2} + a_{13} T^w_{0,\omega_2} + b_1 l_{0,\omega_2} \right) \\
&- \mu^f_{1,\omega_2} \left(a_{21} T^r_{0,\omega_2} + a_{22} T^f_{0,\omega_2} + a_{23} T^w_{0,\omega_2} + b_2 l_{0,\omega_2} \right) \\
&- \mu^w_{1,\omega_2} \left(a_{31} T^r_{0,\omega_2} + a_{32} T^f_{0,\omega_2} + a_{33} T^w_{0,\omega_2} + b_3 l_{0,\omega_2} \right) \\
&- \sum_{t=1}^{N_T} \Big\{ \mu^r_{t,\omega_2} e_1 T^a_{t-1,\omega_2} + \mu^w_{t,\omega_2} e_3 T^a_{t-1,\omega_2} + \mu^f_{t,\omega_2} e_2 T^a_{t-1,\omega_2} \\
&\qquad + \underline{\lambda}_{t,\omega_2} \underline{l} + \overline{\lambda}_{t,\omega_2} \overline{l} + \underline{\epsilon}_{t,\omega_2} \underline{T}^r_t + \overline{\epsilon}_{t,\omega_2} \overline{T}^r_t \Big\}
\end{aligned} \tag{F.32}$$

From the equality between primal and dual objective of the lower-level problem, it follows that the sum of terms $\widetilde{\pi}_{t,\omega_2} l_{t,\omega_2}$ is equal to the sum of products between dual variables and parameters of the primal constraints of the lower-level problem, minus $\rho v_{t,\omega_2}$, which are all linear in the bilevel formulation.

By solving (F.32) on $\sum_{t=1}^{N_T} \widetilde{\pi}_{t,\omega_2} l_{t,\omega_2}$ and taking the expectation with respect to Ω_2 and Ω_3 on both sides of the equation, we are able to replace all the bilinear terms in (F.30), thus obtaining the linear reformulation of the objective function that follows

$$\begin{aligned}\phi(\mathbf{x},\mathbf{y}) = \mathbb{E}_{\Omega_2,\Omega_3}\Bigg\{ & -\mu^r_{1,\omega_2}\left(a_{11}T^r_{0,\omega_2} + a_{12}T^f_{0,\omega_2} + a_{13}T^w_{0,\omega_2} + b_1 l_{0,\omega_2}\right) \\ & -\mu^f_{1,\omega_2}\left(a_{21}T^r_{0,\omega_2} + a_{22}T^f_{0,\omega_2} + a_{23}T^w_{0,\omega_2} + b_2 l_{0,\omega_2}\right) \\ & -\mu^w_{1,\omega_2}\left(a_{31}T^r_{0,\omega_2} + a_{32}T^f_{0,\omega_2} + a_{33}T^w_{0,\omega_2} + b_3 l_{0,\omega_2}\right) \\ & -\sum_{t=1}^{N_T}\Big\{\mu^r_{t,\omega_2} e_1 T^a_{t-1,\omega_2} + \mu^w_{t,\omega_2} e_3 T^a_{t-1,\omega_2} + \mu^f_{t,\omega_2} e_2 T^a_{t-1,\omega_2} \\ & + \underline{\lambda}_{t,\omega_2}\underline{l} + \overline{\lambda}_{t,\omega_2}\overline{l} + \underline{\epsilon}_{t,\omega_2}\underline{T}^r_t + \overline{\epsilon}_{t,\omega_2}\overline{T}^r_t - \rho v_{t,\omega_2} \\ & + \widetilde{\pi}_{t,\omega_2} l^i_{t,\omega_3} - \pi^s_{t,\omega_2}(l_{t,\omega_2} + l^i_{t,\omega_3}) - \psi^{\uparrow}_{t,\omega_2}\Delta E^{\uparrow}_{t,\omega_2,\omega_3} - \psi^{\downarrow}_{t,\omega_2}\Delta E^{\downarrow}_{t,\omega_2,\omega_3}\Big\}\Bigg\}\end{aligned} \tag{F.33}$$

F.3.3 Final problem formulation

As a result of the reformulations above, the bilevel program can be expressed as the following equivalent single-level MILP

$$\begin{aligned}&\underset{\mathbf{x},\mathbf{y}}{\text{Maximize}} && \phi(\mathbf{x},\mathbf{y}) \text{ in (F.33)} \\ &\text{s.t.} && \text{(F.31a)–(F.31c), (F.5)–(F.7)} \\ & && \text{(F.11), (F.23)–(F.26), (F.13)–(F.15)} \\ & && \text{(F.16)–(F.18)} \\ & && \left.\begin{array}{l} l_{t,\omega_2} - \underline{l} \geq 0 \\ \underline{\lambda}_{t,\omega_2} \leq 0 \\ l_{t,\omega_2} - \underline{l} \leq z^2_{t,\omega_2} M^2 \\ \underline{\lambda}_{t,\omega_2} \geq -(1 - z^2_{t,\omega_2}) M^2 \end{array}\right\} \quad \text{linearisation of (F.19)} \end{aligned} \tag{F.34a}$$

$$\left.\begin{array}{l} l_{t,\omega_2} - \overline{l} \leq 0 \\ \overline{\lambda}_{t,\omega_2} \geq 0 \\ l_{t,\omega_2} - \overline{l} \geq -z^3_{t,\omega_2} M^3 \\ \overline{\lambda}_{t,\omega_2} \leq (1 - z^3_{t,\omega_2}) M^3 \end{array}\right\} \quad \text{linearisation of (F.20)} \tag{F.34b}$$

$$\left.\begin{aligned} & T^r_{t,\omega_2} + v_{t,\omega_2} - \underline{T}^r_t \geq 0 \\ & \underline{\epsilon}_{t,\omega_2} \leq 0 \\ & T^r_{t,\omega_2} + v_{t,\omega_2} - \underline{T}^r_t \leq z^4_{t,\omega_2} M^4 \\ & \underline{\epsilon}_{t,\omega_2} \geq -(1 - z^4_{t,\omega_2}) M^4 \end{aligned}\right\} \quad \text{linearisation of (F.21)} \tag{F.34c}$$

$$\left.\begin{aligned} & T^r_{t,\omega_2} - v_{t,\omega_2} - \overline{T}^r_t \leq 0 \\ & \overline{\epsilon}_{t,\omega_2} \geq 0 \\ & T^r_{t,\omega_2} - v_{t,\omega_2} - \overline{T}^r_t \geq z^5_{t,\omega_2} M^5 \\ & \overline{\epsilon}_{t,\omega_2} \leq (1 - z^5_{t,\omega_2}) M^5 \end{aligned}\right\} \quad \text{linearisation of (F.22)} \tag{F.34d}$$

$$z^1_{t,\omega_2}, z^2_{t,\omega_2}, z^3_{t,\omega_2}, z^4_{t,\omega_2}, z^5_{t,\omega_2} \in \{0,1\} \tag{F.34e}$$

The bilevel problem can be solved as a single-level one having the same objective function as the upper-level problem (F.33), and constraints given by the concatenation of

- the constraints of the upper-level problem (F.31a)–(F.31c), (F.5)–(F.7)
- the stationarity conditions in the KKT system of the lower-level problem (F.11), (F.13)–(F.15) and the linearisation of the stationarity condition (F.12) i.e.the system (F.23)–(F.26)
- the equality constraints of the lower-level problem (F.16)–(F.18)
- the linearisation of the complementarity conditions (F.19)–(F.22), i.e.the systems (F.34a)–(F.34d)
- the integrality conditions (F.34e) for the binary variables introduced by the Fortuny-Amat linearisations of the complementarity constraints.

The resulting problem can be solved as a single-level MILP due to the linearity of both the objective function and the constraints, while integer variables are introduced by the Fortuny-Amat linearisation of the complementarity conditions. Problems of this type can be solved using commercial off-the-shelf optimisation software. In this work the problem is formulated in the GAMS environment and solved by employing the CPLEX solver.

F.4 Numerical results and discussion

We describe here the numerical results obtained by running model (F.34) on a small test-case based on real-world data.

The example simulates a single bidding round at the spot market for the retailer, which optimises its bid and real-time market operation using a 48-hour horizon. Uncertainties on the future realisation of spot and real-time market prices, outdoor temperature and inflexible load are modelled through scenarios.

For the sake of simplicity, we limit the number of consumers to three. Indeed, this number is sufficient to draw quantitative conclusions on the behaviour of the model, at the same time allowing the visualisation of relevant variables for each consumer. Incidentally, we stress that although there is no theoretical limit on the number of consumers that can be considered in the model – adding one consumer translates into adding one set of lower-level KKT conditions to the constraints of the upper-level program – there is a certain computational burden implied by the increasing number of integer variables.

Aggregation of consumers into classes characterised by similar building dynamics, behaviour and therefore consumption is paramount for obtaining a tractable, yet realistic, model for the retailer problem. In general, clustering of consumers is widely applied in decision making problems. For instance, clustering techniques for modelling electricity consumption have been proposed in [25], where their importance for electricity providers is also underlined. Clustering the driving behaviour of electric car owners is proposed in [26] for optimising their charging and discharging. Similarly, the three consumers included in this example can be regarded as three classes each grouping a number of consumers with similar behaviour, i.e.building dynamics, heating preferences, etc. Indeed we will treat the three consumers as groups by assigning them different probabilities, i.e.by varying the distribution (or proportion) of consumers belonging to a certain class.

In the following section, we present the parameters chosen to model consumer heating dynamics. Then, we describe how scenarios have been generated in order to model uncertainties. Finally, the results of the example are discussed.

F.4.1 Parameters in the model of building dynamics

The consumer optimisation problem described in Section F.2.2 includes among its constraints a state space model of consumer building dynamics.

Parameter	Value	Unit
a_{11}	0.4103	-
a_{12}	0.5586	-
a_{13}	0.0028	-
a_{21}	0.1092	-
a_{22}	0.8801	-
a_{23}	0.0078	-
a_{31}	0.0022	-
a_{32}	0.0310	-
a_{33}	0.9668	-
b_1	0.0044	°C/kWh
b_2	0.0173	°C/kWh
b_3	4.2332	°C/kWh
e_1	0.0284	-
e_2	0.0029	-
e_3	0	-
$\underline{l}$	0	kWh
$\overline{l}$	0.33	kWh
ρ	30	€/°C

Table F.1: Parameter values considered for the LP model representing the consumer's heating dynamics

Table F.1 summarises the values used for the parameters as well as their units. The chosen parameter values are the ones used in [18], exception made for a lower hourly consumption limit $\overline{l}$ for electricity and lowered b_1, b_2 and b_3 values, due to the choice of a smaller gain for the heat pump, which is decreased by a factor of 3. These changes aim at better spreading the electricity consumption over the day, rather than having few daily consumption spikes as in [18]. We do not discuss here the physical meaning of the parameters, and just refer the interested reader to [18] and [27] for discussion on the physical interpretation of the parameters and on how they can be estimated.

Besides, we consider time-varying comfort bands $[\underline{T}^r_t \quad \overline{T}^r_t]$, so that there is a higher reference for indoor temperature during the day and a lower one during the night. In order to model different consumer preferences, we assume that the three consumer groups have different comfort bands. As one can see in Figure F.1, the first consumer is the most flexible, as it accepts temperatures in a range of 5°C, while the range is narrowed down to 2°C for the third consumer. It is worth mentioning that these temperature ranges need not be constant as in this example, but could e.g. be wider during working hours and narrower when consumers are expected to be at home.

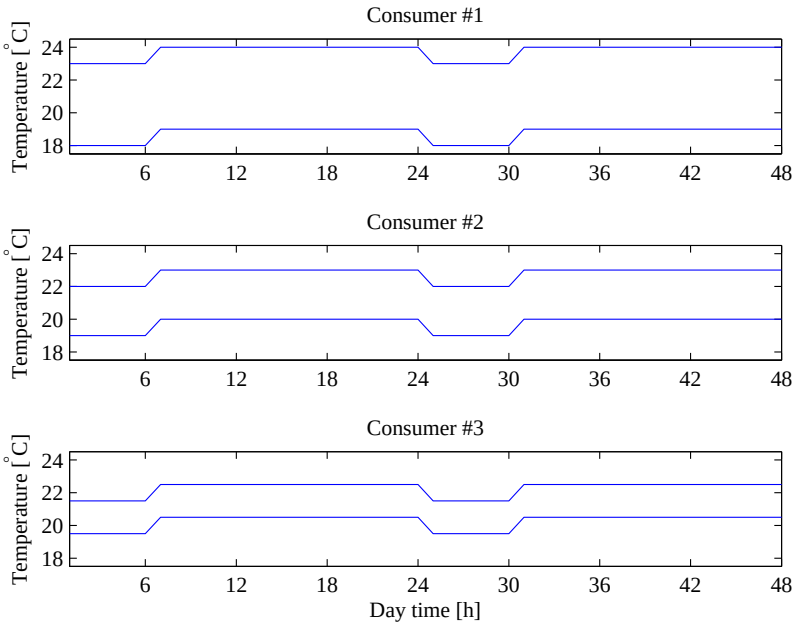

Figure F.1: Comfort bands $[\underline{T}_t^r \quad \overline{T}_t^r]$ for the three consumer groups. The consumer flexibility decreases from top to bottom

F.4.2 Scenario generation

This section describes the methodology employed for generating scenarios for the market quantities (spot and regulation prices), inflexible load and temperature required as inputs to the model. All the employed methodologies are rather simplistic answers to complicated problems, i.e.modelling of weather- and market-related stochastic processes, which are out of the scope of this paper. The interested reader is referred to [28] and [29] and to [30] and [31], respectively for an introduction to modelling of stochastic processes related to weather and electricity markets.

As far as the spot market price π^s_{t,ω_2} is concerned, we use the observed spot market prices in the DK-2 (Eastern Denmark) market area of NordPool, the Scandinavian power exchange, as mean value for the scenarios. We choose arbitrarily to consider prices pertaining to the 15-16th March 2011, which are available at [32] along with other market data for NordPool. In order to generate scenarios, we simulate a multivariate Gaussian process with an exponentially decreasing covariance structure, i.e.the (i, j)-th element of the covariance matrix is given by

$$C(i, j) = \sigma^2 e^{-|i-j|/\tau} \tag{F.35}$$

The parameter σ is the standard deviation of the process. We consider a constant standard deviation $\sigma = €6.67$, which is the approximate RMSE value for the spot market price forecasting model in the work in [33][3]. Furthermore we point out that the time-lags considered for these scenarios are at least 13 hours, which is the look-ahead time of the scenarios for the first hour of the first day considered. The parameter τ sets the exponential decay of correlation with respect to the time lag. We choose the value $\tau = 7$ hours in the example. The choice of model (F.35) is justified by the fact that, despite being relatively simple, it allows us to consider the dynamics of market prices and to easily enforce a realistic value for the standard deviation of the forecast error.

Finally, scenarios are generated by adding the coloured Gaussian noise to the observed spot market price. Figure F.2 shows both the observed spot market price and the obtained scenarios.

Scenarios for the real-time market prices $\pi^{\uparrow}_{t,\omega_2}$ and $\pi^{\downarrow}_{t,\omega_2}$ are generated from the spot price scenarios using a model based on the average values of the ratios

$$\alpha^{\uparrow}_t = \frac{\pi^{\uparrow}_t}{\pi^s_t} \qquad \alpha^{\downarrow}_t = \frac{\pi^{\downarrow}_t}{\pi^s_t} \tag{F.36}$$

[3] This work considers the DK-1 (i.e.Western Denmark) price area of NordPool. Generally the price difference between DK-1 and DK-2 is negligible

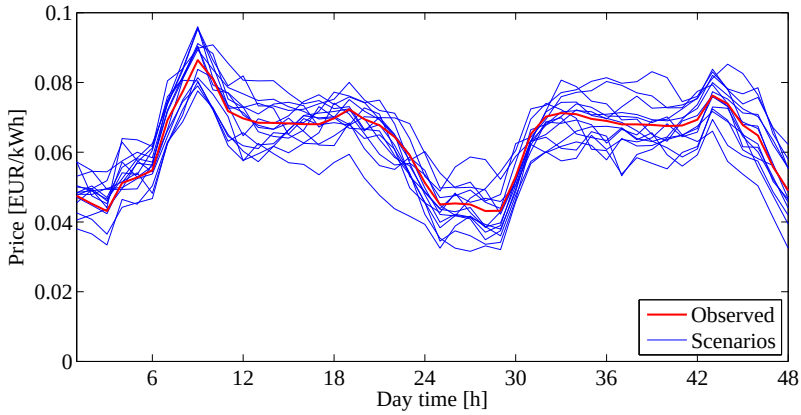

Figure F.2: Observed spot market price in the DK-2 price area of NordPool and generated scenarios for the period 15-16th March 2011

These averages are calculated for the three winter months in the DK-2 price area of NordPool using data from [32], resulting in the values $\widetilde{\alpha}^{\uparrow} = 1.19$ and $\widetilde{\alpha}^{\downarrow} = 0.95$. Scenarios can then be generated from the model as functions of the spot price scenarios

$$\pi^{\uparrow}_{t,\omega_2} = \widetilde{\alpha}^{\uparrow}\pi^{s}_{t,\omega_2} \qquad \pi^{\downarrow}_{t,\omega_2} = \widetilde{\alpha}^{\downarrow}\pi^{s}_{t,\omega_2} \tag{F.37}$$

As a consequence of the use of this model, there is a single regulation price scenario associated to each spot price realisation. This is clearly a simplified model for the regulation prices. We point out, though, that there is no obstacle in using third-stage scenarios in the proposed model, besides that of modelling the stochastic regulation prices. Furthermore, this simplification does not introduce significant distortions in the results of the model, since both regulation penalties $\psi^{\uparrow}_{t,\omega_2}$ and $\psi^{\downarrow}_{t,\omega_2}$ are different from 0 at any time and for all scenarios. In other words, the scenarios $\pi^{\uparrow}_{t,\omega_2}$ and $\pi^{\downarrow}_{t,\omega_2}$ represent the expected real-time market prices conditioned on the realisation of the spot market price π^{s}_{t,ω_2}. Furthermore, it should be noticed that model (F.36) is not a very good predictor of the balancing market prices, especially as far as the up-regulation price is concerned (the standard deviations of the ratios in (F.36) are 0.76 and 0.12, respectively). While developing a state-of-the-art forecasting tool for the regulation prices is out of the scope of this paper, one should keep in mind that more sophisticated forecasting models should be used in realistic applications. The reader should notice that the choice of model (F.36) implies no loss of generality, as the scenarios for the regulation prices are exogenous to the optimisation model.

Scenarios for T^a are formed by gathering temperature observations available at the [34][4]. Measurements are picked from a single location during different days of March 2011 with similar temperature patterns. The obtained scenarios are shown in Figure F.3. In total $N_{\Omega_2} = 14$ second stage scenarios are considered in this example, for reasons of data availability. In a more realistic setup one would want to make use of more advanced modelling of weather-related variables. We refer the reader interested in the subject to [28] for a presentation of scenario-generation techniques applied to weather-related variables.

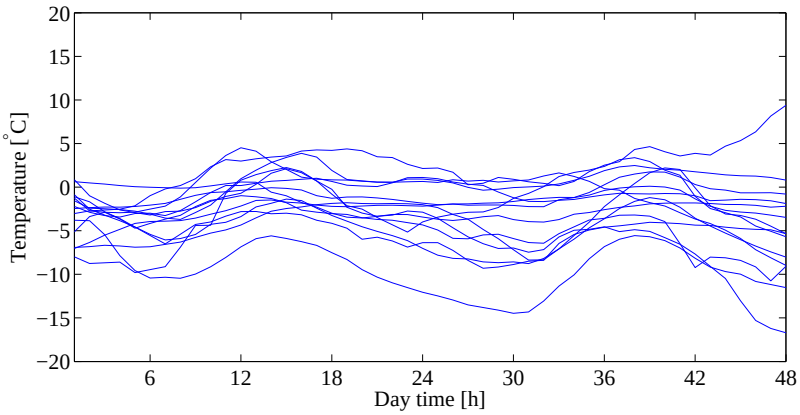

Figure F.3: Scenarios for temperature T^a_{t,ω_2} obtained from measurements during March 2011 available at ??

Finally the third-stage scenarios for the inflexible load l^i_{t,ω_3} are generated with a model similar to the one used for the spot price π^s_{t,ω_2}. The observed load in DK-2, available at [32], is scaled and used as mean value of the process. The scaling is done so that the inflexible load is approximately about 85% of the total load, which is the share of the residual household load after subtracting the consumption due to heating in Denmark [35]. We emphasise, though, that the share of total consumption represented by heating varies from country to country. Coloured Gaussian noise with a covariance structure of the same form of (F.35) is then added to the load pattern. The standard deviation is here set to $\sigma = 0.0075$kWh. As Figure F.4 highlights, the variance of the inflexible load is relatively smaller than the variance of the spot price, reflecting the easier predictability of the load compared to market quantities. Ideally the standard

[4]The geographical displacement between the locations of the temperature and market datasets is justified by reasons of data accessibility. This displacement is equivalent to considering that temperature and market price scenarios are independent from each other. We assume that the results obtained in this paper would hold, at least qualitatively, using consistent datasets.

deviation of the inflexible load would be a function of the size of the considered customer group, decreasing in relative terms with respect to the size owing to smoothing of the errors. In total a number of third-stage scenarios $N_{\Omega_3} = 10$ is selected. Note that the number of scenarios should be large enough to guarantee a faithful representation of the uncertainties involved in the problem. Once more we stress that developing refined models for the uncertainty is outside the scope of this paper.

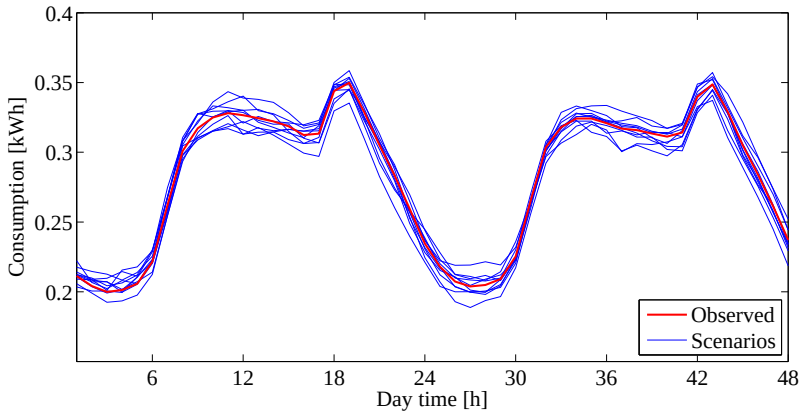

Figure F.4: Scenarios for the inflexible part of the load l^i_{t,ω_3} for the period 15-16th March 2011

F.4.3 Numerical results

The results of the illustrative example are discussed in this section. First, we assess the differences in consumer behaviour and market performance of the retailer between the cases of fixed-price, Time-Of-Use (TOU) price and dynamic-price contracts between retailer and consumers. Then, different distributions of consumer groups are considered in order to discuss how dynamic prices imposed by the retailer impact the market players, and how this impact is influenced by consumer behaviour.

F.4.3.1 Advantages of dynamic pricing

In order to compare the fixed-, TOU- and the dynamic-price case, the model is run three times on the same dataset. In the first run the price charged by the

Day time	1–7	8–10	11–14	15–16	17–20	21–23	24
Type	valley	flat	peak	flat	peak	flat	valley
Price	0.1	0.2	0.3	0.2	0.3	0.2	0.1

Table F.2: Details of the Time-Of-Use (TOU) pricing scheme employed. Prices are in €/kWh

retailer is set to be constant over time to the value €0.2/kWh, which amounts to replacing (F.5)–(F.7) with the equation $\widetilde{\pi}_{t,\omega_2} = €0.2/\text{kWh}$.

In the second run, the Time-Of-Use (TOU) pricing scheme illustrated in Table F.2 is employed. In this scheme, consumption is charged €0.3/kWh during peak hours, €0.2/kWh during flat hours, and €0.1/kWh during valley hours. Notice that, since there are 8 hours for each group, the average TOU price is equal to the price in the fixed-price scheme, i.e.€0.2/kWh.

In the third run, the original model (F.34) is simulated. We remind the reader that the price in model (F.34) is dynamic, but must have a daily mean $\pi^{AVG} = €0.2/\text{kWh}$, which is equal to the fixed price and to the average of the TOU price. Furthermore the price must always fall within the range $[0.1, 0.3]$€/kWh. In all the cases considered the distribution of the consumer groups is set to $[0.3, 0.4, 0.3]$, which means that 30% of the consumers have highly flexible behaviour, 40% are balanced and 30% have low flexibility.

The dynamics of $\widetilde{\pi}_{t,\omega_2}$ and of the flexible load l_{t,ω_2} are shown in Figures F.5, F.6 and F.7 for each consumer type, in the fixed-, TOU- and dynamic-price case, respectively. Mean, median and range (i.e.maximum and minimum value) across scenarios are shown for these variables, which, except for $\widetilde{\pi}_{t,\omega_2}$ in the fixed- and TOU-price case, are scenario-dependent.

In the fixed-price case, there is no economic incentive for the consumer to modify his/her consumption schedule according to the price signal sent by the retailer. In practice the optimisation consists of a trade-off between consumption (and therefore cost) minimisation and aversion to deviations from the comfort band. In this example, the consumer chooses to allocate all of its consumption during the first hours of the simulation horizon, as shown in Figure F.5.

The situation changes in the TOU-price case, where the consumers prefer to allocate their flexible consumption during valley hours, which are characterised by low prices. Clearly, consumption takes place during peak hours only when necessary, i.e.during few hours for consumer type 2 and for the least flexible consumer type 3.

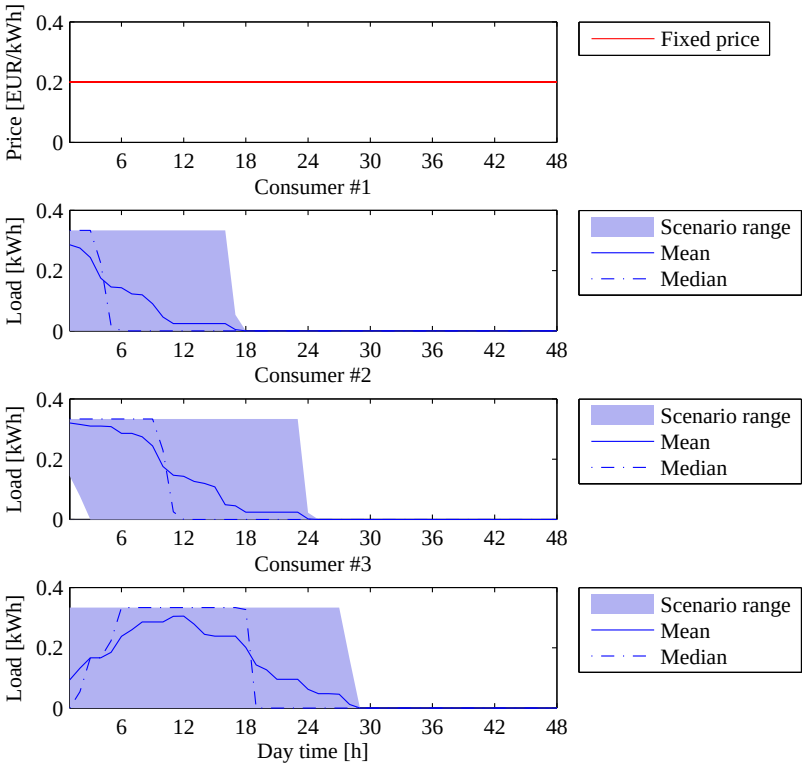

Figure F.5: Flexible consumption (l) patterns for the consumer types with fixed price $\widetilde{\pi}$

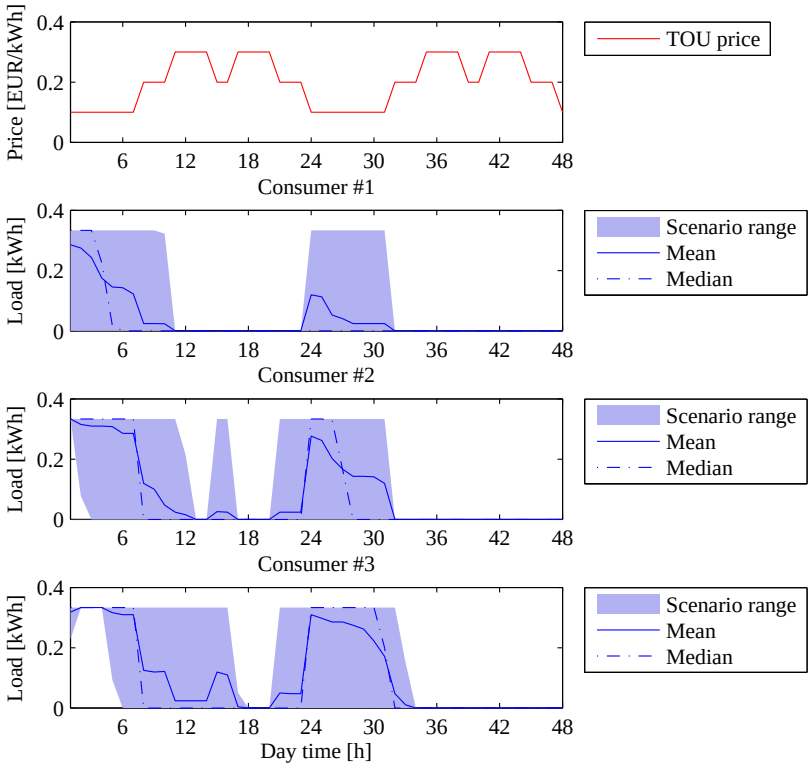

Figure F.6: Flexible consumption (l) patterns for the consumer types with Time-Of-Use (TOU) based price $\widetilde{\pi}$

In the dynamic price case, the consumer adapts to the price signal submitted by the retailer. Remarkably, the price plotted in Figure F.7 is on average lower during night time, i.e.hours 0–8 and 21–32. The consumer response follows the price signal: indeed, flexible consumption takes place more likely in time periods where the price tends to be low. This appears to hold rather generally across all the consumer groups considered.

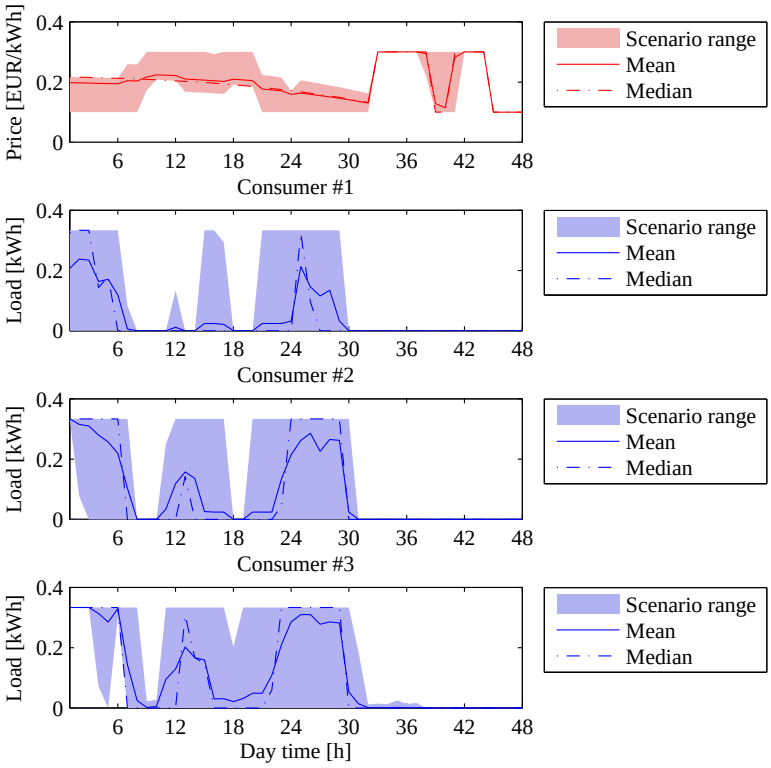

Figure F.7: Flexible consumption (l) patterns for the consumer types with dynamic price $\widetilde{\pi}$

Analysing the results further, one notices scenarios where the price chosen by the retailer implies multiple solutions for the consumer. In this case, the consumer is indifferent with respect to choosing any of these solutions, and might therefore pick randomly or decide according to a secondary criterion (e.g.choosing, among the solutions delivering the minimum cost, the one minimising the consumption).

The results presented here refer to the case where the consumer selects, among the optimal solutions, the one that yields the best profit for the retailer. In mathematical terms, this is the *optimistic* or *strong Stackelberg solution* [36]. Notice that by definition every solution to the MPEC in the general form (F.1) is a strong Stackelberg solution. In practice this means that the results of the bilevel model could be too optimistic, unless there is a reason why the consumer would choose the strong Stackelberg solution instead of any other element in his/her optimal set $\mathbf{y} \in \mathcal{S}(\mathbf{x})$. For example, the retailer could communicate, along with the price signal, a suggested consumption level to choose in case multiple solutions are found. As an alternative, one could modify the setup of the lower level problem so that it always has a unique solution. In other words, one must define a lower level problem as a variational inequality where the functional is *strongly monotone* on the feasible set, see [16]. Future research in this direction is needed.

Let us now consider the relationship between the total consumption $l_{t,\omega_2} + l^i_{t,\omega_3}$ and the price π^s_{t,ω_2} paid by the retailer at the spot market under the dynamic-pricing scheme. As one can see in Figure F.8, total consumption peaks when the spot price is at the lowest point, i.e.during the night in both the first and the second day included in the horizon. Furthermore, another peak of smaller intensity and shorter duration is observed around the 13th hour of the simulation, where the spot price appears on average to have a local valley. An intuitive explanation for this is that part of the load cannot be postponed to the following night (or shifted to the previous one) without violating the comfort band; therefore accepting a locally minimum price is a good compromise. Observing this type of behaviour was one of the reasons behind the choice of a model capturing the dynamics in the consumer flexibility. Finally, the energy E^s purchased by the retailer at the spot market resembles the pattern of the average consumption, though shifted somewhat up due to the lower expected costs for down-regulation compared to up-regulation.

Finally, it is of interest to analyse the impact of the introduction of dynamic prices on the retailer's energy imbalance. Indeed demand response, if managed with correct policies, has the potential to reduce both the magnitude and the total cost of regulation. Deviations from the day-ahead schedule and imbalance penalties are shown in Figure F.9, F.10 and F.11, in the cases of fixed, TOU and dynamic price, respectively. It is worth pointing out that generally the retailer prefers being long, i.e.contracting more energy at the spot market than needed on average. This is confirmed by the prevalence of down-regulation in the three figures. Furthermore, we remark that in the TOU-price case in Figure F.10, the largest imbalances are moved to the valley hours. In a similar fashion, the retailer manages to move the largest imbalances away from periods where regulation prices peak under dynamic pricing. This is illustrated in Figure F.11.

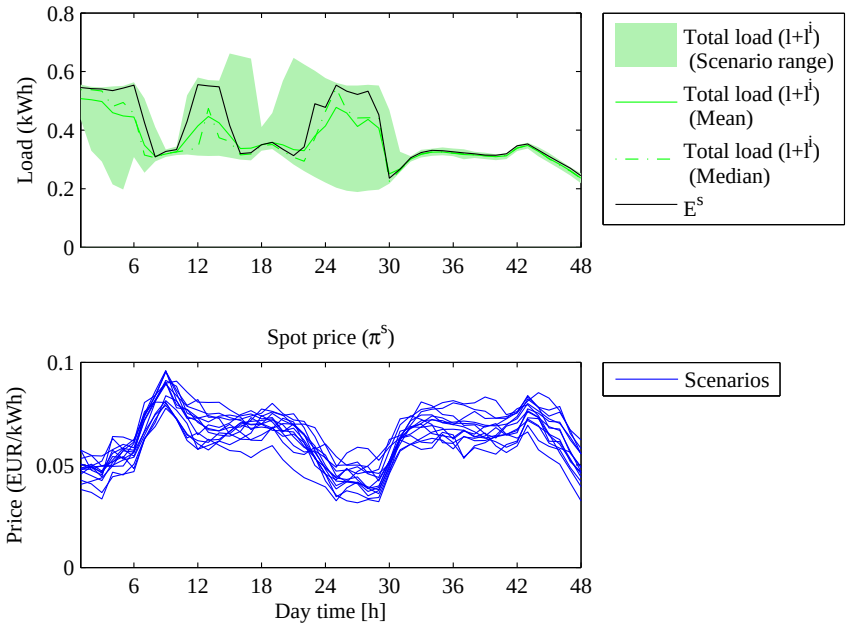

Figure F.8: Total consumption (aggregating flexible and inflexible load $l + l^i$) and spot market offer E^s versus spot market price π^s

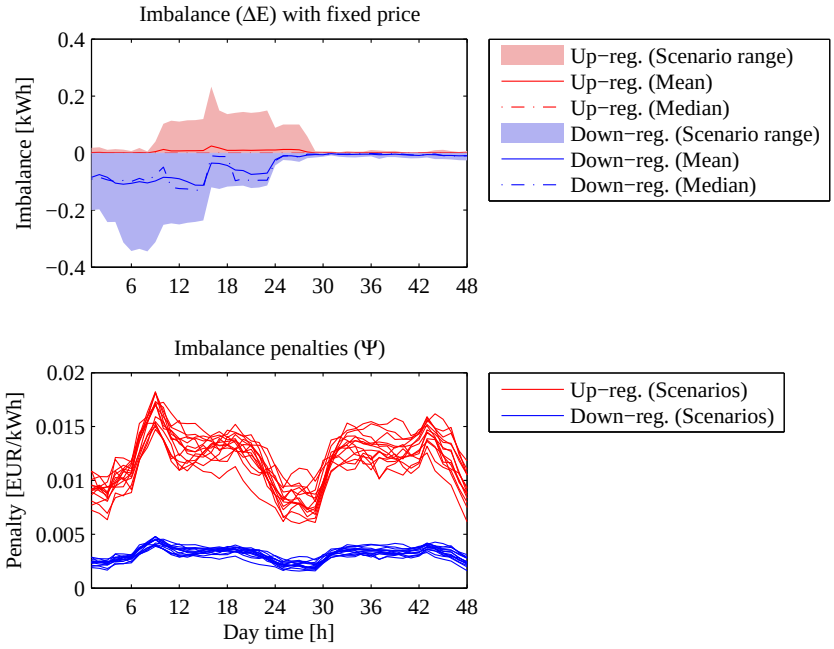

Figure F.9: Retailer energy imbalance $\Delta E^{\uparrow}_{t,\omega_2,\omega_3}$ (up-regulation), $\Delta E^{\downarrow}_{t,\omega_2,\omega_3}$ (down-regulation) and imbalance penalties $\psi^{\uparrow}_{t,\omega_2}$ (up-regulation), $\psi^{\downarrow}_{t,\omega_2}$ (down-regulation) with fixed consumer price $\widetilde{\pi}$

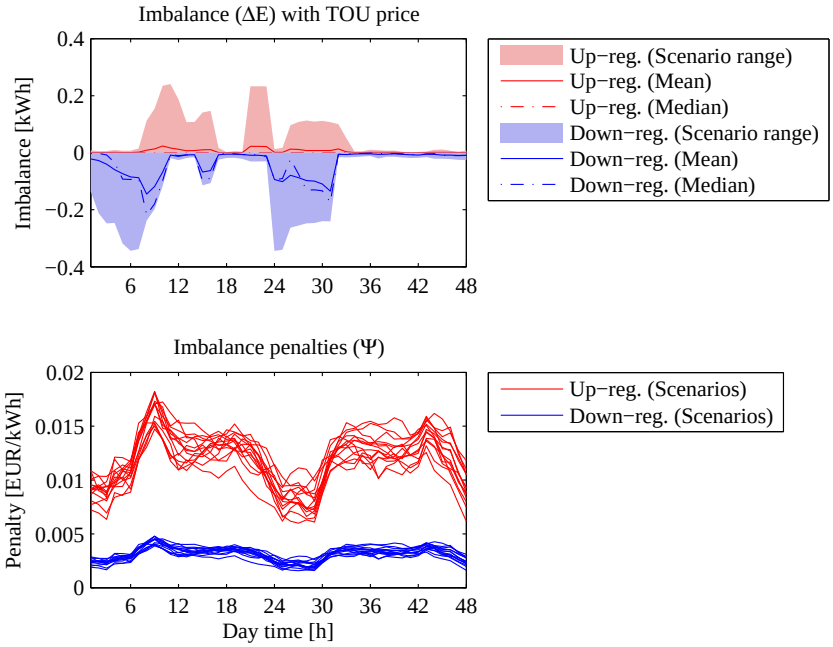

Figure F.10: Retailer energy imbalance $\Delta E^{\uparrow}_{t,\omega_2,\omega_3}$ (up-regulation), $\Delta E^{\downarrow}_{t,\omega_2,\omega_3}$ (down-regulation) and imbalance penalties $\psi^{\uparrow}_{t,\omega_2}$ (up-regulation), $\psi^{\downarrow}_{t,\omega_2}$ (down-regulation) with Time-Of-Use (TOU) based consumer price $\widetilde{\pi}$

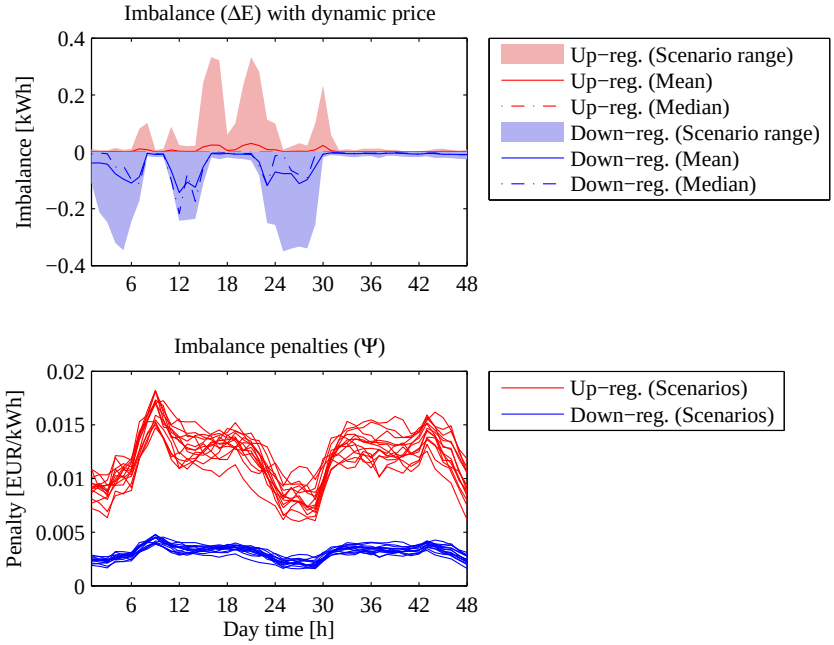

Figure F.11: Retailer energy imbalance $\Delta E^{\uparrow}_{t,\omega_2,\omega_3}$ (up-regulation), $\Delta E^{\downarrow}_{t,\omega_2,\omega_3}$ (down-regulation) and imbalance penalties $\psi^{\uparrow}_{t,\omega_2}$ (up-regulation), $\psi^{\downarrow}_{t,\omega_2}$ (down-regulation) with dynamic consumer price $\widetilde{\pi}$

The main results for the retailer in the simulations with fixed, TOU and dynamic price are summarised in Table F.3. It emerges from these results that the retailer improves its performance when it is allowed to send a dynamic price signal to its flexible consumers. The expected profit $\phi(\mathbf{x}, \mathbf{y})$ rises by approximately 5% compared to the fixed-price case, both due to an increase in revenues and a cost reduction. On the contrary, the TOU-pricing scheme yields the lowest profits among the three cases considered.

The retailer revenues consist of returns of the sale of energy for flexible and inflexible consumption at the price imposed by the retailer, that is

$$\sum_{t=1}^{N_T} \widetilde{\pi}_{t,\omega_2} l_{t,\omega_2} + \widetilde{\pi}_{t,\omega_2} l^i_{t,\omega_3} \tag{F.38}$$

The two components, averaged over the scenarios used in this example, are presented separately in the table. In the case with TOU-price, revenues from the flexible part of the load are dramatically lower if compared to the corresponding quantities with fixed- and dynamic-price. This clearly indicates that this pricing scheme is the most favourable to the consumers. With dynamic pricing, the total revenues are maximised, indicating that the retailer is fully exploiting its market power over the consumers.

The costs for the retailer are presented in two different formulations. In the first formulation they are calculated by summing the payment for purchasing power at the spot market and the cost (revenue) of buying (selling) energy at the real-time market

$$\sum_{t=1}^{N_T} \pi^s_{t,\omega_2} E^s_t + \pi^{\uparrow}_{t,\omega_2} \Delta E^{\uparrow}_{t,\omega_2,\omega_3} - \pi^{\downarrow}_{t,\omega_2} \Delta E^{\downarrow}_{t,\omega_2,\omega_3} \tag{F.39}$$

The payment at the spot market is lowest with dynamic-pricing, i.e.when the retailer can indirectly shift the load by communicating a price signal to the consumer, while the TOU pricing scheme ranks second. The results in the real-time market seem, at a superficial analysis, counterintuitive, since the revenues are lower in the dynamic-price case than in the fixed-price one. However, it is not straightforward from this formulation to understand whether dynamic prices can help to achieve better results in terms of imbalance costs. For this reason we consider reformulation (F.30) and break down the retailer costs in the following way

$$\sum_{t=1}^{N_T} \pi^s_{t,\omega_2} (l_{t,\omega_2} + l^i_{t,\omega_3}) + \psi^{\uparrow}_{t,\omega_2} \Delta E^{\uparrow}_{t,\omega_2,\omega_3} + \psi^{\downarrow}_{t,\omega_2} \Delta E^{\downarrow}_{t,\omega_2,\omega_3} \tag{F.40}$$

where the first term can be considered as the spot market costs if the retailer had perfect information on future consumption, and the last two terms are

Retailer performance index		Pricing		
		Fixed	TOU	Dynamic
Profits		2.3139	2.2296	2.4286
Revenues	flexible load	0.7050	0.4300	0.7180
	inflexible load	2.7155	2.8865	2.7868
	total	3.4205	3.3164	3.5049
Costs	spot market	1.2146	1.1676	1.1578
	regulation market	-0.1080	-0.0808	-0.0814
	total	1.1067	1.0868	1.0763
Costs (reform.)	perfect information	1.0970	1.0781	1.0680
	real-time penalties	0.0096	0.0088	0.0083
	total	1.1067	1.0868	1.0763

Table F.3: Market performance of the retailer in the simulations with fixed and dynamic price. All the values are averages for the considered scenarios expressed in €

the imbalance penalties, i.e.the cost of imperfect information. As shown in Table F.3, not only the spot market "virtual" payment under perfect information, but also the imbalance costs behave according to intuition. Indeed, the dynamic pricing scheme (which is optimal) performs best, followed by the case with TOU price (which is suboptimal, but designed to reduce costs on average), while the fixed price case ranks last. This confirms that demand response can be employed both for reducing the cost of energy procurement (i.e.peak-shifting) and for cutting the regulation cost.

The results of the simulations for the consumers are summarised in Table F.4. Note that the consumer costs in this table are equal to the retailer revenues in Table F.3. As already mentioned in the discussion above, the electricity procurement payments for the consumers are maximised under the dynamic pricing scheme, and lowest with TOU price. Especially the fact that the consumer payments for the flexible part of the load are highest with dynamic pricing tells us that dynamic prices alone do not necessarily result in higher benefit for the flexible consumers. In this example, the consumer is better off with TOU- or fixed-price contracts than with a dynamic-price one with equal average prices over the day. Reductions in the average real-time consumer price could be considered as an incentive for consumers to switch to dynamic-price contracts. Therefore, determining an average value making dynamic real-time prices beneficial also for consumers is an interesting problem for which models of this type could be employed. Finally we point out that, despite the electricity procurement costs for the consumers are higher in the dynamic-price case compare to the fixed pricing scheme, the average price paid by the flexible part of the load

Consumer result index		Unit	Pricing		
			Fixed	TOU	Dynamic
Costs	flexible load	€	0.7050	0.4300	0.7180
	inflexible load	€	2.7155	2.8865	2.7868
	total	€	3.4205	3.3164	3.5049
Price	flexible load	€/kWh	0.2000	0.1136	0.1885
	inflexible load	€/kWh	0.2000	0.2126	0.2053

Table F.4: Consumer results in the simulations with fixed and dynamic price. All the values are averages for the considered scenarios

decreases quite sensibly. This implies that the total electricity consumption is higher in the dynamic-price case.

To conclude, we can interpret the reduction of the market costs for the retailer in the dynamic-price case as an increase of social welfare. This is because the transfer of money from consumers to retailer cancels out in a social welfare calculation. Since there were no deviations from the comfort band in any of the cases and scenarios considered in the example, we can conclude that the consumer benefit is constant. As a result, the social welfare is given by the generation costs changed in sign. These cannot be directly calculated, since this model does not include the supply side. Nevertheless, we can consider the reduction in retailer market costs as a proxy for the reduction of generation cost. On the other hand, the increase in consumer payments to the retailer implies that the redistribution of this additional welfare between the players might not be fair under this retailer-consumer configuration. Once again, though, we point out that these considerations hold for the considered example and with the considered setup. Different dynamic price contracts, i.e.different parameters in the constraints (F.5)–(F.7), could yield a fairer redistribution of the welfare.

F.4.3.2 Impact of consumer flexibility

We now consider how different levels of demand flexibility impact the results for both the retailer and the consumer. This is done by carrying out two additional simulations with different distributions into the consumer groups described in Section F.4.1. In the first run of the model, aimed at simulating a situation of high demand flexibility, we consider the consumer group distribution $[0.6, 0.3, 0.1]$. The situation is reversed to the distribution $[0.1, 0.3, 0.6]$ in the last run of the model, simulating low demand flexibility. Both cases are compared to the reference case in the previous section, where demand flexibility

Retailer performance index		Unit	Flexibility		
			High	Medium	Low
Profits		€	2.3199	2.4286	2.5311
Revenues	flexible load	€	0.5517	0.7180	0.8757
	inflexible load	€	2.7969	2.7868	2.7767
	total	€	3.3486	3.5049	3.6524
Costs	spot market	€	1.1058	1.1578	1.2057
	regulation market	€	-0.0771	-0.0814	-0.0845
	total	€	1.0287	1.0763	1.1212
Costs (reform.)	perfect information	€	1.0211	1.0680	1.1114
	real-time penalties	€	0.0076	0.0083	0.0099
	total	€	1.0287	1.0763	1.1212

Table F.5: Market performance of the retailer in simulations with different demand flexibility. All the values are averages for the considered scenarios

is medium due to the choice of the distribution $[0.3, 0.4, 0.3]$.

Table F.5 illustrates the retailer market performance in the three cases of demand flexibility, this time only with dynamic price. Observe that higher demand flexibility results in lower average profits for the retailer. This is the result of two contrasting trends. On the one side, total revenues for electricity sale diminish as demand flexibility increases. This is in line with the expectations that retailers have lower market power, i.e.ability to impose prices to the demand, as consumers get more flexible. On the other side, total market costs drop as well with higher consumer flexibility. This drop is due to cuts both in spot market costs for electricity procurement (perfect information row in Table F.5) and in regulation penalty costs. Nevertheless the overall effect is still of decreasing retailer profits with increasing flexibility, because the cuts in market costs are not large enough to offset the reduction in revenues.

The results for the consumer are shown in Table F.6. As already pointed out, demand experiences a cut in the electricity costs as it gets more and more flexible. This is due to a quite dramatic drop in the cost of flexible load and only a slight increase in the cost of must-serve load. Therefore, there is a clear economic signal suggesting the demand to adopt more flexible consumption preferences, and to increase the share of flexible demand. The decrease in the average price per kWh paid for flexible load confirms that a more cost-effective load pattern is adopted by the consumer.

Consumer result index		Unit	Flexibility		
			High	Medium	Low
Costs	total	€	3.3486	3.5049	3.6524
	flexible load	€	0.5517	0.7180	0.8757
	inflexible load	€	2.7969	2.7868	2.7767
Price	flexible load	€/kWh	0.1870	0.1885	0.1921
	inflexible load	€/kWh	0.2060	0.2053	0.2045

Table F.6: Consumer results in simulations with different demand flexibility. All the values are averages for the considered scenarios

F.5 Conclusions

This paper presents a game theoretical model for the participation of energy retailers in electricity markets with flexible demand and real-time consumer prices. The hierarchical structure in the relation between retailers and consumers, pertaining to the so-called Stackelberg (or leader-follower) games, is imposed by the formulation as a bilevel optimisation problem. The model has three-stages to reflect the fact that decisions are made day-ahead, real-time and ex-post with different information structure on the stochastic variables involved. Furthermore a dynamic model for the demand flexibility based on realistic consumer preferences is employed.

In an illustrative example, the model is simulated in a realistic setup, which allows the comparison of the results obtained using the optimal dynamic price with the ones under fixed and time-of-use pricing schemes. We show that, in the dynamic-price case, the retailer, while maximising its profits, sends the consumer a price-incentive to shift his/her demand to periods of the day characterised by low spot market prices. Similarly, a drop in the imbalance costs borne by the retailer, due to deviations of the actual consumption from the energy contracted day-ahead, is experienced when switching from a fixed or a time-of-use to a real-time consumer price regime. It turns out that the dynamic pricing scheme minimises the retailer net payments in the day-ahead and real-time markets. On the contrary, the fixed price yields the highest costs among the pricing schemes considered, while the time-of-use price has a middle performance.

We link the reduction of procurement and regulation costs, obtained by shifting the load, to an increase in social welfare. As simulations show, though, the redistribution of the additional welfare is not fair in the dynamic-price scheme considered, as the retailer absorbs entirely the added welfare. Indeed, the consumer payments to the retailer are highest under the dynamic-pricing scheme

in the considered example. On the contrary, the time-of-use setup yields the lowest costs for the consumers among the pricing schemes considered. These results, however, do not account for the effect of competition among retailers. In any case, particular care should be taken in designing pricing schemes that can effectively motivate consumers participation in real-time price programmes.

Finally, through a sensitivity analysis it is shown that, once real-time contracts are in place, there is an economic incentive for the consumers to increase their flexibility.

Future extensions of this research could move in several directions. Different utility functions to model the trade-off for the consumer between electricity price and comfort could be defined and simulated. For example, the lower and upper bounds of the comfort band could be linear functions of the price, or a quadratic penalty for deviations of the temperature from a reference could be used. Furthermore, different forms of consumer flexibility could be considered, for example by modelling the consumption of "intelligent appliances" such as price-responsive washing machines and electric vehicles. Besides, a different setup ensuring a unique solution to the lower-level optimisation problem could be proposed so as to improve the controllability of the load from the retailer perspective, i.e.to ensure that the strong Stackelberg solution is also unique. Furthermore, the effect of renewable power on market prices could be introduced in the model, thus paving the way for an assessment of the value of demand response programmes in the integration of renewable generation in the system. Additionally, the optimisation model for the retailer could be refined by considering a diversified portfolio including e.g.futures and options, and by including risk management. Finally, competition among retailers could be modelled in the framework of *Equilibrium Programs with Equilibrium Constraints* (EPECs)

Acknowledgements

Pierre Pinson and Henrik Madsen are partly funded by the iPower platform project, supported by DSF (Det Strategiske Forskningsråd) and RTI (Rådet for Teknologi og Innovation), which are hereby acknowledged. Furthermore, DSF (Det Strategiske Forskningsråd) is to be accredited for partly funding the work of Pierre Pinson, Henrik Madsen and Juan M. Morales through the Ensymora project (no. 10-093904/DSF). Juan M. Morales is also supported by the H.C. Ørsted research fellowship granted by the Technical University of Denmark. Besides, we thank Rasmus Halvgaard from DTU Informatics and Trine Krogh Boomsma from the Department of Mathematical Sciences at the University of

Copenhagen for useful discussions and comments on our work. Energinet.dk and the Department of Agronomy at Iowa State University are acknowledged for making public the data used in this research. Finally, we thank the Editor of this Journal, Richard Tol, and two anonymous referees for providing us with relevant comments that undoubtedly improved the quality of this paper.

References F

[1] T. Jónsson, P. Pinson, and H. Madsen, "On the market impact of wind energy forecasts," *Energy Economics*, vol. 32, no. 2, pp. 313–320, 2010.

[2] J. M. Morales and A. J. Conejo, "Simulating the impact of wind production on locational marginal prices," *IEEE Transactions on Power Systems*, vol. 26, no. 3, pp. 820–828, 2011.

[3] J. Torriti, M. G. Hassan, and M. Leach, "Demand response experience in Europe: policies, programmes and implementation," *Energy*, vol. 35, no. 4, pp. 1575–1583, 2010.

[4] M. Parvania and M. Fotuhi-Firuzabad, "Demand response scheduling by stochastic SCUC," *IEEE Transactions on Smart Grids*, vol. 1, no. 1, pp. 89–98, 2010.

[5] R. Sioshansi, "Evaluating the impact of real-time pricing on the cost and value of wind generation," *IEEE Transactions on Power Systems*, vol. 25, no. 2, pp. 741–748, 2010.

[6] M. D. Ilić, L. Xie, and J.-Y. Joo, "Efficient coordination of wind power and price-responsive demand – Part I: theoretical foundations," *IEEE Transactions on Power Systems*, vol. 26, no. 4, pp. 1875–1884, 2011.

[7] M. D. Ilić, L. Xie, and J.-Y. Joo, "Efficient coordination of wind power and price-responsive demand – Part II: case studies," *IEEE Transactions on Power Systems*, vol. 26, no. 4, pp. 1884–1893, 2011.

[8] A. A. S. Algarni and K. Bhattacharya, "A generic operations framework for discos in retail electricity markets," *IEEE Transactions on Power Systems*, vol. 24, no. 1, pp. 356–367, 2009.

[9] H. Oh and R. J. Thomas, "Demand-side bidding agents: Modeling and simulation," *IEEE Transactions on Power Systems*, vol. 23, no. 3, pp. 1050–1056, 2008.

[10] O. Corradi, H. Ochsenfeld, H. Madsen, and P. Pinson, "Controlling the electricity consumption by forecasting its response to varying prices," *IEEE Transactions on Power Systems*, 2011. In press.

[11] A. J. Conejo, J. M. Morales, and L. Baringo, "Real-time demand response model," *IEEE Transactions on Smart Grid*, vol. 1, pp. 236–242, dec 2010.

[12] D. T. Nguyen, M. Negnevitsky, and M. de Groot, "Pool-based demand response exchange – concept and modeling," *IEEE Transactions on Power Systems*, vol. 26, no. 3, pp. 1677–1685, 2011.

[13] H. von Stackelberg, *Market Structure and Equilibrium*. Springer Berlin Heidelberg, 2011.

[14] H. Madsen, *Time Series Analysis*. Chapman & Hall/CRC, 2007.

[15] S. Borenstein, "The trouble with electricity markets: understanding California's restructuring disaster," *Journal of Economic Perspectives*, vol. 16, no. 1, pp. 191–211, 2002.

[16] Z.-Q. Luo, J.-S. Pang, and D. Ralph, *Mathematical Programs with Equilibrium Constraints*. Cambridge University Press, 1996.

[17] D. Luenberger, *Linear and Nonlinear Programming*. Addison-Wesley Publishing Company, 1984.

[18] R. Halvgaard, N. K. Poulsen, H. Madsen, and J. B. Jørgensen, "Economic model predictive control for building climate control in a smart grid," in *IEEE PES Conference on Innovative Smart Grid Technologies (ISGT)*, (Washington, USA), 2012.

[19] H. Kwakernaak and R. Sivan, *Linear Optimal Control Systems*. Wiley-Interscience, 1 ed., 1972.

[20] A. J. Conejo, E. Castillo, R. Mínguez, and R. García Bertrand, *Decomposition Techniques in Mathematical Programming. Engineering and Science Applications*. Springer, 2006.

[21] J. Fortuny-Amat and B. McCarl, "A representation and economic interpretation of a two-level programming problem," *Journal of the Operational Research Society*, vol. 32, no. 9, pp. 783–792, 1981.

[22] M. V. Pereira, S. Granville, M. H. C. Fampa, R. Dix, and L. A. Barroso, "Strategic bidding under uncertainty: A binary expansion approach," *IEEE Transactions on Power Systems*, vol. 20, no. 1, pp. 180–188, 2005.

[23] M. T. Vespucci, M. Innorta, and G. Cervigni, "A Mixed Integer Linear Programming model of a zonal electricity market with a dominant producer," *Energy Economics*, 2012. In Press.

[24] M. Carrión, J. M. Arroyo, and A. J. Conejo, "A bilevel stochastic programming approach for retailer futures market trading," *IEEE Transactions on Power Systems*, vol. 24, no. 3, 2009.

[25] G. Chicco, R. Napoli, F. Piglione, P. Postolache, M. Scutariu, and C. Toader, "Load pattern-based classification of electricity customers," *IEEE Transactions on Power Systems*, vol. 19, no. 2, pp. 1232–1239, 2004.

[26] T. K. Kristoffersen, K. Capion, and P. Meibom, "Optimal charging of electric drive vehicles in a market environment," *Applied Energy*, vol. 88, no. 5, pp. 1940–1948, 2011.

[27] H. Madsen and J. Holst, "Estimation of continuous-time models for the heat dynamics of a building," *Energy and Buildings*, vol. 22, no. 1, pp. 67–79, 1995.

[28] M. Dubrovsky, "Creating daily weather series with use of the weather generator," *Environmetrics*, vol. 8, no. 5, pp. 409–424, 1997.

[29] H. Madsen, *Statistically Determined Dynamical Models for Climate Processes*. PhD thesis, Technical University of Denmark, 1985.

[30] R. Weron, *Modeling and forecasting electricity loads and prices*. Wiley, 2006.

[31] T. Jónsson, *Forecasting and decision-making in electricity markets with focus on wind energy*. PhD thesis, Technical University of Denmark, 2012.

[32] Energinet website. `http://energinet.dk/EN/El/Engrosmarked/Udtraek-af-markedsdata/Sider/default.aspx`, 2011. Last access: December 2011.

[33] T. Jónsson, P. Pinson, H. A. Nielsen, H. Madsen, and T. S. Nielsen, "Forecasting electricity spot prices accounting for wind power predictions," *IEEE Transactions on Sustainable Energy*, 2012. In press.

[34] Iowa Environmental Mesonet website. `http://mesonet.agron.iastate.edu/agclimate/info.phtml`, 2011. Last access: December 2011.

[35] Danish Energy Association, "Dansk elforsyning statistik 2009," 2010.

[36] P. Loridan and J. Morgan, "Weak via strong Stackelberg problems: New results," *Journal of Global Optimization*, vol. 8, pp. 263–287, 1996.

Paper G

Electricity Market Clearing With Improved Scheduling of Stochastic Production

Authors:
Juan Miguel Morales, Marco Zugno, Salvador Pineda, Pierre Pinson

Submitted to:
European Journal of Operational Research.

Electricity Market Clearing With Improved Scheduling of Stochastic Production

Juan Miguel Morales[1], Marco Zugno[2], Salvador Pineda[1], Pierre Pinson[2]

Abstract

In this paper, we consider an electricity market that consists of a day-ahead and a balancing settlement, and includes a number of stochastic producers. We first introduce two reference procedures for scheduling and pricing energy in the day-ahead market: on the one hand, a conventional network-constrained auction purely based on the least-cost merit order, where stochastic generation enters with its expected production and a low marginal cost; on the other, a counterfactual auction that also accounts for the projected balancing costs using stochastic programming. Although the stochastic clearing procedure attains higher market efficiency in expectation than the conventional day-ahead auction, it suffers from fundamental drawbacks with a view to its practical implementation. In particular, it requires flexible producers (those that make up for the lack or surplus of stochastic generation) to accept losses in some scenarios. Using a bilevel programming framework, we then show that the conventional auction, if combined with a *suitable* day-ahead dispatch of stochastic producers (generally different from their expected production), can substantially increase market efficiency and emulate the advantageous features of the stochastic optimization ideal, while avoiding its major pitfalls.

A two-node power system serves as both an illustrative example and a proof of concept. Finally, a more realistic case study highlights the main advantages of a smart day-ahead dispatch of stochastic producers.

[1]Centre for Electric Power and Energy, Technical University of Denmark, Elektrovej, bld. 325, DK-2800 Kgs. Lyngby, Denmark

[2]DTU Informatics, Technical University of Denmark, Richard Petersens Plads, bld. 305, DK-2800 Kgs. Lyngby, Denmark

G.1 Introduction

The penetration of stochastic production in electric energy systems is notably increasing worldwide, primarily owing to a booming wind power industry. There is a broad consensus in the research community that today's electricity market designs are to be revisited so that stochastic producers can enter the competition in a fair and efficient manner.

In its most basic form, an electricity market consists of a forward (typically day-ahead) market and a balancing market. On the one hand, the day-ahead market is required to accommodate the generation from the *inflexible* power plants, i.e. from those generating units that need advance planning in order to efficiently and reliably set their production levels. On the other, the balancing market clears the energy deployed to maintain the constant balance of supply and demand over periods of time with finer resolution, commonly spanning from minutes to one hour. Being cleared shortly before real time, balancing markets allow the trade of energy between *flexible* firms, which can adjust their output quickly, and stochastic producers, whose generation is predictable only with limited accuracy at the day-ahead stage.

Conventionally the day-ahead and the balancing markets are settled independently. Furthermore, with respect to the participation of stochastic producers, the day-ahead market is typically cleared considering their expected production at a very low marginal cost (e.g., zero). The eventual energy adjustments needed to cope with the associated forecast errors are left then to the flexible units participating in the balancing market. Consequently, if this market is not provided with enough flexible capacity, balancing costs may escalate dramatically. It is expected that this problem becomes exacerbated as the penetration of stochastic production increases [1, 2, 3].

To face this challenge, two main solution strategies have been considered, namely:

1. To establish reserve markets, where flexible capacity is procured sufficiently in advance of energy delivery and then made available to the balancing market, where it is dispatched if needed. The reserve demand in these markets is *exogenously* specified by the Transmission System Operator, which opens up a number of different ad-hoc criteria, see e.g. [4].

2. To clear the forward market using stochastic programming [5], which allows modeling future balancing needs and costs in a probabilistic framework, thus yielding the day-ahead energy dispatch that minimizes the expected system operating costs. One of the major advantages of this

approach is that it *endogenously* solves for the optimal amount of reserve capacity to be left to the balancing market, weighing the expected costs and benefits of such capacity [6, 7, 8, 9].

Ideally, the stochastic solution method attains maximum market efficiency (as it minimizes the expected system operating cost) and therefore, it is used here as a reference in this respect. For its practical application within a market environment, though, it must be first complemented with a set of prices and payments that make market participants satisfied with the resulting day-ahead dispatch. In this vein, [6] and [10] define prices for both energy and reserve capacity. However, determining who should pay for such reserve and to which extent is still a major source of conflict and debate [11].

In this paper, we follow the approach of [12] and [13], where the stochastic dispatch is supported by energy prices only. However, this approach is not without its problems either. Indeed, [13] illustrate that the energy-only market settlement associated with the stochastic dispatch requires flexible producers to accept losses for some realizations of the stochastic production, which also raises concerns on its practical applicability.

Starting from this point, the objective of this paper is to show that, if cleared with an appropriate value of stochastic production, *generally different from the expected value*, the conventional settlement of the day-ahead market can notably approach the behavior of the ideal stochastic dispatch, while sidestepping its theoretical drawbacks. For this purpose, we construct a bilevel programming formulation that determines the *optimal* value of stochastic production that should be used to clear the day-ahead market under the conventional settlement.

The rest of this paper is organized as follows. Section G.2 presents the conventional and stochastic dispatch models that we use as references in our work, and provides the mathematical insight to calculate the optimal day-ahead schedule of stochastic production under the conventional market settlement. Section G.3 discusses results from a small example and a case study. More specifically, the example serves to illustrate the different dispatch models, which are subsequently compared and tested using a more realistic setup in the case study. Lastly, Section G.4 concludes the paper.

G.2 Dispatch Models

Consider the sequence of a day-ahead and a balancing market. The day-ahead market is cleared on day $d-1$ (e.g., by 10 am) and covers energy transactions for

delivery on day d, typically on an hourly basis. The balancing market settles the energy imbalances with respect to the day-ahead production and consumption schedule. These imbalances are computed throughout day d, usually over time intervals ranging from minutes to 1 hour.

Let us begin by outlining a standard model for the dispatch of energy. This will serve to present the notation and provide a starting point for the developments of the rest of the paper. The setting will be an electric power system comprising a collection N of nodes.

G.2.1 Conventional Dispatch *(ConvD)*

Let p_G and p_W denote the vectors of decisions on the day-ahead dispatch of conventional and stochastic producers, respectively. For simplicity and without loss of generality, the demand at each node n of the system, l_n, is considered to be known with certainty. We also assume that power flows in the transmission network are determined by the vector δ^0 of nodal voltage angles.

The conventional economic dispatch model (ConvDM) identifies the optimal schedule (p_G^*, p_W^*) that minimizes day-ahead generating costs, $\mathcal{C}^{\mathrm{D}}(p_G, p_W)$, as follows:

$$\underset{p_G, p_W, \delta^0}{\text{Minimize}} \quad \mathcal{C}^{\mathrm{D}}\left(p_G, p_W\right) \tag{G.1a}$$

$$\text{s.t.} \quad h^{\mathrm{D}}\left(p_G, p_W, \delta^0\right) - l = 0 : \lambda^{\mathrm{D}} \,, \tag{G.1b}$$

$$g^{\mathrm{D}}\left(p_G, \delta^0\right) \leq 0 \,, \tag{G.1c}$$

$$p_W \leq \widehat{W} \,, \tag{G.1d}$$

where $\widehat{W}$ is the forecast vector of stochastic production. The equality constraints (G.1b) enforce the day-ahead balancing conditions, stating that the dispatch plus net power flow equals the demand at each node. The inequalities (G.1c) include upper and lower bounds to the dispatch of conventional producers and scheduled power flows, as well as declarations of non-negative variables. Constraints (G.1d) limit the day-ahead schedule of stochastic producers to their expected generation.

The dispatch model (G.1) can be understood as a network-constrained auction that follows a least-cost merit-order principle, i.e., the cheapest generators are dispatched first. Consequently, because stochastic producers enter the market with very low or zero marginal cost, their dispatch up to the forecast mean $\widehat{W}$ is prioritized.

Notice that the vector of dual variables associated with constraint (G.1b), which is indicated in (G.1) by λ^{D}, constitutes the vector of day-ahead locational marginal prices.

Once the optimal day-ahead schedule (p_G^*, p_W^*) has been obtained from (G.1), the balancing market must deal with the energy imbalance caused by the stochastic production. Consider a specific realization vector of this production, denoted by $W_{\omega'}$. The energy imbalance is then given by $W_{\omega'} - p_W^*$, which represents a surplus of generation, if positive, or a shortage, if negative. To accommodate an excess of production, several actions may be taken, namely:

- To decrease the power production of flexible generating units. In market terms, this is equivalent to say that flexible producers repurchase a certain amount $r_{\omega'}^-$ of energy in the balancing market.
- To spill a part $W_{\omega'}^{\mathrm{spill}}$ of the stochastic production.

Similarly, to balance a deficit of generation, the following actions may be taken:

- To increase the power output of flexible units, which is equivalent to say that flexible producers sell an additional amount $r_{\omega'}^+$ of energy in the balancing market.
- To shed a portion $l_{\omega'}^{\mathrm{shed}}$ of the demand. This action is, in general, very costly, as the so-called *value of lost load* is normally very high.

It should be noticed that the previous decision vectors $r_{\omega'}^-$, $r_{\omega'}^+$, $W_{\omega'}^{\mathrm{spill}}$, and $l_{\omega'}^{\mathrm{shed}}$ have been intentionally augmented with the subscript ω' to underline their implicit dependence on the specific realization $W_{\omega'}$ of stochastic production. For ease of presentation, we group all these decision variables into one single vector $y_{\omega'}$ (the notation introduced here will become relevant later on in the illustrative example of Section G.3). Thus, the vector $y_{\omega'}^*$ that minimizes the cost of balancing the energy deviation $W_{\omega'} - p_W^*$ is solution to the following optimization problem:

$$\underset{y_{\omega'}, \delta_{\omega'}}{\text{Minimize}} \quad \mathcal{C}^{\mathrm{B}}\left(y_{\omega'}\right) \tag{G.2a}$$

$$\text{s.t.} \quad h^{\mathrm{B}}\left(y_{\omega'}, \delta_{\omega'}, \delta^{0*}\right) + W_{\omega'} - p_W^* = 0 : \lambda_{\omega'}^{\mathrm{B}} \,, \tag{G.2b}$$

$$g^{\mathrm{B}}\left(y_{\omega'}, \delta_{\omega'}, p_G^*; W_{\omega'}\right) \leq 0 \,, \tag{G.2c}$$

where $\delta_{\omega'}$ is the vector of nodal voltage angles at the balancing stage. The equality constraints (G.2b) ensure that generating units and loads are redispatched so that the system remains in balance. The vector $\lambda_{\omega'}^{\mathrm{B}}$ of dual variables

associated with these constraints define the locational marginal prices at the balancing market. Similarly to (G.1c), the inequalities (G.2c) comprise upper and lower bounds on the re-dispatch of generating units, load shedding, wind spillage, actual power flows, and declarations of nonnegative variables.

If we now denote the optimal vector of balancing actions by $y^*_{\omega'}$, the overall cost of operating the power system under the realization $W_{\omega'}$ of stochastic production is given by $\mathcal{C}^{\mathrm{D}}\left(p^*_G, p^*_W\right) + \mathcal{C}^{\mathrm{B}}\left(y^*_{\omega'}\right)$.

It is important to stress that both constraints (G.2b) and (G.2c), and hence also the balancing costs $\mathcal{C}^{\mathrm{B}}\left(y_{\omega'}\right)$, are dependent on the optimal day-ahead schedule $\left(p^*_G, p^*_W, \delta^{0*}\right)$. Since the conventional dispatch model (G.1) is blind to such dependency, the market becomes more and more inefficient as the penetration of stochastic production increases. In this vein, the stochastic dispatch model presented next intends to capture precisely the interaction between day-ahead and balancing decisions.

G.2.2 Stochastic Dispatch *(StochD)*

Consider that the electricity production from stochastic producers can be efficiently modeled by a finite set Ω of scenarios, each characterized by a vector of power values W_ω and a probability of occurrence π_ω. It must hold that $\pi_\omega \geq 0$, for all $\omega \in \Omega$, and $\sum_{\omega\in\Omega} \pi_\omega = 1$. The scenario set Ω is assumed to be available to the Transmission System Operator.

The stochastic dispatch model writes as follows:

$$\underset{p_G, p_W, \delta^0; y_\omega, \delta_\omega, \forall\omega}{\text{Minimize}} \quad \mathcal{C}^{\mathrm{D}}\left(p_G, p_W\right) + \mathbb{E}_\omega\left[\mathcal{C}^{\mathrm{B}}\left(y_\omega\right)\right] \tag{G.3a}$$

$$\text{s.t.} \quad h^{\mathrm{D}}\left(p_G, p_W, \delta^0\right) - l = 0 : \lambda^{\mathrm{D}} \,, \tag{G.3b}$$

$$g^{\mathrm{D}}\left(p_G, \delta^0\right) \leq 0 \,, \tag{G.3c}$$

$$p_W \leq \overline{W} \,, \tag{G.3d}$$

$$h^{\mathrm{B}}\left(y_\omega, \delta_\omega, \delta^0\right) + W_\omega - p_W = 0 \,, \quad \forall\omega \in \Omega \,, \tag{G.3e}$$

$$g^{\mathrm{B}}\left(y_\omega, \delta_\omega, p_G; W_\omega\right) \leq 0 \,, \quad \forall\omega \in \Omega \,, \tag{G.3f}$$

where $\overline{W}$ is the vector of capacities of stochastic producers and $\mathbb{E}_\omega[\cdot]$ is the expectation operator over the scenario set Ω. Notice that, based on this set, the dispatch problem (G.3) explicitly models and thus anticipates the balancing operation of the power system by means of constraints (G.3e) and (G.3f) and the expectation of the balancing costs in the objective function (G.3a). This way, the stochastic programming problem (G.3) yields the day-ahead dispatch (p^*_G, p^*_W)

that maximizes market efficiency, provided that the scenario set Ω is properly constructed. As we shall see later, according to (G.3), flexible producers may be dispatched *out of merit order* in the day-ahead market to provide the power system with sufficient flexible capability to cope with the energy imbalances caused by stochastic producers in real time.

G.2.3 Improved Dispatch of Stochastic Producers *(ImpD)*

In an attempt to increase the performance of the conventional dispatch model (G.1), we address now the following question: *Which value $p_W^{\max}$ should the forecast vector $\widehat{W}$ in* (G.1d) *be replaced with to maximize market efficiency?* The answer to this question is naturally given by the following bilevel programming problem:

$$\underset{p_G,p_W,\delta^0,p_W^{\max};y_\omega,\delta_\omega,\forall\omega}{\text{Minimize}} \quad \mathcal{C}^{\mathrm{D}}\left(p_G,p_W\right)+\mathbb{E}_\omega\left[\mathcal{C}^{\mathrm{B}}\left(y_\omega\right)\right] \tag{G.4a}$$

$$\text{s.t.} \quad h^{\mathrm{B}}\left(y_\omega,\delta_\omega,\delta^0\right)+W_\omega-p_W=0\ ,\ \ \forall\omega\in\Omega\ , \tag{G.4b}$$

$$g^{\mathrm{B}}\left(y_\omega,\delta_\omega,p_G;W_\omega\right)\leq 0\ ,\ \ \forall\omega\in\Omega\ , \tag{G.4c}$$

$$0\leq p_W^{\max}\leq\overline{W}\ , \tag{G.4d}$$

$$\left(p_G,p_W,\delta^0\right)\in\arg\Big\{\underset{x_G,x_W,\theta}{\text{Minimize}} \quad \mathcal{C}^{\mathrm{D}}\left(x_G,x_W\right) \tag{G.4e}$$

$$\text{s.t.} \quad h^{\mathrm{D}}\left(x_G,x_W,\theta\right)-l=0:\lambda^{\mathrm{D}}\ , \tag{G.4f}$$

$$g^{\mathrm{D}}\left(x_G,\theta\right)\leq 0\ , \tag{G.4g}$$

$$x_W\leq p_W^{\max}\Big\}\ . \tag{G.4h}$$

The lower-level problem (G.4e)–(G.4h) is equivalent to the conventional dispatch (G.1), except for the upper bound of the day-ahead schedule of stochastic producers in (G.4h), which is, in this case, endogenously computed by the upper-level problem (G.4a)–(G.4d) to minimize the sum of day-ahead dispatch costs and the expected balancing costs. Consequently, the bilevel model (G.4) manages to dispatch stochastic producers not only based on their marginal costs (which are often very low or zero), but also on the cost of their uncertainty (which is estimated by (G.4a)–(G.4d)).

If the conventional dispatch model (G.1) is linear—note that this includes the family of dispatch models that consider piecewise linear supply costs functions, a DC power-flow network model, a piecewise linear approximation of the transmission losses, ramping constraints, etc. (see e.g. [14])—the lower-level prob-

lem (G.4e)–(G.4h) can be replaced by its KKT conditions. In turn, the associated complementarity conditions can be recast using the equivalent mixed-integer formulation proposed by [15]. The steps required to transform a bilevel programming problem of the type of (G.4), with a linear lower level, into a manageable single-level optimization problem are well known in the technical literature (see e.g. [16]) and are omitted here for conciseness. However, this transformation is illustrated later, in Section G.3, using a small example.

For ease of comparison, the short form "ImpD" is used to refer to the conventional dispatch model (G.1) where $\widehat{W}$ in (G.1d) is replaced with the optimal value of $p_W^{\max}$ that results from (G.4).

G.2.4 Energy-only Market Settlement

We now introduce a standard settlement scheme whereby market participants are paid for energy only.

Consider a certain market participant k and define E_k^{D} as the amount of energy sold (if positive) or purchased (if negative) in the day-ahead market, and $E_{k\omega'}^{\mathrm{B}}$ as the amount of energy sold (if positive) or purchased (if negative) in the balancing market in scenario ω'. These quantities are directly derived from the power schedule that is solution to the dispatch model under consideration. The payment to (if positive) or from (if negative) market participant k under scenario ω' is then given by

$$\lambda_{s(k)}^{\mathrm{D}} E_k^{\mathrm{D}} + \lambda_{s(k)\omega'}^{\mathrm{B}} E_{k\omega'}^{\mathrm{B}} \ , \tag{G.5}$$

where $s(k)$ indicates the node where market participant k is located. The locational day-ahead market price $\lambda_{s(k)}^{\mathrm{D}}$ is obtained from either ConvD, StochD, or ImpD, while the locational balancing market price $\lambda_{s(k)\omega'}^{\mathrm{B}}$ is computed from (G.2) after the day-ahead market is cleared and the actual realization ω' of the stochastic production becomes known.

[13] shows that, if generating units are fully dispatchable from zero to their maximum capacities (the problem of pricing in markets with non-convexities is not treated here; see e.g. [17] for further information on this topic), the energy-only settlement scheme (G.5) under the stochastic dispatch model (G.3) guarantees cost recovery for flexible producers *only in expectation*. This expectation is, besides, contingent on the probabilistic characterization of the stochastic production at a market-wide level, which is in possession of the TSO and out of the control of the individual producers. Furthermore, we show in the illustrative example of Section G.3 that StochD may actually dispatch flexible units in the day-ahead market in a loss-making position.

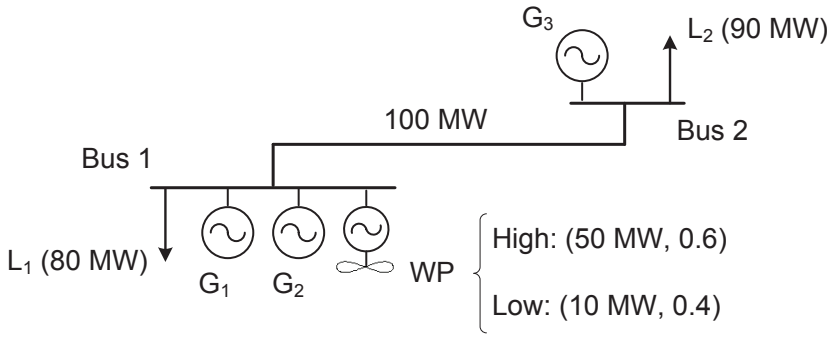

Figure G.1: Two-bus power system.

On the contrary, the conventional dispatch model, either in the traditional form of ConvD or in the variant ImpD proposed in this paper, ensures cost recovery for flexible producers for any possible realization of the stochastic production.

G.3 Results and Discussion

In this section, we first make use of a small two-node system to intuitively illustrate the main features of the previously discussed dispatch models. Then, we provide meaningful results from a more realistic case study.

G.3.1 Illustrative Example

The different dispatch models are illustrated next using the two-node system depicted in Fig. G.1. This small system consists of one line, two loads (L_1 and L_2), three conventional generators (G_1, G_2, and G_3), and one wind power plant (WP). The capacity and reactance of the line are 100 MW and 0.13 pu, respectively. Loads L_1 and L_2 are assumed to be inelastic and equal to 80 and 90 MW, respectively. The demand that is involuntarily shed is valued at \$200/MWh. The stochastic power output of the wind farm is modeled by two plausible scenarios, which are referred to as *high* (50 MW) and *low* (10 MW), with probabilities of occurrence equal to 0.6 and 0.4.

Data for the conventional units are collated in Table G.1, where $\overline{P}$ is the unit capacity; C is the price offer for energy sale in the day-ahead market; C^+ and C^-

Table G.1: Unit data— Two-bus system

Unit	G_1	G_2	G_3
$\overline{P}$ (MW)	100	110	50
C (\$/MWh)	35	30	10
C^+ (\$/MWh)	40	–	–
C^- (\$/MWh)	34	–	–
R^+ (MW)	20	0	0
R^- (MW)	40	0	0

are, respectively, the price offers for energy sale and purchase in the balancing market; and R^+ and R^- are, in that order, the upper bounds of the energy sale and purchase offers in the balancing market. Note that, in comparative terms, unit G_1 is expensive, but flexible; unit G_2 is a little bit cheaper, but inflexible; and unit G_3 is very cheap, but inflexible. Therefore, G_1 is the only unit in the system that can be re-dispatched to provide balancing energy. Besides, observe that, for this unit, $C^+ > C$ and $C^- < C$, meaning that producer G_1 is willing to be flexible in return for a price premium on the energy traded during the balancing operation [12].

The marginal cost of the energy produced by the wind farm is considered to be zero. The expected wind power production is $50 \times 0.6 + 10 \times 0.4 = 34$ MW.

G.3.1.1 Dispatch Models

Firstly, we consider the conventional dispatch model (G.1), which writes for this particular example as follows:

$$\text{Min. } 35p_{G_1} + 30p_{G_2} + 10p_{G_3} \tag{G.6a}$$

$$\text{s.t. } p_{G_1} + p_{G_2} + p_W - 80 = -\frac{\delta_2^0}{0.13}\,, \tag{G.6b}$$

$$p_{G_3} - 90 = \frac{\delta_2^0}{0.13}\,, \tag{G.6c}$$

$$p_{G_1} \leq 100\,, \quad p_{G_2} \leq 110\,, \quad p_{G_3} \leq 50\,, \tag{G.6d}$$

$$-100 \leq \frac{\delta_2^0}{0.13} \leq 100\,, \tag{G.6e}$$

$$p_W \leq 34\,, \tag{G.6f}$$

$$p_{G_1}\,,\ p_{G_2}\,,\ p_{G_3}\,,\ p_W \geq 0\,, \tag{G.6g}$$

where bus 1 is considered as the reference node, i.e. $\delta_1^0 = 0$. Optimization problem (G.6) aims at minimizing the day-ahead production costs (G.6a). The dispatch problem is built upon a DC modeling of the transmission network, which leads to the set of nodal power balance equations (G.6b) and (G.6c), and includes generation and transmission capacity limits, (G.6d) and (G.6e), respectively. As it is customary, constraint (G.6f) limits the dispatch of the wind power plant to its expected production. Constraints (G.6g) enforce the nonnegative character of production quantities.

Observe that, according to the dispatch model (G.6), the day-ahead market is settled irrespective of the potential impact that the resulting day-ahead program $\{p^*_{G_1}, p^*_{G_2}, p^*_{G_3}, p^*_W\}$ may have on the subsequent balancing operation. The day-ahead market is thus cleared purely based on a least-cost merit-order principle. This way, the wind farm is first dispatched to 34 MW (its expected production), followed by generating units G_3 and G_2, in that order, which are dispatched to 50 and 86 MW, respectively, to cover the total system load of 170 MW. Unit G_1 (the flexible producer) is consequently left out of the day-ahead schedule. Afterwards, during the balancing operation of the power system, energy adjustments to the day-ahead schedule are required to cope with the uncertain wind power production. Specifically, if the power output of the wind farm turns out to be *high* (50 MW), the wind power producer seeks to sell the leftover $50 - 34 = 16$ MW in this market. However, the only flexible unit in the system, unit G_1, cannot purchase the extra wind, as it cannot decrease its production below zero. As a result, these 16 MW of free wind power have to be spilled. On the other hand, if the eventual wind generation is *low* (10 MW), there is a wind generation deficit of $34 - 10 = 24$ MW. This deficit has to be covered in the balancing market, but generating unit G_1 can only increase its production 20 MW at most. Consequently, the remaining $24 - 20 = 4$ MW are obtained from costly load curtailment.

We can alternatively compute the day-ahead generation schedule using the stochastic dispatch model (G.3), which writes as follows:

$$\text{Min. } 35p_{G_1} + 30p_{G_2} + 10p_{G_3} + 0.6\Big(40r^+_{G_1h} - 34r^-_{G_1h} + 200\left(l^{\text{shed}}_{1h} + l^{\text{shed}}_{2h}\right)\Big) + 0.4\Big(40r^+_{G_1l} - 34r^-_{G_1l} + 200\left(l^{\text{shed}}_{1l} + l^{\text{shed}}_{2l}\right)\Big) \tag{G.7a}$$

$$\text{s.t. (G.6b)} - \text{(G.6e)}\,, \text{(G.6g)}\,, \tag{G.7b}$$

$$p_W \leq 50\,, \tag{G.7c}$$

$$r^+_{G_1h} - r^-_{G_1h} + l^{\text{shed}}_{1h} + 50 - p_W - W^{\text{spill}}_h = \frac{(\delta^0_2 - \delta_{2h})}{0.13}\,, \tag{G.7d}$$

$$r^+_{G_1l} - r^-_{G_1l} + l^{\text{shed}}_{1l} + 10 - p_W - W^{\text{spill}}_l = \frac{(\delta^0_2 - \delta_{2l})}{0.13}\,, \tag{G.7e}$$

$$l_{2h}^{\text{shed}} = -\frac{(\delta_2^0 - \delta_{2h})}{0.13} \,, \tag{G.7f}$$

$$l_{2l}^{\text{shed}} = -\frac{(\delta_2^0 - \delta_{2l})}{0.13} \,, \tag{G.7g}$$

$$p_{G_1} + r_{G_1 h}^{+} \leq 100 \,, \;\; p_{G_1} + r_{G_1 l}^{+} \leq 100 \,, \tag{G.7h}$$

$$p_{G_1} - r_{G_1 h}^{-} \geq 0 \,, \;\; p_{G_1} - r_{G_1 l}^{-} \geq 0 \,, \tag{G.7i}$$

$$-100 \leq \frac{\delta_{2h}}{0.13} \leq 100 \,, \;\; -100 \leq \frac{\delta_{2l}}{0.13} \leq 100 \,, \tag{G.7j}$$

$$r_{G_1 h}^{+} \leq 20 \,, \;\; r_{G_1 l}^{+} \leq 20 \,, \tag{G.7k}$$

$$r_{G_1 h}^{-} \leq 40 \,, \;\; r_{G_1 l}^{-} \leq 40 \,, \tag{G.7l}$$

$$W_h^{\text{spill}} \leq 50 \,, \;\; W_l^{\text{spill}} \leq 10 \,, \tag{G.7m}$$

$$l_{1h}^{\text{shed}} \leq 80 \,, \;\; l_{1l}^{\text{shed}} \leq 80 \,, \;\; l_{2h}^{\text{shed}} \leq 90 \,, \;\; l_{2l}^{\text{shed}} \leq 90 \,, \tag{G.7n}$$

$$r_{G_1 h}^{+} \,, r_{G_1 l}^{+} \,, r_{G_1 h}^{-} \,, r_{G_1 l}^{-} \,, W_h^{\text{spill}}, W_l^{\text{spill}}, l_{1h}^{\text{shed}} \,, l_{1l}^{\text{shed}} \,, l_{2h}^{\text{shed}} \,, l_{2l}^{\text{shed}} \geq 0 \,, \tag{G.7o}$$

where subscripts "h" and "l" index the corresponding augmented variable with scenario "high" and "low", respectively. Note that the cleared amount of wind production in the day-ahead market, p_W, is limited to its capacity (50 MW) through constraint (G.7c).

Optimization problem (G.7) includes the scenario-based modeling of the balancing operation through the set of constraints (G.7d)–(G.7o). Balancing actions comprise the production increase/decrease of flexible unit G_1 ($r_{G_1}^{+}/r_{G_1}^{-}$), wind spillage (W^{spill}), and load shedding (l_1^{shed}, l_2^{shed}). The stochastic dispatch model seeks to minimize the overall expected system costs (G.7a), which consists of the day-ahead dispatch costs plus the expectation of the balancing operation costs. Constraints (G.7d)–(G.7g) enforce the power balances per node and scenario. Inequalities (G.7h)–(G.7j) impose generation and transmission capacity limits at the balancing stage. Constraints (G.7k) and (G.7l) limit the balancing energy provided by unit G_1 to its "flexible capacity", which is specified through R^{+} and R^{-} in Table G.1 for production increases and decreases, respectively. Inequalities (G.7m) and (G.7n) cap, in that order, the amount of wind power that is spilled and the amount of load that is shed to the actual wind power production and the actual load consumption. Finally, the set of constraints (G.7o) constitute positive variable declarations.

The essential feature of the stochastic dispatch model (G.7) is that the day-ahead generation schedule $\{p_{G_1}, p_{G_2}, p_{G_3}, p_W\}$ is determined considering its projected implications for the subsequent balancing operation of the power system. Following this rationale, only 10 MW of wind power production are cleared in the day-ahead market. Furthermore, the flexible, but expensive, generating unit G_1

is dispatched to 40 MW in order to exploit its capability of reducing its power output during the balancing operation. Thus, if scenario *high* materializes, the 40-MW wind production surplus can be sold to unit G_1 instead of being curtailed. Besides, since the share of unit G_1 in the day-ahead schedule is increased up to 40 MW, unit G_2 is only dispatched to 70 MW, even though this unit is \$5/MWh cheaper than unit G_1. Therefore, the least-cost merit-order principle that drives the conventional dispatch model is here violated.

We compute next the amount of wind power production that should clear the day-ahead market to maximize power system efficiency under the conventional dispatch model. For this purpose, we solve the following bilevel programming problem:

$$\text{Min. } 35p_{G_1} + 30p_{G_2} + 10p_{G_3} + 0.6\Big(40r^{+}_{G_1h} - 34r^{-}_{G_1h} + 200\left(l^{\text{shed}}_{1h} + l^{\text{shed}}_{2h}\right)\Big) + 0.4\Big(40r^{+}_{G_1l} - 34r^{-}_{G_1l} + 200\left(l^{\text{shed}}_{1l} + l^{\text{shed}}_{2l}\right)\Big) \tag{G.8a}$$

$$\text{s.t. } r^{+}_{G_1h} - r^{-}_{G_1h} + l^{\text{shed}}_{1h} + 50 - p_W - W^{\text{spill}}_{h} = \frac{(\delta^0_2 - \delta_{2h})}{0.13}\,, \tag{G.8b}$$

$$r^{+}_{G_1l} - r^{-}_{G_1l} + l^{\text{shed}}_{1l} + 10 - p_W - W^{\text{spill}}_{l} = \frac{(\delta^0_2 - \delta_{2l})}{0.13}\,, \tag{G.8c}$$

$$l^{\text{shed}}_{2h} = -\frac{(\delta^0_2 - \delta_{2h})}{0.13}\,, \tag{G.8d}$$

$$l^{\text{shed}}_{2l} = -\frac{(\delta^0_2 - \delta_{2l})}{0.13}\,, \tag{G.8e}$$

$$p_{G_1} + r^{+}_{G_1h} \le 100\,,\ \ p_{G_1} + r^{+}_{G_1l} \le 100\,, \tag{G.8f}$$

$$p_{G_1} - r^{-}_{G_1h} \ge 0\,,\ \ p_{G_1} - r^{-}_{G_1l} \ge 0\,, \tag{G.8g}$$

$$-100 \le \frac{\delta_{2h}}{0.13} \le 100\,,\ \ -100 \le \frac{\delta_{2l}}{0.13} \le 100\,, \tag{G.8h}$$

$$r^{+}_{G_1h} \le 20\,,\ \ r^{+}_{G_1l} \le 20\,, \tag{G.8i}$$

$$r^{-}_{G_1h} \le 40\,,\ \ r^{-}_{G_1l} \le 40\,, \tag{G.8j}$$

$$W^{\text{spill}}_{h} \le 50\,,\ \ W^{\text{spill}}_{l} \le 10\,, \tag{G.8k}$$

$$l^{\text{shed}}_{1h} \le 80\,,\ \ l^{\text{shed}}_{1l} \le 80\,,\ \ l^{\text{shed}}_{2h} \le 90\,,\ \ l^{\text{shed}}_{2l} \le 90\,, \tag{G.8l}$$

$$r^{+}_{G_1h}, r^{+}_{G_1l}, r^{-}_{G_1h}, r^{-}_{G_1l}, W^{\text{spill}}_{h}, W^{\text{spill}}_{l}, l^{\text{shed}}_{1h}, l^{\text{shed}}_{1l}, l^{\text{shed}}_{2h}, l^{\text{shed}}_{2l} \ge 0\,, \tag{G.8m}$$

$$0 \le p^{\max}_{W} \le 50\,, \tag{G.8n}$$

$$\left(p_{G_1}, p_{G_2}, p_{G_3}, p_W, \delta^0_2\right) \in \arg\Big\{ \underset{x_{G_1}, x_{G_2}, x_{G_3}, x_W, \theta}{\text{Minimize}} \ 35x_{G_1} + 30x_{G_2} + 10x_{G_3} \tag{G.8o}$$

$$\text{s.t. } x_{G_1} + x_{G_2} + x_W - 80 = -\frac{\theta}{0.13} : \lambda^{\text{D}}_1\,, \tag{G.8p}$$

$$x_{G_3} - 90 = \frac{\theta}{0.13} : \lambda_2^{\mathrm{D}} \,, \tag{G.8q}$$

$$x_{G_1} \leq 100 : \overline{\mu}_{G_1} \,, \quad x_{G_2} \leq 110 : \overline{\mu}_{G_2} \,, \quad x_{G_3} \leq 50 : \overline{\mu}_{G_3} \,, \tag{G.8r}$$

$$-100 \leq \frac{\theta}{0.13} \leq 100 : (\underline{\mu}_{\delta}, \overline{\mu}_{\delta}) \,, \tag{G.8s}$$

$$x_W \leq p_W^{\max} : \overline{\rho} \,, \tag{G.8t}$$

$$\left. x_{G_1} \,,\; x_{G_2} \,,\; x_{G_3} \,,\; x_W \geq 0 : (\underline{\mu}_{G_1}, \underline{\mu}_{G_2}, \underline{\mu}_{G_3}, \underline{\rho}) \right\} \,, \tag{G.8u}$$

where the dual variables of the lower-level problem (G.8o)–(G.8u) have been made explicit after the corresponding constraint, separated by a colon.

Notice that $p_W^{\max}$ is a decision variable of the upper-level problem that enters the lower-level problem as a constant. This variable is limited to the capacity of the wind farm through constraint (G.8n). The remaining equations are the same as those in the conventional and stochastic dispatch models (G.6) and (G.7).

For the bilevel programming problem (G.8) to be processed by optimization solvers, it has to be first transformed into an equivalent single-level optimization problem. To this end, we can replace the lower-level minimization problem (G.8o)–(G.8u) with its KKT conditions, which are as follows:

$$35 + \lambda_1^{\mathrm{D}} + \overline{\mu}_{G_1} - \underline{\mu}_{G_1} = 0 \,, \tag{G.9a}$$

$$30 + \lambda_1^{\mathrm{D}} + \overline{\mu}_{G_2} - \underline{\mu}_{G_2} = 0 \,, \tag{G.9b}$$

$$10 + \lambda_2^{\mathrm{D}} + \overline{\mu}_{G_3} - \underline{\mu}_{G_3} = 0 \,, \tag{G.9c}$$

$$\lambda_1^{\mathrm{D}} + \overline{\rho} - \underline{\rho} = 0 \,, \tag{G.9d}$$

$$\frac{\lambda_1^{\mathrm{D}} - \lambda_2^{\mathrm{D}} + \overline{\mu}_{\delta} - \underline{\mu}_{\delta}}{0.13} = 0 \,, \tag{G.9e}$$

$$\text{(G.6b)} - \text{(G.6e)} \,, \text{(G.6g)} \,, \tag{G.9f}$$

$$p_W \leq p_W^{\max} \,, \tag{G.9g}$$

$$\overline{\mu}_{G_1}(p_{G_1} - 100) = 0 \,,\; \overline{\mu}_{G_2}(p_{G_2} - 110) = 0 \,,\; \overline{\mu}_{G_3}(p_{G_3} - 50) = 0 \,, \tag{G.9h}$$

$$\underline{\mu}_{\delta}\left(\frac{\delta_2^0}{0.13} + 100\right) = 0 \,,\; \overline{\mu}_{\delta}\left(\frac{\delta_2^0}{0.13} - 100\right) = 0 \,, \tag{G.9i}$$

$$\overline{\rho}(p_W - p_W^{\max}) = 0 \,, \tag{G.9j}$$

$$\underline{\mu}_{G_1} p_{G_1} = 0 \,,\; \underline{\mu}_{G_2} p_{G_2} = 0 \,,\; \underline{\mu}_{G_3} p_{G_3} = 0 \,,\; \underline{\rho}\, p_W = 0 \tag{G.9k}$$

$$\underline{\mu}_{G_1} \,, \overline{\mu}_{G_1} \,, \underline{\mu}_{G_2} \,, \overline{\mu}_{G_2} \,, \underline{\mu}_{G_3} \,, \overline{\mu}_{G_3} \,, \underline{\rho} \,, \overline{\rho} \,, \underline{\mu}_{\delta} \,, \overline{\mu}_{\delta} \geq 0 \,. \tag{G.9l}$$

Besides, the complementarity conditions (G.9h)–(G.9k) can be recast using the mixed-integer linear formulation introduced by [15]. For example, consider a

Table G.2: Comparison of expected system operation costs ($)— Two-bus system

	Total	Day ahead	Balancing	Load curtailment
ConvD	3720	3080	320	320
StochD	3184	4000	−816	0
ImpD	3520	3200	320	0

large enough constant M. The complementarity condition (G.9j) can be equivalently formulated as

$$\begin{aligned} \overline{p} &\leq Mu\,, \\ p_W^{\max} - p_W &\leq \overline{W}(1-u)\,, \end{aligned}$$

where u is a binary variable, i.e. $u \in \{0,1\}$, and $\overline{W}$ is the capacity of the wind farm, equal to 50 MW. Notice that both quantities in the left-hand side of the inequalities above must be nonnegative as a result of (G.9g) and (G.9l).

After all these transformations, the bilevel program (G.8) leads to a single-level mixed-integer linear programming problem that can be readily processed by off-the-shelf optimization software and results in $p_W^{\max *} = 30$ MW. Consequently, under ImpD (the conventional settlement with a smart day-ahead dispatch of the wind farm), only 30 MW of wind power production are cleared in the day-ahead market, which avoids expensive load curtailment if scenario *low* eventually realizes. The conventional units are cleared following a least-cost merit order. In particular, generating units G1, G2, and G3 are dispatched to 0, 90, and 50 MW, respectively. As a consequence, 20 MW of wind power have to be spilled if scenario *high* realizes.

Table G.2 provides the breakdown of the expected system operation cost under each dispatch model. Logically, both StochD and ImpD outperform ConvD. Observe, moreover, that both StochD and ImpD result in a more costly day-ahead dispatch, which leads, however, to savings in the balancing operation stage without load shedding. In fact, the stochastic dispatch model is able to reduce costs at the balancing operation phase through a more efficient integration of the wind production. However, the energy-only market settlement associated with this dispatch model requires the flexible producer G_1 to accept economic losses if scenario *low* comes true, as we show in the following section.

Table G.3: Day-ahead and balancing energy prices (\$/MWh)–Two-bus system

	$\lambda^{\mathrm{D}}_n, \forall n \in N$	$\lambda^{\mathrm{B}}_{n\omega}, \forall n \in N$	
		High	Low
ConvD	30	0	200
StochD	30	25.67	36.50
ImpD	30	0	75

G.3.1.2 Prices and Revenues

Energy prices resulting from each of the dispatch models are shown in Table G.3. Note that these prices do not differ between buses, because no network congestion occurs in any of the two wind power scenarios considered. Observe that, for the three dispatch models, the resulting day-ahead electricity price is \$30/MWh, which is the marginal cost of unit G_2. In the case of ConvD, the value of lost load (\$200/MWh) determines the balancing energy price in scenario *low*, where load shedding actions need to be undertaken if the day-ahead generation schedule given by this dispatch model is implemented. In both ConvD and ImpD, the balancing electricity price is set to \$0/MWh in scenario *high* due to the occurrence of wind curtailment.

Given the energy prices in Table G.3 and the dispatch results previously discussed, we can determine the profit made by each market participant in expectation and per scenario according to each dispatch model (see Table G.4). For example, the payment to the flexible generator G_1 in scenario *low* under StochD is given by $40 \times 30 = \$1200$. Since its marginal cost is equal to \$35/MWh, the profit that generator G_1 makes in this scenario is equal to $1200 - 40 \times 35 = -\$200$. Here we bump into one of the most controversial features of StochD, namely, the likelihood that flexible units incur economic losses in some scenarios, even though the recovery of costs is guaranteed in expectation. Actually, notice that unit G_1 enters the day-ahead dispatch in a loss-making position, because its marginal cost, \$35/MWh, is higher than the resulting day-ahead market price, \$30/MWh. Therefore, under StochD, being flexible may involve higher risk than being inflexible, which may potentially discourage power producers from providing balancing service. In contrast, ConvD and the proposed ImpD ensure revenue adequacy in the day-ahead market and per scenario, and therefore they do not suffer from this problem.

Table G.4: Profit ($) of market participants–Two-bus system

	Agent	Expected	Per scenario	
			High	Low
ConvD	G_1	1320	0	3300
	G_2	0	0	0
	G_3	1000	1000	1000
	WP	−900	1020	−3780
	L_1	−2400	−2400	−2400
	L_2	−2380	−2700	−1900
StochD	G_1	24	173.33	−200
	G_2	0	0	0
	G_3	1000	1000	1000
	WP	916	1326.66	300
	L_1	−2400	−2400	−2400
	L_2	−2700	−2700	−2700
ImpD	G_1	320	0	800
	G_2	0	0	0
	G_3	1000	1000	1000
	WP	300	900	−600
	L_1	−2400	−2400	−2400
	L_2	−2700	−2700	−2700

Table G.5: Generator data (* = {+, −}). Powers in MW

Unit	Type	Bus #	$\overline{P}$	R^*
1	U76	1	152	40
2	U76	2	152	40
3	U100	7	300	70
4	U197	13	591	180
5	U12	15	60	60
6	U155	15	155	30
7	U155	16	155	30
8	U400	18	400	0
9	U400	21	400	0
10	U50	22	300	0
11	U155	23	310	60
12	U350	23	350	40

G.3.2 Case Study

We now consider a 24-bus power system that is based on the single-area version of the IEEE Reliability Test System [18]. It includes 34 lines, 17 loads, and 12 generating units. The nodal location, type, capacity, and flexibility parameters of these units are collated in Table G.5. Energy offers submitted by power producers in the day-ahead market consist of the four incremental cost/power blocks listed in Table 9 of [18], assuming the fuel costs used by [19]. We consider that nuclear and hydro power producers offer their production at zero price. Price premiums of 5% and 4% are assumed for the energy sold and purchased, respectively, in the balancing market. This means that flexible producers are willing to sell (purchase) energy in the balancing market at a price 5% higher (4% lower) than their energy offer price in the day-ahead market. Nuclear and hydro units are assumed to be inflexible and therefore, they do not provide balancing energy.

Two wind farms are located at nodes 5 and 7. The per-unit power production of these wind farms is modeled using Beta distributions, as in [20]. The shape parameters of these Beta distributions, denoted by (α, β), are equal to $(0.71, 0.08)$ and $(3.78, 1.62)$, respectively. Thus, the per-unit forecast power outputs of the wind farms at nodes 5 and 7 are 0.9 and 0.7, in that order. Furthermore, the power outputs of both wind farms are assumed to be correlated with a correlation coefficient ρ. Correlated samples from the previous Beta distributions are obtained using the sampling procedure described by [21]. An original scenario set comprising 10 000 wind power samples is first generated and then reduced to

100 using the fast forward selection algorithm presented by [22]. The marginal costs of the wind farms are assumed to be zero.

Loads are considered to be inelastic with a value of lost load equal to \$1000/MWh. These loads are geographically distributed among buses as indicated in Table 5 of [18]. The total system demand is 2000 MW. The capacities of lines 1–5, 5–10, and 7–8 are doubled (up to 350 MW) so that higher amounts of wind power production can be injected at buses 5 and 7.

The single-level mixed-integer linear programming problem that results from the bilevel program (G.4) has been solved using CPLEX 12.3.0 under GAMS on a Windows-based personal computer Intel(R) Core(TM) i5 with four processors clocking at 2.4 GHz and 6 GB of RAM. Solution time is kept below 30 seconds in all instances.

The stochastic dispatch model (G.3) has, among others, two properties that make it particularly useful to facilitate the large-scale integration of stochastic production in electricity markets, namely, its ability to avoid the uneconomic scheduling of stochastic production capacity and its ability to efficiently accommodate generation from stochastic producers that are spatially correlated. We show below that these two properties are conferred, to a large extent, on the conventional dispatch model (G.1), if solved for an appropriate value of stochastic production, generally different from the mean. This is actually what we refer to as ImpD.

Figure G.2 shows the expected cost of the power system operation as a function of the wind power penetration level, for the three dispatch models. The wind power penetration level is defined as the ratio of the forecast wind power production to the total system demand and is increased by augmenting the capacity installed at both wind farms by the same amount. The figure is arranged in two illustrations, each corresponding to a different correlation coefficient between wind farms. Observe that from a certain penetration level, the expected cost resulting from the implementation of the conventional dispatch begins to significantly diverge from the expected cost yielded by the other two dispatch models. Furthermore, note that this "breaking point", roughly identified on the graphs using a vertical dashed line, occurs for lower penetration levels if the correlation coefficient between wind sites increases. Indeed, the breaking point moves approximately from 38% to 33% if the correlation coefficient goes from 0.35 to 0.75. In contrast, StochD and ImpD are significantly less affected by correlated winds, as they both account for the wind production variability to decide the wind generation schedule. Furthermore, notice that, in the case of ConvD, the expected cost exhibits an increasing trend after a high enough wind power penetration level, whereas both StochD and ImpD guarantee that an increase in wind power capacity never leads to an increase in the expected cost.

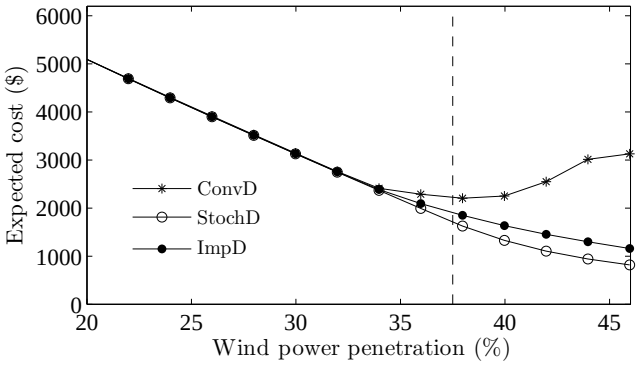

(a) $\rho = 0.35$

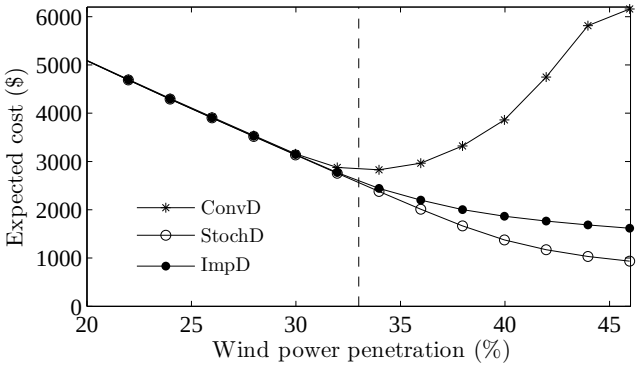

(b) $\rho = 0.75$

Figure G.2: Impact of the wind power penetration level and spatial correlation on the expected cost of the system operation. Total system demand = 2000 MW.

Table G.6: Highlights of profits. Wind penetration 38% ($\rho = 0.35$)

		Unit			
		1	6	11	12
ConvD	Expected profit ($)	379.8	359.7	724.9	389.1
StochD	Expected profit ($)	45.6	48.4	99.7	64.9
	Average losses ($)	−17.4	−10.9	−17.6	−11.5
	Probability profit < 0	0.81	0.71	0.71	0.75
ImpD	Expected profit ($)	170.2	263.7	531.6	178.7

We now show that, unlike ConvD or ImpD, the stochastic dispatch leads to a conflicting energy-only settlement of the market, because it requires flexible producers to incur losses in some scenarios. Let us consider a wind power penetration level of 38%. In this instance, generators 1, 2, 6, 7, 11 and 12 are mostly the units providing balancing energy. Table G.6 includes the expected profit made by some of these units in these conditions under the three dispatch models. For the case of StochD, the average losses incurred by the selected units and the probability of their profit being eventually negative are also shown. Note that this probability is remarkably high.

Lastly, observe that the expected profit made by the selected units is significantly higher under ConvD than under ImpD. This is so because, under the conventional dispatch where the expected wind power production is cleared, there is a considerable transfer of money from the wind power producers to the flexible producers, as the wind power producers have to bear the cost of a very inefficient balancing operation. ImpD manages to substantially mitigate this effect by clearing an amount of wind power production—not necessarily equal to the mean—that avoids high balancing costs.

G.4 Conclusions

This paper deals with the clearing of a day-ahead electricity market that includes a significant number of stochastic producers. Our study uses two reference models for generation scheduling: on the one hand, a conventional network-constrained auction based on a least-cost merit order for dispatch, where stochastic generation enters with its expected production and a very low marginal cost; on the other, a full stochastic dispatch method that maximizes market efficiency by anticipating balancing costs. The conventional dispatch may turn out to be very uneconomical, while the stochastic one leads to an energy-only market settlement that does not guarantee cost recovery for flexible producers is some scenarios.

We show that the conventional auction, if cleared with an appropriate value of stochastic production, generally different from the mean, can significantly approach the stochastic dispatch ideal. We construct a bilevel program that optimally computes this value. Our analysis prompts two fundamental conclusions, namely:

1. Current day-ahead markets should not clear the expected stochastic production by default. There is indeed room for substantial improvement in market efficiency by abandoning this practice, in particular in those markets with a high share of stochastic generation.

2. The amount of stochastic production to be cleared in the day-ahead market should be driven not only by the marginal cost of stochastic generation, which is usually very low or zero, but also by the cost of its uncertainty, understood as its economic impact due to system balancing.

As future research, it is necessary to develop computationally efficient methods that allow us to determine a day-ahead schedule for stochastic producers better in terms of market efficiency than their expected power outputs without having to directly solve a computationally costly bilevel program. Likewise, the idea introduced in this paper is compatible with the implementation of reserve capacity markets or the flexible ramping products that are currently under development in CAISO [23] and Midwest ISO [24]. The combination of these strategies may bring current market efficiency closer to the full stochastic optimization ideal.

References G

[1] H. Holttinen, "Impact of hourly wind power variations on the system operation in the Nordic countries," *Wind Energy*, vol. 8, no. 2, pp. 197–218, 2005.

[2] R. Doherty and M. O'Malley, "A new approach to quantify reserve demand in systems with significant installed wind capacity," *IEEE Transactions on Power Systems*, vol. 20, no. 2, pp. 587–595, 2005.

[3] U. Helman, C. Loutan, G. Rosenblum, M. Rothleder, J. Xie, H. Zhou, and M. Kuo, "Integration of renewable resources: Operational requirements and generation fleet capability at 20% rps," tech. rep., California Independent System Operator (CAISO), 2010. `http://www.caiso.com/2804/2804d036401f0.pdf`.

[4] E. Ela, M. Milligan, and B. Kirby, "Operating reserves and variable generation," Tech. Rep. NREL/TP-5500-51978, National Renewable Energy Laboratory, 2011. `http://www2.econ.iastate.edu/tesfatsi/OperatingReservesVariableGenerationSurvey.NRELAug2011.pdf`.

[5] J. R. Birge and F. Louveaux, *Introduction to Stochastic Programming*. Series in Operations Research and Financial Engineering, Springer, 2 ed., 2011.

[6] F. D. Galiana, F. Bouffard, J. M. Arroyo, and J. F. Restrepo, "Scheduling and pricing of coupled energy and primary, secondary, and tertiary reserves," *Proceedings of the IEEE*, vol. 93, no. 11, pp. 1970–1983, 2005.

[7] F. Bouffard and F. D. Galiana, "Stochastic security for operations planning with significant wind power generation," *IEEE Transactions on Power Systems*, vol. 23, no. 2, pp. 306–316, 2008.

[8] J. M. Morales, A. Conejo, and J. Pérez-Ruiz, "Economic valuation of reserves in power systems with high penetration of wind power," *IEEE Transactions on Power Systems*, vol. 24, no. 2, pp. 900–910, 2009.

[9] A. Papavasiliou, S. Oren, and R. O'Neill, "Reserve requirements for wind power integration: A scenario-based stochastic programming framework," *IEEE Transactions on Power Systems*, vol. 26, no. 4, pp. 2197–2206, 2011.

[10] S. Wong and J. D. Fuller, "Pricing energy and reserves using stochastic optimization in an alternative electricity market," *IEEE Transactions on Power Systems*, vol. 22, pp. 631–638, May 2007.

[11] W. W. Hogan, "On an energy only electricity market design for resource adequacy," tech. rep., Center for Business and Government, Harvard University, 2005. `http://www.ferc.gov/EventCalendar/files/20060207132019-hogan_energy_only_092305.pdf`.

[12] G. Pritchard, G. Zakeri, and A. Philpott, "A single-settlement, energy-only electric power market for unpredictable and intermittent participants," *Operations Research*, vol. 58, pp. 1210–1219, Jul./Aug. 2010.

[13] J. M. Morales, A. Conejo, K. Liu, and J. Zhong, "Pricing electricity in pools with wind producers," *IEEE Transactions on Power Systems*, vol. 27, no. 3, pp. 1366–1376, 2012.

[14] A. Motto, F. Galiana, A. Conejo, and J. Arroyo, "Network-constrained multiperiod auction for a pool-based electricity market," *IEEE Transactions on Power Systems*, vol. 17, no. 3, pp. 646–653, 2002.

[15] J. Fortuny-Amat and B. McCarl, "A representation and economic interpretation of a two-level programming problem," *Journal of the Operational Research Society*, pp. 783–792, 1981.

[16] R. Fernández-Blanco, J. Arroyo, and N. Alguacil, "A unified bilevel programming framework for price-based market clearing under marginal pricing," *IEEE Transactions on Power Systems*, vol. 27, no. 1, pp. 517–525, 2012.

[17] M. Bjørndal and K. Jörnsten, "Equilibrium prices supported by dual price functions in markets with non-convexities," *European Journal of Operational Research*, vol. 190, no. 3, pp. 768–789, 2008.

[18] C. Grigg, P. Wong, P. Albrecht, R. Allan, M. Bhavaraju, R. Billinton, Q. Chen, C. Fong, S. Haddad, S. Kuruganty, *et al.*, "The IEEE reliability test system-1996," *IEEE Transactions on Power Systems*, vol. 14, no. 3, pp. 1010–1020, 1999.

[19] F. Bouffard, F. D. Galiana, and A. J. Conejo, "Market-clearing with stochastic security–Part II: case studies," *IEEE Transactions on Power Systems*, vol. 20, no. 4, pp. 1827–1835, 2005.

[20] A. Fabbri, T. Gomez San Roman, J. Rivier Abbad, and V. Mendez Quezada, "Assessment of the cost associated with wind generation prediction errors in a liberalized electricity market," *IEEE Transactions on Power Systems*, vol. 20, no. 3, pp. 1440–1446, 2005.

[21] J. M. Morales, A. Conejo, and J. Pérez-Ruiz, "Simulating the impact of wind production on locational marginal prices," *IEEE Transactions on Power Systems*, vol. 26, no. 2, pp. 820–828, 2011.

[22] H. Heitsch and W. Römisch, "Scenario reduction algorithms in stochastic programming," *Computational Optimization and Applications*, vol. 24, pp. 187–206, Feb.-Mar. 2003.

[23] K. Abdul-Rahman, H. Alarian, M. Rothleder, P. Ristanovic, B. Vesovic, and B. Lu, "Enhanced system reliability using flexible ramp constraint in CAISO market," in *Power and Energy Society General Meeting, 2012 IEEE*, pp. 1–6, 2012.

[24] N. Navid and G. Rosenwald, "Market solutions for managing ramp flexibility with high penetration of renewable resource," *IEEE Transactions on Sustainable Energy*, vol. 3, no. 4, pp. 784–790, 2012.

Paper H

A Robust Optimization Approach to Energy and Reserve Dispatch in Electricity Markets

Authors:
Marco Zugno, Antonio J. Conejo

Published as:
Technical Report–2013–05.

A Robust Optimization Approach to Energy and Reserve Dispatch in Electricity Markets

Marco Zugno[1], Antonio J. Conejo[2]

Abstract

To a large extent, electricity markets worldwide still rely on deterministic procedures for clearing energy and reserve auctions. However, larger and larger shares of the production mix consist of renewable sources whose nature is stochastic and non-dispatchable, as their output is not known with certainty and cannot be controlled by the operators of the production units. Stochastic programming models for the joint determination of the day-ahead energy and reserve dispatch, necessary for coping with the real-time output deviations from these sources, have been proposed in the literature. In this work, we take an alternative approach and cast the problem as an adaptive robust optimization problem. The day-ahead and reserve schedules determined in this fashion yield the minimum system cost, accounting for the cost of the redispatching decisions at the balancing stage, in the worst-case realization of the stochastic production within a specified uncertainty set. In a case-study based on a 24-node system, we assess the degree of suboptimality of the robust solution with respect to the optimal dispatch obtained with a stochastic programming approach, and compare their worst-case cost. Furthermore, we discuss the robustness of these two alternative approaches with respect to changes in the distribution of the uncertainty, as well as their computational properties.

[1]DTU Compute, Technical University of Denmark, Matematiktorvet, bld. 322, DK-2800 Kgs. Lyngby, Denmark

[2]Department of Electrical Engineering, University of Castilla–La Mancha, Campus Universitario, Ciudad Real, 13071 Spain

Nomenclature

Decision Variables

$\mathbf{x}$ Vector of decision variables at the dispatching stage, including energy dispatch, upward and downward reserve, and network state variables at the nodes of the system;

$\mathbf{\Delta w}$ Forecast error for stochastic power production;

$\mathbf{y}$ Vector of decision variables at the balancing stage, including energy redispatch, load shedding, stochastic power spillage and actual state variables at the nodes of the system.

Parameters

$\mathbf{c_x}$ Coefficients in the cost function associated with the day-ahead dispatching (energy and reserve);

$\mathbf{c_y}$ Coefficients in the cost function associated with the redispatching at the balancing stage;

$\mathbf{d}$ Demand at each node of the system (considered known with certainty);

$\widehat{\mathbf{w}}$ Conditional expectation of stochastic power production.

H.1 Introduction

In recent years, renewable electricity production sources have experienced an unprecedented growth in installed capacity worldwide. Such a development is explained both by technological advance, which has made production from sources like wind and solar cheaper, and by governmental support aimed at promoting sustainability. Sources of this type are fundamentally different from conventional means of electricity generation. Indeed, they are stochastic, i.e., their production is not known with certainty in advance, and non-dispatchable, i.e., the power plant operators have partial or no control on the output level.

Owing to the features described above, an increasing penetration of renewables challenges the traditional way electricity markets are operated. In particular, deterministic schemes have been employed for years to assess the amount of

reserve capacity, the availability of which is needed in order to cope with unforeseen events in the system. Typically, mechanisms for reserve determination are based on deterministic $N-1$ or $N-k$ criteria, which guarantee the functioning of the system in the event of loss of the largest unit, or of the k largest units in the system, respectively. As the penetration of stochastic generation sources in power system grows, reserves are increasingly used to cover the fluctuations of the power output from renewables, thus calling for stochastic decision-making tools.

In parallel, market-clearing procedures for energy markets are also challenged by the growth of stochastic production capacity. For example, the day-ahead market is cleared according to a deterministic least-cost dispatch principle based on the offers and bids submitted by suppliers and consumers. Stochastic production is normally dispatched at a point forecast of its output distribution. However, this procedure does not account for the projected cost of the dispatch at the balancing stage, and is therefore suboptimal, see [1].

The existing literature on the subject shows that system cost can be significantly reduced in expectation by jointly optimizing the day-ahead dispatch and the reserve in a stochastic programming framework, see [2]. However, models of this type require that the market operator has an accurate probabilistic description of the joint distribution of uncertain production at different locations in the grid, which is far from trivial. Furthermore, such models may require unreasonable solution time as the discrete number of scenarios used to approximate the distribution of the uncertainty increases.

An alternative framework to stochastic programming for dealing with problems under uncertainty is robust optimization. In this framework, stochastic variables are assumed to take values within an uncertainty set. Then, a robust decision is determined as the solution to an optimization problem that must be feasible for any realization of the uncertainty, and optimal in the worst-case choice of the stochastic parameters in the aforementioned set. The modeling effort is reduced in robust optimization to a description of a meaningful set over which the uncertain parameters may take values in, i.e., the support of the density function rather than the full probability distribution required by the stochastic programming approach.

The equivalent of stochastic programming with recourse in robust optimization is adaptive robust optimization. This framework aims at minimizing the total cost in the worst-case realization of the uncertainty, assuming that recourse actions can be taken as a response to the realization of the uncertainty. For an introduction to robust optimization, and to its adaptive version, we refer the interested reader to [3].

Recent applications of adaptive robust optimization focusing on electricity markets are presented in [4], [5] and [6], which study the unit commitment problem under uncertain load or production from stochastic sources. In all these works, a cutting-plane approach is employed to exploit the convex dependence of the objective function on the first-stage decision, see [7]. Then, the resulting *max-min* problem resulting from the sequential enforcement of the worst-case (maximum-cost) parameter realization and decision on the optimal recourse action is cast as a single-level bilinear program. This problem is then solved either with an outer-approximation technique [4], or as a Mixed Integer Linear Program (MILP) after linearization through binary expansion [5, 6].

The main features of the model presented in this paper are threefold:

1. We apply adaptive robust optimization to the problem of determining the optimal day-ahead energy and reserve dispatch in a single time-period, rather than to unit commitment. The problem we consider is particularly interesting as it resembles the current design of electricity markets in Europe, where decisions on unit commitment are left to the power producers, and the market operator determines sequentially the amount of reserves needed and the optimal day-ahead energy dispatch. Note that the extension of the proposed model to a multi-period setting does not entail any conceptual complication. We propose the joint determination of day-ahead dispatch and reserve akin to the one in [2], though in a robust optimization framework.

2. We propose a reformulation of the inner *max-min* problem for the determination of the uncertainty and recourse decision that can accommodate general polyhedral sets for the uncertainty and converges to an exact solution. Our approach is more flexible than the binary reformulation in [5] and [6] in that it allows to model any polyhedral uncertainty set, still using a comparable number of binary variables. In comparison to the approach in [4], which is more flexible with respect to the choice of the uncertainty set, our reformulation guarantees convergence to an exact solution.

3. We compare the results obtained from the robust optimization approach with the ones from the corresponding stochastic programming version of the model.

The structure of the paper is the following. In Section H.2, we introduce the formulation of the problem. Algorithms for solving this problem are then described in Section H.3. Then, Section H.4 presents results from a simple illustrative example and from a larger case study based on the 24-node IEEE Reliability Test-System in [8]. Finally, conclusions are presented in Section H.5.

H.2 Problem Formulation

When an electric energy system includes stochastic production sources, the joint determination of the optimal day-ahead energy and reserve dispatch can be formulated as the following problem of optimization under uncertainty:

$$\min_{\mathbf{x}} \quad \mathbf{c_x}^T\mathbf{x} + \mathcal{Q}_{\mathcal{W}}(\mathbf{x}) \tag{H.1a}$$

$$\text{s.t.} \quad \mathbf{F}\mathbf{x} = \mathbf{d} - \widehat{\mathbf{w}} \,, \tag{H.1b}$$

$$\mathbf{G}\mathbf{x} \geq \mathbf{g} \,. \tag{H.1c}$$

The vector $\mathbf{x}$ of decision variables includes energy dispatch, upward and downward reserve as well as state variables at each node of the transmission network.

For the sake of clarity, we split the set of constraints into two groups. Group (H.1b) only includes equalities, which represent the balancing conditions. Such constraints guarantee that for each node of the transmission network, the day-ahead energy dispatch for production and the net power inflow, which are either a subset or linearly dependent on a subset of the variables $\mathbf{x}$, are equal to the net demand, i.e., consumption, $\mathbf{d}$, minus the forecast stochastic power production, $\widehat{\mathbf{w}}$. The second set of constraints (H.1c) includes upper and lower bounds to the energy and reserve dispatch, to the scheduled power flows, as well as declarations of nonnegative variables.

The objective function (H.1a) is equal to the sum of the cost associated with the day-ahead decision $\mathbf{c_x}^T\mathbf{x}$ and a measure of the stochastic optimal recourse cost, $\mathcal{Q}_{\mathcal{W}}(\mathbf{x})$. Such a measure is a function of the first-stage decision only, and is parameterized on the distribution $\mathcal{W}$ of the uncertainty, in this case stochastic power generation. In stochastic programming, typical choices of $\mathcal{Q}_{\mathcal{W}}(\mathbf{x})$ are the expectation or the conditional value at risk (or a combination of these) over a discrete set of scenarios approximating the actual distribution of the uncertainty. In a robust optimization framework, instead, we seek to minimize the recourse cost in the worst-case realization of the stochastic parameters within an uncertainty set. The determination of the worst-case recourse cost, or redispatch cost, writes as the following *max-min* programming problem, parameterized on the first-stage decision $\mathbf{x}$:

$$\mathcal{Q}_{\mathcal{W}}(\mathbf{x}) = \max_{\boldsymbol{\Delta}\mathbf{w}} \min_{\mathbf{y}} \mathbf{c_y}^T\mathbf{y} \tag{H.2a}$$

$$\text{s.t.} \ \mathbf{P}\mathbf{y} = -\boldsymbol{\Delta}\mathbf{w} - \mathbf{Q}\mathbf{x} \,, \qquad : \boldsymbol{\lambda} \,, \tag{H.2b}$$

$$\mathbf{L}\mathbf{y} \geq \mathbf{l} - \mathbf{M}\mathbf{x} - \mathbf{N}\boldsymbol{\Delta}\mathbf{w} \,, \qquad : \boldsymbol{\mu} \,, \tag{H.2c}$$

$$\text{s.t.} \ \mathbf{H}\boldsymbol{\Delta}\mathbf{w} \leq \mathbf{h} \,. \tag{H.2d}$$

Model (H.2) has a *max-min* structure that allows the determination of the minimum recourse cost in the worst-case realization of the uncertainty. Indeed, the maximization problem chooses the worst-case realization of the stochastic deviation $\mathbf{\Delta w}$ of stochastic power production from the conditional mean forecast within the polyhedral uncertainty set defined by the set (H.2d) of linear inequalities. After the worst-case realization of the uncertainty is chosen, the recourse cost is minimized in the *min* problem in (H.2a). The vector $\mathbf{y}$ of optimization variables of this problem consists of the energy redispatch for each producer, load shedding, spillage of stochastic production and the network state variable at each node in the balancing stage. The set of equations (H.2b) ensure that redispatch plus additional net flow equals the error of stochastic power prediction at each node. Notice that (H.2b) depends on the first-stage network state variables included in the day-ahead decision vector $\mathbf{x}$. Furthermore, the problem is constrained by the set (H.2c) of linear inequalities, which include upper and lower bounds on energy redispatch, load shedding, stochastic power spillage, actual power flows and declarations of nonnegative variables. Notice that reserve, which is included in the day-ahead decision vector $\mathbf{x}$, limits the provision of backup power at the recourse stage. Furthermore, stochastic power spillage is limited above by the actual stochastic power production $\widehat{\mathbf{w}} + \mathbf{\Delta w}$.

H.2.1 Reformulation as a Min-Max Bilinear Problem

The formulation in the above section cannot be immediately employed in practice. Indeed, the direct substitution of $\mathcal{Q}_{\mathcal{W}}(\mathbf{x})$ as defined in (H.2) results in a *min-max-min* problem, for which a general-purpose solution algorithm is not available. However, following the derivations in [4], [5] and [6], it is possible to reformulate it as a *min-max* problem by substituting the right-hand side *max* problem with its dual. This results in the following formulation:

$$\min_{\mathbf{x}} \ \mathbf{c_x}^T\mathbf{x} + \max_{\mathbf{\Delta w}} \max_{\boldsymbol{\lambda},\boldsymbol{\mu}} \ (-\mathbf{\Delta w} - \mathbf{Q}\mathbf{x})^T\boldsymbol{\lambda} + (\mathbf{l} - \mathbf{M}\mathbf{x} - \mathbf{N}\mathbf{\Delta w})^T\boldsymbol{\mu} \tag{H.3a}$$

$$\text{s.t. } \mathbf{P}^T\boldsymbol{\lambda} + \mathbf{L}^T\boldsymbol{\mu} = \mathbf{c_y} \ , \tag{H.3b}$$

$$\boldsymbol{\mu} \geq 0 \ , \tag{H.3c}$$

$$\text{s.t. } \mathbf{H}\mathbf{\Delta w} \leq \mathbf{h} \ , \tag{H.3d}$$

$$\text{s.t. } \mathbf{F}\mathbf{x} = \mathbf{d} - \widehat{\mathbf{w}} \ , \tag{H.3e}$$

$$\mathbf{G}\mathbf{x} \geq \mathbf{g} \ . \tag{H.3f}$$

It should be noticed that model (H.3) is in fact a *min-max* programming problem. Indeed, the mid- and right-hand-side maximization problems can be merged into a single maximization problem in the optimization variables $\mathbf{\Delta w}$, $\boldsymbol{\lambda}$ and $\boldsymbol{\mu}$. Furthermore, we remark that the optimization problem resulting from

this merging is a bilinear one, as it involves cross-products between $\boldsymbol{\Delta}\mathbf{w}$ and the lower-level decision variables $\boldsymbol{\lambda}$ and $\boldsymbol{\mu}$ in the objective function (H.3a).

We conclude the section with the following two observations, which will turn out useful in Section H.3.

1. The problem resulting from the merging of the mid and the right-hand-side maximization problems (H.3a)–(H.3c) is bilinear and defined over a polyhedral set. As a consequence, its optimal solution is one of the vertices of this set.
2. Since the vector $\mathbf{x}$ of day-ahead decision variables only appears in the objective function and not in the constraints, the feasible polyhedron is independent of the day-ahead decision, and hence it has a finite number of vertices.

H.2.2 Reformulation as a Linear Min-Max Problem with Equilibrium Constraints

Let us consider again formulation (H.3). We notice that it is possible to swap the order of the mid and right-hand-side maximization problems, thus first optimizing over the variables $\boldsymbol{\lambda}, \boldsymbol{\mu}$, and then over $\boldsymbol{\Delta}\mathbf{w}$. Furthermore, not all the terms of the objective function depend on $\boldsymbol{\Delta}\mathbf{w}$, and the constraints are separable for the two sets of variables. As a result, we can reformulate (H.3) as follows:

$$\min_{\mathbf{x}} \mathbf{c_x}^T\mathbf{x} + \max_{\boldsymbol{\lambda},\boldsymbol{\mu}} \; -(\mathbf{Q}\mathbf{x})^T\boldsymbol{\lambda} + (\mathbf{l}-\mathbf{M}\mathbf{x})^T\boldsymbol{\mu} + \max_{\boldsymbol{\Delta}\mathbf{w}} \; -\left(\boldsymbol{\lambda}^T + \boldsymbol{\mu}^T\mathbf{N}\right)\boldsymbol{\Delta}\mathbf{w} \quad \text{(H.4a)}$$

$$\text{s.t. } \mathbf{H}\boldsymbol{\Delta}\mathbf{w} \le \mathbf{h}\,, \qquad \boldsymbol{\xi}\,, \quad \text{(H.4b)}$$

$$\text{s.t. } \mathbf{P}^T\boldsymbol{\lambda} + \mathbf{L}^T\boldsymbol{\mu} = \mathbf{c_y}\,, \quad \text{(H.4c)}$$

$$\boldsymbol{\mu} \ge 0\,, \quad \text{(H.4d)}$$

$$\text{s.t. } \mathbf{F}\mathbf{x} = \mathbf{d} - \widehat{\mathbf{w}}\,, \quad \text{(H.4e)}$$

$$\mathbf{G}\mathbf{x} \ge \mathbf{g}\,, \quad \text{(H.4f)}$$

where we indicate with $\boldsymbol{\xi}$ the set of dual variables relative to constraints (H.4b) for the right-hand-side maximization problem.

The *max-max* programming problem comprising the mid and the right-hand-side optimization problems in (H.4) can be cast as a Mathematical Program with Equilibrium Constraints (MPEC), see [GCF+12]. However, before doing

so, we point out that since the right-hand-side maximization problem is linear, the strong duality theorem holds. Therefore, the following relationship holds at optimality:

$$-\left(\boldsymbol{\lambda}^T + \boldsymbol{\mu}^T\mathbf{N}\right)\boldsymbol{\Delta}\mathbf{w} = \mathbf{h}^T\boldsymbol{\xi}\,. \tag{H.5}$$

Differently from the term on the left-hand side of (H.5), the one on the right-hand side is linear, as it does not involve cross-products between optimization variables. Therefore, considering (H.4) and (H.5) renders the problem below whose objective function is linear in the optimization variables:

$$\min_{\mathbf{x}}\ \mathbf{c_x}^T\mathbf{x} + \max_{\boldsymbol{\lambda},\boldsymbol{\mu},\boldsymbol{\Delta}\mathbf{w},\boldsymbol{\xi}} -(\mathbf{Q}\mathbf{x})^T\boldsymbol{\lambda} + (\mathbf{l}-\mathbf{M}\mathbf{x})^T\boldsymbol{\mu} + \mathbf{h}^T\boldsymbol{\xi} \tag{H.6a}$$

$$\text{s.t. } \mathbf{0} \le \boldsymbol{\xi} \perp \mathbf{h} - \mathbf{H}\boldsymbol{\Delta}\mathbf{w} \ge \mathbf{0}\,, \tag{H.6b}$$

$$\mathbf{H}^T\boldsymbol{\xi} = -\boldsymbol{\lambda} - \mathbf{N}^T\boldsymbol{\mu}\,, \tag{H.6c}$$

$$\mathbf{P}^T\boldsymbol{\lambda} + \mathbf{L}^T\boldsymbol{\mu} = \mathbf{c_y}\,, \tag{H.6d}$$

$$\boldsymbol{\mu} \ge \mathbf{0}\,, \tag{H.6e}$$

$$\text{s.t. } \mathbf{F}\mathbf{x} = \mathbf{d} - \widehat{\mathbf{w}}\,, \tag{H.6f}$$

$$\mathbf{G}\mathbf{x} \ge \mathbf{g}\,. \tag{H.6g}$$

Notice that formulations (H.1)–(H.2), (H.3) and (H.6) are equivalent.

H.3 Solution Algorithm

In this section, we present two iterative schemes to solve the *min-max-min* problem (H.1)–(H.2), both of which are based on the cutting-plane algorithm in [9] within a Benders' decomposition scheme [10].

H.3.1 Benders-Dual Cutting-Plane Algorithm

Let us consider reformulation (H.3). Because of the observations in the last paragraph of Section H.2.1, the solution to the inner level bilinear maximization problem belongs to a set of finite cardinality K, which does not depend on the first-stage decisions. Indicating the elements of this set as $(\boldsymbol{\Delta}\mathbf{w}_k, \boldsymbol{\lambda}_k, \boldsymbol{\mu}_k)$, with $k = 1, \ldots, K$, we can alternatively reformulate problem (H.1)–(H.2) as follows:

$$\min_{\mathbf{x},\beta}\ \mathbf{c_x}^T\mathbf{x} + \beta \tag{H.7a}$$

$$\text{s.t. } \beta \ge -\boldsymbol{\Delta}\mathbf{w}_k^T\boldsymbol{\lambda}_k + \left(\mathbf{l} - \mathbf{N}\boldsymbol{\Delta}\mathbf{w}_k\right)^T\boldsymbol{\mu}_k - \left(\boldsymbol{\lambda}_k\mathbf{Q} + \boldsymbol{\mu}_k\mathbf{M}\right)\mathbf{x}\,, \quad \forall k\,, \tag{H.7b}$$

$$\mathbf{F}\mathbf{x} = \mathbf{d} - \widehat{\mathbf{w}}\,, \tag{H.7c}$$

$$\mathbf{G}\mathbf{x} \ge \mathbf{g}\,. \tag{H.7d}$$

As one can see, the term β in the objective function is bounded from below by the pointwise maximum of a finite set of linear functions in the first-stage decision variables $\mathbf{x}$. This implies that the optimal objective function value of (H.7) is a convex, piecewise linear function in $\mathbf{x}$. The following cutting-plane algorithm, proposed for robust optimization problems with recourse by [7], is guaranteed to converge to the optimal solution in a finite number of steps.

1. Set upper and lower bounds $\mathrm{UB} = +\infty$ and $\mathrm{LB} = -\infty$, and initialize the iteration index $i \leftarrow 1$.

2. Define the relaxed master problem (MP) as the minimization of (H.7a), subject to (H.7c) and (H.7d), and fix a reasonable lower bound for β, i.e., lower than the expected objective value of the inner problem. Fix a feasible solution $(\mathbf{x}_1^*, \beta_1^*)$ to the relaxed MP.

3. Solve either the following subproblem

$$\mathrm{SP}_1 : \max_{\boldsymbol{\Delta w}, \boldsymbol{\lambda}, \boldsymbol{\mu}} \quad \left(-\boldsymbol{\Delta w} - \mathbf{Q}\mathbf{x}_i^*\right)^T \boldsymbol{\lambda} + \left(\mathbf{l} - \mathbf{M}\mathbf{x}_i^* - \mathbf{N}\boldsymbol{\Delta w}\right)^T \boldsymbol{\mu} \tag{H.8a}$$

$$\text{s.t.} \quad \mathbf{P}^T\boldsymbol{\lambda} + \mathbf{L}^T\boldsymbol{\mu} = \mathbf{c_y} \,, \tag{H.8b}$$

$$\boldsymbol{\mu} \geq 0 \,, \tag{H.8c}$$

$$\mathbf{H}\boldsymbol{\Delta w} \leq \mathbf{h} \,, \tag{H.8d}$$

or

$$\mathrm{SP}_2 : \max_{\boldsymbol{\lambda}, \boldsymbol{\mu}, \boldsymbol{\Delta w}, \boldsymbol{\xi}} \quad -\left(\mathbf{Q}\mathbf{x}_i^*\right)^T \boldsymbol{\lambda} + \left(\mathbf{l} - \mathbf{M}\mathbf{x}_i^*\right)^T \boldsymbol{\mu} + \mathbf{h}^T\boldsymbol{\xi} \tag{H.9a}$$

$$\text{s.t.} \quad \mathbf{0} \leq \boldsymbol{\xi} \perp \mathbf{h} - \mathbf{H}\boldsymbol{\Delta w} \geq \mathbf{0} \,, \tag{H.9b}$$

$$\mathbf{H}^T\boldsymbol{\xi} = -\boldsymbol{\lambda} - \mathbf{N}^T\boldsymbol{\mu} \,, \tag{H.9c}$$

$$\mathbf{P}^T\boldsymbol{\lambda} + \mathbf{L}^T\boldsymbol{\mu} = \mathbf{c_y} \,, \tag{H.9d}$$

$$\boldsymbol{\mu} \geq \mathbf{0} \,. \tag{H.9e}$$

Notice that (H.8) and (H.9) correspond to the merging of the mid and right-hand-side optimization problems in (H.3), and to the right-hand-side problem in (H.6), respectively, where the first-stage variables are fixed. Let us indicate the optimal SP objective function value as $z_i^{\mathrm{SP}^*}$. Update the upper bound $\mathrm{UB} = \min\{\mathrm{UB}, \mathbf{c_x}\mathbf{x}_i^* + z_i^{\mathrm{SP}^*}\}$. Add to the relaxed MP the Benders cut (H.7b) corresponding to the SP solution $(\boldsymbol{\Delta w}_i^*, \boldsymbol{\lambda}_i^*, \boldsymbol{\mu}_i^*)$ determined at this stage.

4. Solve the relaxed MP, fix $\mathbf{x}_{i+1}^*$ at the solution and $z_{i+1}^{\mathrm{MP}^*}$ at the objective function value. Update $\mathrm{LB} = z_{i+1}^{\mathrm{MP}^*}$.

5. If $\mathrm{UB} - \mathrm{LB} < \tau$, where τ is a small tolerance value, then stop. Otherwise, update $i \leftarrow i + 1$ and go back to 3.

The above approach is named *Benders-dual cutting plane algorithm* in [11], since the cuts generated in step 3 of the algorithm above are based on the optimal dual solution of the lower-level problem in (H.2).

H.3.2 Primal Cut Algorithm

Similarly to the previous approach, the *primal cut algorithm* [11] is based on the fact that the solution to the lower-level optimization problem in (H.3) is at one of the vertices of the feasibility set. Because the feasibility set for $\mathbf{\Delta w}$ is completely decoupled from the feasibility set of the variables $(\boldsymbol{\lambda}, \boldsymbol{\mu})$, the worst-case realization of the uncertainty $\mathbf{\Delta w}$ is at a vertex of its feasibility set defined by $\mathbf{H\Delta w} \leq \mathbf{h}$.

We indicate with $\mathbf{\Delta w}_k$ the vertices of the feasibility set for the uncertain stochastic power production $\mathbf{\Delta w}$, and assign a copy $\mathbf{y_k}$ of the vector of recourse decision variables to each of these vertices. Hence, one can reformulate problem (H.1)–(H.2) in the following way:

$$\min_{\mathbf{x},\mathbf{y}_k,\beta} \quad \mathbf{c_x}^T\mathbf{x} + \beta \tag{H.10a}$$

$$\text{s.t.} \quad \beta \geq \mathbf{c_y}^T\mathbf{y}_k \,, \qquad \forall k \,, \tag{H.10b}$$

$$\mathbf{P}\mathbf{y}_k = -\mathbf{\Delta w}_k - \mathbf{Q}\mathbf{x} \,, \qquad \forall k \,, \tag{H.10c}$$

$$\mathbf{L}\mathbf{y}_k \geq \mathbf{l} - \mathbf{M}\mathbf{x} - \mathbf{N}\mathbf{\Delta w}_k \,, \qquad \forall k \,, \tag{H.10d}$$

$$\mathbf{F}\mathbf{x} = \mathbf{d} - \widehat{\mathbf{w}} \,, \tag{H.10e}$$

$$\mathbf{G}\mathbf{x} \geq \mathbf{g} \,. \tag{H.10f}$$

Notice that cuts (H.10b) are affine in the primal recourse variables $\mathbf{y_k}$, as opposed to cuts (H.7b), which depend on the dual variables. Besides, we remark that there is a copy $\mathbf{y}_k$ of the recourse variables and of constraints (H.10b), (H.10c) and (H.10d) for each vertex $\mathbf{\Delta w}_k$.

The following comments are in order:

- Differently from (H.7), model (H.10) includes energy redispatch, load shedding, stochastic power spillage, and network state variables at the balancing stage as decision variables. Furthermore, there is one such set of decisions for each vertex of the uncertainty set.
- The number of vertices, and therefore of Benders cuts, in (H.10) is smaller than that in (H.7). This is because in (H.10) there is one Benders cut per vertex of the uncertainty set, and not per vertex of the joint feasibility set of $(\mathbf{\Delta w}, \boldsymbol{\lambda}, \boldsymbol{\mu})$, which has higher dimensionality.

- On the other hand, the increase in size of the relaxed MP in a Benders scheme is much larger every time a vertex is added to the MP. Indeed, this entails adding a set of balancing market variables (recourse for a specific realization of the uncertainty), as well as a Benders cut (H.10b) and a set of feasibility constraints (H.10c)–(H.10d) for the balancing stage.

The primal cut algorithm is akin to the one described in Section H.3.1, with the following differences: the master problem used in step 2 is (H.10); at the end of step 3, we add a set $\mathbf{y_k}$ of recourse variables and a set of constraints (H.10b)–(H.10d), where we fix $\boldsymbol{\Delta}\mathbf{w}$ at the current solution $\boldsymbol{\Delta}\mathbf{w}_i^*$ of the subproblem.

As documented in [11] and [6], the primal cut algorithm, which is the one used in this work, generally guarantees a faster convergence to the optimal solution than the Benders-dual cutting plane one.

H.3.3 Choice of the Subproblem and of its Solution Method

In the description of the cutting-plane algorithm in Section H.3.1, we left open the choice of the subproblem and of relative solution method in step 3.

To our knowledge, the existing literature on the topic exclusively considers subproblem (H.8). The solution of this optimization problem is far from being trivial, since the presence of bilinear terms in the objective function (H.3a) renders the problem non-convex. In [4], an outer-approximation algorithm is proposed to solve this problem with general uncertainty sets. However, since the subproblem is non-convex, only local convergence is guaranteed for this method. As an alternative, exact linearization methods based on the use of integer variables are proposed in [5] and [6]. However, the uncertainty set is restricted to the particular case of polyhedral budgeted sets.

In this work, we propose the use of subproblem (H.9). The only nonlinearity in this problem is the presence of complementarity conditions (H.9b), where the $\perp$ operator implies that $\boldsymbol{\xi}(\mathbf{h} - \mathbf{H}\boldsymbol{\Delta}\mathbf{w}) = \mathbf{0}$. Notice that complementarity conditions can be linearized by making use of binary variables as proposed by [12]. Alternatively, one could employ the approach of [13], which is based on SOS-1 variables. In this work, the former implementation is chosen.

In comparison to the models in [5], [6] and [4], the proposed model has the following characteristics:

1. As compared to the method in [4], our approach converges to the global optimal solution. However, the model in [4] considers general convex uncertainty set, while our model is valid for any type of polyhedral set.

2. In comparison to the approach in [5] and [6], our approach retains the convergence to the global optimum while allowing us to consider any type of polyhedral sets. The number of binary variables employed in the linearization of the complementarity conditions (H.6b) grows linearly with the number of inequality constraints used to define the uncertainty set. Hence, in the case where the uncertainty set is a multidimensional interval with a total budget for deviations, the number of binary variables is comparable to the one in the binary expansions in [5] and in [6]

H.4 Results and Discussion

In this section, we present results obtained by employing the proposed model on different application studies. Section H.4.1 describes an example based on a simple two-node system, to illustrate the functioning of the model. A larger study based on the 24-node IEEE Reliability Test-System, the specifications of which can be found in [8], is considered in Section H.4.2.

H.4.1 Illustrative Example

Let us consider the two-node system depicted in Figure H.1. The line between the two nodes of the system has a capacity of 60 MW and a reactance of 0.13 pu. The load at each node is known with certainty and equal to 110 MWh and 30 MWh at node 1 and 2, respectively, during the market period considered. Furthermore, two wind farms are located at each node. The day-ahead production forecast is equal to 20 MWh and 25 MWh for wind farms 1 and 2, respectively. Notice that we make the assumption that the length of a market period is one hour. Hence, a forecast production equal to 20 MWh corresponds to an average output of 20 MW during the considered period. However, for the sake of clarity we will hereinafter employ the unit MWh for energy production and dispatch, and MW for reserve and capacity.

The characteristics of the units in the system are listed in Table H.1. The capacity of each unit is indicated with $P^{\max}$, the per unit cost of production with C, while C^+ and C^- represent the costs for each MW of available upward and downward reserve, respectively. Production from unit 1 is costly, but the unit is highly flexible, which is reflected in its low costs for reserve. On the

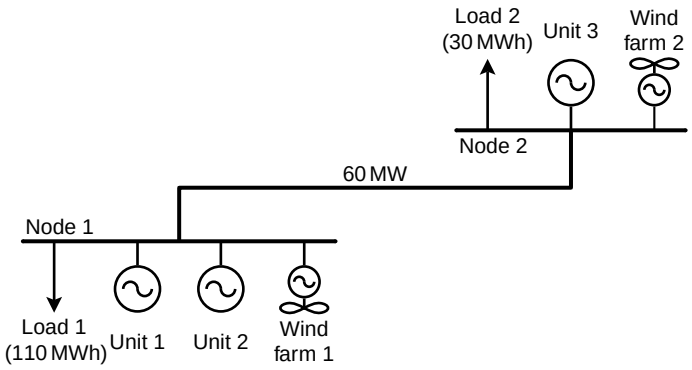

Figure H.1: Two-node system

contrary, unit 3 has a low marginal cost of production but is inflexible. Unit 2 has balanced characteristics.

Table H.1: Characteristics of the units in the two-node system

	Unit 1	Unit 2	Unit 3
$P^{\max}$ (MW)	120	80	70
C (\$/MWh)	32	20	12
C^+ (\$/MW)	7	11	15
C^- (\$/MW)	5	6	14

Model (H.1) for this example writes as follows:

$$\min_{\mathbf{p},\mathbf{r}^+,\mathbf{r}^-,\boldsymbol{\delta}^0} \; 32p_1 + 20p_2 + 12p_3 + 7r_1^+ + 11r_2^+ + 15r_3^+ + 5r_1^- + 6r_2^- + 14r_3^- + \mathcal{Q}_{\mathcal{W}}(\mathbf{p},\mathbf{r}^+,\mathbf{r}^-,\boldsymbol{\delta}^0) \tag{H.11a}$$

$$\text{s.t. } p_1 + p_2 + 20 = 110 - \frac{\delta_2^0}{0.13}\,, \tag{H.11b}$$

$$p_3 + 25 = 30 + \frac{\delta_2^0}{0.13}\,, \tag{H.11c}$$

$$p_1 + r_1^+ \le 120\,, \quad p_2 + r_2^+ \le 80\,, \quad p_3 + r_3^+ \le 70\,, \tag{H.11d}$$

$$p_1 - r_1^- \ge 0 \quad , \quad p_2 - r_2^- \ge 0 \quad , \quad p_3 - r_3^- \ge 0\,, \tag{H.11e}$$

$$-60 \le \frac{\delta_2^0}{0.13} \le 60\,, \tag{H.11f}$$

$$p_1, p_2, p_3, r_1^+, r_2^+, r_3^+, r_1^-, r_2^-, r_3^- \ge 0\,. \tag{H.11g}$$

Constraints (H.11b) and (H.11c) enforce power balance at node 1 and 2, re-

spectively. We choose node 1 as the reference node, i.e., we set $\delta_1^0 = 0$. Hence $-\delta_2^0/0.13$ represents the energy flow from node 1 to node 2. Constraints (H.11d) ensure that the sum of the day-ahead dispatch p and the upward reserve r^+ is not greater than the maximum power output. Similarly, (H.11e) enforces that the scheduled downward reserve r^- is not greater than the dispatch p. As a result of (H.11f), the scheduled flow between the two nodes is within the transmission capacity. Finally, non-negativity of the variables is enforced by (H.11g).

At the balancing stage, the actual wind power production can deviate from the day-ahead forecast. Table H.2 reports forecast, maximum deviation (in absolute value) and the resulting minimum and maximum values of production for the two wind farms considered. We make the further assumption that production from

Table H.2: Day-ahead forecast, maximum deviation at the balancing stage and resulting lower and upper bounds for production from each wind farm. Values in MWh

	$\widehat{w}$	$\Delta w^{\max}$	$\underline{w}$	$\overline{w}$
Wind farm 1	20	15	5	35
Wind farm 2	25	20	5	45

the two wind farms cannot deviate by $\Delta w^{\max}$ at the same time. On the contrary, the sum between the ratios of their deviation divided by the relative $\Delta w^{\max}$ cannot be greater than $\Gamma = 1.4$. Constant Γ is referred to in the literature as the *budget of uncertainty*. Imposing this constraint implies that, if the deviation of one wind farm's production is equal to $\Delta w^{\max}$, then the other wind farm can deviate at most by $0.4 \times \Delta w^{\max}$.

Under the non restrictive assumption that the marginal cost for redispatch is equal to the day-ahead dispatch cost, and assuming a load-shedding cost equal to \$ 200/MWh, the worst-case recourse cost $\mathcal{Q}_{\mathcal{W}}(\mathbf{p}, \mathbf{r}^+, \mathbf{r}^-, \boldsymbol{\delta}^{\mathbf{0}})$ is equal to the objective function value of the following *max-min* problem, which corresponds to model (H.2):

$$\max_{\mathbf{\Delta w}} \min_{\substack{\mathbf{p}^+, \mathbf{p}^-, \\ \mathbf{l}^{\mathrm{sh}}, \mathbf{w}^{\mathrm{sp}}, \boldsymbol{\delta}}} \; 32(p_1^+ - p_1^-) + 20(p_2^+ - p_2^-) + 12(p_3^+ - p_3^-) + 200(l_1^{\mathrm{sh}} + l_2^{\mathrm{sh}}) \tag{H.12a}$$

$$\text{s.t. } p_1^+ - p_1^- + p_2^+ - p_2^- + \Delta w_1 - w_1^{\mathrm{sp}} + l_1^{\mathrm{sh}} = -\frac{\delta_2 - \delta_2^0}{0.13} \,, \tag{H.12b}$$

$$p_3^+ - p_3^- + \Delta w_2 - w_2^{\mathrm{sp}} + l_2^{\mathrm{sh}} = \frac{\delta_2 - \delta_2^0}{0.13} \,, \tag{H.12c}$$

$$p_1^+ \le r_1^+ \,, \quad p_2 \le r_2^+ \,, \quad p_3 \le r_3^+ \,, \tag{H.12d}$$

$$p_1^- \le r_1^- \,, \quad p_2^- \le r_2^- \,, \quad p_3^- \le r_3^- \,, \tag{H.12e}$$

$$l_1^{\text{sh}} \leq 110\,, \quad l_2^{\text{sh}} \leq 30\,, \tag{H.12f}$$

$$w_1^{\text{sp}} \leq 20 + \Delta w_1\,, \quad w_2^{\text{sp}} \leq 25 + \Delta w_2\,, \tag{H.12g}$$

$$-60 \leq \frac{\delta_2}{0.13} \leq 60\,, \tag{H.12h}$$

$$p_1^+, p_2^+, p_3^+, p_1^-, p_2^-, p_3^-, l_1^{\text{sh}}, l_2^{\text{sh}}, w_1^{\text{sp}}, w_2^{\text{sp}} \geq 0\,, \tag{H.12i}$$

$$\text{s.t. } -15 \leq \Delta w_1 \leq 15\,, \quad -20 \leq \Delta w_2 \leq 20\,, \tag{H.12j}$$

$$\Delta w_1 = \Delta w_1^+ - \Delta w_1^-\,, \quad \Delta w_2 = \Delta w_2^+ - \Delta w_2^-\,, \tag{H.12k}$$

$$\frac{\Delta w_1^+ + \Delta w_1^-}{15} + \frac{\Delta w_2^+ + \Delta w_2^-}{20} \leq 1.4\,. \tag{H.12l}$$

The minimization problem enforces a minimum-cost redispatch in the electric energy system. Equations (H.12b) and (H.12c) guarantee the nodal power balance at the balancing stage. Symbols p^+ and p^- represent upward and downward redispatch, Δw the deviation of wind power production from the day-ahead forecast, w^{sp} and l^{sh} represent wind power spillage and load shedding, respectively, while δ represent the actual nodal network state. Constraints (H.12d) and (H.12e) enforce that the redispatch is not greater than the amount of upward and downward reserve established at the day-ahead stage, respectively. Constraints (H.12f) and (H.12g) guarantee that load shedding and wind power spillage are not greater than the actual consumption and wind power production. The actual transmission constraints are enforced by (H.12h). Finally, non-negative variables are defined in (H.12i).

The maximization problem in model (H.12) picks the worst case realization of deviation $\mathbf{\Delta w}$ of the wind power production from the day-ahead forecast $\widehat{\mathbf{w}}$. The feasible space is polyhedral. Inequalities (H.12j) define the intervals over which the deviation of wind power production can occur. Equations (H.12k) split the deviation into its positive and negative parts Δw^+ and Δw^-. Finally, constraint (H.12l) enforces the uncertainty budget.

Table H.3(a) displays the results of model (H.11)–(H.12) in terms of day-ahead energy and reserve dispatch. These results can be compared to the ones obtained using a similar model based on stochastic programming and reported in Table H.3(b). The latter model is obtained by replacing $\mathcal{Q}_{\mathcal{W}}(\cdot)$ in (H.11) with the expected value of the recourse cost over a discrete set of scenarios, rather than with its worst-case value determined by model (H.12). The scenarios used in the stochastic programming model are 100 random samples drawn from a uniform distribution defined over the uncertainty set (H.12j)–(H.12l). While the day-ahead energy dispatch coincides, the following comments on reserve are in order:

1. As far as upward reserve is concerned, the robust optimization model yields more conservative results than the stochastic programming model.

Indeed, no realization of the wind power deviation within the uncertainty set results in load-shedding events with the former approach. On the contrary, with the latter approach load shedding can take place if its cost is offset in expectation by the savings in terms of reserve.

2. No downward reserve is scheduled with the robust optimization approach. This is explained by the fact that there is no cost associated to wind power spillage. Hence, the worst-case realization of the wind power deviation is always negative, i.e., an underproduction, which requires no downward redispatch at the balancing stage.

3. With the robust optimization approach, units with the lowest aggregate cost of reserve and production, e.g., unit 3, are preferred to units with lower reserve cost but higher marginal costs, e.g., unit 1. This is a straightforward result of the focus on the worst-case realization of the uncertainty in (H.12). On the contrary, the stochastic programming model schedules reserve from units with lower capacity cost and higher operating costs, since the latter are weighted by the probability of actual deployment of the reserves.

Table H.3: Results for day-ahead dispatch and reserve using the robust optimization and the stochastic programming approach

(a) Robust Optimization

	Unit 1	Unit 2	Unit 3
p (MWh)	0	30	65
r^+ (MW)	0	21	5
r^- (MW)	0	0	0

(b) Stochastic Programming

	Unit 1	Unit 2	Unit 3
p (MWh)	0	30	65
r^+ (MW)	9.60	8.47	0
r^- (MW)	0	1.26	0

In the following section, we assess the impact of the increased robustness of the proposed approach on the costs of dispatch, reserve and redispatch in a more realistic setup.

H.4.2 Simulation Study

The results presented in this section are obtained from a modified version of the 24-node IEEE Reliability Test-System in [8].

We include six wind farms at different locations throughout the grid. Table H.4 reports the nodal location, as well as day-ahead forecast, maximum deviation at the balancing stage and the resulting minimum and maximum power production. The total forecast wind power production is 554 MWh. We consider the peak hour, where consumption totals 2850 MWh, thus wind power is expected to cover slightly less than 20 % of the load.

Table H.4: Nodal location, day-ahead forecast, maximum deviation at the balancing stage and resulting lower and upper bounds for production from each wind farm. Values in MWh

Wind farm	Node	$\widehat{w}$	$\Delta w^{\max}$	$\underline{w}$	$\overline{w}$
1	3	120	55.20	64.80	175.20
2	5	96	40	56	136
3	7	140	60	80	200
4	16	52	52	0	104
5	21	36	33.60	2.40	69.60
6	23	110	66	44	176

Besides the intervals reported in Table H.4 and the budget constraint of the type of (H.12l), we introduce another type of linear constraints for the deviation of wind power production. The objective of these constraints is to limit the difference between deviations for adjacent wind farms, e.g., for units q_1 and q_2:

$$-\rho_{q_1 q_2} \leq \frac{\Delta w_{q_1}}{\Delta w_{q_1}^{\max}} - \frac{\Delta w_{q_2}}{\Delta w_{q_2}^{\max}} \leq \rho_{q_1 q_2} \ . \tag{H.13}$$

We remark that solving the bilinear model (H.3) including constraints of this type is not straightforward, while in the proposed model (H.6) they can be included with little effort. Table H.5 reports the values of ρ employed in this study. Note that $\rho_{q_1 q_2}$ is a measure of the spatial correlation between wind farms q_1 and q_2.

Capacity on the transmission lines connecting the node pairs $(15, 21)$, $(14, 16)$ and $(13, 23)$ is reduced to 400 MW, 250 MW and 250 MW, respectively. This is done in order to introduce bottlenecks in the transmission system. The production cost of the units is linearized by making use of a piecewise-linear approximation. Four blocks with constant marginal cost are employed for each

Table H.5: Values of ρ employed for constraints (H.13) in the 24-node system

Wind farms		ρ
1	2	0.4
1	4	0.3
2	3	0.5
4	5	0.4
5	6	0.5

power plant. As far as reserve provision is concerned, we assume that nuclear plants are totally inflexible and thus unable to provide reserve. For coal units, the reserve cost per MW is equal to one fourth of the marginal cost of its most expensive block. Oil units are assumed to be more flexible and their reserve cost is one tenth of the marginal cost of the most expensive block. Notice, however, that these units have the highest production cost among the plants considered. Finally, the load-shedding cost is set to \$1000/MWh.

H.4.2.1 Comparison with the Stochastic Programming Approach

In this section we discuss the results in terms of system cost for the day-ahead dispatch and reserve schedules for the 24-node system, determined with the proposed robust optimization model and with a stochastic programming approach.

The uncertainty set in the robust optimization model is defined by the intervals in Table H.4, constraints of the type (H.13) with the parameters defined according to Table H.5 and a budget of uncertainty $\Gamma = 3.5$.

For the model based on stochastic programming, 500 scenarios drawn from independent truncated Gaussian distributions model the wind power uncertainty at each site. The Gaussian distributions are scaled so that the upper and lower bounds in Table H.4 represent the 95% confidence interval. Scenarios falling out of this interval, as well as the ones violating constraints (H.13) or exceeding the uncertainty budget are discarded.

Table H.6 breaks down the system cost for the two approaches into day-ahead costs (for dispatch and reserve) and balancing costs (for redispatch and load-shedding). The latter are reported both in expectation, calculated over a validation set of 1000 scenarios drawn from the same distribution as the one used in the optimization of the stochastic programming model, and in the worst-case realization of the uncertainty within the set described above.

As one can notice, the reserve costs are comparable for the two approaches. Indeed, the higher level of conservatism of robust optimization is almost completely offset by the cost for downward reserve in the stochastic programming approach. However, the dispatch cost and, notably, the expected costs in the balancing stage are lower for the stochastic programming approach, which benefits from the possibility of redispatching downward rather than spilling wind power. In total, the stochastic programming approach outperforms the robust optimization one in terms of expected cost by about 2.8%. However, the stochastic programming approach incurs a worst-case cost as high as three times the worst-case cost with the robust optimization model.

Table H.6: Comparison of system cost with the robust optimization and the stochastic programming approaches. Values in $

Cost	Robust Optimization		Stochastic Programming	
Dispatch	17 897.52		17 512.07	
Upward reserve	489.72		355.59	
Downward reserve	0		130.28	
Total day-ahead	18 387.25		17 997.95	
	Expected	Worst-case	Expected	Worst-case
Redispatch	339.32	2989.46	147.82	2634.55
Load-shedding	0	0	72.83	43 586.85
Total balancing	339.32	2989.46	220.64	46 221.40
Total aggregate	18 726.56	21 376.72	18 218.59	64 219.34

H.4.2.2 Robustness of Decision to Varying Distribution Type

The degree of suboptimality of the robust decision highlighted in the previous section might be an overestimation. In practice, the actual distribution of stochastic parameters can only be estimated by the decision-maker. Thus, the scenarios employed as input to stochastic programming models represent the uncertainty with a limited accuracy.

Table H.7 illustrates the expectation of the system cost incurred by the robust optimization and by the stochastic programming models if the uncertainty has a different distribution than the one considered in Section H.4.2.1. We now consider that deviations of wind power production at different locations follow independent uniform distributions defined on the same support as the Gaussian distribution employed in Section H.4.2.1 to determine the stochastic program-

ming solution. As one can notice, the expected value of system cost is rather stable if the solution obtained with the robust optimization model is employed. On the contrary, the cost incurred by the stochastic programming solution increases by roughly \$1000 compared to the one in Table H.6, mostly owing to increasing load-shedding cost.

Table H.7: Comparison of system cost with the robust optimization and the stochastic programming approaches under a different distribution. Values in \$

Cost	Robust Optimization	Stochastic Programming
Dispatch	17 897.52	17 512.07
Upward reserve	489.72	355.59
Downward reserve	0	130.28
Total day-ahead	18 387.25	17 997.95
Redispatch (exp.)	576.75	335.06
Load-shedding (exp.)	0	923.26
Total balancing (exp.)	576.75	1258.32
Total aggregate (exp.)	18 964.00	19 256.27

This comparison confirms the results in [4], which shows the stability of results of the robust approach to changes in the shape of the distribution. In practice, if the actual distribution of the uncertainty is more fat-tailed than the model from which scenarios are drawn, as in the case above, the performance of the stochastic programming solution degrades faster than the one of the robust optimization solution.

For completeness of the analysis, we consider the inverse case, where scenarios drawn from a uniform distribution are used as input to the stochastic programming model. Then, the expected system cost is determined over a set of scenarios drawn from a normal distribution and truncated consistently with the uncertainty set. The expected system cost for the two approaches is reported in Table H.8. Notably, the amount of reserve in the stochastic programming solution is significantly higher in this case than in the case in Table H.6 where uncertainty is normally distributed. As a result, this solution is rather robust when the actual distribution of the uncertainty has lower weight on the tails, such as in this case. Indeed, no load-shedding events are observed, and the total expected system cost is lower than that for the robust optimization solution.

Table H.8: Comparison of system cost with the robust optimization and the stochastic programming approaches under a different distribution. Values in $

Cost	Robust Optimization	Stochastic Programming
Dispatch	17 897.52	17 512.87
Upward reserve	489.72	433.42
Downward reserve	0	209.45
Total day-ahead	18 387.25	18 155.74
Redispatch (exp.)	361.10	139.36
Load-shedding (exp.)	0	0
Total balancing (exp.)	361.10	139.36
Total aggregate (exp.)	18 748.34	18 295.10

H.4.2.3 Computational Results

In this section, we briefly discuss the computational properties of the robust optimization and of the stochastic programming approaches. The models have been implemented in GAMS and solved using CPLEX 12, running on a laptop equipped with a 4-core processor clocking at 2.66 GHz.

Solution times for the 24-node system are illustrated in Figure H.2. The robust optimization model converged in 29.11 s after four iterations of the cutting-plane algorithm. The solution time in this case is plotted as a horizontal dashed line in the figure since robust optimization is scenario-free. The solid line in the figure represents the time for solving the stochastic programming approach as a function of the number of scenarios. As one can see, the computation time for the stochastic programming model increases with the number of scenarios. The robust optimization model solves more quickly than the stochastic optimization one as soon as the number of scenarios is higher than 300.

H.5 Conclusions

In this work, we consider the problem of jointly determining day-ahead energy dispatch and reserve capacity in an electricity market with large penetration of stochastic generation sources. The problem is cast as an adaptive robust optimization model, the solution of which minimizes the system cost in terms of dispatch, reserve and redispatch in the worst-case realization of the uncertain

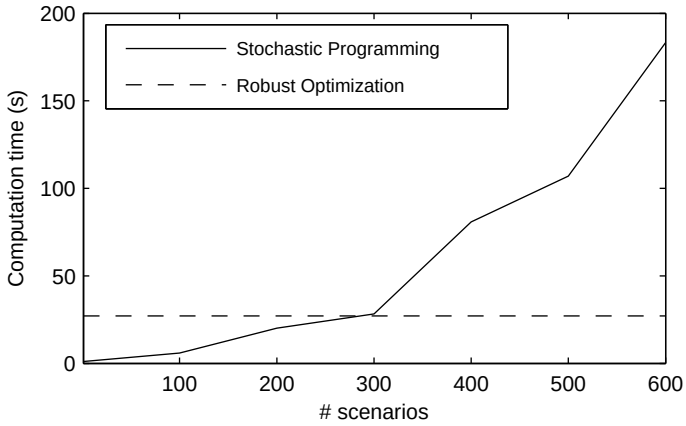

Figure H.2: Computation time for the robust optimization approach, and for the stochastic programming approach as a function of the number of scenarios

production.

We propose a novel reformulation of the problem that allows us to consider polyhedral sets of any type to model the support of the uncertainty distribution. Such a reformulation is employed as the subproblem within a well-known cutting-plane algorithm for adaptive robust optimization problems with right-hand side uncertainty. The proposed scheme, besides providing more flexibility in modeling uncertainty with general polyhedral sets, retains properties of convergence to the global optimum as well as of tractability of the methods proposed in the literature on the subject.

Through a case-study based on the 24-node IEEE Reliability Test-System, we assess the degree of suboptimality of the robust solution with respect to the stochastic programming approach. System cost increase in expectation by about 2.8%. However, the robust solution cuts worst-case cost by over two thirds. Furthermore, we show that the proposed model is rather robust to changes in the probability distribution. Indeed, the robust solution can actually outperform the stochastic programming one if the model for the distribution of the uncertainty used in the latter one underestimates the probability density on the tails. Finally, we show that for the proposed model, the robust optimization approach has better computational properties than a reasonably sized equivalent stochastic programming model.

Future research on the topic should be carried out in different directions. Firstly, the complementary problem of modeling uncertainty sets for spatially

distributed stochastic production, which is not considered here, should be studied. In parallel, dynamic properties could also be considered both in terms of modeling uncertainty sets, and by extending the model to a multi-period setting. Furthermore, reformulations of the robust optimization problem should be thought of in order to account for uncertainty sets with different structure, e.g., ellipsoidal sets. Finally, the combination of the proposed model with methods for determining ex-post the amount of downward reserve should be investigated as well, in order to reduce the gap of the robust approach with the stochastic programming one in terms of expected system cost.

H.6 Complete Min-Max-Min Optimization Model

A description of the symbols employed in these appendices is included in Table H.9.

The complete *min-max-min* model used in this work to determine the robust energy and reserve dispatch is the following optimization problem:

$$\min_{\mathbf{p},\mathbf{r}^+,\mathbf{r}^-,\boldsymbol{\delta^0}} \sum_k C_k p_k + C_k^+ r_k^+ + C_k^- r_k^- + \mathcal{Q}_{\mathcal{W}}(\mathbf{p},\mathbf{r}^+,\mathbf{r}^-,\boldsymbol{\delta^0}) \tag{H.14a}$$

$$\text{s.t.} \sum_{k\in G_i} p_k = \sum_{j\in N_i} B_{ij}\left(\delta_i^0 - \delta_j^0\right) + d_{s(i)} - \widehat{w}_{q(i)} \;, \qquad \forall i \;, \tag{H.14b}$$

$$\delta_1^0 = 0 \;, \tag{H.14c}$$

$$p_k + r_k^+ \le P_k^{\max} \;, \qquad \forall k \;, \tag{H.14d}$$

$$p_k - r_k^- \ge 0 \;, \qquad \forall k \;, \tag{H.14e}$$

$$B_{ij}\left(\delta_i^0 - \delta_j^0\right) \le T_{ij}^{\max} \;, \qquad \forall i,j \in N_i \;, \tag{H.14f}$$

$$p_k, r_k^+, r_k^- \ge 0 \;, \qquad \forall k \;, \tag{H.14g}$$

where the worst-case recourse cost for energy redispatching at the balancing stage is yielded by the following *max-min* optimization model:

$$\mathcal{Q}_{\mathcal{W}}(\mathbf{p},\mathbf{r}^+,r^-,\boldsymbol{\delta}^0) = \tag{H.15a}$$

$$\max_{\substack{\boldsymbol{\Delta}\mathbf{w},\\ \boldsymbol{\Delta}\mathbf{w}^+,\boldsymbol{\Delta}\mathbf{w}^-}} \; \min_{\substack{\mathbf{p}^+,\mathbf{p}^-,\\ \mathbf{l}^{\mathrm{sh}},\mathbf{w}^{\mathrm{sp}},\boldsymbol{\delta}}} \sum_k C_k\left(p_k^+ - p_k^-\right) + \sum_s V^{\mathrm{sh}} l_s^{\mathrm{sh}} \tag{H.15b}$$

Table H.9: List of symbols

Symbol	Type	Description
k	index	index for production block
i, j	index	index for network node
q, u	index	index for wind farm
s	index	index for load
G_i	set	set of production blocks k at node i
N_i	set	set of nodes j connected by a transmission line to node i
W_q	set	set of wind farms u neighboring wind farm q
$s(i)$	set	load at node i of the network (if any)
$q(i)$	set	wind farm at node i of the network (if any)
$i(k)$	set	node where production block k is located
$i(s)$	set	node where load s is located
$i(q)$	set	node where wind farm q is located
C_k	parameter	per unit cost of energy dispatch and redispatch for unit k
C_k^+	parameter	per unit cost of upward reserve for unit k
C_k^-	parameter	per unit cost of downward reserve for unit k
d_s	parameter	load from consumer s
$\widehat{w}_q$	parameter	forecast wind power production for wind farm q
B_{ij}	parameter	susceptance of line connecting nodes i and j
$T_{ij}^{\max}$	parameter	capacity of line connecting nodes i and j
V^{sh}	parameter	per unit cost of load-shedding
$\Delta w_q^{\max}$	parameter	maximum forecast error for output of wind farm q
Γ	parameter	budget of uncertainty for forecast error of wind power production
ρ_{qu}	parameter	maximum deviation of forecast error between wind farms q and u
p_k	variable	energy dispatch for production block k
r_k^+	variable	upward reserve dispatch for production block k
r_k^-	variable	downward reserve dispatch for production block k
δ_i^0	variable	network state variable at node i at the day-ahead stage
Δw_q	variable	forecast error for production from wind farm q
Δw_q^+	variable	positive part of forecast error for production from wind farm q
Δw_q^-	variable	negative part of forecast error for production from wind farm q
p_k^+	variable	upward energy redispatch for production block k
p_k^-	variable	downward energy redispatch for production block k
l_s^{sh}	variable	load shedding for demand s
w_q^{sp}	variable	wind power spillage for wind farm q
δ_i	variable	network state variable (voltage angle) at node i at the balancing stage

$$\text{s.t.} \sum_{k \in G_i} \left(p_k^+ - p_k^-\right) + l_{s(i)}^{\text{sh}} + \Delta w_{q(i)} - w_{q(i)}^{\text{sp}} = \sum_{j \in N_i} B_{ij} \left(\delta_i - \delta_i^0 - \delta_j + \delta_j^0\right) \ , \quad : \lambda_i \ , \quad \forall i \ , \tag{H.15c}$$

$$\delta_1 = 0 \ , \qquad : \nu \ , \tag{H.15d}$$

$$p_k^+ \leq r_k^+ \ , \qquad : \mu_k^+ \ , \qquad \forall k \ , \tag{H.15e}$$

$$p_k^- \leq r_k^- \ , \qquad : \mu_k^- \ , \qquad \forall k \ , \tag{H.15f}$$

$$l_s^{\text{sh}} \leq d_s \ , \qquad : \epsilon_s^{\text{sh}} \ , \qquad \forall s \ , \tag{H.15g}$$

$$w_q^{\text{sp}} \leq \widehat{w}_q + \Delta w_q \ , \qquad : \epsilon_q^{\text{sp}} \ , \qquad \forall q \ , \tag{H.15h}$$

$$B_{ij} \left(\delta_i - \delta_j\right) \leq T_{ij}^{\max} \qquad : \sigma_{ij} \ , \qquad \forall i, j \in N_i \ , \tag{H.15i}$$

$$p_k^+, p_k^- \geq 0 \, , \forall k \, , l_s^{\text{sh}} \geq 0 \, , \forall s \, , w_q^{\text{sp}} \geq 0 \, , \forall q \, , \tag{H.15j}$$

$$\text{s.t.} \ \Delta w_q = \Delta w_q^+ - \Delta w_q^- \ , \qquad \forall q \ , \tag{H.15k}$$

$$\Delta w_q^+ \leq \Delta w_q^{\max} \ , \qquad \forall q \ , \tag{H.15l}$$

$$\Delta w_q^- \leq \Delta w_q^{\max} \ , \qquad \forall q \ , \tag{H.15m}$$

$$\sum_q \frac{\Delta w_q^+ + \Delta w_q^-}{\Delta w_q^{\max}} \leq \Gamma \ , \tag{H.15n}$$

$$\frac{\Delta w_q}{\Delta w_q^{\max}} - \frac{\Delta w_u}{\Delta w_u^{\max}} \leq \rho_{qu} \ , \qquad \forall q, u \in W_q \ , \tag{H.15o}$$

$$\Delta w_q^+, \Delta w_q^- \geq 0 \ , \qquad \forall q \ . \tag{H.15p}$$

(H.15q)

Notice that (H.14) is the complete formulation of (H.1) for the problem at hand. Similarly, (H.15) corresponds to (H.2).

H.7 Optimization Model Used Within the Cutting-Plane Algorithm

In this section, we carry out in detail the mathematical development that leads to the single-level maximization problem (H.6).

Let us first replace the right-hand side minimization problem in (H.15) with its dual. Notice that the dual variables are indicated in (H.15) after a colon separating them from the corresponding constraints. We then swap the order of the

resulting *max-max* problem, so that the right-hand-side maximization problem is the one involving variables $\boldsymbol{\Delta}\mathbf{w}, \boldsymbol{\Delta}\mathbf{w}^+, \boldsymbol{\Delta}\mathbf{w}^-$. These operations render the following problem:

$$\max_{\substack{\boldsymbol{\lambda},\boldsymbol{\nu},\boldsymbol{\mu}^+,\boldsymbol{\mu}^- \\ \boldsymbol{\epsilon}^{\mathrm{sh}},\boldsymbol{\epsilon}^{\mathrm{sp}},\boldsymbol{\sigma}}} \sum_i -\lambda_i \sum_{j\in N_i} B_{ij}\left(\delta_i^0 - \delta_j^0\right) + \sum_k \left(\mu_k^+ r_k^+ + \mu_k^- r_k^-\right) \tag{H.16a}$$

$$+ \sum_s d_s \epsilon_s^{\mathrm{sh}} + \sum_q \widehat{w}_q \epsilon_q^{\mathrm{sp}} + \sum_{i,j\in N_i} T_{ij}^{\max}\sigma_{ij} \tag{H.16b}$$

$$+ \max_{\boldsymbol{\Delta}\mathbf{w},\boldsymbol{\Delta}\mathbf{w}^+,\boldsymbol{\Delta}\mathbf{w}^-} -\sum_i \lambda_i \Delta w_{q(i)} + \sum_q \epsilon_q^{\mathrm{sp}} \Delta w_q \tag{H.16c}$$

$$\text{s.t. } \Delta w_q = \Delta w_q^+ - \Delta w_q^- \qquad : \gamma_q\ , \quad \forall q\ , \tag{H.16d}$$

$$\Delta w_q^+ \le \Delta w_q^{\max} \qquad : \xi_q^+\ , \quad \forall q\ , \tag{H.16e}$$

$$\Delta w_q^- \le \Delta w_q^{\max} \qquad : \xi_q^-\ , \quad \forall q\ , \tag{H.16f}$$

$$\sum_q \frac{\Delta w_q^+ + \Delta w_q^-}{\Delta w_q^{\max}} \le \Gamma \qquad : \eta\ , \tag{H.16g}$$

$$\frac{\Delta w_q}{\Delta w_q^{\max}} - \frac{\Delta w_u}{\Delta w_u^{\max}} \le \rho_{qu} \qquad : \omega_{qu}\ , \ \forall q, u \in W_q\ , \tag{H.16h}$$

$$\Delta w_q^+, \Delta w_q^- \ge 0 \qquad \forall q\ , \tag{H.16i}$$

$$\text{s.t. } \lambda_{i(k)} + \mu_k^+ \le C_k\ , \qquad \forall k\ , \tag{H.16j}$$

$$-\lambda_{i(k)} + \mu_k^- \le -C_k\ , \qquad \forall k\ , \tag{H.16k}$$

$$\lambda_{i(s)} + \epsilon_s^{\mathrm{sh}} \le V^{\mathrm{sh}}\ , \qquad \forall s\ , \tag{H.16l}$$

$$-\lambda_{i(q)} + \epsilon_q^{\mathrm{sp}} \le 0\ , \qquad \forall q\ , \tag{H.16m}$$

$$\begin{aligned} &\nu - \left(\sum_{j\in N_1} B_{1j}\right)\lambda_1 + \left(\sum_{j\in N_1} B_{1j}\lambda_j\right) \\ &\quad + \sum_{j\in N_1} B_{1j}\left(\sigma_{1j} - \sigma_{j1}\right) = 0\ , \end{aligned} \tag{H.16n}$$

$$\begin{aligned} &-\left(\sum_{j\in N_i} B_{ij}\right)\lambda_i + \left(\sum_{j\in N_i} B_{ij}\lambda_j\right) \\ &\quad + \sum_{j\in N_i} B_{ij}\left(\sigma_{ij} - \sigma_{ji}\right) = 0\ , \end{aligned} \qquad \forall i \ne 1\ , \tag{H.16o}$$

$$\mu_k^+, \mu_k^- \le 0\ , \forall k\ , \epsilon_s^{\mathrm{sh}} \le 0\ , \tag{H.16p}$$

$$\forall s\ , \epsilon_q^{\mathrm{sp}} \le 0\ , \forall q\ , \sigma_{ij} \le 0\ , \forall i, j \in N_i\ , \tag{H.16q}$$

which is the complete formulation of the mid and right-hand-side maximization

problems in (H.4).

Then, we replace the objective function of the right-hand-side maximization problem in (H.16) with the one of its dual problem:

$$-\sum_i \lambda_i \Delta w_{q(i)} + \sum_q \epsilon_q^{\mathrm{sp}} \Delta w_q = \sum_q \Delta w_q^{\max} \left(\xi_q^+ + \xi_q^-\right) + \Gamma\eta + \sum_{q,u\in W_q} \rho_{qu}\omega_{qu} \ . \tag{H.17}$$

Finally, we include the Karush-Kuhn-Tucker conditions for the right-hand-side optimization problem, and cast (H.16) as the following single-level maximization problem:

$$\max_{\substack{\boldsymbol{\lambda},\nu,\boldsymbol{\mu}^+,\boldsymbol{\mu}^-,\boldsymbol{\epsilon}^{\mathrm{sh}},\boldsymbol{\epsilon}^{\mathrm{sp}},\boldsymbol{\sigma}\\ \boldsymbol{\Delta w},\boldsymbol{\Delta w}^+,\boldsymbol{\Delta w}^-,\\ \boldsymbol{\gamma},\boldsymbol{\xi}^+,\boldsymbol{\xi}^-,\eta,\boldsymbol{\omega}}} \quad \sum_i -\lambda_i \sum_{j\in N_i} B_{ij}\left(\delta_i^0 - \delta_j^0\right) + \sum_k \left(\mu_k^+ r_k^+ + \mu_k^- r_k^-\right) \tag{H.18a}$$

$$+ \sum_s d_s \epsilon_s^{\mathrm{sh}} + \sum_q \widehat{w}_q \epsilon_q^{\mathrm{sp}} + \sum_{i,j\in N_i} T_{ij}^{\max}\sigma_{ij} \tag{H.18b}$$

$$+ \sum_q \Delta w_q^{\max}\left(\xi_q^+ + \xi_q^-\right) + \Gamma\eta + \sum_{q,u\in W_q} \rho_{qu}\omega_{qu} \tag{H.18c}$$

$$\text{s.t. } \Delta w_q = \Delta w_q^+ - \Delta w_q^- \ , \qquad \forall q \ , \tag{H.18d}$$

$$0 \le \xi_q^+ \perp \Delta w_q^+ - \Delta w_q^{\max} \le 0 \ , \qquad \forall q \ , \tag{H.18e}$$

$$0 \le \xi_q^- \perp \Delta w_q^- - \Delta w_q^{\max} \le 0 \ , \qquad \forall q \ , \tag{H.18f}$$

$$0 \le \eta \perp \sum_q \frac{\Delta w_q^+ + \Delta w_q^-}{\Delta w_q^{\max}} - \Gamma \le 0 \ , \tag{H.18g}$$

$$0 \le \omega_{qu} \perp \frac{\Delta w_q}{\Delta w_q^{\max}} - \frac{\Delta w_u}{\Delta w_u^{\max}} - \rho_{qu} \le 0 \ , \qquad \forall q,u \in W_q \ , \tag{H.18h}$$

$$\gamma_q + \sum_{u\in W_q} \frac{\omega_{qu} - \omega_{uq}}{\Delta w_q^{\max}} + \lambda_{q(i)} - \epsilon_q^{\mathrm{sp}} = 0 \qquad \forall q \ , \tag{H.18i}$$

$$0 \le \Delta w_q^+ \perp -\gamma_q + \xi_q^+ + \frac{\eta}{\Delta w_q^{\max}} \ge 0 \ , \qquad \forall q \ , \tag{H.18j}$$

$$0 \le \Delta w_q^- \perp \gamma_q + \xi_q^- + \frac{\eta}{\Delta w_q^{\max}} \ge 0 \ , \qquad \forall q \ , \tag{H.18k}$$

$$\lambda_{i(k)} + \mu_k^+ \le C_k \ , \qquad \forall k \ , \tag{H.18l}$$

$$-\lambda_{i(k)} + \mu_k^- \le -C_k \ , \qquad \forall k \ , \tag{H.18m}$$

$$\lambda_{i(s)} + \epsilon_s^{\mathrm{sh}} \le V^{\mathrm{sh}} \ , \qquad \forall s \ , \tag{H.18n}$$

$$-\lambda_{i(q)} + \epsilon_q^{\mathrm{sp}} \le 0 \ , \qquad \forall q \ , \tag{H.18o}$$

$$\nu - \left(\sum_{j\in N_1} B_{1j}\right)\lambda_1 + \left(\sum_{j\in N_1} B_{1j}\lambda_j\right) + \sum_{j\in N_1} B_{1j}\left(\sigma_{1j} - \sigma_{j1}\right) = 0\,, \tag{H.18p}$$

$$-\left(\sum_{j\in N_i} B_{ij}\right)\lambda_i + \left(\sum_{j\in N_i} B_{ij}\lambda_j\right) + \sum_{j\in N_i} B_{ij}\left(\sigma_{ij} - \sigma_{ji}\right) = 0\,, \quad \forall i \neq 1\,, \tag{H.18q}$$

$$\mu_k^+, \mu_k^- \leq 0\,, \forall k\,, \epsilon_s^{\mathrm{sh}} \leq 0\,, \forall s\,, \tag{H.18r}$$

$$\epsilon_q^{\mathrm{sp}} \leq 0\,, \forall q\,, \sigma_{ij} \leq 0\,, \forall i, j \in N_i\,, \tag{H.18s}$$

which is the complete formulation of the right-hand side maximization problem in (H.6).

Acknowledgement

The authors would like to thank Juan Miguel Morales from the Department of Applied Mathematics and Computer Science and Pierre Pinson from the Center for Electrical power and Energy (CEE), both at the Technical University of Denmark, for their insightful comments on this work.

References H

[1] G. Pritchard, G. Zakeri, and A. Philpott, "A single-settlement, energy-only electric power market for unpredictable and intermittent participants," *Operations Research*, vol. 58, no. 4(2), pp. 1210–1219, 2010.

[2] J. M. Morales, A. J. Conejo, and J. Pérez-Ruiz, "Economic valuation of reserves in power systems with high penetration of wind power," *IEEE Transactions on Power Systems*, vol. 24, no. 2, pp. 900–910, 2009.

[3] D. Bertsimas, D. G. Brown, and C. Caramanis, "Theory and applications of robust optimization," *SIAM Review*, vol. 53, no. 3, pp. 464–501, 2011.

[4] D. Bertsimas, E. Litvinov, X. A. Sun, J. Zhao, and T. Zheng, "Adaptive robust optimization for the security constrainted unit commitment problem," *IEEE Transactions on Power Systems*, vol. 28, no. 1, pp. 52–63, 2012.

[5] R. Jiang, J. Wang, and Y. Guan, "Robust unit commitment with wind power and pumped storage hydro," *IEEE Transactions on Power Systems*, vol. 27, pp. 800–810, May 2012.

[6] L. Zhao and B. Zeng, "Robust unit commitment problem with demand response and wind energy," in *2012 IEEE Power & Energy Society General Meeting*, pp. 1–8, 2012.

[7] A. Thiele, T. Terry, and M. Epelman, "Robust linear optimization with recourse," IOE Technical Report TR09-01, University of Michigan, mar 2010.

[8] C. Grigg, P. Wong, P. Albrecht, R. Allan, M. Bhavaraju, R. Billinton, Q. Chen, C. Fong, S. Haddad, S. Kuruganty, *et al.*, "The IEEE reliability

test system-1996. A report prepared by the reliability test system task force of the application of probability methods subcommittee," *IEEE Transactions on Power Systems*, vol. 14, no. 3, pp. 1010–1020, 1999.

[9] J. E. Kelley, "The cutting-plane method for solving convex programs," *SIAM Journal of the Society for Industrial and Applied Mathematics*, vol. 8, no. 4, pp. 703–712, 1960.

[10] A. J. Conejo, E. Castillo, R. Mínguez, and R. García-Bertrand, *Decomposition Techniques in Mathematical Programming: Engineering and Science Applications*, ch. 5, pp. 197–199. Berlin: Springer, 2006.

[11] B. Zeng, "Solving two-stage robust optimization problems by a constraint-and-column generation method," tech. rep., Department of Industrial and Management Syst. Engineering, University of South Florida, 2011.

[12] J. Fortuny-Amat and B. McCarl, "A representation and economic interpretation of a two-level programming problem," *Journal of the Operational Research Society*, pp. 783–792, 1981.

[13] S. Siddiqui and S. A. Gabriel, "An SOS1-based approach for solving MPECs with a natural gas market application," *Networks and Spatial Economics*, pp. 1–23, 2012.

Bibliography

[AAR+12] Khaled H. Abdul-Rahman, Hani Alarian, Mark Rothleder, Petar Ristanovic, Bogdan Vesovic, and Bo Lu. Enhanced system reliability using flexible ramp constraint in CAISO market. In *Power and Energy Society General Meeting, 2012 IEEE*, pages 1–6. IEEE, 2012.

[BBC11] Dimitris Bertsimas, David G. Brown, and Constantine Caramanis. Theory and applications of robust optimization. *SIAM Review*, 53(3):464–501, 2011.

[BL11] John R. Birge and François Louveaux. *Introduction to Stochastic Programming*. Springer Series in Operations Research and Financial Engineering. Springer, New York, second edition, 2011.

[Bor02] Severin Borenstein. The trouble with electricity markets: understanding California's restructuring disaster. *Journal of Economic Perspectives*, 16(1):191–211, 2002.

[BSS06] Mokhtar S. Bazaraa, Hanif D. Sherali, and Chitharanjan Marakada Shetty. *Nonlinear programming: Theory and algorithms*. Wiley-Interscience, Hoboken, New Jersey, third edition, 2006.

[CD88] William S. Cleveland and Susan J. Devlin. Locally weighted regression: An approach to regression analysis by local fitting. *Journal of the American Statistical Association*, 83(403):596–610, 1988.

[Ene08] Energinet.dk. *Regulation C2: The balancing market and balance settlement*, dec 2008.

[Ene12] Energinet.dk. *Ancillary services to be delivered in Denmark – Tender conditions*, oct 2012.

[Ene13a] Energinet.dk. Website, 2013. http://energinet.dk/EN/Sider/default.aspx.

[Ene13b] Energistyrelsen. Website, 2013. http://www.ens.dk/da-dk/Sider/forside.aspx.

[FGRM05] Alberto Fabbri, Tomás Gómez San Román, Juan Rivier Abbad, and Víctor H. Méndez Quezada. Assessment of the cost associated with wind generation prediction errors in a liberalized electricity market. *IEEE Transactions on Power Systems*, 20(3):1440–1446, 2005.

[FM81] José Fortuny-Amat and Bruce McCarl. A representation and economic interpretation of a two-level programming problem. *Journal of the Operational Research Society*, pages 783–792, 1981.

[GCF+12] Stephen A. Gabriel, Antonio J. Conejo, J. David Fuller, Benjamin F. Hobbs, and Carlos Ruiz. *Complementarity Modeling in Energy Markets*, volume 180 of *International Series in Operations Research & Management Science*. Springer, New York, 2012.

[Glo12] Global Wind Energy Council. Global wind statistics 2012. Report, 2012. http://www.gwec.net/wp-content/uploads/2013/02/GWEC-PRstats-2012_english.pdf.

[GWA+99] Cliff Grigg, Peter Wong, Paul Albrecht, Ron Allan, Murty Bhavaraju, Roy Billinton, Quan Chen, Clement Fong, Suheil Haddad, Sastry Kuruganty, et al. The IEEE reliability test system-1996. A report prepared by the reliability test system task force of the application of probability methods subcommittee. *IEEE Transactions on Power Systems*, 14(3):1010–1020, 1999.

[Jón12] Tryggvi Jónsson. *Forecasting and Decision-Making in Electricity Markets with Focus on Wind Energy*. PhD thesis, Technical University of Denmark, 2012. http://orbit.dtu.dk/fedora/objects/orbit:110048/datastreams/file_10102096/content.

[KJ60] James E. Kelley Jr. The cutting-plane method for solving convex programs. *Journal of the Society for Industrial & Applied Mathematics*, 8(4):703–712, 1960.

[KW94] Peter Kall and Stein W. Wallace. *Stochastic Programming*. John Wiley & Sons, Chichester, 1994.

[LPR96] Zhi-Quan Luo, Jong-Shi Pang, and Daniel Ralph. *Mathematical Programs with Equilibrium Constraints*. Cambridge University Press, Cambridge, UK, 1996.

[LY08] David G. Luenberger and Yinyu Ye. *Linear and Nonlinear Programming*, volume 116 of *International Series in Operations Research and Management Science*. Springer, New York, third edition, 2008.

[Mad07] Henrik Madsen. *Time Series Analysis*. Chapman & Hall/CRC, 2007.

[MCPR09] Juan M. Morales, Antonio J. Conejo, and Juan Pérez-Ruiz. Economic valuation of reserves in power systems with high penetration of wind power. *IEEE Transactions on Power Systems*, 24(2):900–910, 2009.

[Nor12] Nordic Energy Regulators. Nordic market report 2012. report, 2012. `https://www.nordicenergyregulators.org/upload/Reports/NMR%202012%20-%20publication.pdf`.

[Nor13a] Nord Pool Spot. Nord Pool Spot — Europe's leading power markets. Presentation, 2013.

[Nor13b] Nord Pool Spot. The Nordic electricity exchange and the Nordic model for a liberalized electricity market. Technical report, Nord Pool Spot, 2013.

[Nor13c] Nord Pool Spot. Website, 2013. `http://www.nordpoolspot.com/`.

[PK10] Pierre Pinson and George Kariniotakis. Conditional prediction intervals of wind power generation. *IEEE Transactions on Power Systems*, 25(4):1845–1856, 2010.

[PMN+09] Pierre Pinson, Henrik Madsen, Henrik Aa. Nielsen, George Papaefthymiou, and Bernd Klöckl. From probabilistic forecasts to statistical scenarios of short-term wind power production. *Wind Energy*, 12(1):51–62, 2009.

[PZP10] Geoffrey Pritchard, Golbon Zakeri, and Andrew Philpott. A single-settlement, energy-only electric power market for unpredictable and intermittent participants. *Operations Research*, 58(4-Part-2):1210–1219, 2010.

[RS64] Howard Raiffa and Robert Schlaifer. *Applied Statistical Decision Theory*. Division of Research — Harvard Business school, Boston, 1964.

[THL10] Jacopo Torriti, Mohamed G. Hassan, and Matthew Leach. Demand response experience in Europe: Policies, programmes and implementation. *Energy*, 35(4):1575–1583, 2010.

[Web10] Christoph Weber. Adequate intraday market design to enable the integration of wind energy into the European power systems. *Energy Policy*, 38(7):3155–3163, 2010.

[Wer06] Rafał Weron. *Modeling and Forecasting Electricity Loads and Prices*. John Wiley & Sons, 2006.